



Dipl.-Ing. Andreas Schwarz, BSc.

# Decoding Hand Movements From Human EEG

## **DOCTORAL THESIS**

to achieve the university degree of  
Doktor der technischen Wissenschaften

submitted to

**Graz University of Technology**

### **Supervisor**

Gernot R. Müller-Putz, Prof. Dr. Dipl.-Ing.  
Institute of Neural Engineering

Graz, 6 2020

## **AFFIDAVIT**

I declare that I have authored this thesis independently, that I have not used other than the declared sources/resources, and that I have explicitly indicated all material which has been quoted either literally or by content from the sources used. The text document uploaded to TUGRAZonline is identical to the present doctoral thesis.

---

Date, Signature

# Abstract

Severely motor impaired persons are substantially limited in their daily life routine. Depending on their grade of motor impairment, even tasks of daily routine like eating, drinking or personal hygiene are not viable without the help of a permanent caregiver. Up to this point, this group is waiting for an intervention, making regaining grasp functions their priority choice. A possible way for restoring their basic independence would be via a brain-computer interface (BCI) to control assistive devices, e.g. an upper limb motor neuroprosthesis or a robotic arm. The BCI circumvents damaged parts of the central nervous system by directly recording and processing brain signals from the scalp. The goal of this thesis was to evaluate whether brain patterns of natural grasp/reach-and-grasp movements can be identified and decoded from the electroencephalogram (EEG) and further used in a non-invasive EEG-based BCI.

In several consecutive experiments in able bodied study participants, EEG correlates of grasp/reach-and-grasp actions could be identified in EEGs' low frequency time domain (LFTD) signals and decoded against each other and a rest condition. In addition, it could further be shown that these correlates could be used online in a non-invasive BCI, where able bodied study participants gained control over a virtual robotic arm in a simulation environment.

Further investigations were conducted incorporating bimanual movements. Results obtained from an able bodied population indicated that these movements were not only significantly different to their unimanual counterparts, but also decodable. Finally, a single case study performed in one tetraplegic end user could show that unimanual and bimanual executed reach-and- attempted grasp actions could be successfully decoded. This thesis shows that natural grasp/reach-and-grasp movements can be identified and decoded from the low frequency time domain and used to drive a BCI. However, further research is necessary to improve inter alia the decoding performance, before a successful transfer to motor impaired end users is feasible.

# Kurzfassung

Menschen mit schwerer Bewegungsbeeinträchtigung, wie beispielsweise Personen mit einer hohen Querschnittlähmung, haben einen beträchtlichen Teil Ihrer persönlichen Freiheit eingebüßt und sind in ihrer täglichen Routine vollkommen auf die externe Hilfe einer Pflegekraft angewiesen. Abhängig vom Grad der Beeinträchtigung sind oft alltägliche Dinge wie Nahrungsaufnahme, Trinken oder auch die persönliche Hygiene nicht mehr alleine zu bewerkstelligen. Diese Personengruppe hofft und wartet auf vielversprechende Ansätze, um zumindest einen Teil ihrer persönlichen Freiheit wiederzugewinnen, wobei deren Hauptaugenmerk auf der Wiedererlangung der Greiffunktion liegt. Eine durchaus vorstellbare Herangehensweise bietet sich via Brain-Computer-Interface (BCI): Es bietet einen alternativen Kommunikationskanal zum (beschädigten) zentralen Nervensystem im Rückenmark, indem es direkt Hirnsignale mit Hilfe des Elektroenzephalogramms (EEG) auf dem Skalp erfasst und interpretiert.

Das Ziel der vorliegenden Dissertation war es festzustellen, ob designierte Gehirnmuster für Greifbewegungen aus dem EEG identifiziert und mittels moderner Machine-learning Methoden auch dekodiert werden können. Des Weiteren wurde untersucht, ob diese Gehirnmuster geeignet sind, um in einem BCI eingesetzt werden zu können.

In mehreren aufeinanderfolgenden Experimenten konnte nicht nur die Existenz solcher Gehirnmuster im niederfrequenten Zeitbereich des EEG gezeigt werden, sondern auch dass diese Muster sowohl untereinander als auch gegen eine Ruhe Kondition dekodiert werden können. In einem weiteren Experiment mit gesunden, nicht bewegungsbeeinträchtigten Studienteilnehmern wurden diese Gehirnmuster dazu benutzt um mittels eines BCIs in Echtzeit die Kontrolle eines virtuellen Roboterarms zu übernehmen.

Basierend auf den Erfahrungen mit Personen mit hohem Querschnitt, wurde das Forschungsfeld um die Identifikation und Dekodierung von Gehirnmustern beruhend auf bimanualen Greifbewegungen erweitert. Die gewonnenen Resultate zeigen, dass auch bimanuale Bewegungen individuelle Gehirnmuster erzeugen, die sich nicht nur von ihren unimanualen Gegenständen signifikant unterscheiden, sondern auch also solche, erfolgreich dekodiert werden können.

Im letzten Versuchsaufbau dieser Dissertation wurde der konzeptionelle Beweis für die Übertragbarkeit der vorliegenden Resultate auf einen Versuchsteilnehmer mit hohem Querschnitt angetreten: Es konnte erfolgreich gezeigt werden, dass die Gehirnmuster der ausgeführten und versuchten Greifbewegungen des Versuchsteilnehmers kombiniert und dekodiert werden können. Dementsprechend konnte in dieser Dissertation gezeigt werden, dass designierte Gehirnmuster für Griff und Greifbewegungen aus dem EEG identifiziert und mittels moderner Machine-learning Methoden auch dekodiert werden können. Jedoch muss festgestellt werden, dass unter anderem, aber vor allem die Leistung und Genauigkeit der EEG basierenden Dekodierung noch zu unzuverlässig sind, um

gefährlos im Alltag verwendet zu werden. Dementsprechend ist eine weitere Erforschung des Themas vonnöten.

# Danksagung (Acknowledgements)

An dieser Stelle ist all jenen zu danken, die mich auf dem Weg zu dieser Dissertationsschrift begleitet haben. Jeder von Ihnen hat seinen für Ihn möglichen Teil beigetragen - als Unterstützer, Freund, Partner, Kritiker.

Ich danke Prof. Gernot R. Müller-Putz für die Chance, mich als Wissenschaftler zu beweisen.

Ferner danke ich Reinhold Scherer, Selina Wriessnegger und Rüdiger Rupp, die mir stets mit Rat und Tat zur Seite standen und mir geholfen haben, meine Ideen im wissenschaftlichen Sinn zu strukturieren. Besonderer Dank gilt meinen Kommilitonen Joana Pereira, Patrick Ofner, Josef Faller, David Steyrl und natürlich Andreas Pinegger, die substantiell zum Erfolg meiner wissenschaftlichen Studien und Publikationen beigetragen haben.

Die in dieser Dissertation vorgestellten Studien wären nicht durchführbar gewesen ohne die professionelle und tatkräftige Unterstützung von Maria Katharina Höller, Marcel Zube und Daniel Hackhofer, die mir als Assistenten bei meinen Experimenten zur Seite standen. Besonderen Dank und Anerkennung für seine handwerklichen Leistungen möchte ich meinem Freund Dietmar Schäfauer aussprechen, der sämtliche Aufbauten in meinen Experimenten gefertigt hat.

Ein weiterer Dank gilt der Europäischen Union und dem Horizon 2020 Projekt “MoreGrasp” (643955), der Technischen Universität Graz und dem Land Steiermark, durch die dieses Dissertationsvorhaben finanziert wurde.

Mein tiefster Dank gilt meinem familiären und freundschaftlichen Umfeld: Meinen Großeltern, Eltern, meinem Bruder und meiner Familie, die mein Fortkommen mehr als über das Ihnen mögliche Maß gefördert haben. Meinen Freunden, Reinhard Hutter, Michael Schaffernak, Thomas Wiesner, Patrik Fritzer, Kerstin Strommer, Jakob DeVries und Christian Mathis, für Eure Freundschaft und Euren Beitrag zu meiner geistigen Gesundheit - im hoffentlich positiven Sinn.

Von tiefstem Herzen danke ich meiner Partnerin Katharina Haring, für Ihre Liebe und Geduld mit mir sowie Ihr Gespür zu wissen, wann ein sprichwörtlicher “Tritt in den Hintern” notwendig ist.

# Contents

<b>1</b>	<b>Introduction</b>	<b>1</b>
1.1	Severe motor impairment - causes and intervention . . . . .	1
1.2	Brain-computer interfaces . . . . .	2
1.2.1	BCI signal acquisition . . . . .	4
1.2.2	Modulatable brain signals . . . . .	5
1.2.3	BCI feature translation . . . . .	10
1.2.4	Application interface and application . . . . .	10
1.2.5	Closed loop BCI feedback . . . . .	11
1.3	Non-invasive BCIs for motor control: State-of-the-art . . . . .	11
1.4	Current limitations in BCIs control modalities for motor control . . . . .	13
1.5	Aims of this thesis . . . . .	15
1.6	Organization of this thesis . . . . .	15
<b>2</b>	<b>Methodology and results</b>	<b>16</b>
2.1	Decoding reach and reach-and-grasp actions from human EEG . . . . .	17
2.1.1	Decoding natural reach-and-grasp actions from human EEG . . . . .	17
2.1.2	Decoding hand movements from human EEG to control a robotic arm in a simulation environment . . . . .	21
2.2	Decoding unimanual and bimanual reach-and-grasp actions from human EEG . . . . .	25
2.2.1	Unimanual and Bimanual Reach-and-Grasp Actions Can Be Decoded From Human EEG . . . . .	25
2.2.2	Case study: Unimanual and Bimanual Reach-and-Grasp Actions Can Be Decoded From Human EEG of a tetraplegic end user . . . . .	29
2.2.3	Combining frequency and time-domain EEG features for classification of self-paced reach-and-grasp actions . . . . .	41
<b>3</b>	<b>Discussion</b>	<b>44</b>
3.1	EEG-based decoding of executed grasp/hand movements . . . . .	44
3.1.1	Offline - Analysis of EEG correlates and identifying hyperparameters . . . . .	44
3.1.2	Online - Controlling a robotic arm in a simulation environment using a BCI . . . . .	46
3.1.3	EEG based decoding of unimanual and bimanual reach-and-grasp movements . . . . .	47
3.1.4	Decoding of unimanual and bimanual reach-and-attempted grasp of an tetraplegic end user . . . . .	48
3.2	Boosting decoding performance . . . . .	49

3.3	Limitations of this thesis . . . . .	51
3.3.1	On the decoding performance . . . . .	51
3.3.2	On the Suitability of MRCPs . . . . .	51
3.4	Conclusion . . . . .	52
3.5	Outlook - Towards a successful transfer to end user . . . . .	52
<b>4</b>	<b>Appendix</b>	<b>75</b>
4.1	Appendix A: Author Contributions . . . . .	75
4.2	Appendix B: Core Publications . . . . .	76
4.3	Appendix C: Publication List (peer reviewed) . . . . .	123



## List of Acronyms and Symbols

ALS	Amyotrophic lateral sclerosis
AIS	ASIA impairment score
ASIA	American Spinal Injury Association
AT	Assistive technologies
BCI	Brain-computer interface
BOLD	Blood oxygenation level dependent
BP	Bereitschaftspotential/readiness potential
CAR	Common average reference
CNS	Central nervous system
CNV	Contingent negative variation
CP	Cerebral palsy
CSP	Common spatial patterns
ECoG	Electrocorticogram
EEG	Electroencephalogram
EOG	Electrooculogram
EP	Evoked potentials
EPSP	Excitatory postsynaptic potentials
ERD/S	Event-related desynchronization/synchronization
ERP	Event-related potential
FES	Functional electrical stimulation
fNIRS	Functional near infrared spectroscopy
FNR	False negative rate
FPR	False positive rate
GFP	Global field power
ITR	Information transfer rate
LDA	Linear discriminant analysis
LED	Light emitting diode
LFP	Local field potential
LFTD	Low frequency time domain
MEG	Magnetoencephalography
MI	Motor imagery
MRC	Medical research council scale for muscle strength
MRCPP	Movement-related cortical potential
MS	Multiple sclerosis
MVI	Motor vehicle injury

SCI	Spinal cord injury
SCP	Slow cortical potential
sLDA	Shrinkage based linear discriminant analysis
SMA	Supplementary motor area
SSEP	steady-state evoked potential
SSVEP	Steady state visual evoked potential
STD	Standard deviation
SUA	Single unit activity
SVM	Support vector machine
TNR	True negative rate
TPC	Trials per condition
TPR	True positive rate
VEP	Visual evoked potential
w.r.t.	with respect to
WOI	Window of interest

# 1 Introduction

## 1.1 Severe motor impairment - causes and intervention

Chronic motor impairment has a critical impact on a person's daily life routine. Depending on the severity of the impairment, tasks and chores of daily routine, such as personal hygiene, eating and drinking or getting dressed present a serious challenge. In the worst case, these tasks cannot be performed without external help anymore. Potential reasons for motor impairment can be trauma to the spinal cord [1,2], stroke [3,4] or neuropathological conditions such as cerebral palsy (CP) [5], multiple sclerosis (MS) [6] or amyotrophic lateral sclerosis (ALS) [7,8].

Naturally, all affected persons seek intervention to regain and retain the maximum of voluntary motor control and to cushion the effect of stroke, neuropathological conditions or trauma. Stroke patients undergo an intensive period of physiotherapeutic rehabilitation to regain lost functions such as inter alia aphasia, neglect motor functions - often with notable success [9,10]. Persons suffering from neuropathological diseases such as ALS or MS attempt to delay the degradation of motor functions and cushion its effects [7,11].

Trauma to the spinal cord, also known as spinal cord injury (SCI) is another cause for motor impairment. Depending on the lesion location and the extent of the damage to the spinal cord (e.g. complete or incomplete interruption), persons may be affected by impairment of body functions from waist to feet (sacral and lumbar sections), while damage of thoracic and cervical sections can lead to severe limitations of vegetative functions as well as chronic paralysis of both, lower and upper limb functions (also known as tetraplegic condition) [1]. Trauma to the spinal cord is not uncommon: according to numbers published by the AUVA in Austria 2018, there were overall more than 4000 reported cases of persons with SCI with around 200 new incidents per year [12]. Main causes for a SCI trauma are downfalls and motor vehicle injuries (MVI) [13]. While not all SCI injuries result in severe chronic motor impairment conditions, roughly 51% of the traumatic injuries occur on cervical level (C-level), causing paraplegic or tetraplegic conditions [14].

Especially for tetraplegic persons, the impact of the motor impairment on their daily and social routine is severe: in most cases, personal assistance is required all times, limiting their independence and personal intimacy. Unsurprisingly, when asking them which of the lost body functions they would like to regain most, more than three quarters of them report their arm/hand function as their priority choice - even before dysreflexia or sexual functions [15–17].

For a small tetraplegic population, basic arm/hand function can be restored through muscle and tendon transfers within the limb. In this surgical intervention, rewiring of

still voluntary controllable muscles (and tendons) is performed to allow basic arm/hand functions such as elbow flexion or regaining functional grasping function. It has been shown that persons using this technique are able to operate their urine catheters, use cutlery or can even open bottle caps [18]. However, inclusion criteria such as lesion height (C6 and below) and MRC scales [19] of the designated muscles (4 or more) significantly limit the target population of this procedure. When surgical or physiotherapeutic interventions reach their limits, technical interventions, called assistive technologies (AT), target to assist motor impaired persons in their daily life routine.

“AT include any devices and technologies whose primary purpose is to maintain or improve an individual’s functioning and independence .” [20,21]

AT devices can be highly generalizable and based on low technology such as walking cans or crutches, but also highly individualized with high technology items such as electric wheelchairs, text-to-speech communication devices or motor neuroprosthetic devices [22,23]. One can state that the more severe the (motor) impairment of a person becomes, the higher the need for a more individualized and often complex solution gets. Some technologies are still on prototype level and have not emerged from the research lab towards broad public applicability yet. The following sections discuss one of these technologies, the so-called brain-computer interfaces (BCIs) and their applicability for severe motor impaired, which is this thesis’ main field of research.

## 1.2 Brain-computer interfaces

Brain-computer interfaces (BCIs) enable its users to interact with their environment only by thought [24]. They circumvent the central nervous system (CNS) by recording brain activity in real time and interpreting it using machine learning methods [25–27]. In this way, users are able to directly interact with their environment or control any (assistive) devices. The scientific BCI community has identified five application scenarios for BCIs [28]:

1. BCIs can replace lost functions of the CNS e.g. for communication or controlling assistive devices [29–32].
2. BCIs can restore lost functions of the CNS e.g. by circumventing the CNS to address muscle stimulation in a paralysed person using an upper limb motor neuroprosthesis [33–35].
3. BCIs can improve functions of the CNS e.g. as a tool for rehabilitation in stroke, thus generally increasing the chance of recovery of stroke patients. [36–42].
4. BCIs can enhance functions e.g. through monitoring stress or attention levels. These so called passive BCIs (pBCI) do not provide active control, rather they enhance the (e.g. environmental) conditions for optimizing the interaction between human and machine [43–46].

- BCI technology can be used as a research tool, thus providing further insights in the functionality of the brain.

Classic BCIs operate as closed loop systems, meaning that users receive direct feedback based on a specific action. Figure 1.1 depicts the head components of a typical BCI system. In the following sections, these components are further discussed.

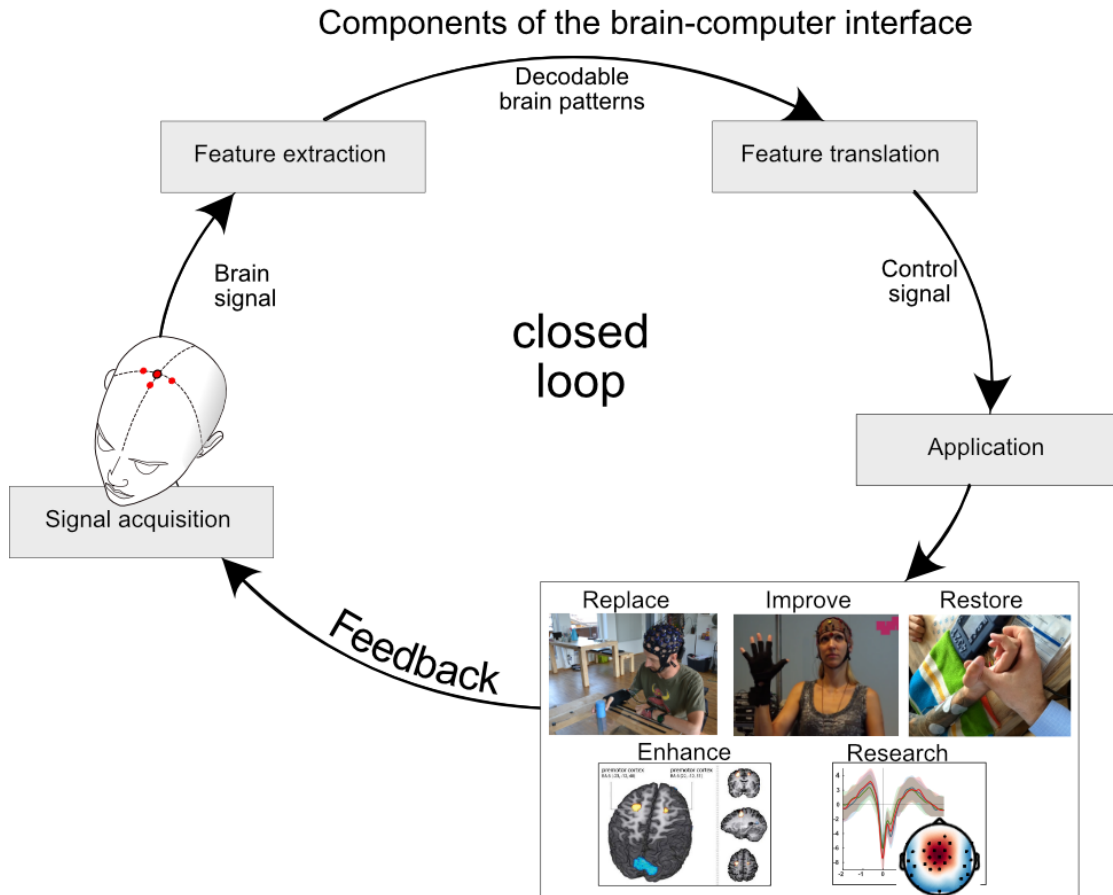


**Figure 1.1:** Closed loop structure of a standard brain computer interface. *Signal acquisition:* Brain signals can be recorded invasively or non-invasively, however, the most common approach is using electroencephalography (EEG), which is a non-invasive method. *Feature extraction:* Signals are preprocessed to optimize the ratio between useful brain patterns and noise. Depending on the mental strategy, decodable brain patterns are extracted. *Feature translation:* Machine learning methods are applied to decode the brain patterns and translate them into a command signal. *Application:* the generated control signal is processed by the application. The application gives feedback, e.g. the application performs the designated action if the command was recognized correctly, or an error notification in case of a wrong detection.

## 1.2.1 BCI signal acquisition

There are several methods available for the acquisition of brain signals, roughly dividable in non-invasive and invasive methods [47]: In general, non-invasive approaches record brain signals without penetrating the scalp of the individual, while invasive measurement methods usually rely on surgical interventions.

### 1.2.1.1 Non-invasive signals

The electroencephalogram (EEG) is one of the most commonly applied techniques to record brain signals. Developed by Hans Berger in the early 1920's, Berger recorded for the first time human EEG [48]. The EEG measures potential differences between electrodes, originating mainly from the sum of excitatory postsynaptic potentials (EPSPs) of large populations (scaling  $10^4$  to  $10^7$ ) of neurons with the same perpendicular alignment to the cortex surface. The intensity (voltage) of this effect is dependent on the alignment of the firing neurons as well as on the distance of the firing neurons to the electrode. A perpendicular alignment to the cortex surface intensifies the effect (summation), while a random alignment attenuates it (deletion). Since the voltage potential spreads by means of volume conduction, the effect decreases with the square of the distance [49–51].

EEG is widespread in medical use, it is one of the main diagnostic tools for epilepsy or sleeping disorders. It is also one of the main acquisition tools for neuroscience research due to its comparatively low cost and mobility. It provides sufficient temporal resolution for real time applications, which makes it a good candidate for time dependent analysis or real time operations for BCIs. Recent advances in EEG hardware research and miniaturization technology allowed the construction of compact and mobile EEG recording systems which can provide a dense grid of electrodes for high resolution measurements [52].

Other non-invasive measurement techniques for BCIs include inter alia magnetoencephalography (MEG), which measures changes in the magnetic field caused by electrical currents that occur in the brain [53]. These changes are measured by highly sensitive magnetometers. Though it can be successfully used as a signal acquisition tool for a BCI [54, 55], current MEG recording devices are large and stationary devices and therefore more suitable for research purposes than for mobile BCIs at end users' homes.

Contrary to EEG and MEG, which measure brain activity based on electrical activity, functional near infrared spectroscopy (fNIRS) and functional magnetic resonance imaging (fMRI) rely on metabolic changes in the brain tissue, which are caused on neuronal activity. Neuronal activity is linked to the oxygenation/deoxygenation level of the localized blood flow (neurovascular coupling), which is also called hemodynamic response or blood oxygen level dependent (BOLD) response. This response can be measured using light emitters and detectors in the near infrared level mounted on the scalp which measure the blood oxygenation level. Due to the nature of the BOLD response, measurable changes in the signal can take up to several seconds. Nevertheless, it has been shown that signal acquisition using fNIRS can successfully be applied for BCIs [56–60]. In the case of fMRI, the BOLD activity is mapped on an image of the user's brain, which is

recorded in advance using magnetic resonance imaging (MRI). The fMRI is mainly used in brain research however it is highly suitable to supplement EEG measurements [61].

### **1.2.1.2 Invasive signal acquisition**

Invasive signal acquisition requires surgical intervention and close-mesh follow up monitoring. It can be performed on different spatial scales ranging from the electrocorticogram (ECoG) over multi unit activity (MUA) using microelectrodes arrays to single unit activities (SUA) which measure neuronal spikes of a single neuron using a single microelectrode. The ECoG uses an electrode grid, usually consisting between 4 and 256 electrodes, and is placed either outside (epidural) or under (subdural) the dura mater. The ECoG electrodes record directly electrical potentials associated with brain activity from the cortex [62]. ECoG recordings are performed for advanced diagnosis of epilepsy and is considered the “gold standard” for defining epileptogenic zones. It has also been shown that ECoG is an excellent signal acquisition tool for BCIs [63–65]. From the technical point, ECoG offers significantly improved signal-to-noise ratio and is less prone to external artefacts, thus allowing the decoding of signals such as individual finger movements [66]. Even more invasive is the direct insertion of microelectrodes into the cortex to measure single activity, which are able to measure neuronal spikes [62,67] or local field potentials (LFP). Microelectrodes can also be bundled to microelectrode arrays [68] and used to measure the activity of multiple units (MUA). Recordings from microelectrode/array level benefit from extraordinary signal-to-noise ratio (SNR) and spatial resolution, allowing the decoding of movement intentions with high accuracy [69].

## **1.2.2 Modulatable brain signals**

In general, feature extraction targets to find a suitable representation of the designated brain pattern and process it for a machine learning algorithm. There exist quite a variation of different brain activities suitable as features for a BCI.

BCIs for control usually rely on the intentional control of the user. As such, users must choose to perform a mental task, with the goal of sending a message or a command each time they want to use the BCI [24]. These tasks may be an internal process such as an imagination of a mental task (e.g. imagining repetitive squeezing a stress ball, or subtraction of numbers) or elicited by an external stimulus (e.g. focusing on a blinking light source). Both examples would lead to changes in brain patterns which eventually could be detected by a BCI.

### **1.2.2.1 Event-related desynchronization/synchronization**

Brain activity contains recurrent rhythmic activity, so called oscillations. They can be quantified in frequency, power and also phase. These oscillations occur with reference to a certain event (time-locked), but with arbitrary (random) phase characteristic (non-phase-locked). Pfurtscheller et al. have shown that voluntary movement execution or the

imagination of mental tasks [70], lead to increased brain activity and a desynchronisation of neural activity when compared to baseline [71–73]. This desynchronisation is reflected by a relative decrease of power in  $\mu$  (8-13Hz) and beta band (18-24Hz), also known as event-related desynchronisation (ERD). In a similar way, a conscious state of resting entails synchronisation in brain activity and leads to a relative power increase in said bands, known as event-related synchronisation (ERS) (see Figure 1.2).

Pfurtscheller’s work is especially associated with motor imagery (MI), which describes the mental imagination of movements of hands or feet, e.g. hand opening and closing or plantar flexion/extension of both feet [74, 75]. However, also other mental imagination tasks lead to power modulations such as repetitive mental subtraction, auditory imagery (imagine singing a song) or spatial navigation [70, 76].

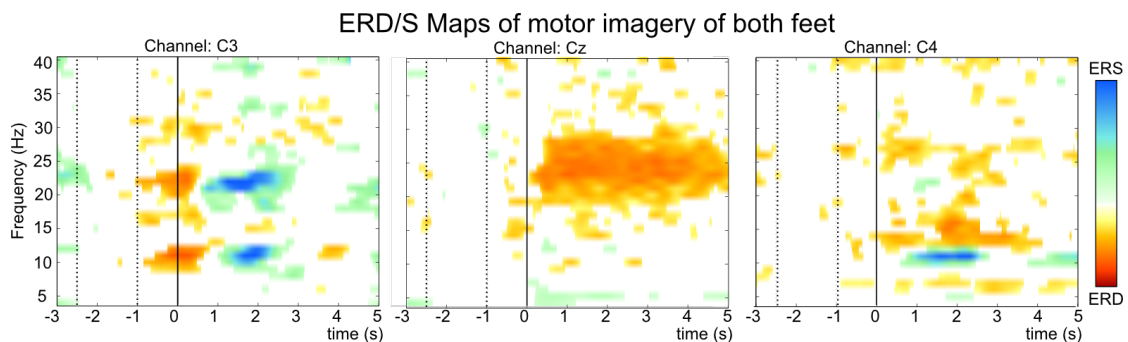


**Figure 1.2: Time-Frequency (ERD/S) Maps for mental imagery of both feet (80 trials) for channels C3, Cz and C4 (international 10/20 system).** Recording of the data followed the GRAZ-BCI paradigm [74]. The reference period for calculation was determined with 2.5 to 1 second before presenting the instructions to the participant ( $t = 0s$ ). Maps were calculated using methods as described [77]. Colored patches represent significant differences with respect to the reference period (non-parametric, t-percentile bootstrap significance test,  $\alpha = 0.05$ ). As can be seen over channel Cz, a significant desynchronisation occurs in the beta range (hot colors). Simultaneously over both channels C3 and C4 a relative power increase could be observed (ERS, cold colors). Taken and modified from Schwarz et al. 2015 [78].

MI-based BCIs are widely known and have been used to establish communication [79] and control of operate assistive devices [33, 35, 80]. There is general agreement that the use of MI-based BCIs is a skill, which means the user must be properly trained to achieve successful BCI control. If the user cannot correctly perform the desired mental commands, even the most advanced signal processing algorithm could not properly identify them. Studies such as performed by Müller-Putz and colleagues have shown, that an extended training period (in this case 53 consecutive training sessions) could lead to stable BCI control higher than 90% [80]. Nevertheless, other studies have also shown that about 15-30% of the population can not operate a MI-based BCI [81].



### 1.2.2.2 Event-related potentials (ERP)

Contrary to the oscillation based brain activities, ERPs are not only time, but also the phase-locked responses in brain activity. They describe transient reflections of a sensory, cognitive or motor process in the brain [82, 83].

Depending on the stimuli (e.g. internally driven, or excited externally by a paradigm), ERPs consist of a series of positive and negative amplitude deflections over time which are categorized based on the sign and the latency with respect to the stimulus, e.g. a N100 means a negative deflection 100ms after the stimulus presentation [83] (see Figure 1.3).

ERPs can be successfully used for BCI control [24], since features based on the positive and negative amplitude deflections, are considered robust and stable at the user level. Moreover, due to the time and phase locked property of the signal, each elicited potential can be reliably attributed to a certain stimulus. The most prominent BCI use of ERPs are certainly P300 BCIs which utilizes external stimuli to elicit discriminable brain activity. A common strategy for P300 based BCIs is to utilize an oddball paradigm: Users are instructed to concentrate on a single stimulus (target stimulus) in a series of stimuli (non-target stimulus) presented with high pace, whereas the ratio of target to non-target stimulus is about 20% targets to 80% non-targets. In contrast to the non-target stimuli, whenever the target stimulus is presented to the user, a positive deflection around 300ms after stimulus presentation can be observed, which is pronounced strongest in central parietal regions (see Figure 1.3 [84]).

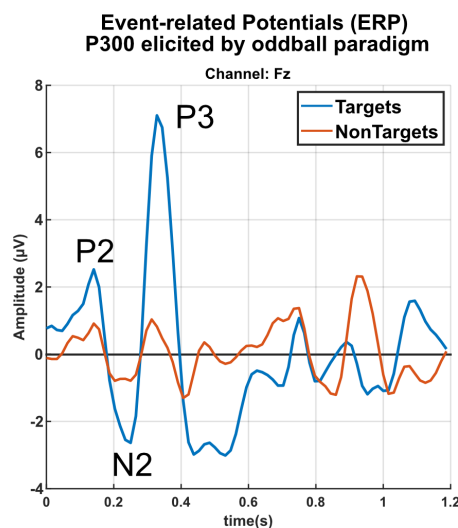


**Figure 1.3: Event-related potentials: P300.** Average of 400 target and 1200 non-target trials from one participant operating a matrix speller (as described in [85]). Singular components of the ERP such as the P2, N2 and N4 are visible. The P300 elicited by the oddball paradigm is significantly larger in target than in non-target trials.

This difference between target and non-target stimuli can eventually be decoded by a classification algorithm [27]. P300 BCIs were initially designed for communication

purposes [85–88], e.g. between a completely paralyzed person and its environment. Recent advances however have shown that this approach would also allow severely motor impaired persons tasks beyond communication - e.g. regaining the ability for painting or composing music [30, 89].

ERPs also occur as a reaction when persons make or witness an error [90–92]. The so-called error-related potential (Errp) is localized over fronto/central and parietal central regions and consists of two components: the error-related negativity which describes a negative deflection 50-100 ms after the perceived error and the error-related positivity which occurs directly afterwards. The morphology is dependent on the erroneous task/perceived error [93, 94]. In the context of BCI research, studies have shown that Errps can be exploited to correct BCI based misclassifications [95–100] by detection of the occurring Errp and thus could potentially contribute to BCI stability.

The contingent negative variation (CNV) represents another phenomenon in the context of ERPs: it describes a negative deflection elicited by a warning stimulus (e.g. “Be Ready!”) in preparation of an imperative stimulus (“GO!”). It has been shown that voluntary modulation of these slow cortical potentials can be trained [101] and also used for BCIs [102].

ERPs also reflect motor processes in the brain. This type of ERPs are commonly known as movement-related cortical potentials (MRCPs) and can manifest not only after a certain event, but also before and during the event, e.g. the movement onset of the hand [82, 103] [104–107]. MRCPs contain a number of sub components, whereas the Bereitschaftspotential (BP) is probably the most known and best investigated subcomponent of MRCPs. It was discovered in the early 1960ies by Prof. Hans Kornhuber and his doctoral student at that time, Lüder Deecke who investigated voluntary hand and feet movements using EEG. They found a *”langsam ansteigendes oberflächen-negatives Hirnpotential von 10-15 $\mu$ V”*, which they called the Bereitschaftspotential [105,106]. Pre-movement components of the BP can already be found up to 2 s before the movement onset (early BP component) over supplementary motor areas (SMA) and are characterized as a negative deflection in EEG. Around 0.5 - 0.25 s before the movement onset, this deflection becomes a much steeper negative gradient (late BP component) and is strongest over central/contra lateral premotor and primary motor areas. Maximum peak negativity occurs around the movement onset (BP) and is strongest over the central motor cortex. Measuring the exact timing of the movement onset is not trivial and often introduces a systematic measuring error (e.g. a delay). Thereafter positive deflections occur (e.g. refferent potential around 0.25 -0.3 s after movement onset, see Figure 1.4) before returning the EEG back to baseline [103,108]. A detailed review on MRCP components can be found in [103].

Studies have shown that different movement tasks elicit changes in the morphology of MRCPs, even before the designated movement is executed [110–112] and as well as information about movement force and speed [108,113].

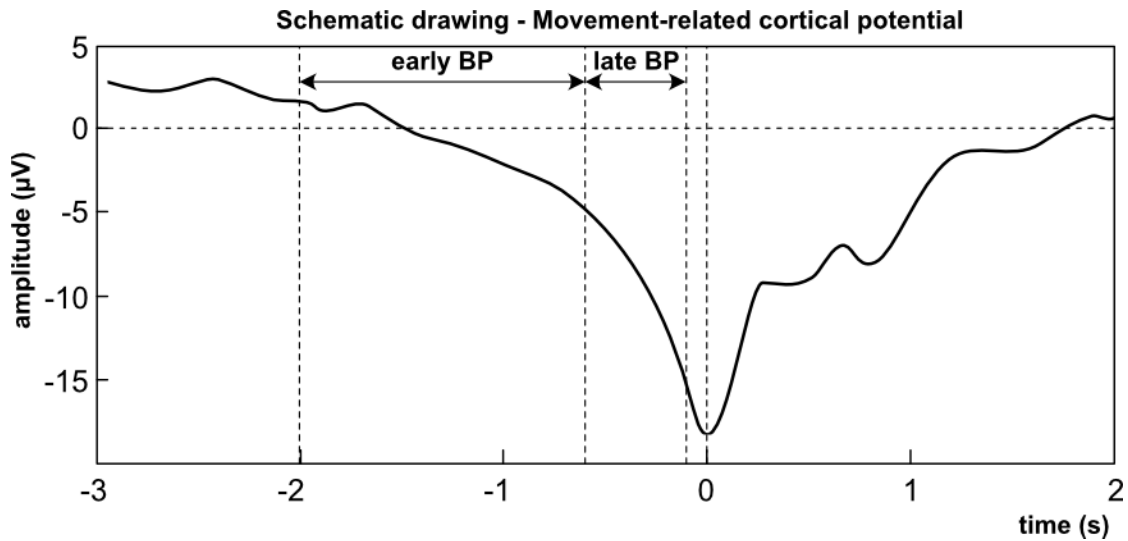


**Figure 1.4: Movement-related cortical potentials (schematic drawing).** Around 2s before the actual movement onset a negative deflection can already be observed (early BP). This deflection increases becomes a much steeper gradient around 0.5 to 0.25s before the movement onset (late BP). The strong negative deflection at time = 0s (movement onset) represents the Bereitschaftspotential. [108]. Taken and modified from [109].

### 1.2.2.3 Slow Cortical potentials (SCP)

Slow cortical potentials (SCPs) are positive or negative electrical shifts in the cortical activity. They can last from several hundred milliseconds up to several seconds with regards to the eliciting event [114]. Importantly, they can be externally triggered or self-triggered. While negative deflections are assumed to occur in states of behavioural or cognitive preparation [115], positive deflections indicate a reduction in cortical activity, e.g. during behavioural inhibition [114] [116].

### 1.2.2.4 Steady-state evoked potentials

When presenting a stimulus with a steady frequency, a sinusoid brain response is elicited with the same frequency as the stimulus frequency, called steady-state evoked potential (SSEP) [117]. This brain feature is elicited by visual, auditory and somatosensory stimuli and thus can be exploited for a BCI, e.g.: When presenting users three lights with different flickering frequencies, they can focus on a specific light (target) which elicits a measurable, oscillatory brain response with the target frequency. It has already been shown that SSEPs can be used to drive BCIs using visual (SSVEP) [118–120], auditory (SSAEP) [121–123] or somatosensory stimuli [124–126]. However this type of BCIs strictly rely on an external stimulus source thus the control signal cannot be initiated internally.

### 1.2.3 BCI feature translation

The main goal of any BCI system is to translate brain patterns (e.g. as described in the previous section) to control commands with a minimum of erroneous translations. The most popular approach for this task is the use of classification algorithms [27].

The classification algorithm is a function which attempts to label each incoming observation into a set of categories. In a supervised training approach, the basis for identifying the correct label is a training data set of observations, where the categories are already known [25, 127].

In terms of BCI use, an observation would be features such as amplitude or power values of brain pattern generated by a single action of a user, whereas the category indicates the type of action, e.g. a reach-and-grasp action towards a glass. Naturally there could be more categories which are also called classes or conditions (e.g. reach-and-grasp of a spoon, or a no-movement condition). Hence, the classification algorithm would attempt to identify the reach-and-grasp action as such and would attempt to categorize correctly as a reach-and-grasp action of a glass.

The performance of a classification algorithm is strongly dependent on the suitability of the algorithm to interpret the provided features of an observation as well as the number and the quality of the observations of the training set. While the first can be tuned using a priori knowledge about the data and its provided features, the latter is prone to unfathomable trade offs and practical necessities.

In general, EEG-based BCI experiments lack training data. The main reason for this is that training data is usually not transferred or accumulated through different BCI sessions due to the significant decrease in signal to noise ratio by changes in sensor position and the conducting impedance between sensors and skin (reattaching the cap leads inevitably to EEG nonstationarities). Additionally, one needs to keep in mind that for training classification algorithms involving more than one condition (which is usually the case) hundreds of observations requiring an action (e.g. reaching and grasping a glass) from the user. Hence only the minimum amount of training data is recorded per session to avoid user fatigue and decrease in user compliance. This fact further limits the selection of classification algorithms to a set, capable of dealing with comparatively small amounts of training data. Most popular classification methods are still the linear discriminant analysis (LDA) [128, 129], support vector machines (SVM) [130] or nonlinear, decision tree based algorithms such as random forests [131–133]. Lotte and colleagues provided a review of classification algorithms currently used for BCIs [27].

### 1.2.4 Application interface and application

The application interface transforms the output of the classification stage to a suitable control signal for the designated application. In the best case, each BCI control command maps to one unique application command. For instance, a single BCI command can operate a toggle switch [134–137]. Whereas a direct control modality is desired, the number of conditions a BCI is trained on is usually limited (each condition needs their own set of training data).

However, indirect control modalities allow access to a large set of application commands with comparatively few or even only one BCI command available. Application commands are organized in subsets, which can be selected by navigating through individual layers of subsets. Though the selection process for an application command takes longer, this trade-off is made deliberately in exchange for limited BCI control commands. Scanning paradigms are certainly the most commonly used indirect control strategies used for BCIs (which can actually be operated by a toggle 1 condition switch) [31,138,139]: A scanning line sequentially highlights each command for a fixed time. When the scanning line reaches the desired command, the user can select it with the help of the BCI (e.g. MI of both feet) and eventually the command is selected. Naturally this selection procedure strongly relies on BCI control with high accuracy. To further support stable BCI control performance, Scherer et al. introduced evidence accumulation to a row-column based indirect scanning procedure. Here the designated application command had to be selected 2 out of 3 times to be ultimately acknowledged as command. Though this puts further strains on the time needed to make a selection (and eventually the information transfer rate (ITR)), they could achieve stable BCI control [140–142].

### **1.2.5 Closed loop BCI feedback**

When humans interact with their environment, they usually receive feedback. For instance, when grasping a glass of water, there is a vast sensoric spectrum of impressions to deal with, like the surface structure of the glass itself, its temperature or the overall weight just to name a few.

Per definition, a BCI operates in a manner of closed loop, which means that users need to receive feedback based on their actions [24]. In order to provide meaningful feedback, it has to be in context to the designated action. While the first is a technical issue which has to be addressed, the human mind is able to adapt to the latter, e.g. when reversing a car and one has no direct line of sight, a reversing assistant gives auditory feedback with increasing frequency the smaller the distance to an obstacle is. Here the human mind adapts to the lack of visual feedback and accepts feedback based on auditory information. In any case, the type of feedback presentation for BCIs strongly relies on the application. It can be given visually [143–145], auditory [121,146] even through tactile feedback [147–151]. However, also combinations of different feedback modalities are possible. For instance, in case of a BCI driven upper limb neuroprosthesis, it is quite conceivable that users receive feedback by observing his enhanced arm grasping an object while they receive feedback of the grasp force via vibrotactile feedback presented on a shoulder actuator [152].

## **1.3 Non-invasive BCIs for motor control: State-of-the-art**

Besides communication, restoring voluntary motor control for humans with paralyzed limbs is one of the most prominent use cases of a BCI [28]. The BCI hereby acts as a bridge to overcome the incapacitated part of the central nervous system (e.g. a lesion

at the cervical level of the spinal cord): it attempts to decode the movement intention of the user and eventually generates a control signal for an assistive device such as a prosthesis, an orthosis or an upper limb motor neuroprostheses. Motor neuroprostheses [153, 154] are generally based on the principle of functional electrical stimulation (FES): electrodes which can either be placed on the skin surface or implanted on muscle motor points apply short constant-current pulses which depolarize the nerve and elicit an action potential. This leads to contractions of still innervated muscle fibres. Depending on the electrode placement, various upper limb/hand movements as well as basic grasps can be formed [155–157].

Over the last two decades a number of BCI groups have made attempts to realize BCIs for motor control. In another proof-of-concept study including one tetraplegic participant (lesion height C5), Heasman et al. achieved BCI control of an implanted neuroprosthesis via toggle switch [158]. The participant was able to voluntarily modulate his occipital alpha rhythm (8-13 Hz) by opening and closing his eyes, which eventually triggered the switch to either open or close the hand via neuroprosthesis. In a series of 13 trials, the tetraplegic end user completed 10 trials successfully.

Notably, the group of Pfurtscheller and especially Müller-Putz have been continuously pursuing BCIs for motor control over the years. Their initial proof-of-concept study involved BCI control of an electrically driven hand orthosis (left hand) which supported a tetraplegic end user (lesion height C4) to open and close the hand [80]. Their single study participant performed different kinds of motor imagery (MI) tasks to modulate his brain patterns. These MI tasks led to power changes especially in the alpha (8-12 Hz) and beta band (18-30 Hz) and could eventually be classified using a linear discriminant analysis classifier (LDA). Over the course of 53 experimental sessions (160 trials per condition (TPC) each), they identified mental strategies with the most discriminable features, which were ultimately the MI of both feet versus right hand. Eventually the study participant achieved a stable performance of 95%. Relying on the same study participant as well as the same feature space for BCI control, they could show the feasibility of their so called MI-BCI also when using a FES-based upper limb neuroprosthesis (left hand) [35]. Furthermore, the group could show that the MI-BCI is also applicable when using an invasive upper limb motor neuroprosthesis such as the FreeHand<sup>TM</sup> system [159]. In three days training, the study participant was able to switch between different neuroprosthesis modes (e.g. switching between palmar and lateral grasp) using the BCI. In this case, the study participant performed motor imagery of the left hand to switch between grasping patterns of the neuroprosthesis, which was implanted in the right hand [33].

In a later study, the Müller-Putz et al. investigated the feasibility of SSVEP based BCI control of a two axis electrical lower arm prosthesis [160]. The prosthesis had attached four LEDs which flickered with different frequencies (6,7,8 and 13 Hz). Each study participant (n=4) had to perform a series of commands (e.g. rotate the wrist) which were triggered by focusing on the designated flickering light which could be decoded from the EEG. Study results indicated that for this four condition approach, classification accuracy ranged between 44% and 88% (160 TPC, probability threshold 25%). A follow up

study by Ortner et al. in 6 healthy participants applied the concept on a hand orthosis with comparable results [161].

One of the major problems of using BCIs for motor control was the limited number of derived control signals for actual control. Müller-Putz and colleagues eventually could show in a cohort of able bodied participants that with a temporal coding approach, the control modalities of their initially 2 class MI-BCI could be increased. With the additional temporal coding, e.g. short MI of right hand movements vs long MI of right hand movements, their system could provide enough control modalities to successfully operate both hand (open/close) and elbow (flexion/extension) control [162].

In a first approach to provide a more intuitive form of control for the user, Tavella et al. provided a proof-of-concept study in healthy participants (n=4): their asynchronous MI-BCI approach involved MI of the hand to which the neuroprosthesis was attached to. Previous studies refrained from this approach for the fear of incorporating artefacts in their analysis or introducing a confounder due to feedback observation (the end user performs the MI of the hand, which then performs the movement and the observation has a potential effect on the MI) [163]. They could show that their study participants were able to grab a pen and write words or short sentences incorporating only a comparatively small set of erroneous attempts.

In a later attempt Rohm and Kreilinger picked up the concept of the hybrid BCI [164,165] to control an hybrid neuroprosthesis via both MI-BCI based switch and a shoulder operated joystick [166,167]. This study also included the temporal coding approach described in [162]. As an additional control modality, the shoulder operated joystick allowed analogue control of elbow flexion/extension as well opening/closing of the hand. The study was conducted over a whole year and included 415 single BCI sessions. Unfortunately, the authors could not determine any improvements in performance as could be shown by [80], rather their participant scored on average around 70% accuracy with the BCI.

## **1.4 Current limitations in BCIs control modalities for motor control**

The previous section has shown the development of BCIs intended for motor control with an intentional focus on the action/control strategy of the user. In general, one can say that these strategies were rather abstract and did not often have any intuitive association to the intended movement at all. Pfurtscheller and Müller-Putz used in their proof-of-concept study MI of foot movement to control the participants' neuroprosthesis [80]. In follow up studies, Müller-Putz included the opposite hand to allow BCI control the FreeHand<sup>TM</sup> system [33], or required even staring at flickering lights to elicit a control command [160]. Some approaches required the closing of both eyes to induce changes in alpha rhythm, which is not only unpractical in daily life, but can potentially lead to dangerous situations [158].

Although initial attempts by Tavella et. al. were made to adjust the control modality to a more natural form by using MI of the same hand as a toggle switch, it is still a form of repetitive imagination of a task to elicit a brain pattern which can be decoded [163]. In a

real application scenario, these control modalities are too abstract and counterintuitive to allow meaningful control of an assistive device e.g. a neuroprosthesis. In a potential hazardous situation, where people rather react by instinct, this might even lead to reduced control performance.

Therefore, decisive investigations towards a more natural form of BCI based upper limb/hand motor control are necessary. Moreover, an approximation towards natural grasping as it is performed by non-impaired persons is desirable. A future control strategy ideally consists of one non-repetitive task which is similar to the task that has to be performed by the assistive device. In case of upper limb/hand movements, this inevitably leads to the use of different grasps as control modalities. For instance, a tetraplegic end user attempts or imagines a palmar grasp with the right hand, the BCI correctly decodes this intention and instructs the neuroprosthesis (attached also on the right hand) to form a palmar grasp.

The human hand has 27 degrees of freedom, hence a large amount of different hand gestures and grasps are possible to interact with the environment. However, in case of controlling assistive devices such as an upper limb motor neuroprosthesis, this range is limited to the capabilities of the device and its potential control interface. A selection for the most used and practical grasping options is required. Most actions of daily life can be handled using palmar, pincer and lateral grasps [168], hence a restriction to these grasp types would seem feasible.

On close inspection however, most of the time it is not enough to include only grasping. In most cases, a grasp towards an object implies a reaching movement. Prehension experiments initiated by Jeannerod and colleagues show that there is a direct synergy between reaching and grasping [169–171] (see for a review [172]): they could quantify that the hand already preshapes during the reaching movement towards the object. Here, the maximum grip aperture between thumb and index finger (tips) occurs around 70% of movement completion. This indicates not only that a substantial part of the grasping procedure already happens during the reaching movement: From a neurophysiological aspect, grasping information might be already encoded during preparation and reaching movement.

Nevertheless, it still remains to be seen whether neural correlates for grasp or reach-and-grasp actions can be found and decoded from human EEG. So far, invasive studies using ECoG measurements performed by Pistohl and colleagues indicate that there is discriminative information for detection of grasps and their classification in amplitude modulations of frequencies below 6 Hz [173–175]. This frequency range coincides to the full extent with the low frequency time domain (LFTD), where MRCPs are prominent [103]. EEG studies investigating LFTD could already confirm that continuous decoding of reaching movements is possible [176–178], using center out tasks. Recently, Agashe and colleagues showed that EEG based LFTD signals of various reach-and-grasp hold synergies with their designated movement kinematics. They report correlation coefficients ( $r$ ) of 0.3 to 0.6 between the predicted movement kinematics extracted from the LFTD and the actual movement kinematics [111]. Furthermore, initial investigations of Jochumsen et al. could show that MRCPs hold information about the force and the



speed when performing a palmar grasp [113].

These studies indicate that the LFTD and the occurring MRCPs potentially could hold discriminative information to decode grasping or reach-and-grasping actions from human EEG. Hence, this thesis targets further investigations on the EEG based decoding of grasp and reach-and-grasp actions from MRCPs.

## 1.5 Aims of this thesis

Summarizing the current limitations, BCIs for upper limb motor control rely on rather abstract control modalities, which are often counterintuitive and do not reflect the actual task at hand. A more natural form of control is required, ideally an approximation towards natural grasping, as it is performed by non-impaired persons. Hence the main goals of this thesis are to

1. Identify EEG correlates which are associated with natural grasp and reach-and-grasp actions as they are performed in daily life. Recent studies suggest that LFTD and MRCPs potentially hold discriminable information for detection and decoding of grasps and reach-and-grasp actions. Hence the focus of the investigations presented in this thesis will be on examining EEG correlates of this frequency range.
2. Investigate whether these EEG correlates can be successfully decoded on a single trial basis and
3. Assess their feasibility in a noninvasive online BCI.

## 1.6 Organization of this thesis

So far, **Chapter 1, Introduction**, has provided an overview of the BCI research field. It gives an overview over the most relevant neurophysiological signals and defines the components of a standard BCI. Furthermore it provides an outline of the current state-of-the-art BCIs used for (upper limb/hand) motor control and shows the limitation of the current BCI control modalities. In conclusion, the section identifies and defines the goals for this thesis. **Chapter 2, Methodology and results**, summarizes all relevant experiments and studies performed in context of this thesis. **Chapter 3, Discussion**, discusses the findings of this thesis and compares it to other work in the literature. Furthermore it critically assesses its limitations and explains future prospects to overcome these limitations. **Chapter 4, Appendix A**, lists the author contributions to the included publications. **Appendix B** holds all publications which were conducted in the course of this thesis. **Appendix C** provides an overview of all publications of the author of this thesis.

## 2 Methodology and results

The following chapter summarizes all studies and methodologies conducted with respect to this thesis. The underlying journal and conference publications can be found in Chapter 4, Appendix. Figure 2.1 depicts the findings within the timeline of the thesis.

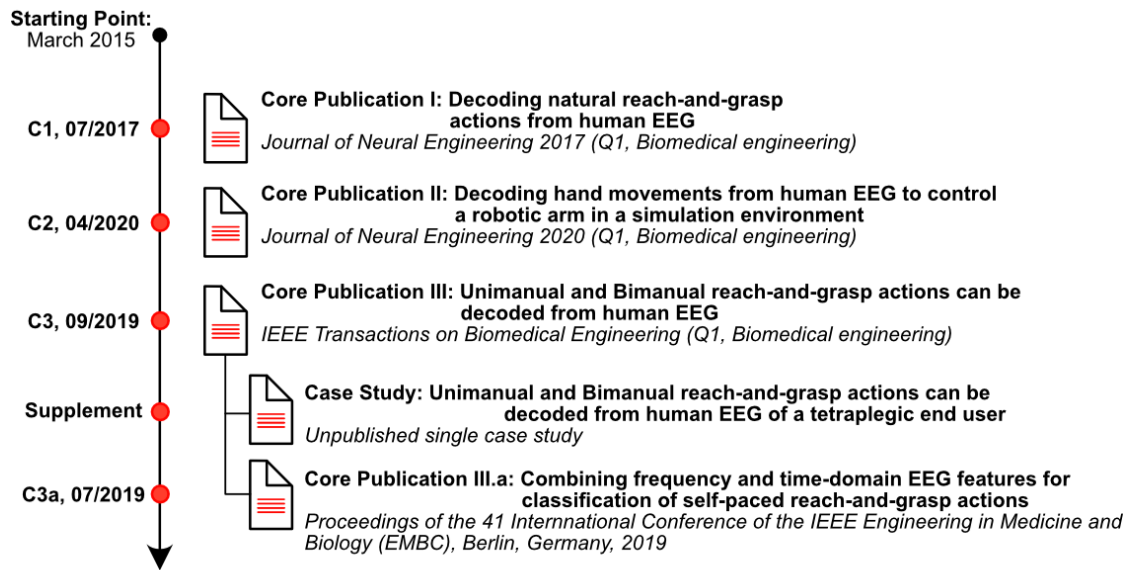


**Figure 2.1: Core publication overview of the thesis.** Investigations have already started with the start of the PhD in March 2015. Studies for Core publications 2 and 3 were done in parallel.

## 2.1 Decoding reach and reach-and-grasp actions from human EEG

### 2.1.1 Decoding natural reach-and-grasp actions from human EEG

Schwarz Andreas, Ofner Patrick, Pereira Joana, Sburlea Andreea and Gernot Müller-Putz, “Decoding natural reach-and-grasp actions from human EEG.”, *Journal of Neural Engineering*, Feb 2018; 15(1):016005, <https://doi.org/10.1088/1741-2552/aa8911>, [179]

#### 2.1.1.1 Summary

This study analyzed whether EEG correlates of executed reach-and-grasp actions could be found and discriminated from each other and from a no-movement condition. Following the practical approach described by Popovic et al [168], the conditions investigated were restrained to palmar, pincer and lateral grasp on objects of daily life (see Figure 2.2) as well as a no-movement condition for a comparative baseline. Following a cue-guided experiment (see Figure 2.3), 15 abled participants performed 72 reach-and-grasp actions using palmar, pincer and lateral grasps each. Additionally 72 trials were recorded where they performed no-movement at all.

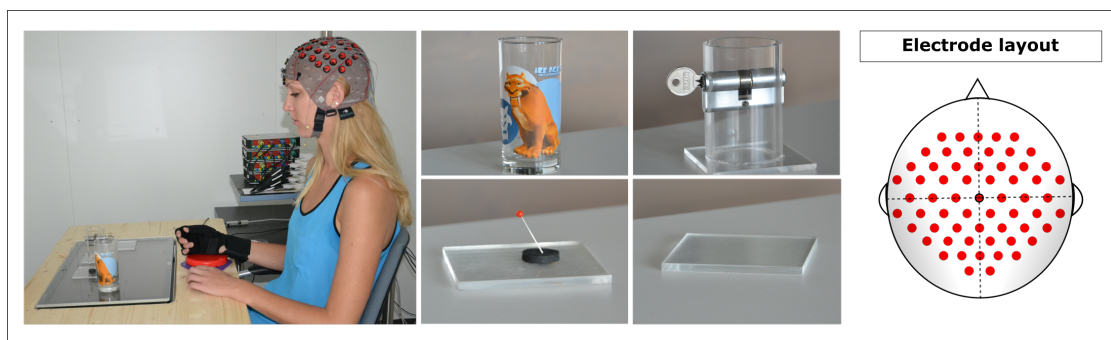


**Figure 2.2: Experimental setup, Left:** Participant is seated on the table and focuses her gaze on a fixation cross presented on the in-built screen. **Center:** Objects for grasping (i) a glass, a key, a needle, and an empty plexiglass retainer which represents the no grasp condition. **Right:** 61 electrodes were used to record EEG over frontal, central and parietal regions using a 5 percent grid.

#### 2.1.1.2 Contribution to the PhD thesis

This initial study laid the foundation for all upcoming investigations within this PhD thesis. We could successfully identify EEG correlates in the LFTD (0.3-3 Hz), namely MRCPs, which represented the executed palmar, pincer and lateral reach-and-grasp actions. The MRCPs were characterized by a strong negative deflection at the movement onset (Bereitschaftspotential, [108]) followed by a refferent positive potential around 300ms. Thereafter, a second positive deflection occurred before returning to baseline (see

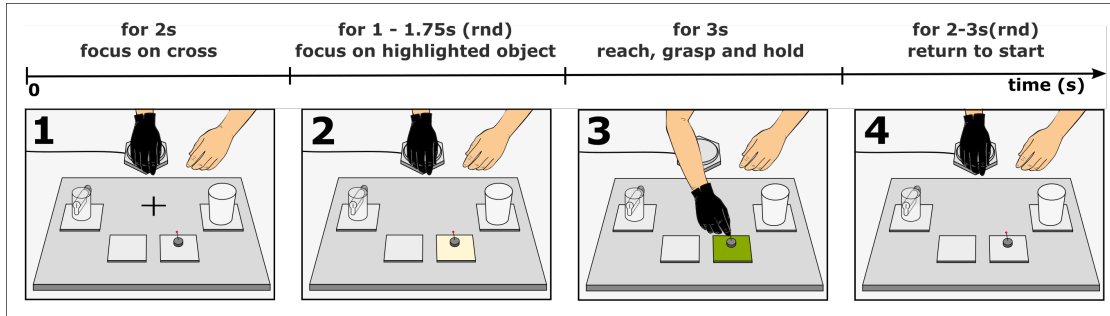


**Figure 2.3: Experimental paradigm, sequential view.** At trial start participants focus their gaze on the cross shown on the screen (1). After 2 seconds, one of the four objects is highlighted in white. Participants are instructed to focus on the white tile (3). Once the tile turned green (variable time), participants immediately reached-and-grasped for the designated object until the green highlighting vanished. Thereafter the returned to starting position (4) and the inter trial interval started (2-3 seconds).

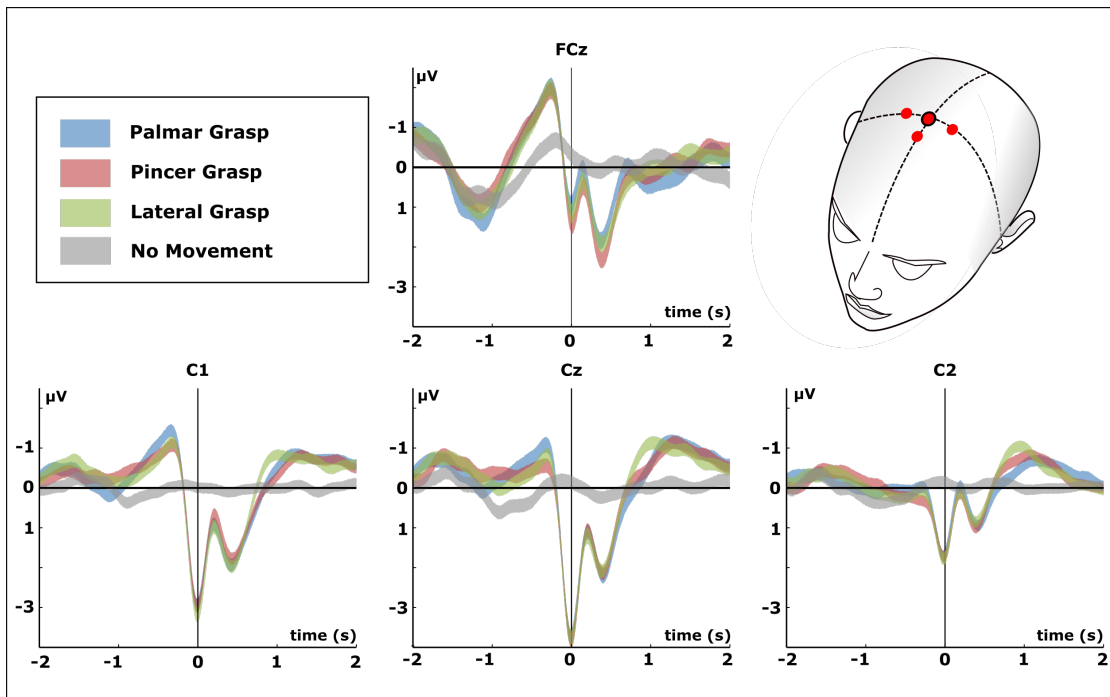


**Figure 2.4: Movement-related cortical potentials (MRCPs)** of cue-guided reach-and-grasp actions (colored) and the no-movement condition (grey) for channels FCz, C1, Cz and C2 (bidirectional filtered, 4th order, 0.3-3 Hz). The shaded areas represent the 95% confidence interval, calculated using non-parametric t-percentile bootstrap testing ( $\alpha = 0.05$ ).

Figure 2.4). We could show that on group level, the correlates of the movement conditions were significantly different before and during the reach-and-grasp actions to the movement condition. Additionally, significant differences between movement conditions could be found in the first second after movement onset.

The goal of this study was not only to assess the decodability of the investigated conditions, but also to determine tunable parameters to boost decoding accuracy. In this work we could show that on average, the highest decoding accuracy could be reached by extracting features from the first second after the movement onset. With respect to the performed behavioural analysis, this period fully reflects the reaching and preshaping of the hand before the grasp is finished. Binary decoding of reach-and-grasps versus the no-movement conditions yielded on average around 93.5% STD +/- 4.2%. Even for participants with movement versus movement decoding accuracies close to chance level, movement versus rest achieved around 85%. Binary movement versus movement decoding, e.g. lateral versus palmar grasp, yielded on a grand average basis of 72.4% STD +/- 5.8%.

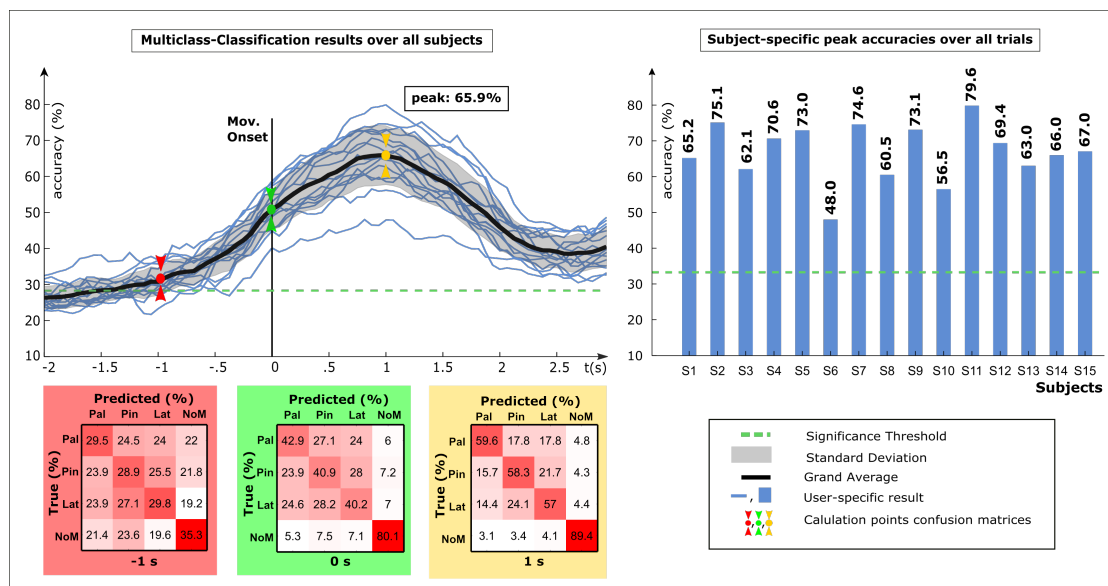


**Figure 2.5: Offline cross-validated (10x5) multiclass classification performance using a 1000ms feature window.** **Left:** Grand average over all study participants. The colored markers represent calculation points for underlying confusion matrices. The confusion matrices underwent row-wise normalization. **Right:** Participant specific peak accuracy is higher in general than the global grand average due to participant specific time variation in reaching peak accuracy.

In a multiclass decoding setting, where we included all three reach-and-grasp conditions as well as the no movement conditions, we could reach 65.9% STD +/- 8.1 % (see Figure 2.5). We also investigated how the performance changed when reducing the electrode setup to a smaller configuration. Our analysis showed that when reducing the electrode grid from 61 channels distributed over the whole scalp to only 25 channels

located primarily over sensorimotor areas, the previously mentioned multiclass performance dropped only by less than 3 %.

This suggested for future endeavours including e.g. a motor impaired end user population that a trade-off between performance and electrode density and hereby mobility is well within reach.

## 2.1.2 Decoding hand movements from human EEG to control a robotic arm in a simulation environment

Schwarz Andreas, Maria Katharina Höller, Joana Pereira and Gernot Müller-Putz, “Decoding hand movements from human EEG to control a robotic arm in a simulation environment.”, *Journal of Neural Engineering*, 17(3):030610, 2020. <https://doi.org/10.1088/1741-2552/ab882e>, [180]

### 2.1.2.1 Summary

In this study we investigated whether EEG-based decoding of two different grasps and one wrist supination condition can be done in real time by a BCI. Fifteen abled bodied participants took part in the experiment. They were immersed in a desktop based simulation environment and gained control of the robotic arm of an avatar in a wheelchair. The avatar was seated in front of a desk and had to perform actions of daily life, e.g. grasping a glass of water (palmar grasp) or a spoon (lateral grasp) or turning on a big radio knob on a vintage radio (wrist supination). Although the simulation environment mimicked a setting of daily life, the paradigm was implemented in a cue-based way: The robotic arm of the avatar reached towards the interacting object, but stopped shortly before it. The study participants were asked to finish the designated task, e.g. in case of the glass, they had to execute a palmar grasp, in case of the spoon, a lateral grasp (see Figure 2.6).

Based on the parameters investigated in section 2.1.1, we defined a calibration phase where we recorded 60 TPC for each condition without giving feedback. Thereafter, a regularized linear discriminant classifier [129] was trained on the best performing time point within the trial with respect to the real movement onset. In the subsequent evaluation phase (45 TPC), participants controlled a robotic arm and interacted with the virtual objects in case of a correct classification. In case of an incorrect classification, the virtual robotic arm performed a shaking movement on the horizontal plane.

### 2.1.2.2 Contribution to the PhD thesis

We could show for the first time in a large population of gender balanced, abled participants (n=15) that executed, single hand/wrist movements could be successfully decoded online from EEG using features extracted from the LFTD. In the online experiment, 14 out of 15 participants scored significantly higher than chance with 48% of correctly classified movement trials (3 condition scenario, adjusted chance level 40%, [181, 182] (see Figure 2.7).

Underlying EEG correlates of the initial calibration data in the LFTD showed significant differences between conditions in the first 0.5 s after the movement onset. These differences were found mainly over sensorimotor areas contralateral to the executing hand at channel locations C1 and C3. Importantly, we could show that these differences were retained to a large extent in the evaluation phase, where participants received feedback based on their actions (see Figure 2.8).

## Simulation Environment, Paradigm & Experimental Timeline

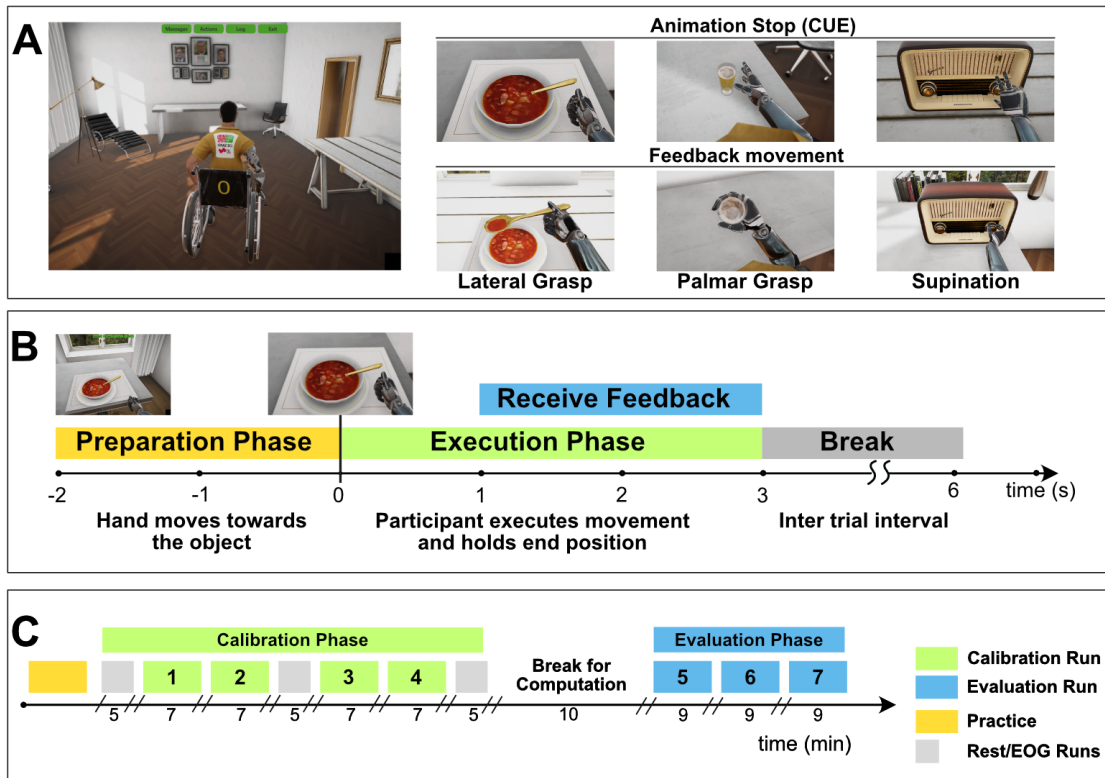


**Figure 2.6: Simulation environment, paradigm and experimental setup.** (A) Study participants were immersed in a desktop-based simulation environment and were asked to interact with three different objects of daily life via a motor impaired avatar with a robotic arm. At the start of each trial, the robotic arm of the avatar reached for an object, but stopped shortly before interacting with it. (B) The study participants were instructed to complete the movement. In case of a correct classification, the robotic hand interacted with the objects on the table (evaluation phase only), e.g the robotic hand turned on the vintage radio. Thereafter we introduced a break for 2 to 3 seconds (random length). (C) the experiment was subdivided in the calibration phase for data gathering (4 runs á 15 TPC, no feedback) and the evaluation phase (3 runs á 15 TPC).



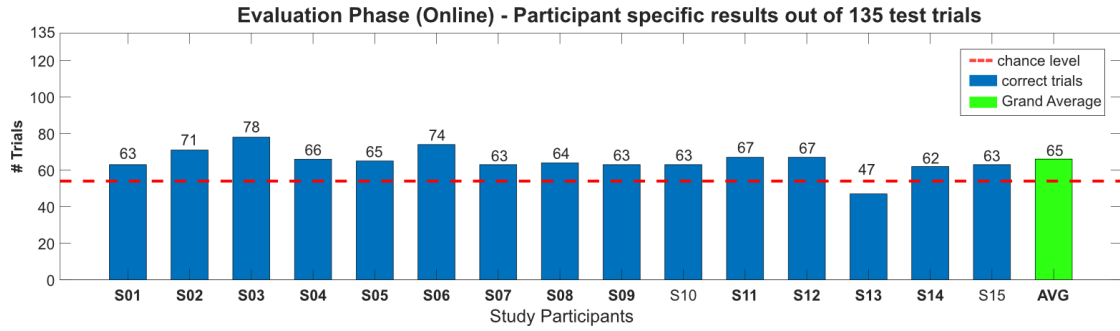


**Figure 2.7: Participant-specific performance of the online evaluation.** In total 135 correct trials could be achieved. To score significantly higher than chance, 54 trials out of 135 trials had to be correctly classified (alpha = 0.05, adjusted Wald interval [181, 182]).

In this study we applied a novel paradigm to instruct and interact with the users. The desktop based simulation environment not only allowed us to recreate daily life situations, e.g. grasping a glass or a spoon. Moreover, we designed the simulation environment in a way so that we could avoid brisk cue presentation and its inevitably accompanying elicited visually evoked potentials (VEP). This is of particular importance since they can potentially mask and contaminate motor potentials.

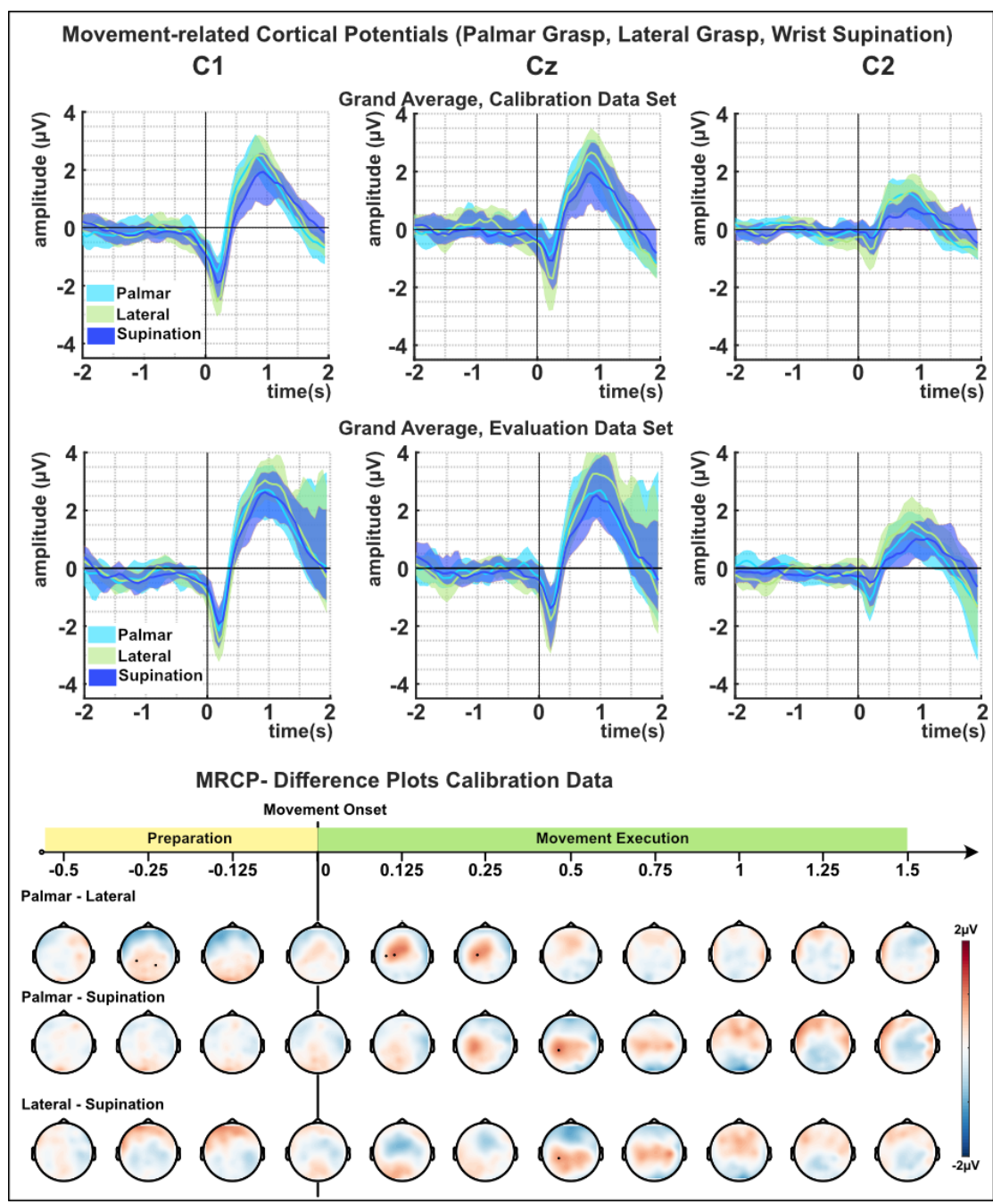


**Figure 2.8: Movement related cortical potentials (causal filtered, 4th order, 0.3-3Hz).** Top and central row show the grand average and the bootstrapped confidence interval ( $\alpha = 0.05$ ) for all conditions for channels C1, Cz and C2 (0.3-3Hz, causally filtered). Time = 0s represents the movement onset. The bottom figure depicts differences between the conditions on a topographical scale, on a grand average basis. Black dots on the scalp represent channels which showed significant differences between conditions (calculated using non-parametric paired sample two-tailed permutation tests based on t-statistics,  $\alpha = 0.05$ ).

## 2.2 Decoding unimanual and bimanual reach-and-grasp actions from human EEG

### 2.2.1 Unimanual and Bimanual Reach-and-Grasp Actions Can Be Decoded From Human EEG

Schwarz Andreas, Pereira Joana, Kobler Reinmar, Gernot Müller-Putz, “Unimanual and Bimanual Reach-and-Grasp Actions Can Be Decoded From Human EEG.”, in *IEEE Transactions on Biomedical Engineering (TBME)*, 09/2019, vol. 67, no. 6, pp. 1684-1695, June 2020, <https://dx.doi.org/10.1109/TBME.2019.2942974>, [183]

#### 2.2.1.1 Summary

During our work with tetraplegic spinal cord end users (see [152]) we came to understand that single limb control is not enough to provide meaningful control in daily life situations. The second hand is often used in a supporting or stabilizing function. Hence with this study, we investigated the EEG correlates in the LFTD for both unimanual and bimanual reach-and-grasp actions. The aim was to find significant differences which eventually could be used for subsequent decoding between unimanual and bimanual tasks, as well as against a rest condition. Fifteen able bodied participants performed self initiated reach-and-grasp actions on objects of daily life (see Figure 2.9). Unimanually, with both left and right hand, they reached and grasped for a glass (palmar grasp) or a spoon (lateral grasp).

As for bimanual tasks, they either reach-and-grasped a pot on its handles (double lateral grasp) or a jar with a spoon attached (mixed grasping of palmar and lateral grasp). Additionally we recorded periods of resting, where participants sat comfortably and relaxed. In this way, we recorded 80 trials for 7 different conditions, 4 unimanual (left/right, palmar/lateral), 2 bimanual (double lateral/mixed palmar/lateral) and 1 rest condition.

#### 2.2.1.2 Contribution to the PhD thesis

In this study we could show that unimanual and bimanual reach-and-grasp actions can be decoded from the LFTD of human EEG. Our multiclass classification approach consisted of all 6 movement conditions and one rest condition. It was evaluated on a (unseen) test set consisting of one third of the gathered data. On average, participants performed at 38.6% +/- STD 6.6% peak performance approximately 1 s +/- STD 200 ms after the movement onset (see Figure 2.10). This confirms our findings from section 2.1.1, where the most discriminable features could be found in the first second after the movement onset [179].

Underlying EEG correlates of paired conditions ‘Left Hand’, ‘Right Hand’ and Bimanual showed significant lateralization effects already occur around one second before the movement onset but also during and shortly after the movement onset (see Figure 2.11).

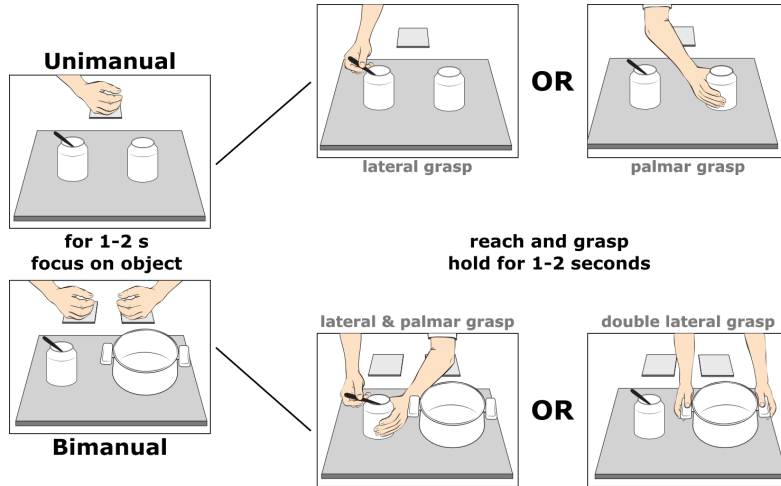


**Figure 2.9: Experimental paradigm.** Though self-initiated, we instructed the participants to fixate their gaze on the object they want to grasp for 1-2 s before initiating the reach-and-grasp action. Once they grasped the object, they were tasked to hold the object for at least 1-2 seconds, before returning to their starting position. For unimanual conditions, participants grasped a glass (palmar grasp) or a spoon (lateral) grasp with both left and right hand. For the bimanual conditions they grasped the handles of a pot (double lateral grasp) or a jar with a stuck spoon (left hand palmar grasp for support, right hand lateral grasp on the spoon).

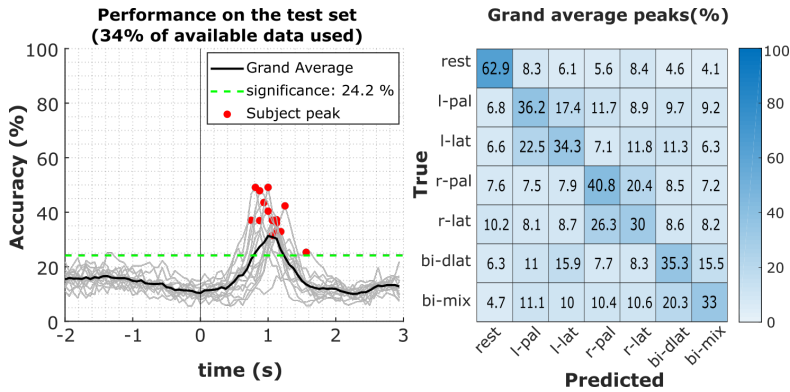


**Figure 2.10: Multiclass decoding performance of the unseen test set for all participants.** **Left:** The evaluation was performed within a window of interest of [-2 3] s whereas time = 0s refers to the movement onset. The bold black line shows the grand average over all participants. Grey lines indicate the participant specific performances, red dots represent their peak accuracy. Peak accuracies are spread over the time course of one second, indicating a considerable inter participant variability. Nevertheless, all participants performed significantly better than chance (adjusted chance level at 24.2%,  $\alpha = 0.05$ , [181,182]). **Right:** Grand average, row-wise normalised confusion matrix of participant specific peak accuracies. As can be seen, true positive rates (TPR) for the rest condition exceed any other movement condition TPRs by more than 20 percent. Discrimination between bimanual conditions as well as same hand conditions yield higher false positive and false negative rates while parings involving different hands have considerably lower true positive or false positive rates.

For the bimanual conditions no distinct lateralization effect could be observed. Investigations on the scalp topographic level showed these differences mainly over sensorimotor areas (see Figure 2.12).

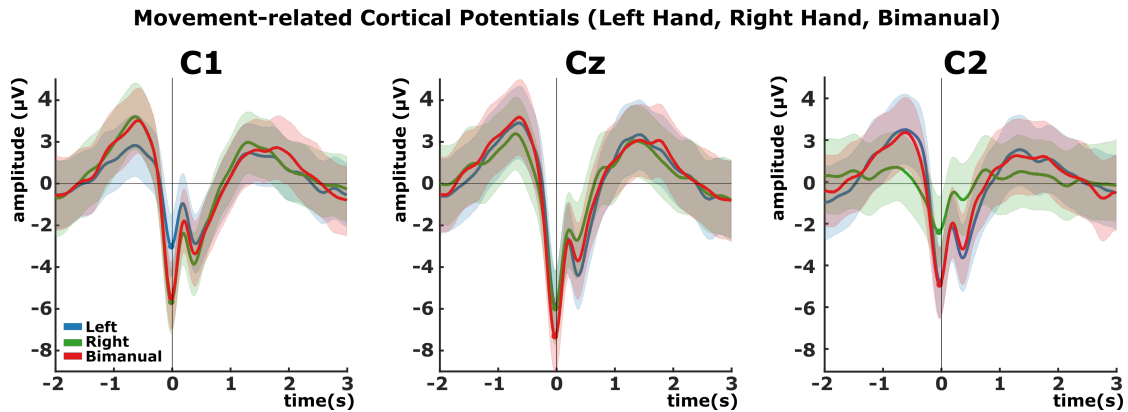


**Figure 2.11: Movement-related cortical potentials of unimanual and bimanual reach-and-grasp actions (bidirectional filtered, order 4, 0.3-3Hz).** Grand average over all participants of grouped unimanual and bimanual conditions (e.g. all left hand conditions together). Additionally, colored shaded areas show the 95% confidence interval calculated using non-parametric t-percentile bootstrap statistics ( $\alpha = 0.05$ ) for channels C1, Cz and C2.

Results of this study indicated that a discrimination between unimanual and bimanual movements is not only possible but the occurring lateralization effect even fosters discrimination between unimanual and bimanual conditions.

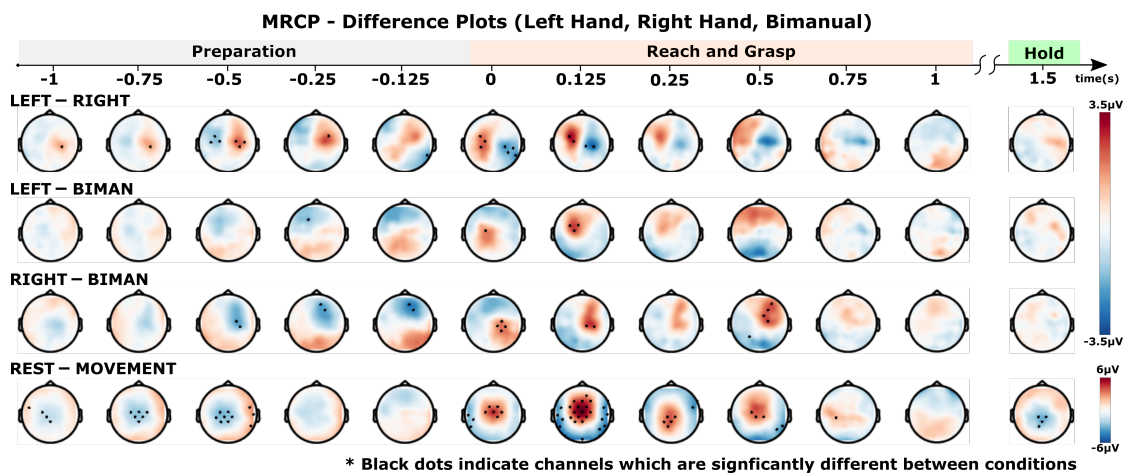


**Figure 2.12:** Topographical plots showing the difference between grouped conditions (groupA-groupB) of left hand, right hand and bimanual tasks. The time range depicted ranges from one second before the movement onset (time = -1s) to 1.5 s after the movement onset. Small dots represent channels which have been significantly different between groups (determined using non-parametric paired sample two-tailed permutation tests based on t-statistics,  $\alpha = 0.05$ ).

## 2.2.2 Case study: Unimanual and Bimanual Reach-and-Grasp Actions Can Be Decoded From Human EEG of a tetraplegic end user

The following chapter describes an unpublished single case study which is considered for future publication.

”Unimanual and Bimanual Reach-and-Grasp Actions Can Be Decoded From Human EEG of a tetraplegic end user”, in preparation<sup>1</sup>

### 2.2.2.1 Introduction

In section 2.2.1, we could show in an abled bodied population (n=15) that unimanual and bimanual reach-and-grasp actions could be decoded from the EEG LFTD. In a single-trial multiclass classification approach consisting of 6 unimanual and bimanual movement conditions as well as one rest condition, participants reached peak accuracies of 38.6 % +/- STD 6.6% on a previously unseen test data set. Underlying EEG correlates indicated significant differences of movement-related cortical potentials between conditions from around 1s before to 1.25 s after the movement onset. However, it still remained unclear whether these results could be transferred to e.g. users without voluntary hand/finger control - a condition not uncommon in people with high spinal cord injury [152]. In such a scenario, a combination of both executed and attempted movements, respectively, would come to bear: While the reaching movement towards an object can still be executed, the grasp is attempted by the end user. Recent findings have suggested that the attempted movements provide a similar neural representation to executed movements and can also be decoded [184, 185].

In the current single case study, we investigated in one high spinal cord injured end user, whether the combination of executed and attempted unimanual and bimanual reach-and-grasp actions can be decoded from the LFTD of EEG. Additionally we were interested, whether significant differences of MRCPs could be found.

### 2.2.2.2 Methods

**Study Participant** This study was approved by the local ethical commission of the Medical University of Graz (EK: 30-439 ex 17/18). The study participant SCI1 was a 31 year old tetraplegic male participant. He suffered a traumatic injury at cervical level 4 (C4) after a motor vehicle incident (MVI). Clinical assessment performed according to the ASIA impairment scale (AIS) file him as sensory incomplete B. [186]

Regarding residual voluntary motor functions, the study participant has no voluntary lower limb, hand or wrist control, however he still retains shoulder and elbow function for both arms (MRC [19], grade 4-5). His predominant hand is the right hand which he uses to operate most assistive devices in daily life (leather wrist bands, customized pens and cutlery, also touch screens). The study participant was informed about the study procedure and the scientific goals of the study and he also gave written consent.

---

<sup>1</sup>Schwarz Andreas, Pereira Joana, Zube Marcel, Gernot Müller-Putz

**Experimental setup** The recording was conducted in a secluded room at the home of the study participant. In front of the participant, we placed a customized table with an in built monitor. On the monitor, we placed objects of daily life for reach-and-attempted grasping. For unimanual conditions (performed with both left and right hand) we placed a jar (palmar grasp) and a jar with a spoon (lateral grasp on the spoon). For bimanual conditions, we used a pot to be grasped at both handles (double lateral grasp) and the jar with the spoon (right hand lateral grasp on the spoon, left hand palmar grasp on the glass for stabilization). Table 1 lists all conditions performed in the experiment. In unimanual runs, both unimanual objects were placed on the table in a comfortable reaching and grasping position for the participant. We also switched positions (left or right) of the objects regularly, so that each object was on each side of the table the same often. For bimanual runs we put only one object at a time on the table, since the range of motion of the study participant was limited.

The participant was then tasked to reach and attempt to grasp the designated objects in front of him. At the start of each trial, his hand(s) were located on pressure plates directly in front of him (for unimanual conditions, one pressure plate was placed in the centre). In a self initiated manner, the participant focused his gaze first on the object for 1 to 2 seconds before he started the reaching and attempted grasping movement (see Figure 2.13). While it was evident that he could not perform a fully functional grasp on the objects before him, he attempted the designated grasp (see Figure 2.14). After a period of 1 to 2 seconds, the participant released position and went back to the starting position. Thereafter, he paused for at least 4 seconds before initiating the next trial. In this way, we recorded 80 trials per condition (TPC) in runs á 20 TPC. As for the bimanual conditions we recorded 40 trials alternating for each object.

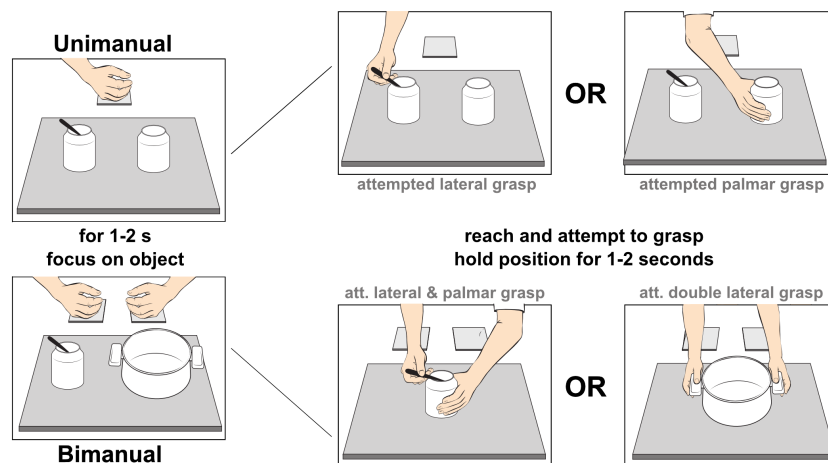


**Figure 2.13: Experimental paradigm:** In a self-initiated manner, the participant was tasked focusing his gaze for 1-2 s on the designated object before initiating the reach and attempted grasp. Although the participant was not able to perform a fully functioning grasp on any object, he still attempted the grasp and touched them. After 1-2 seconds, the participant returned his hand(s) back on the pressure plates.



Additionally, we recorded at the start, half time and end of the experiment 3 minutes of resting data as well as 2 minutes of eye movements following the protocol already described in [183].



**Figure 2.14: The study participant performs unimanual and bimanual reach and grasp actions.** (A) attempted palmar grasp, (B) attempted lateral grasp, (C) attempted double lateral grasp, (D) attempted mixed grasping action (left hand palmar grasp, right hand lateral grasp).

**Data recording and preprocessing** Data recording and preprocessing was performed identical to the processing steps described in section 2.2.1, [183], section A-F. Summarizing, we used 58 active electrodes (g.tec medical engineering GmbH) positioned over frontal, central and parietal regions of the scalp. Additionally, we recorded the electrooculogram (EOG) using 6 additional active electrodes at locations superior and inferior to the left and right eye as well as the outer canthi. All signals were sampled with 256 Hz and bandpass-filtered (0.01-100Hz) using a 8th order Chebyshev filter. Additionally, we placed a notch filter at 50Hz to suppress the power line noise.

For recording the movement onset as well as the grasp onset (the moment the participant touched the designated object), we used force-sensing resistors. All datastreams were synchronized using the TOBI signal server [187, 188].

We applied a 4th order, zero-phase highpass Butterworth filter at 0.3 Hz on all recorded

**Table 2.1:** Experimental Conditions

<b>TYPE</b>	<b>OBJECT</b>	<b>GRASP TYPE</b>
<b>Unimanual</b> (performed w. left or right hand separately)	Jar	Palmar
	Spoon	Lateral
<b>Bimanual</b>	Pot with Handles	Double Lateral
	Jar with Spoon	Palmar (left Hand) Lateral (right Hand)
<b>Rest</b>	Cross on Screen	No movement performed
<b>Eye Movement</b>	Instructions on screen	-

data. To correct the recorded data for ocular based artefacts, we trained a subspace subtraction algorithm [189–191] on the recorded eye movements and applied it on the movement and rest data. Thereafter we defined a window of interest (WOI) of -2s to 3s with respect to the movement onset for each trial. We epoched the recorded rest data to extract 81 trials as an additional condition.

We further rejected trials with potential artefact contamination using statistical parameters between 0.3 and 35 Hz (see [183] for parameters) from the subsequent analysis (12% of all trials were rejected).

**Movement-related cortical potentials** Calculation of the MRCPs follows closely the approach described in [183], section G. We initially applied a common average reference filter (CAR) and resampled the all data to 16 Hz to save computational load. Thereafter we applied a 4th order zero-phase highpass filter (Butterworth) with a cut-off frequency of 3 Hz to attenuate higher signal components. To ease comparison to the findings in [183], we calculated the global field power over all channels and normalized all data by the average GFP of the rest condition [192].

We eventually epoched all data according to the WOI and calculated the mean over all trials for each condition. We also calculated a 95% confidence interval for each condition using non-parametric t-percentile bootstrap statistics.

Additionally, we pooled all conditions for each left hand, right hand and bimanual and calculated mean and bootstrapped confidence interval.

**Single trial classification** Single trial classification was performed identically to the approach described in [183] section H (see Appendix for further details). In summary, we resampled all data to 16 Hz and applied a 4th order zero-phase highpass filter (Butterworth) with a cut-off frequency of 3 Hz. Thereafter, we divided all available data (all movement trials as well as all extracted rest trials) into a calibration set (the first

recorded 66% of all movement trials) and an unseen test set (the last 33% of the recorded data). Using the calibration data, we determined the best performing (in terms of accuracy) classification model. We epoched all trials of the calibration data set according to the WOI and calculated an individual classification model for each time point within the WOI: For each time point, we applied 10 times 5 fold cross validation and divided the calibration data in training and validation set. Thereafter, we trained a shrinkage based linear discriminant classification model [129] with features extracted from the training set. These features were taken from all 58 EEG channels in 0.125s steps from a causal 1 s window  $[-1:0.125\ 0]$  s, whereas  $\text{time} = 0\text{s}$  is the investigated time point in the WOI. In this way, we extracted 9 features per channel, in total 522 features per observation. This approach was repeated for every time point within the WOI ( $n = 80$ ). To determine the best performing classifier, we took the means of the accuracies of the cross-validated results for each time point and chose the one with the highest mean accuracy. We also determined a normalized confusion matrix for the best performing classification model. For this, we row-wise normalized the confusion matrix (CM) so that every row sums up to 1. Hence, reported true positive (TPR) and false positive rates (FPR) were also subject to this normalization step. Finally, we applied the best performing classification model on the unseen test data set (33% of all recorded data).

### 2.2.2.3 Results

**Behavioural deviation from the experimental protocol in bimanual tasks** It was not possible for the study participant to simultaneously reach with both hands (forwards) towards the object: This would have led to an unstable torso position resulting in tilting forwards. Instead he eventually performed the bimanual tasks in a slightly sequential order as can be seen in Figure 2.15.

**Movement-related cortical potentials** Figure 2.16 depicts the average MRCPs for the pooled conditions of left hand, right hand and bimanual conditions for channels C1, Cz and C2 over the central motor cortex. Already 1s before the movement onset, a strong negative shift occurs which reaches its peak around the movement onset (“Bereitschaftspotential“, [106, 108]). This negative peak is larger for left hand conditions on the right side, and for right hand conditions on the left side, indicating a distinct lateralization effect. For the bimanual conditions, no distinct lateralization effect at  $\text{time} = 0\text{s}$  can be observed. Around 300ms after the movement onset, a positive peak for all conditions can be observed, which corresponds in timing to the “reafferent potential”. Around 1 to 1.5 s after the movement onset a second positive peak can be observed for the conditions before returning to baseline.

Figure 2.17 shows the MRCPs for same hand and bimanual conditions for channels C1, Cz and C2 located over the central motor cortex. Again a strong negative shift can be observed culminating around the movement onset followed by the positive potential around 300ms after the movement onset. For left hand conditions (Figure 21, 1st row) the negative peak at the movement onset is stronger pronounced on the right side (C2) while for right hand conditions on the left side (C1) (Figure 22.16, 2nd row). A pronounced

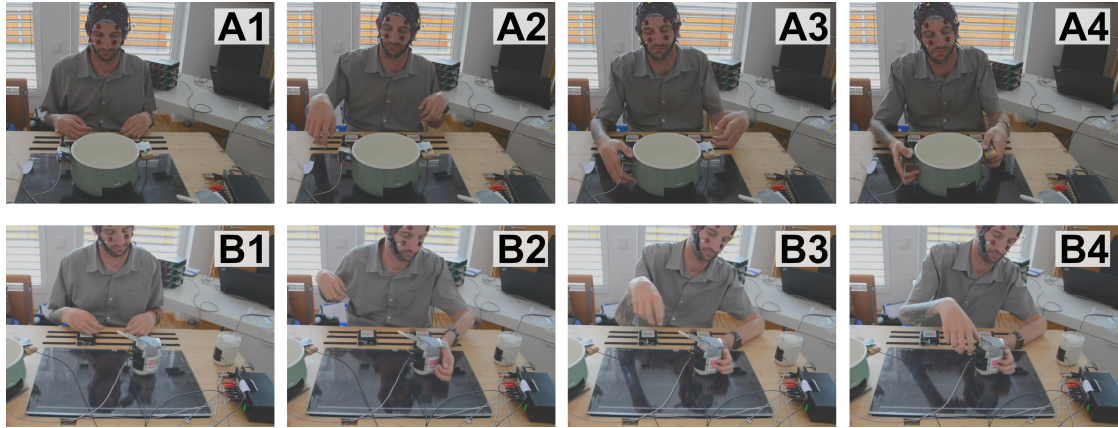


**Figure 2.15: Behavioural deviation from experimental protocol in bimanual tasks.** (A, B) show the trial time course. Due to torso instability the study participant was unable to simultaneously reach with both arms forward towards the object. Instead he performed sequential reach-and- attempted grasp actions. (A) bimanual reach and attempted grasp towards the pot (double lateral grasp). (B) bimanual reach and attempted grasp towards the jar with the spoon.

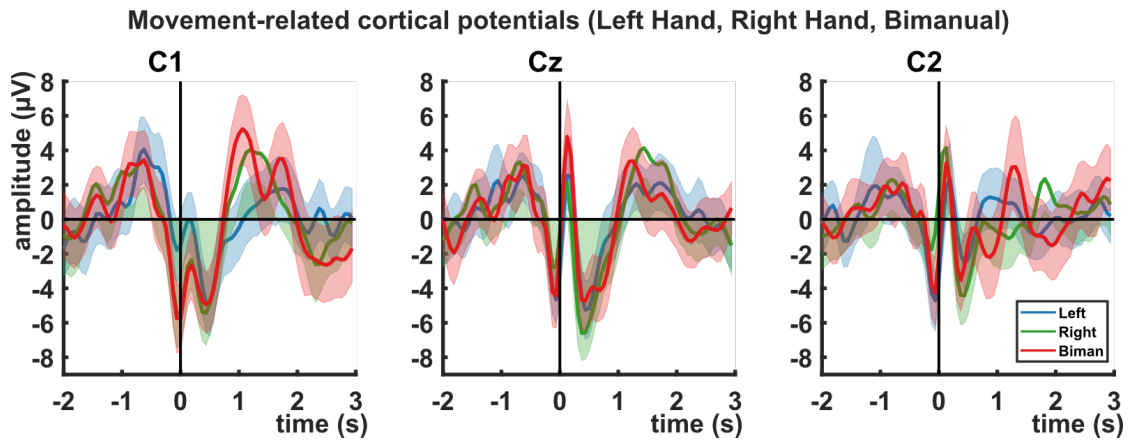


**Figure 2.16: Movement-related cortical potentials for Left hand, right hand and bimanual conditions (pooled):** Averages and 95% confidence intervals of left hand, right hand and bimanual conditions (pooled) for channels C1, Cz and C2. The black perpendicular line represents the movement onset.

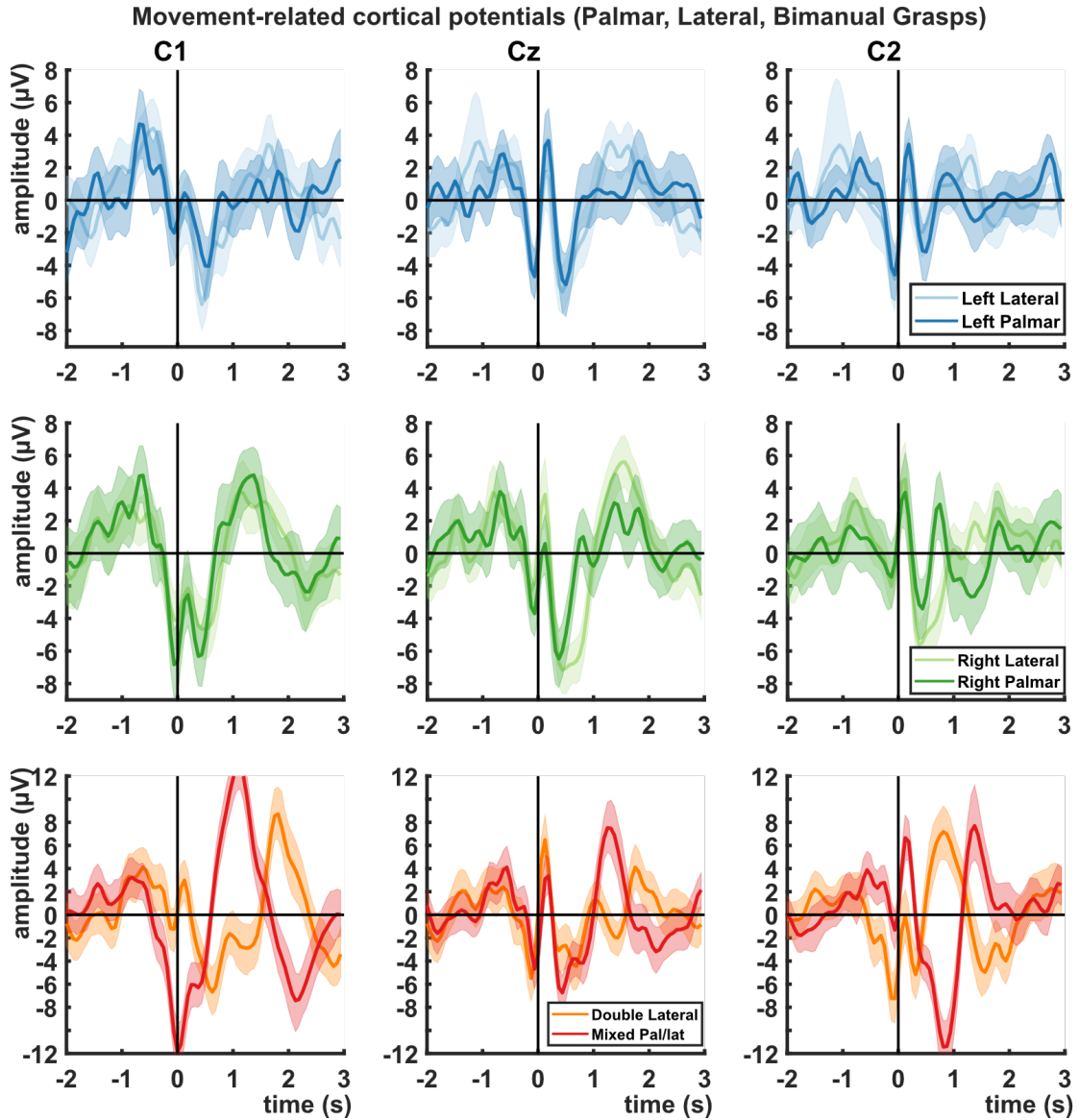


**Figure 2.17:** Movement-related cortical potentials for same hand and bimanual conditions. Averages and 95% confidence intervals for all conditions for channels C1, Cz and C2. MRCPs are time locked to the movement onset (time = 0s, black perpendicular line). The first row shows the MRCPs for left hand conditions, the second row for right hand conditions. The last row depicts the MRCPs for the bimanual conditions.

difference in MRCP morphology can be observed between both bimanual conditions, since timing for both conditions is different due to sequential handling of the reach and grasp actions.

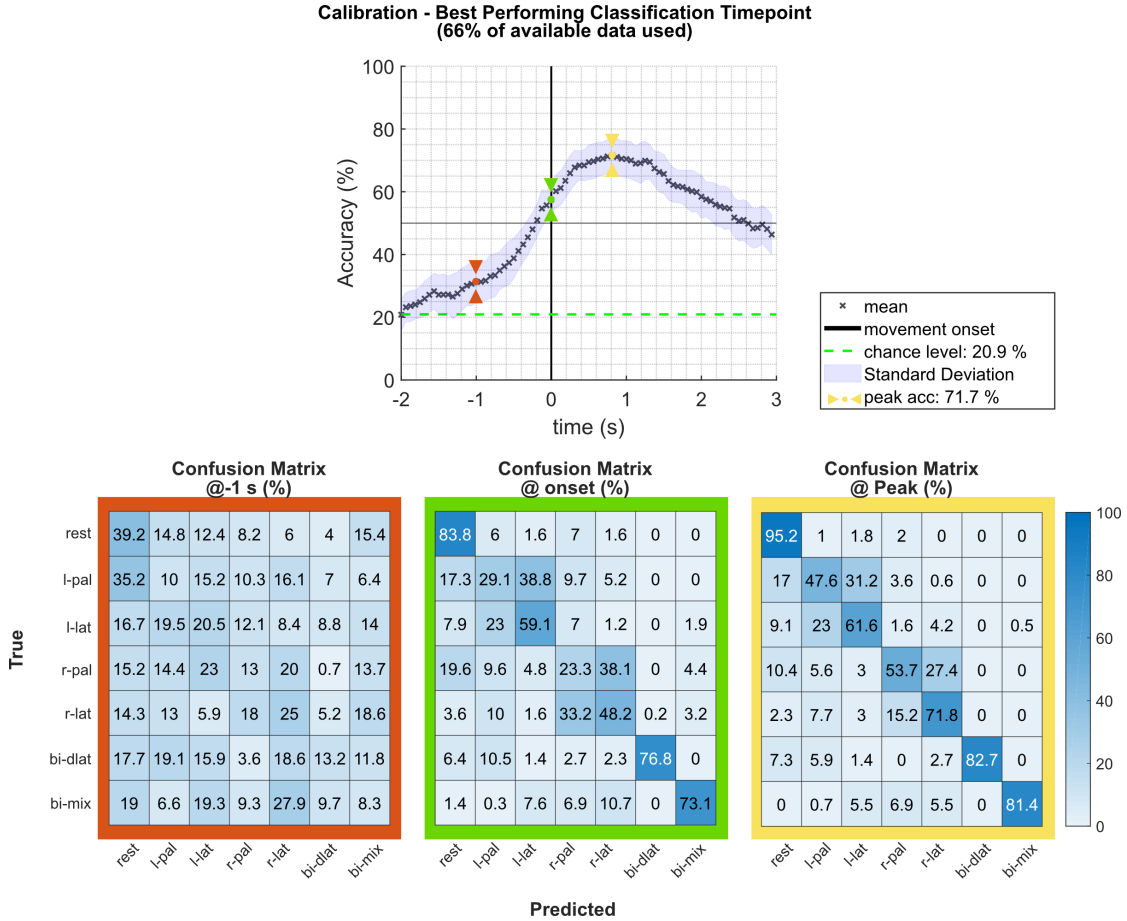


**Figure 2.18: Calibration set, mean of the cross-validated classification results.** (Top) Accuracy averages (%) over all tested timepoints within the WOI (black crosses). Peak performance is reached around 900ms after the movement onset (black vertical line). (Bottom) Confusion matrices for 3 points of interest within the WOI (row-wise normalized): 1s before the movement onset (red), at time of the movement onset (green) and when reaching peak performance (yellow). Condition abbreviations: rest (Rest), l-pal (left palmar), l-lat (left lateral), r-pal (right palmar), r-lat (right lateral), bi-dlat (bimanual double lateral, Pot), bi-mix (bimanual mixed palmar/lateral).

**Single trial multiclass classification** For the single trial multiclass classification we initially determined the best performing classification model (in terms of accuracy) within the WOI. Figure 2.18 (top) depicts the results for each time point within the WOI (averaged over all cross validated results). The best performing classification model was found 0.875 s after the movement onset with a peak accuracy of 71.1% (adjusted chancel

level 20.9%, [181,182]). Figure 2.18 (bottom) shows the row-wise normalized confusion matrices for 3 points of interest within the WOI. It can be seen that around 1 s before the movement onset (bottom left, highlighted red), all entries of the confusion matrix are around chance level (with the exception of the rest class). At the point of movement onset (bottom center, highlighted green), better than chance TPR rates can already be seen for all conditions, especially for the rest and bimanual conditions. Highest false positive rates (FPR) and false negative rates (FNR) can be observed for unimanual same hand conditions. At the point of peak accuracy at 0.875 ms, TPR for all conditions are significantly better than chance level and, above all, the rest and the bimanual conditions. FPR and FNR for same hand unimanual conditions are lower compared to the point of movement onset. We eventually applied the best performing classification model onto the unseen test data set (see Figure 2.19, left). The participant specific peak accuracy was reached again 0.875 s after the movement onset with 57.6% (adjusted chancel level 25.6%, [181,182]). The row-wise normalized confusion matrix shows highest TPR for the rest condition and the bimanual double lateral (pot) condition. Highest FPR and FNR can be found between unimanual same hand conditions (see Figure 2.19, right).

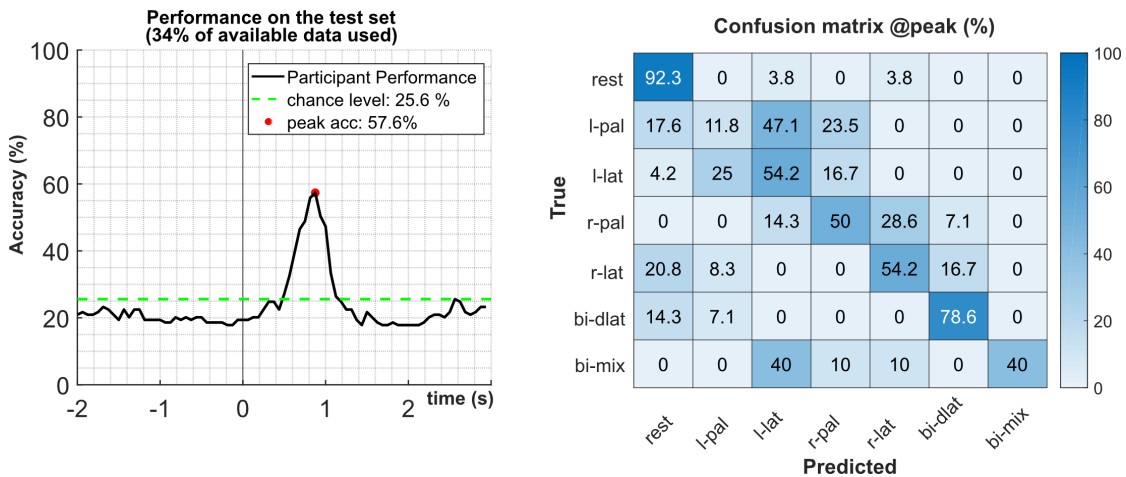


**Figure 2.19: Test set performance results. (Left)** Performance of the best performing classification model applied on the previously unseen test set (black line). **(Right)** Confusion matrix calculated at the point of peak performance (row-wise normalized). Condition abbreviations: rest (Rest), l-pal (left palmar), l-lat (left lateral), r-pal (right palmar), r-lat (right lateral), bi-dlat (bimanual double lateral, Pot), bi-mix (bimanual mixed palmar/lateral).

#### 2.2.2.4 Discussion

In this single case study, we could successfully show that unimanual and bimanual executed reach-and-attempted grasp actions can be successfully decoded from the EEG’s low frequency time domain. We were able to decode six movements and one rest condition with a peak accuracy of 57.6% (adjusted chance level (25.6%) [181,182]). Underlying EEG correlates show significant differences between same and bimanual conditions in

the first second after the movement onset which is the same time window used for feature extraction of the classification model.

**Movement-related cortical potentials** The EEG correlates for unimanual conditions of the study participant show similar characteristics and are comparable to our previous findings in able bodied populations [179, 183] - though with a higher variation. Starting almost 1 s before the movement onset a negative deflection starts, peaking at the movement onset (“Bereitschaftspotential”, [105]) followed by a positive rebound around 300ms after the movement onset, before returning to baseline. When pooling left hand and right hand conditions, a lateralization effect can be observed (lateralized, readiness potential, see [193, 194], whereas the MRCPs are pronounced always strongest on the contralateral side to the executing hand. As for bimanual conditions, the study participant deviated from the initial experimental instruction of simultaneous grasping for fear of tilting forwards. This slightly sequential execution order of both hands is also visible in the EEG correlates: While the initial Bereitschaftspotential around the movement onset is still present, the reaching phase is contaminated by additional positive and negative deflections, most likely induced by the second hand, which changed the morphology of the MRCPs. Moreover, since the bimanual movements were also different in timing against each other, these changes in morphology lead to pronounced significant differences not only against the unimanual conditions, but also against each other.

**Single-trial multiclass classification** For the multiclass approach, we initially determined the best performing classification model on the calibration data set (the 66% of all recorded data (chronological)) within the WOI. Here, we found the best performing classification model 0.875 s after the movement onset with a mean accuracy over all folds of 71.7%. This coincides with the time period where significantly different EEG correlates in the LFTD were found. While the timing is similar to the able bodied study participants in [183], the performance of the tetraplegic study participant exceeds their best calibration results by 29%. A close look at the confusion matrices calculated for the classification model shows that for the bimanual classifications, TPR of more than 80% could be reached. Moreover, the TPRs for rest versus any movement conditions exceeded 95%. While the first can be explained by the deviation in the execution of the bimanual reach and attempted grasp actions, the latter exceeds the average TPR of able bodied in [183] by more than 38%. A potential explanation for this might be that the study participants reaching movement is considerably different from able bodied persons: The reaching movement includes more movement of the shoulder, since he had to compensate for missing voluntary wrist and finger control. This leads inevitably to additional confounders such as (i) the shoulder movement represents an additional movement which changes the morphology of the MRCP itself. (ii) Moreover, the additional shoulder movement could introduce potential muscular-based artefact contamination of the EEG. This has to be taken into consideration when evaluating these results.

When applying the best performing classification results on the unseen test dataset, the classification accuracy yielded 57.6%. Though a performance drop from calibration data



to an unseen test set can be expected, it is higher than in the abled bodied population in [183]. When looking at the calculated confusion matrix for the point of peak accuracy, it can be seen that the classification model was not able to discriminate between the bimanual mixed condition and the lateral grasp of the left hand in the same way anymore. This could be the result of a behavioural change in timing of the execution of the bimanual condition (the discrimination between lateral left hand and other unimanual conditions still was in the same range). Similar to the calibration data set, rest condition and the second bimanual condition (double lateral) performed overly well. Nevertheless, the results indicate that single-trial decoding of executed reach-and-attempted grasp actions is possible.

**Study Limitations** In the current study, the study participant deviated from given instructions for performing the bimanual reach and attempt to grasp conditions. Instead of reaching with both hands simultaneously, he performed the task in a slightly sequential manner. This was because he was afraid of tilting forwards due to lack of sufficient torso stability (due to SCI level).

Due to this deviation, the morphology of the EEG correlates for bimanual conditions changed considerably in comparison to that of able bodied persons shown in [183]. Moreover, due to these different task executions, the differences between unimanual and bimanual tasks increased, which lead to increased decoding performance. Nevertheless, these deviations brought further insights not only for the design of follow up experiments, but also for future application in real world scenarios: Future experimental setups need to take torso instability into account. This could be done by e.g. fixating the torso to the wheelchair with a belt, or redesigning the experimental setup to account for this instability. The first allows a better comparison to studies in abled bodied populations such as [183, 195], the latter reflects a scenario more realistic to a daily life situation of an SCI end user.

The study participant compensated for the lack of voluntary wrist and hand control with overly pronounced elbow and shoulder movements when reaching for the designated objects presented on the table. In this way he did not reach for the object on a plane level parallel to the table, rather he approached them at a slightly sharp angle, whereas the elbow was elevated. In this way it was possible for him to reach and attempt the grasp as well as making contact with the objects. However, these overly pronounced movements, especially the shoulder movements, can have a potential influence on EEG by causing muscle induced artefacts and lead to an increase percentage of rejected trials due to artefact contamination (16%). Hence, for any future experimental setup or online application, causal state of the art EMG correction algorithms such as [196] could come to bear.

### 2.2.2.5 Conclusion

We showed that unimanual and bimanual executed reach-and-attempted grasp actions can be decoded from the low frequency time domain of a tetraplegic end user. We were able to decode six movements and one rest condition against each other with a peak

accuracy of 57.6% on unseen data. EEG correlates showed significant lateralization effects between unimanual condition of the left and the right hand. The correlates further revealed that significant differences between all conditions were pronounced within the first second after the movement onset, which is the same window used for feature extraction of the classification model. Further, we could identify and discuss parameters such as torso stabilisation during tasks as well as a difference in reaching patterns to able bodied persons, which need to be addressed thoroughly in future experiments.

#### **2.2.2.6 Acknowledgements**

The authors thank Rüdiger Rupp for his contribution in the discussion and the planning of this. We deeply thank all members of the Project “MoreGrasp” (‘643955’) who made this experiment possible in the first place. This work was supported by the Horizon 2020 Project MoreGrasp (‘643955’).

### 2.2.3 Combining frequency and time-domain EEG features for classification of self-paced reach-and-grasp actions

Schwarz Andreas, Pereira Joana, Lindner Lydia, Gernot Müller-Putz, “Combining frequency and time-domain EEG features for classification of self-paced reach-and-grasp actions.”, Proc. of the 41st Annual International Conference of the IEEE Engineering in Medicine and Biology Society (EMBC), Berlin, Germany. <https://doi.org/10.1109/EMBC.2019.8857138> [197]

#### 2.2.3.1 Summary

This study was performed on data which was previously recorded for [183] (see section 2.2.1). While we could show in our previous studies [179, 183] that singular reach-and-grasp actions can be decoded from the low frequency domain of human EEG, one has to recognize that the decoding performance was insufficient to provide meaningful control. In the current study we attempted to increase decoding performance by also including band power based features from alpha and beta bands. We arbitrarily selected 10 data sets of self-initiated unimanual (right hand) reach-and-grasp actions (80 TPC) on a glass (palmar grasp) and on a spoon (lateral grasp) from the data sets recorded in [183] (see Figure 2.20 for paradigm). We also included the rest condition where participants sat on a chair in a relaxed state.

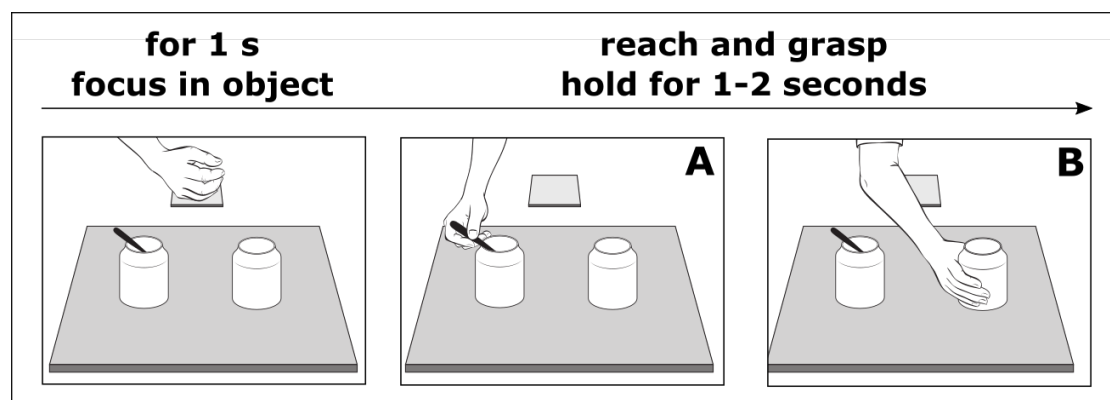


**Figure 2.20: Experimental paradigm.** Though self-initiated, we instructed the participants to fixate their gaze on the object they want to grasp for 1-2 s before initiating the reach-and-grasp action. Once they grasped the object, they were tasked to hold the object for at least 1-2 seconds, before returning to their starting position. Participants grasped a glass (palmar grasp) or a spoon (lateral) grasp with the right hand.

#### 2.2.3.2 Contribution to the PhD thesis

We could show that the overall classification significantly improved for all study participants (Wilcoxon rank sum test,  $\alpha = 0.05$ ) when including features from alpha and beta band for decoding. On average, the peak decoding performance increased by

more than 10% from 65% +/- STD 6.5% to 75% STD +/- 5.8%. Further analysis of the confusion matrix of the grand average peak accuracies revealed that the discrimination between movement classes and rest class benefited the most from the extended feature set (see Figure 2.21).

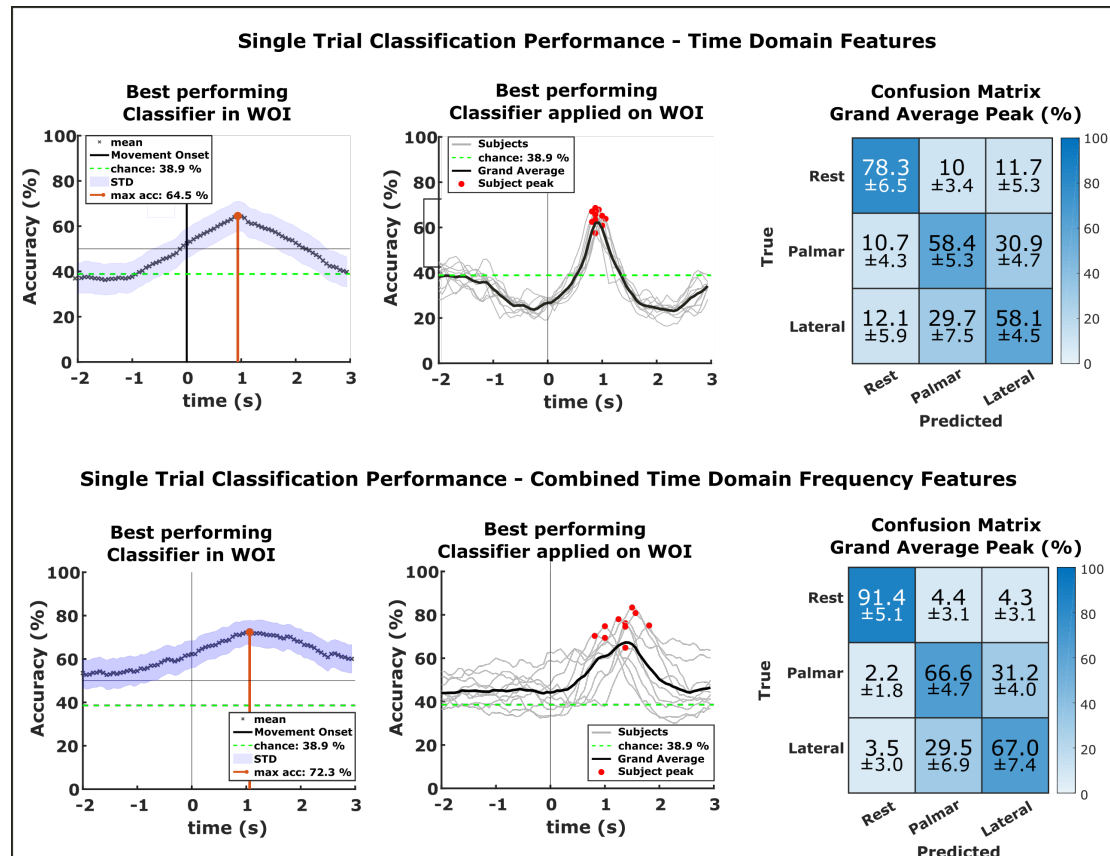
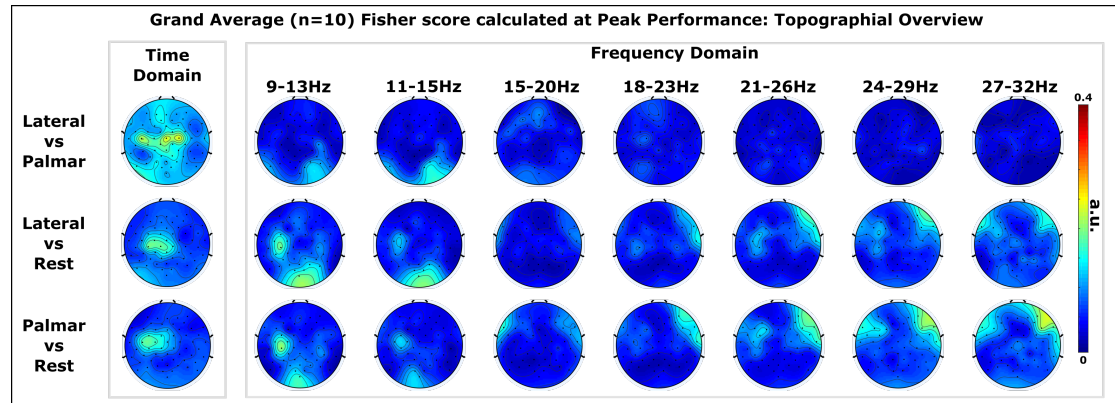


Figure 2.21: Single trial, multiclass based classification performed using time domain features only (top row) and time domain combined with power features from the frequency domain (bottom row). The left column shows all evaluated classification algorithms (regularized linear discriminant algorithm models (sLDA) [129]) within the window of interest (WOI) of [-2 3] s whereas time = 0 s represents the movement onset. The middle column depicts the performance of the best performing classification algorithm. The third column shows the grand averages of the row-wise normalized confusion matrices of the participant specific peak accuracies.

We also evaluated the feature ranking provided by Fisher's score [198] (see Figure 2.22): The quantification attempt showed that for movement versus movement conditions, the most discriminable features can still be found in the LFTD range (0.3-3 Hz). However, for movement versus rest discrimination, especially features from the alpha range not only over the contra lateral motor cortex (to the executing right hand) but also features from the occipital cortex contributed to increased discrimination performance. The contribution of the occipital cortex can be explained by increased alpha

activity typically associated with resting conditions ([48,51]). However, scores achieved from the high beta range over frontal and lateral regions indicate the presence of residual muscular artefacts, hence one must take this into consideration when interpreting the results.

Summarizing, we could state that the combination of both LFTD features and power based features from alpha and band lead to significantly increased performance, especially for movement versus rest decoding, and could effectively contribute to improving BCI control for assistive devices.



**Figure 2.22: Topographical overview of Fisher's Score on both time domain and frequency domain based features.** The first column shows the time domain, columns 2-7 the frequency domain. Hot colors represent higher contribution, cold colors minimal or none.

## 3 Discussion

The goal of this thesis was to evaluate whether natural grasp/reach-and-grasp movements can be decoded from EEG and have the potential to act as a control modality in an non-invasive BCI. In [179], it could show in able bodied study participants that the most used grasp actions of daily life (palmar, lateral and pincer grasp) can be decoded from EEG's low frequency time domain against each other and a resting condition. In a follow up study [180], palmar and lateral grasp together with a wrist supination could be decoded online and able bodied study participants could control a robotic arm in a simulation environment.

Experiences with high spinal cord injured persons have shown that single limb control is not enough to provide meaningful control in daily life situations. The second hand is imperative to them at least in a supporting or stabilizing role. Hence, in [183], investigations towards decoding of grasp/reach-and-grasp actions were extended to also include bimanual grasp/reach-and-grasp actions. Further offline investigations were conducted to boost decoding performance by including features from the frequency domain of alpha and beta band [197].

Lastly, a single case study including a high spinal cord injured end user was done who performed unimanual and bimanual executed reach-and-attempted grasps on objects of daily life. It could be shown that both unimanual and bimanual movements could be decoded from each other as well as a rest condition.

### 3.1 EEG-based decoding of executed grasp/hand movements

#### 3.1.1 Offline - Analysis of EEG correlates and identifying hyperparameters

In section 2.1.1, it was assessed whether EEG correlates of 3 executed reach-and-grasp movements most prominent in daily life (palmar, lateral and pinch grasp, see [179]) can be identified in the LFTD and eventually discriminated against each other and a rest condition. Offline analysis of the data revealed that the morphology of MRCPs in the LFTD significantly changed to a rest condition already 1.5 s before the actual movement onset. In addition, significant differences between MRCPs between grasp conditions (especially between palmar and lateral grasp) could be observed 1 s before the movement onset. These differences concerning the pre-movement phase (movement intention) go in line with findings described by Jochumsen et al. who assessed the decoding of grasping intention in the preparation phase [199] as well as findings from Gu et al. [104] or Oda et al. [200]. However, the main differences in morphology were found in the first second after the movement onset: Starting with the Bereitschaftspotential around the movement onset [108] occurring over the central motor cortex at channel Cz, followed by a positive

reafferent potential around 300ms after the movement onset [103]. This reafferent potential has only been found in this form when performing a combination of movements, in this case a reach-and-grasp. For instance, Ofner et. al, who investigated a broader range of upper limb movements in EEG's LFTD, but also included conditions similar to grasping (e.g. "hand closing") did not report any pronounced reafferent potential 300ms after the movement onset [201]. The same goes for findings presented in [180], where the investigated grasping conditions were performed with a preceding reaching movement. Further analysis of the reaching phase revealed a second positive rebound after 1 s after the movement onset, before returning to baseline. Additionally, a lateralization effect could be observed meaning that MRCPs were pronounced stronger on the contralateral side to the executed hand. Analysis of the behavioural data (kinematic data analysis of a data glove) showed that the average duration from the movement onset to finally grasping the objects took on grand average around 1.1 to 1.25 s. This window fully covered the time span where the majority of the differences between conditions could be found. From that, one can also conclude that information regarding the designated grasp can already be extracted from the reaching phase. This goes in line with initial studies conducted by Jeannerod et al in the 1980s [202,203] investigating (reaching and) grasping kinematics, especially the preshaping of the hand: They attempted to quantify the preshaping of the hand during the reaching movement by constantly measuring the distance between thumb and index finger tip. They could show that the maximum aperture between both is reached around 60-70% of the duration of the reaching movement. A summary review can be found in [172].

The single trial classification approach allowed to test a series of hyperparameters such as the size and location of the time window for feature extraction, or the number of EEG sensors, while avoiding overfitting of the data. It could be shown that the best window for extracting features is within the first second after the movement onset, although better than chance classification could already be reached before the movement onset (which additionally confirms presented findings by Jochumsen et al [199] regarding the pre movement phase). Binary classification results yielded accuracies around 70% for grasp versus grasp classification (adjusted chance level 63.2%, [181, 182]), however for grasp versus a rest condition, accuracies of over 90% could be reached. In the meantime, several studies conducted in able bodied populations have shown similar decoding results [111,204,205], although a direct comparison is often not possible since experimental setup, paradigm and approach differ. In Randazzo and colleagues' experiment [204], study participants (n=4) were instructed to grasp an u-bracket with either palmar or precision grasp in a self initiated manner. They could confirm that for movement versus rest classification, better than chance classification of on average 70% could be reached already before the movement onset. This increased to almost 80% during the reaching movement within 1s after the movement onset. In a follow up study incorporating the same experimental setup, Iturrate et al. [205] achieved similar classification results in an able-bodied population of 10 study participants. Using source localization techniques, they were also able to identify patterns associated with grasping in bilateral regions of the motor and parietal cortex in the time domain (range 1-40 Hz). In another experi-

ment, Agashe et al. [111] investigated reach-and-grasp actions on six different objects in a narrower frequency band between 0.1 and 1 Hz. Contrary to the findings described in section 2.1.1, [179], as well as findings by Randazzo and Iturrate and colleagues, they report that the average peak accuracy of their decoding attempt happened already 250ms after the movement onset. Though a direct comparison between studies is not possible due to fundamental different approaches in methodology, it can be surmised that the information content in the LFTD of reach-and-grasp actions is not only limited to 0.1-1Hz - a fact that has been also underlined by the source analysis performed by Iturrate et al. in [205].

Nevertheless, a still open issue was whether these findings can be successfully transferred for application in a non-invasive BCI.

### **3.1.2 Online - Controlling a robotic arm in a simulation environment using a BCI**

Relying on findings and parameters investigated in section 2.1.1, [179], we initiated a second study which aimed to test the feasibility of MRCPs as features for grasp/hand movements in a non invasive BCI (section 2.1.2, [180]): While this study was still conducted in a population of able-bodied study participants, it was already designed as a precursor for investigations incorporating severely motor impaired end users. Therefore, the study relied on a desktop based simulation environment for presenting instructions and feedback (paradigm) to the study participants. The main idea for this was to reduce the experimental setup to an ecologically valid environment, which is compact enough to be applied at end users' homes. Additionally, we concentrated foremost on the EEG analysis and discrimination of different grasps (palmar and lateral) and one additional hand movement (wrist supination).

EEG analysis of both the recorded calibration data as well as the online data of the BCI was performed using causal filters and showed a negative deflection around the movement onset. This deflection reached its peak shortly after the movement onset. Thereafter a strong positive deflection could be observed before returning to baseline. Contrary to findings presented in [179, 183, 197], no reafferent positive potential 300 ms after the movement onset could be found, which can be attributed to the non-existing reaching movement. On average, the EEG correlates shown in this study are prone to a higher variability, especially after finishing the grasp/hand movement. This can be credited to (i) the additional visual input and its accompanying brain activity as well as (ii) participant expectations when presenting feedback based on their actions. Significant differences between conditions were mainly found in the first 0.5 s after the movement onset on the sensorimotor areas contralateral to the executing (right) hand (locations C1, C3). Interestingly, during feedback presentation significant differences could also be found over the frontal area (Fz) for grasping conditions.

Calibration of the BCI followed closely the approach described in [179]. The single trial classification approach yielded classification performances similar and comparable to the findings presented in [179], yielding on average around 60% accuracy for the 3 class problem (adjusted chance level at 44%, [181, 182]) around 1 s after the move-



ment onset. However when transferring the calculated classification model to the online scenario, where participants received feedback based on their actions, a significant performance loss of more than 10% was encountered. Though a decrease in performance is not uncommon when applying a calibrated classification model on unseen data, post hoc analysis of the data revealed that the gross of the performance loss could be attributed to the estimation of the movement onset in the online part as well as additional activity in frontal regions attributed to user expectation and feedback presentation.

Eventually, discrete online classification results yielded on average around 48% (adjusted chance level at 40.2%, [181,182]) or 65 out of 135 trials for the 3 class approach.

So far, only Ofner et al. have shown in a proof-of-concept study in one participant with SCI asynchronous online decoding of hand movements (hand opening, hand closing) using MRCPs as a feature [184]. Unfortunately, a direct comparison between study is not possible due to substantial differences in approach and protocol. Hence, the findings and the implications of this study stand for themselves.

Nevertheless, a feasibility study in a group of tetraplegic end users has already been initiated, where their capabilities of controlling an upper limb motor neuroprosthesis is assessed (see “The MoreGrasp feasibility study”, [152]). Initial findings have shown that decoding is possible even when end users only attempt the movements (see also [184]). However, these results will be published elsewhere and are not part of this thesis.

### **3.1.3 EEG based decoding of unimanual and bimanual reach-and-grasp movements**

#### **3.1.3.1 Decoding in able bodied study participants**

During the work with high spinal cord injured persons (lesion height at cervical level, C4) within the H2020 project ‘MoreGrasp’ (<http://www.MoreGrasp.eu>) we saw that unimanual grasping support would not be enough to provide effective support in daily life. In most cases, the second hand is used in a supporting function for stabilisation or even in a more active role when an object has to be grasped with both hands. As a consequence, in [183] (see section 2.2.1), we investigated EEG correlates of self-initiated unimanual and bimanual reach-and-grasp actions in the LFTD and whether these correlates were suitable for decoding not only against a rest condition, but also against each other.

EEG analysis of unimanual reach-and-grasp conditions was similar in shape and morphology to findings already presented in Core publication 1 [179]. A strong negative deflection started already up to 1 s before the movement onset and peaked around the movement onset [105,108]. In addition a refferent positive potential around 300 ms after the movement onset could be identified. A second positivity could be observed between 1s and 1.5s second after the movement onset before the potential returned to baseline. The MRCPs were also significantly stronger expressed on the contralateral side to the executing hand. Interestingly, it could be shown that for the bimanual conditions, the “Bereitschaftspotential” was pronounced stronger than for unimanual conditions. Though this difference was not significant on group level, it could be observed for two

thirds of the study participants (n=15). No significant lateralization effects could be found, which proved to be beneficial when it came to decoding between unimanual and bimanual conditions: While binary classification results between unimanual conditions of the same and or between both bimanual conditions yielded results around 68%, combinations involving a unimanual and a bimanual condition yielded results between 74% and 77% (61.4%, adjusted Wald interval [181,182]). Against the rest condition, all movement conditions yielded decoding accuracies between 80% and 90% whereas decoding accuracies for bimanual conditions yielded best results around 87%). Findings on unimanual level go in line with previous findings already presented in this thesis [179] and from other groups [199, 204, 205]. However, the investigations of bimanual reach-and-grasp actions in the LFTD, especially towards objects of daily life, represents a unique feature which has not been assessed in literature.

When compared to the field of MI-based BCIs, where control is often established by repeated mental imagery of a movement task (e.g. unimanually squeezing a training ball, plantar flexion/extension of BCI feet) not only unimanual conditions have been investigated [24, 206, 207], but also bimanual control modalities were tested: Probably best known and popular approach is the experiment by LaFleur and colleagues, who showed the successful control of a quadcopter along a predetermined flight plan in three dimensional space [208] using unimanual and bimanual repetitive movement for control. In a similar approach from the same group, Meng et al. utilized continuous repetitive motor imagery of left hand, right hand and both hand movements as well as relaxation (rest) to control a robotic arm in 3 dimensional space [209]. The 4 conditions corresponded to left, right, up and down movements. Using these commands, study participants (n=13) were able to perform reach-and-grasp actions with the robotic arm. Recently, Vuckovic and colleagues investigated unimanual and bimanual hand movements (slowly waving the designated hand(s) for 3 s) and incorporating analysis of brain oscillations in alpha, beta and gamma range for both executed and imagined movements [195]. Their decoding attempt based on common spatial patterns (CSP) [210] and linear discriminant analysis (LDA) [129] yielded binary classification results between 63% and 75%.

Though MI-based BCIs show promising decoding results and are within the same range of the studies presented in this thesis, they do still rely on repetitive movement executions/imaginings which often do not represent the task at hand. In this way the relation to a natural/intuitive movement control is lost and the command eventually feels unnatural for the user.

#### **3.1.4 Decoding of unimanual and bimanual reach-and-attempted grasp of an tetraplegic end user**

In an attempt to transfer the findings of [183] to motor impaired end users, a proof-of-concept study in one tetraplegic end user was initiated (see section 2.2.2). Aware that the study participant was able to move shoulder and arms but had no voluntary wrist/hand function anymore, the study protocol was adapted accordingly: He was instructed to perform self-initiated executed reaching-and-attempted grasp movement towards the objects presented on the table. Though this combination of executed and attempted movements

has not been evaluated or reported in literature, findings by Blokland et al. [185,211] as well as Rastogi et al. [212] confirmed that attempted movements provide a similar neural representation to that of executed movements. In this context, also Ofner et al. [184] not only investigated attempted arm and hand movements of tetraplegic SCI end users and could show that discriminative information between 5 hand/grasping movements (hand open, palmar grasp, lateral grasp, pronation/supination) can be found in the LFTD: In additional proof-of-concept study they could show that even decoding of self-paced hand open versus hand closing is possible.

In the current study, the EEG correlates of unimanual reach-and-attempted grasp conditions of the tetraplegic study participant were similar in morphology and location to those of able bodied shown in this thesis [179,183]. However, unlike the findings presented in section 2.2.1, EEG correlates of the bimanual conditions were not comparable to previous findings because of significant differences in morphology. The most obvious explanation for this could be the study participants deviation from the given protocol: Instead of simultaneously reaching and attempting to grasp the designated objects with both hands, the study participant performed the task in a slight sequential order. The reason for this deviation was that the tetraplegic study participant did not possess enough torso stability to simultaneously reach forward with both arms without risking tilting forwards. As an additional effect, EEG correlates of bimanual conditions bore more discriminable information against unimanual reach-and-attempted grasp movements than anticipated, thus leading to favourable multiclass classification results. Hence, overall decoding results (single trial, multiclass) exceeded participant specific results reported in [183] by almost 30% for the calibration set and at 8% for the test set.

Additionally, the study participant compensated the lack of voluntary wrist/hand movement capabilities by overly pronouncing elbow and shoulder movements. Hence, despite rigorous artefact handling identically to [183], one cannot rule out that these movements had an additional effect on the movement decoding and one needs to take this into account when interpreting these results.

Nevertheless it could be successfully shown that the combination of an executed reaching with attempted grasping movement can be decoded using features of EEGs LFTD. The findings presented in this proof-of-concept stand on their own, so far no similar attempts involving reach-and-attempted grasp action can be found in literature. The next logical step would be to implement a study on a larger scale of tetraplegic end users including a closely tailored setup based on the end users capabilities.

## 3.2 Boosting decoding performance

To assess whether features on the frequency domain would help increasing decoding accuracies, an offline study on the unimanual data presented in section 2.2.1 was performed: The primary hypothesis was that an extension of the features to include power based features of the frequency domain of alpha and beta range significantly improves overall decoding performance (see section 2.2.3, [197]). Investigations performed by Jochum-

sen and colleagues have already shown that the inclusion of similar features lead to an increased decoding performance for grasp intention [199]. Results shown in section 2.2.3 [197] could not only confirm the findings of Jochumsen and colleagues for the pre movement phase. Moreover, they also showed for the movement conditions and the rest condition significantly better decoding performance than with the LFTD features only. In fact, the combination of both feature spaces increased the average decoding performance by almost 10%. The biggest benefactor was the rest condition with an increased TPR of more than 13%. This is of particular importance, since in a continuous decoding scenario, e.g. it is imperative first to discriminate between movement versus rest rather than decoding movement versus movement. Eventually, decoding performance reached on average 75% for the 3 class scenario (2 grasp, 1 rest condition, adjusted chance level 38.9%, [181,182]). Analysis of the Fischer score [198] performed on the extracted features revealed that for the LFTD features the majority discriminable information is located over the central motor cortex. For the frequency domain features, large contributions could also be found again over the motor cortex. Notably for alpha band based features, strong contributions could be found over the occipital cortex, especially for movement versus rest conditions which can be attributed to increased alpha oscillations during rest periods [83]. The findings of Jochumsen et al as well as the results of this offline study confirm that additional discriminable information can be found in the frequency domain, especially from alpha and beta bands. Though an increase of almost 10% is already notable, it seems possible that further investigations incorporating state of the art processing methods [210,213–215] could further improve performance.

Findings shown in sections 2.1.2 and 2.2.1 indicated a significant performance loss when transferring classification models from offline to an unseen (online) data set. Possible reasons for this are ranging from EEG based nonstationarities elicited through e.g. fatigue, user expectations when receiving feedback or even through feedback presentation itself.

Especially in [180], where study participants attempted to gain online control over a robotic arm in a simulation environment [180], drop in performance was higher than 10%. Though in this particular case an additional confounder was the use of a virtual movement onset rather than a real movement onset, post hoc analysis showed that this accounted only 50% of the performance loss. A possible future solution to minimize this loss could be found in the use of a co-adaptive classification approach [216–218]: When utilizing a co-adaptive training approach, both machine and user are engaged in a mutual learning environment. The user receives feedback based on his actions already minutes after start of BCI use, while the machine is trained/adapted in recurrent training intervals based on the additional data of the user - even during online use. In this way the BCI is not only finitely capable to adjust and contradict EEG nonstationarities such as fatigue or changes in channel impedance, but also eases the offline-to-online transition. Strictly speaking, through the continuous adaptation including real time feedback, this transition is omitted. Studies by Vidaurre et al. as well as Faller et al. have successfully shown in ERD based BCIs and motor imagery the feasibility of the concept in both abled and motor impaired populations [219,220]. In addition, this con-

cept has also been applied and improved by Schwarz and colleagues [78] and extended by an semi-supervised approach, where the BCI is able to perform recurrent updates even with unlabeled data [221]. Efforts should be made to assess the feasibility of the combination of co-adaptive BCIs and MRCP based features.

### **3.3 Limitations of this thesis**

#### **3.3.1 On the decoding performance**

This thesis primary goal was to identify EEG correlates in the LFTD which are associated with grasp/reach-and-grasp actions of daily life and evaluate their decoding potential on a single trial basis. Although EEG correlates could be identified and eventually decoded, the decoding performance is rather low. In the previous section, it was already discussed on how to boost this performance by extending the feature space, or as a future prospect, introducing co-adaptive training approaches. However, decoding approaches conducted within this thesis rarely exceed peak performances of 75-80% on a single subject basis and are comparable with current findings from other groups [111, 199, 205]. They are also within the same range as performances reported of MI-based BCIs [74, 206, 222]. Hence the prospects for enabling an tetraplegic end user to BCI control e.g. an upper limb motor neuroprosthesis, on a direct control basis are rather wanting. Moreover, current decoding performances would at least fail to recognize the intended command in one fourth of a time, or even worse, put the end user in a potential dangerous situation (e.g. spilling hot coffee over his body). Additionally, results from Ofner and colleagues' study regarding asynchronous decoding of attempted hand movements suggests not only an even lower decoding performance ( 68%) but also a false positive detection rate of around 4 false detections per minute [184].

Therefore, the approach presented in this thesis still contains considerable challenges regarding boosting performance to overcome, before a direct BCI control of assistive devices is conceivable.

#### **3.3.2 On the Suitability of MRCPs**

MRCPs are a time-locked and phase-locked response in brain activity to an internal or external cue. The experiments presented in this thesis were time-locked to the movement onset, which was determined with external sensors (e.g. pressure button, data glove, force sensor). As such, a successful detection and decoding always relied on an external reference point and not solely on EEG data. In this way a narrow decoding window could be defined which the classification model used to come to a decision. However, when one attempts to develop a decoder for asynchronous online use, this approach is not feasible anymore: An asynchronous decoder continuously evaluates users' brain signals and attempts to predict their intention. As such, it cannot rely on a reference point anymore, which represents an additional challenge to this approach which is not yet solved [184].

The morphology of MRCPs is influenced by factors such as the level of intention, the preparatory state, movement force and speed (investigated by [113,223]) or the type of movement - e.g. lower limb movements elicit stronger MRCPs than upper limb movements (see [108] for a detailed list of influencing factors). As such, these influences on MRCPs pose additional challenges to any decoding approach: For instance, based on the findings described in [108,113] it is conceivable that a decoder trained on executed reach-and-grasp actions decreases in performance or is even unusable anymore if these actions are performed with a different speed or state of user attention.

In this thesis, MRCPs were extracted from the LFTD, concretely within the range of 0.3-3Hz. Consequently, they are easily masked/contaminated by evoked potentials elicited by external stimuli (auditory, visually, tactile) or ocular based artefacts such as saccades or blinks. While careful experimental planning and state-of-the-art rejection and correction methods (e.g. EOG subspace subtraction or outlier rejection based on statistical parameters [191,219]) can minimize masking/contamination, it is still unknown on how to transfer this to an end users' daily life setting. Especially correction of ocular based activity usually requires sensors positioned near the eyes which represents a challenge for both practical and aesthetic reasons in daily life.

### **3.4 Conclusion**

This thesis identified and evaluated EEG correlates which are associated with natural grasp/reach-and-grasp actions as they are performed in actions of daily life. It could further be shown that these correlates could be decoded against each other and against a rest condition. In addition, their decoding potential has been assessed online using a non-invasive brain-computer interface, where able bodied study participants gained control over a virtual robotic arm in a simulation environment.

Based on the experiences with tetraplegic spinal cord injured end users, who also strongly rely on their second hand in supporting functions, investigations were extended towards bimanual reach-and-grasp actions. It could further be shown that EEG correlates of bimanual reach-and-grasp actions are significantly different from their unimanual counterparts and as such also decodable. Lastly, a non-published proof-of-concept study in one tetraplegic SCI study participant could show that unimanual and bimanual executed reach-and-attempted grasp actions show en grosse similar EEG correlates to those of able bodied participants and were decodable. Though results of this proof-of-concept study need to be confirmed in a larger population, a successful transfer to end users might one day be possible.

### **3.5 Outlook - Towards a successful transfer to end user**

Based on the findings of this thesis, the main focus for future investigations clearly lies on further developing a BCI-based motor control for severely motor impaired users. A suitable device would be an upper limb motor neuroprosthesis [22], since it naturally supports all investigated conditions and can be closely tailored to end users' needs.

Furthermore the combination between a BCI which is able to decode grasp/reach-and-grasp actions combined with the neuroprosthesis which enables end users basic grasping with their own (paralysed) arm is both natural and intuitive. However, for a successful transfer to end users, several challenges have to be taken into account:

(i) Although the potential target group for this technology are tetraplegic SCI end users, their movement capabilities have to be assessed, since residual upper limb functions vary (see “The MoreGrasp feasibility study, [152]). For a successful appliance, end users are required not only to be able to generate discriminable brain patterns, but also need to be able to fulfill the requirements for the designated motor neuroprosthesis. As such, voluntary control of the elbow and the shoulder to execute aimed reaching movements would be required.

(ii) In section 2.2.2, it was already shown that the combination of executed reach-and-attempted grasp movements (both unimanual and bimanual) can be successfully decoded from the EEG of a tetraplegic end user. However further investigations in a larger population are necessary to confirm these findings. In addition, additional steps have to be made to increase the decoding performance (as described previously), before a successful transition to an end user can be made. As a first step, the neuroprosthesis could be fitted with an additional immersive measurement unit (IMU), which in turn supports the BCI with a reference point for a movement onset.

(iii) State-of-the-art EEG recording devices are mobile enough to allow usage outside the lab, even at end users’ home on a daily life basis [52, 152]. Advances within the MoreGrasp project ([152, 224] <http://www.MoreGrasp.eu>), which investigated a the appliance of a multimodal neuroprosthesis for spinal cord injured end users could already show that all required hardware (EEG recording, computational unit, user interface (tablet) and neuroprosthesis) could be mounted on a wheelchair. However, state-of the art smartphones already provide enough performance to process and decode EEG data in real time which allows an even greater degree of miniaturization [225]. The simulation environment used in the experimental setup of 2.1.2 was already designed to be operable on mobile devices [180], and can be closely tailored to the movement capabilities of end users. Another benefit of the simulation environment is that users are already interacting with objects of daily life rather than reacting to abstract cues. Hence it will allow a smoother transition between training and real life application.

iv.) Lastly, it is imperative that end users are compliant and satisfied with the technology provided. While this goes along with high performance and reliability of the assistive device, appearance of and appealing to end users are factors not to be underestimated. It has already been shown in section 2.1.1, [179], that there is no significant difference in decoding performance between recording 64 EEG sensors distributed over the whole scalp and 25 channels located over sensorimotor areas. As such, future EEG sets intended for end user motor control could be designed in a less prominent fashion, and even be appealing to end users.

## Bibliography

- [1] V. W. Lin and C. M. Bono, *Spinal Cord Medicine, Second Edition: Principles & Practice*. Springer Publishing Company, Mar. 2010.
- [2] J. W. McDonald and C. Sadowsky, “Spinal-cord injury,” *The Lancet*, vol. 359, no. 9304, pp. 417–425, 2002.
- [3] G. A. Donnan, M. Fisher, M. Macleod, and S. M. Davis, “Stroke,” *The Lancet*, vol. 371, no. 9624, pp. 1612–1623, 2008.
- [4] J. P. Mohr, P. A. Wolf, M. A. Moskowitz, M. R. Mayberg, and R. Von Kummer, *Stroke E-Book: Pathophysiology, Diagnosis, and Management*. Elsevier Health Sciences, May 2011.
- [5] E. Odding, M. E. Roebroek, and H. J. Stam, “The epidemiology of cerebral palsy: incidence, impairments and risk factors,” *Disabil. Rehabil.*, vol. 28, pp. 183–191, Feb. 2006.
- [6] M. Pugliatti, G. Rosati, H. Carton, T. Riise, J. Drulovic, L. Vécsei, and I. Milanov, “The epidemiology of multiple sclerosis in europe,” *Eur. J. Neurol.*, vol. 13, pp. 700–722, July 2006.
- [7] D. Petrov, C. Mansfield, A. Moussy, and O. Hermine, “ALS clinical trials review: 20 years of failure. are we any closer to registering a new treatment?,” *Front. Aging Neurosci.*, vol. 9, p. 68, Mar. 2017.
- [8] L. C. Wijesekera and P. N. Leigh, “Amyotrophic lateral sclerosis,” *Orphanet J. Rare Dis.*, vol. 4, p. 3, Feb. 2009.
- [9] E. R. Coleman, R. Moudgal, K. Lang, H. I. Hyacinth, O. O. Awosika, B. M. Kissela, and W. Feng, “Early rehabilitation after stroke: a narrative review,” *Curr. Atheroscler. Rep.*, vol. 19, p. 59, Nov. 2017.
- [10] P. Langhorne, J. Bernhardt, and G. Kwakkel, “Stroke rehabilitation,” *Lancet*, vol. 377, pp. 1693–1702, May 2011.
- [11] A. Feinstein, J. Freeman, and A. C. Lo, “Treatment of progressive multiple sclerosis: what works, what does not, and what is needed,” *Lancet Neurol.*, vol. 14, pp. 194–207, Feb. 2015.
- [12] J. Obrist, “AUVA fallzahlen querschnittlähmung österreich.” <https://www.auva.at/cdscontent/?contentid=10007.790539>, Jan. 2018. Accessed: 2020-5-16.



- [13] GBD 2016 Neurology Collaborators, “Global, regional, and national burden of neurological disorders, 1990-2016: a systematic analysis for the global burden of disease study 2016,” *Lancet Neurol.*, vol. 18, pp. 459–480, May 2019.
- [14] M. E. L. van den Berg, J. M. Castellote, I. Mahillo-Fernandez, and J. de Pedro-Cuesta, “Incidence of spinal cord injury worldwide: a systematic review,” *Neuroepidemiology*, vol. 34, pp. 184–92, Feb. 2010.
- [15] G. J. Snoek, M. J. IJzerman, H. J. Hermens, D. Maxwell, and F. Biering-Sorensen, “Survey of the needs of patients with spinal cord injury: impact and priority for improvement in hand function in tetraplegics,” *Spinal Cord*, vol. 42, pp. 526–532, Sept. 2004.
- [16] K. D. Anderson, “Targeting recovery: priorities of the spinal cord-injured population,” *J. Neurotrauma*, vol. 21, pp. 1371–1383, Oct. 2004.
- [17] Y. Namrata, “Priorities of spinal cord injured population – a survey,” *American Journal of Applied Psychology*, vol. 6, no. 6, p. 183, 2017.
- [18] C. Leclercq, M.-A. Lemouel, and T. Albert, “Chirurgische funktionsverbesserung an der oberen extremität von tetraplegikern,” *Handchirurgie, Mikrochirurgie und Plastische Chirurgie*, vol. 37, no. 04, pp. 230–237, 2005.
- [19] Medical-Research-Council, “War memorandum no.7: Aids to the investigation of peripheral nerve injuries,” *Med. Res. Council, London*, 1942.
- [20] World Health Organisation, “WHO on assistive technologies.” <https://www.who.int/disabilities/technology/en/>. Accessed: 2020-5-16.
- [21] A. Cook, J. Polgar, and P. Encarnacao, *Assistive Technologies, Principle and Practice*. Elsevier, Dec 2019.
- [22] R. Rupp and H. J. Gerner, “Neuroprosthetics of the upper extremity - clinical application in spinal cord injury and challenges for the future,” *Operative Neuro-modulation*, pp. 419–426, 2007.
- [23] K. L. Kilgore, H. A. Hoyen, A. M. Bryden, R. L. Hart, M. W. Keith, and P. H. Peckham, “An implanted upper-extremity neuroprosthesis using myoelectric control,” *J. Hand Surg. Am.*, vol. 33, pp. 539–550, Apr. 2008.
- [24] J. R. Wolpaw, N. Birbaumer, D. J. McFarland, G. Pfurtscheller, and T. M. Vaughan, “Brain–computer interfaces for communication and control,” *Clin. Neurophysiol.*, vol. 113, pp. 767–791, June 2002.
- [25] T. Hastie, R. Tibshirani, and J. Friedman, *The Elements of Statistical Learning: Data Mining, Inference, and Prediction, Second Edition*. Springer Science & Business Media, Aug. 2009.

- [26] F. Lotte, M. Congedo, A. Lécuyer, F. Lamarche, and B. Arnaldi, “A review of classification algorithms for EEG-based brain–computer interfaces,” *J. Neural Eng.*, vol. 4, p. R1, Jan. 2007.
- [27] F. Lotte, L. Bougrain, A. Cichocki, M. Clerc, M. Congedo, A. Rakotomamonjy, and F. Yger, “A review of classification algorithms for EEG-based brain-computer interfaces: a 10 year update,” *J. Neural Eng.*, vol. 15, p. 031005, June 2018.
- [28] C. Brunner, N. Birbaumer, B. Blankertz, C. Guger, A. Kübler, D. Mattia, J. del R. Millán, F. Miralles, A. Nijholt, E. Opisso, N. Ramsey, P. Salomon, and G. R. Müller-Putz, “BNCI horizon 2020: towards a roadmap for the BCI community,” *Brain-Computer Interfaces*, vol. 2, no. 1, pp. 1–10, 2015.
- [29] N. Birbaumer, N. Ghanayim, T. Hinterberger, I. Iversen, B. Kotchoubey, A. Kübler, J. Perelmouter, E. Taub, and H. Flor, “A spelling device for the paralysed,” *Nature*, vol. 398, pp. 297–298, Mar. 1999.
- [30] A. Pinegger, H. Hiebel, S. C. Wriessnegger, and G. R. Müller-Putz, “Composing only by thought: Novel application of the P300 brain-computer interface,” *PLoS One*, vol. 12, p. e0181584, Sept. 2017.
- [31] B. Obermaier, G. R. Müller, and G. Pfurtscheller, ““virtual keyboard” controlled by spontaneous EEG activity,” *IEEE Transactions on Neural Systems and Rehabilitation Engineering*, vol. 11, no. 4, pp. 422–426, 2003.
- [32] J. d. R. Millán, R. Rupp, G. Mueller-Putz, R. Murray-Smith, C. Giugliemma, M. Tangermann, C. Vidaurre, F. Cincotti, A. Kubler, R. Leeb, C. Neuper, K. Mueller, and D. Mattia, “Combining brain–computer interfaces and assistive technologies: State-of-the-art and challenges,” *Frontiers in Neuroscience*, vol. 4, p. 161, 2010.
- [33] G. R. Müller-Putz, R. Scherer, G. Pfurtscheller, and R. Rupp, “EEG-based neuroprosthesis control: a step towards clinical practice,” *Neurosci. Lett.*, vol. 382, pp. 169–174, Apr. 2005.
- [34] G. R. Müller-Putz, R. Scherer, G. Pfurtscheller, and others, “Brain-computer interfaces for control of neuroprostheses: from synchronous to asynchronous mode of operation/Brain-Computer interfaces zur steuerung von ...,” *Biomed. Tech.*, 2006.
- [35] G. Pfurtscheller, G. R. Müller, J. Pfurtscheller, H. J. Gerner, and R. Rupp, ““thought”–control of functional electrical stimulation to restore hand grasp in a patient with tetraplegia,” *Neurosci. Lett.*, vol. 351, no. 1, pp. 33–36, 2003.
- [36] N. Mrachacz-Kersting, S. R. Kristensen, I. K. Niazi, and D. Farina, “Precise temporal association between cortical potentials evoked by motor imagination and afference induces cortical plasticity,” *The Journal of Physiology*, vol. 590, no. 7, pp. 1669–1682, 2012.

- [37] N. Mrachacz-Kersting, N. Jiang, A. J. T. Stevenson, I. K. Niazi, V. Kostic, A. Pavlovic, S. Radovanovic, M. Djuric-Jovicic, F. Agosta, K. Dremstrup, and D. Farina, “Efficient neuroplasticity induction in chronic stroke patients by an associative brain-computer interface,” *J. Neurophysiol.*, vol. 115, pp. 1410–1421, Mar. 2016.
- [38] N. Mrachacz-Kersting, N. Jiang, K. Dremstrup, and D. Farina, “A novel Brain-Computer interface for chronic stroke patients,” *Brain-Computer Interface Research*, pp. 51–61, 2014.
- [39] A. Biasiucci, R. Leeb, I. Iturrate, S. Perdakis, A. Al-Khodairy, T. Corbet, A. Schnider, T. Schmidlin, H. Zhang, M. Bassolino, D. Viceic, P. Vuadens, A. Gugisberg, and J. d. R. Millan, “Brain-actuated functional electrical stimulation elicits lasting arm motor recovery after stroke,” *Nature Communications*, vol. 9, 06 2018.
- [40] K. K. Ang, C. Guan, K. S. Phua, C. Wang, L. Zhou, K. Y. Tang, G. J. Ephraim Joseph, C. W. K. Kuah, and K. S. G. Chua, “Brain-computer interface-based robotic end effector system for wrist and hand rehabilitation: results of a three-armed randomized controlled trial for chronic stroke,” *Frontiers in Neuroengineering*, vol. 7, p. 30, 2014.
- [41] A. Ramos-Murguialday, D. Broetz, M. Rea, L. Laeer, O. Yilmaz, F. L. Brasil, G. Liberati, M. R. Curado, E. Garcia-Cossio, A. Vyziotis, W. Cho, M. Agostini, E. Soares, S. Soekadar, A. Caria, L. G. Cohen, and N. Birbaumer, “Brain-machine interface in chronic stroke rehabilitation: A controlled study,” *Annals of Neurology*, vol. 74, no. 1, pp. 100–108, 2013.
- [42] F. Pichiorri, G. Morone, M. Petti, J. Toppi, I. Pisotta, M. Molinari, S. Paolucci, M. Inghilleri, L. Astolfi, F. Cincotti, and D. Mattia, “Brain-computer interface boosts motor imagery practice during stroke recovery,” *Annals of Neurology*, vol. 77, no. 5, pp. 851–865, 2015.
- [43] T. O. Zander, C. Kothe, S. Welke, and M. Roetting, “Utilizing secondary input from passive Brain-Computer interfaces for enhancing Human-Machine interaction,” *Foundations of Augmented Cognition. Neuroergonomics and Operational Neuroscience*, pp. 759–771, 2009.
- [44] T. O. Zander and C. Kothe, “Towards passive brain-computer interfaces: applying brain-computer interface technology to human-machine systems in general,” *J. Neural Eng.*, vol. 8, p. 025005, Apr. 2011.
- [45] L. George and A. Lécuyer, “An overview of research on ”passive” brain-computer interfaces for implicit human-computer interaction,” in *International Conference on Applied Bionics and Biomechanics ICABB 2010 - Workshop W1 ”Brain-Computer Interfacing and Virtual Reality”*, (Venise, Italy), Oct. 2010.

- [46] P. Gerjets, C. Walter, W. Rosenstiel, M. Bogdan, and T. O. Zander, “Cognitive state monitoring and the design of adaptive instruction in digital environments: lessons learned from cognitive workload assessment using a passive brain-computer interface approach,” *Frontiers in Neuroscience*, vol. 8, p. 385, 2014.
- [47] J. d. R. Milan, J. del R. Milan, and J. Carmena, “Invasive or noninvasive: Understanding Brain-Machine interface technology [conversations in BME],” *IEEE Engineering in Medicine and Biology Magazine*, vol. 29, no. 1, pp. 16–22, 2010.
- [48] H. Berger, “Über das Elektrenkephalogramm des Menschen,” *Eur. Arch. Psychiatry Clin. Neurosci.*, vol. 98, no. 1, pp. 231–254, 1933.
- [49] A. Ebner and G. Deuschl, *EEG (Referenzreihe Neurologie)*. Georg Thieme Verlag, Oct. 2010.
- [50] G. Buzsáki, C. A. Anastassiou, and C. Koch, “The origin of extracellular fields and currents — EEG, ECoG, LFP and spikes,” *Nature Reviews Neuroscience*, vol. 13, no. 6, pp. 407–420, 2012.
- [51] D. L. Schomer and F. H. L. da Silva, *Niedermeyer’s Electroencephalography: Basic Principles, Clinical Applications, and Related Fields*. Lippincott Williams & Wilkins, 2011.
- [52] A. Pinegger, S. C. Wriessnegger, J. Faller, and G. R. Müller-Putz, “Evaluation of different EEG acquisition systems concerning their suitability for building a Brain-Computer interface: Case studies,” *Front. Neurosci.*, vol. 10, p. 401, Sept. 2016.
- [53] M. Hämäläinen, R. Hari, R. J. Ilmoniemi, J. Knuutila, and O. V. Lounasmaa, “Magnetoencephalography—theory, instrumentation, and applications to noninvasive studies of the working human brain,” *Rev. Mod. Phys.*, vol. 65, no. 2, p. 413, 1993.
- [54] E. Buch, C. Weber, L. G. Cohen, C. Braun, M. A. Dimyan, T. Ard, J. Mellinger, A. Caria, S. Soekadar, A. Fourkas, and N. Birbaumer, “Think to move: a neuromagnetic brain-computer interface (BCI) system for chronic stroke,” *Stroke*, vol. 39, pp. 910–917, Mar. 2008.
- [55] J. Mellinger, G. Schalk, C. Braun, H. Preissl, W. Rosenstiel, N. Birbaumer, and A. Kübler, “An MEG-based brain-computer interface (BCI),” *Neuroimage*, vol. 36, pp. 581–593, July 2007.
- [56] R. Sitaram, H. Zhang, C. Guan, M. Thulasidas, Y. Hoshi, A. Ishikawa, K. Shimizu, and N. Birbaumer, “Temporal classification of multichannel near-infrared spectroscopy signals of motor imagery for developing a brain-computer interface,” *Neuroimage*, vol. 34, pp. 1416–1427, Feb. 2007.

- [57] S. M. Coyle, T. E. Ward, and C. M. Markham, “Brain–computer interface using a simplified functional near-infrared spectroscopy system,” *J. Neural Eng.*, vol. 4, p. 219, Apr. 2007.
- [58] N. Naseer and K.-S. Hong, “fNIRS-based brain-computer interfaces: a review,” *Front. Hum. Neurosci.*, vol. 9, p. 3, Jan. 2015.
- [59] G. Bauernfeind, R. Scherer, G. Pfurtscheller, and C. Neuper, “Single-trial classification of antagonistic oxyhemoglobin responses during mental arithmetic,” *Medical and biological engineering and computing*, vol. 49, pp. 979–84, 06 2011.
- [60] V. Kaiser, G. Bauernfeind, A. Kreilinger, T. Kaufmann, A. Kübler, C. Neuper, and G. Müller-Putz, “Cortical effects of user training in a motor imagery based brain–computer interface measured by fnirs and eeg,” *NeuroImage*, vol. 85, 05 2013.
- [61] R. J. Huster, S. Debener, T. Eichele, and C. S. Herrmann, “Methods for simultaneous EEG-fMRI: an introductory review,” *J. Neurosci.*, vol. 32, pp. 6053–6060, May 2012.
- [62] E. R. Kandel, J. H. Schwartz, and T. M. Jessell, *Principles of neuroscience. 2000*. New York: McGraw-Hill, 2000.
- [63] E. C. Leuthardt, G. Schalk, J. R. Wolpaw, J. G. Ojemann, and D. W. Moran, “A brain–computer interface using electrocorticographic signals in humans,” *Journal of Neural Engineering*, vol. 1, no. 2, pp. 63–71, 2004.
- [64] G. Schalk and E. C. Leuthardt, “Brain-Computer interfaces using electrocorticographic signals,” *IEEE Reviews in Biomedical Engineering*, vol. 4, pp. 140–154, 2011.
- [65] B. Graimann, J. E. Huggins, A. Schlögl, S. P. Levine, and G. Pfurtscheller, “Detection of movement-related desynchronization patterns in ongoing single-channel electrocorticogram,” *IEEE Trans. Neural Syst. Rehabil. Eng.*, vol. 11, pp. 276–281, Sept. 2003.
- [66] W. Wang, A. D. Degenhart, J. L. Collinger, R. Vinjamuri, G. P. Sudre, P. D. Adelson, D. L. Holder, E. C. Leuthardt, D. W. Moran, M. L. Boninger, A. B. Schwartz, D. J. Crammond, E. C. Tyler-Kabara, and D. J. Weber, “Human motor cortical activity recorded with Micro-ECOG electrodes, during individual finger movements,” *Conf. Proc. IEEE Eng. Med. Biol. Soc.*, vol. 2009, pp. 586–589, 2009.
- [67] E. E. Fetz, “Operant conditioning of cortical unit activity,” *Science*, vol. 163, pp. 955–958, Feb. 1969.

- [68] E. M. Maynard, C. T. Nordhausen, and R. A. Normann, “The utah intracortical electrode array: a recording structure for potential brain-computer interfaces,” *Electroencephalogr. Clin. Neurophysiol.*, vol. 102, pp. 228–239, Mar. 1997.
- [69] L. R. Hochberg, M. D. Serruya, G. M. Friehs, J. A. Mukand, M. Saleh, A. H. Caplan, A. Branner, D. Chen, R. D. Penn, and J. P. Donoghue, “Neuronal ensemble control of prosthetic devices by a human with tetraplegia,” *Nature*, vol. 442, pp. 164–171, July 2006.
- [70] G. Pfurtscheller, C. Brunner, A. Schlögl, and F. Lopes da Silva, “Mu rhythm (de)synchronization and eeg single-trial classification of different motor imagery tasks,” *NeuroImage*, vol. 31, no. 1, pp. 153 – 159, 2006.
- [71] G. Pfurtscheller and A. Aranibar, “Event-related cortical desynchronization detected by power measurements of scalp EEG,” *Electroencephalogr. Clin. Neurophysiol.*, vol. 42, pp. 817–826, June 1977.
- [72] G. Pfurtscheller and A. Aranibar, “Evaluation of event-related desynchronization (ERD) preceding and following voluntary self-paced movement,” *Electroencephalogr. Clin. Neurophysiol.*, vol. 46, pp. 138–146, Feb. 1979.
- [73] G. Pfurtscheller and F. H. L. da Silva, “Event-related EEG/MEG synchronization and desynchronization: basic principles,” *Clinical Neurophysiology*, vol. 110, no. 11, pp. 1842–1857, 1999.
- [74] G. Pfurtscheller and C. Neuper, “Motor imagery and direct brain-computer communication,” *Proc. IEEE*, vol. 89, no. 7, pp. 1123–1134, 2001.
- [75] R. Scherer and C. Vidaurre, “Motor imagery based brain-computer interfaces,” *Smart Wheelchairs and Brain-Computer Interfaces*, pp. 171–195, 2018.
- [76] E. V. C. Friedrich, C. Neuper, and R. Scherer, “Whatever works: a systematic user-centered training protocol to optimize brain-computer interfacing individually,” *PLoS One*, vol. 8, p. e76214, Sept. 2013.
- [77] B. Graimann, J. E. Huggins, S. P. Levine, and G. Pfurtscheller, “Visualization of significant ERD/ERS patterns in multichannel EEG and ECoG data,” *Clin. Neurophysiol.*, vol. 113, pp. 43–47, Jan. 2002.
- [78] A. Schwarz, R. Scherer, D. Steyrl, J. Faller, and G. R. Muller-Putz, “A co-adaptive sensory motor rhythms Brain-Computer interface based on common spatial patterns and random forest,” *Conf. Proc. IEEE Eng. Med. Biol. Soc.*, vol. 2015, pp. 1049–1052, Aug. 2015.
- [79] A. Kübler, F. Nijboer, J. Mellinger, T. M. Vaughan, H. Pawelzik, G. Schalk, D. J. McFarland, N. Birbaumer, and J. R. Wolpaw, “Patients with ALS can use sensorimotor rhythms to operate a brain-computer interface,” *Neurology*, vol. 64, pp. 1775–1777, May 2005.

- [80] G. Pfurtscheller, C. Guger, G. Müller, G. Krausz, and C. Neuper, “Brain oscillations control hand orthosis in a tetraplegic,” *Neurosci. Lett.*, vol. 292, pp. 211–214, Oct. 2000.
- [81] B. Blankertz, C. Sanelli, S. Halder, E. Hammer, A. Kübler, K.-R. Müller, G. Curio, and T. Dickhaus, “Predicting BCI performance to study BCI illiteracy,” *BMC Neurosci.*, vol. 10, no. Suppl 1, p. P84, 2009.
- [82] J. D. Kropotov, *Functional Neuromarkers for Psychiatry: Applications for Diagnosis and Treatment*. Academic Press, May 2016.
- [83] S. Luck and E. Kappenman, “The Oxford Handbook of Event-Related potential components,” in *The Oxford Handbook of Event-Related Potential Components*, Oxford University Press, 1 ed., Dec. 2011.
- [84] L. A. Farwell and E. Donchin, “Talking off the top of your head: toward a mental prosthesis utilizing event-related brain potentials,” *Electroencephalogr. Clin. Neurophysiol.*, vol. 70, pp. 510–523, Dec. 1988.
- [85] S. Halder, A. Pinegger, I. Käthner, S. C. Wriessnegger, J. Faller, J. B. Pires Antunes, G. R. Müller-Putz, and A. Kübler, “Brain-controlled applications using dynamic P300 speller matrices,” *Artif. Intell. Med.*, vol. 63, pp. 7–17, Jan. 2015.
- [86] E. Donchin, K. M. Spencer, and R. Wijesinghe, “The mental prosthesis: assessing the speed of a p300-based brain-computer interface,” *IEEE Trans. Rehabil. Eng.*, vol. 8, pp. 174–179, June 2000.
- [87] C. Guger, S. Daban, E. Sellers, C. Holzner, G. Krausz, R. Carabalona, F. Gramatica, and G. Edlinger, “How many people are able to control a p300-based brain-computer interface (BCI)?,” *Neurosci. Lett.*, vol. 462, pp. 94–98, Sept. 2009.
- [88] D. J. Krusienski, E. W. Sellers, F. Cabestaing, S. Bayouhd, D. J. McFarland, T. M. Vaughan, and J. R. Wolpaw, “A comparison of classification techniques for the P300 speller,” *J. Neural Eng.*, vol. 3, pp. 299–305, Dec. 2006.
- [89] J. I. Münßinger, S. Halder, S. C. Kleih, A. Furdea, V. Raco, A. Hösle, and A. Kübler, “Brain painting: First evaluation of a new Brain-Computer interface application with ALS-Patients and healthy volunteers,” *Front. Neurosci.*, vol. 4, 2010.
- [90] M. Falkenstein, J. Hoormann, S. Christ, and J. Hohnsbein, “ERP components on reaction errors and their functional significance: a tutorial,” *Biol. Psychol.*, vol. 51, pp. 87–107, Jan. 2000.
- [91] M. Falkenstein, J. Hohnsbei, J. Hoormann, and M. Blanke, “Effects of errors in choice reaction tasks on the erp under focused and divided attention,” *Psychophysiol. Brain Res.*, vol. 1, pp. 192–195, 1991.

- [92] P. Ferrez and J. d. R. Millan, “You are wrong!—automatic detection of interaction errors from brain waves,” in *Proceedings of the 19th International Joint Conference on Artificial Intelligence*, pp. 1413–1418, 01 2005.
- [93] C. B. Holroyd and M. G. H. Coles, “The neural basis of human error processing: reinforcement learning, dopamine, and the error-related negativity,” *Psychol. Rev.*, vol. 109, pp. 679–709, Oct. 2002.
- [94] H. T. van Schie, R. B. Mars, M. G. H. Coles, and H. Bekkering, “Modulation of activity in medial frontal and motor cortices during error observation,” *Nat. Neurosci.*, vol. 7, pp. 549–554, May 2004.
- [95] G. Schalk, J. R. Wolpaw, D. J. McFarland, and G. Pfurtscheller, “EEG-based communication: presence of an error potential,” *Clin. Neurophysiol.*, vol. 111, pp. 2138–2144, Dec. 2000.
- [96] A. Kreilinger, C. Neuper, and G. R. Müller-Putz, “Error potential detection during continuous movement of an artificial arm controlled by brain–computer interface,” *Med. Biol. Eng. Comput.*, vol. 50, pp. 223–230, Mar. 2012.
- [97] A. Kreilinger, H. Hiebel, and G. R. Müller-Putz, “Single versus multiple events error potential detection in a BCI-Controlled car game with continuous and discrete feedback,” *IEEE Trans. Biomed. Eng.*, vol. 63, pp. 519–529, Mar. 2016.
- [98] R. Chavarriaga, A. Sobolewski, and J. D. R. Millán, “Errare machinale est: the use of error-related potentials in brain-machine interfaces,” *Front. Neurosci.*, vol. 8, p. 208, July 2014.
- [99] C. Lopes Dias, A. I. Sburlea, and G. R. Müller-Putz, “Masked and unmasked error-related potentials during continuous control and feedback,” *J. Neural Eng.*, vol. 15, p. 036031, June 2018.
- [100] P. W. Ferrez and J. d. R. Millán, “Simultaneous real-time detection of motor imagery and error-related potentials for improved bci accuracy,” *Proceedings of the 4th International Brain-Computer Interface Workshop and Training Course*, pp. 197–202, 2008.
- [101] W. Lutzenberger, T. Elbert, B. Rockstroh, and N. Birbaumer, “The effects of self-regulation of slow cortical potentials on performance in a signal detection task,” *Int. J. Neurosci.*, vol. 9, no. 3, pp. 175–183, 1979.
- [102] T. Hinterberger, S. Schmidt, N. Neumann, J. Mellinger, B. Blankertz, G. Curio, and N. Birbaumer, “Brain-computer communication and slow cortical potentials,” *IEEE Trans. Biomed. Eng.*, vol. 51, pp. 1011–1018, June 2004.
- [103] H. Shibasaki, G. Barrett, E. Halliday, and A. M. Halliday, “Components of the movement-related cortical potential and their scalp topography,” *Electroencephalogr. Clin. Neurophysiol.*, vol. 49, pp. 213–226, Aug. 1980.



- [104] Y. Gu, O. F. do Nascimento, M.-F. Lucas, and D. Farina, “Identification of task parameters from movement-related cortical potentials,” *Med. Biol. Eng. Comput.*, vol. 47, pp. 1257–1264, Dec. 2009.
- [105] H. H. Kornhuber and L. Deecke, “Hirnpotentialänderungen bei Willkürbewegungen und passiven Bewegungen des Menschen: Bereitschaftspotential und reafferente Potentiale,” *Pflüger’s Archiv für die gesamte Physiologie des Menschen und der Tiere*, vol. 284, pp. 1–17, Dec 1964.
- [106] H. H. Kornhuber and L. Deecke, “Hirnpotentialänderungen beim menschen vor und nach willkurbewegungen dargestellt mit magnetbandspeicherung und ruckwärtsanalyse,” in *Pflugers Archiv-European Journal of Physiology*, vol. 281, p. 52, 1964.
- [107] H. H. Kornhuber and L. Deecke, “Brain potential changes in voluntary and passive movements in humans: readiness potential and reafferent potentials,” *Pflugers Arch.*, vol. 468, pp. 1115–1124, July 2016.
- [108] H. Shibasaki and M. Hallett, “What is the Bereitschaftspotential?,” *Clin. Neurophysiol.*, vol. 117, no. 11, pp. 2341–2356, 2006.
- [109] A. Shakeel, M. S. Navid, M. Anwar, S. Mazhar, M. Jochumsen, and I. Niazi, “A review of techniques for detection of movement intention using movement-related cortical potentials,” *Computational and Mathematical Methods in Medicine*, vol. 2015, 12 2015.
- [110] I. K. Niazi, N. Jiang, O. Tiberghien, J. F. Nielsen, K. Dremstrup, and D. Farina, “Detection of movement intention from single-trial movement-related cortical potentials,” *J. Neural Eng.*, vol. 8, p. 066009, Dec. 2011.
- [111] H. A. Agashe, A. Y. Paek, Y. Zhang, and J. L. Contreras-Vidal, “Global cortical activity predicts shape of hand during grasping,” *Front. Neurosci.*, vol. 9, p. 121, Apr. 2015.
- [112] A. I. Sburlea, L. Montesano, R. Cano de la Cuerda, I. M. Alguacil Diego, J. C. Miangolarra-Page, and J. Minguez, “Detecting intention to walk in stroke patients from pre-movement EEG correlates,” *J. Neuroeng. Rehabil.*, vol. 12, p. 113, Dec. 2015.
- [113] M. Jochumsen, I. K. Niazi, N. Mrachacz-Kersting, D. Farina, and K. Dremstrup, “Detection and classification of movement-related cortical potentials associated with task force and speed,” *J. Neural Eng.*, vol. 10, p. 056015, Oct. 2013.
- [114] N. Birbaumer, T. Elbert, A. G. Canavan, and B. Rockstroh, “Slow potentials of the cerebral cortex and behavior,” *Physiol. Rev.*, vol. 70, pp. 1–41, Jan. 1990.

- [115] W. Lutzenberger, T. Elbert, B. Rockstroh, and N. Birbaumer, “Biofeedback produced slow brain potentials and task performance,” *Biol. Psychol.*, vol. 14, pp. 99–111, Feb. 1982.
- [116] H. Gevensleben, B. Albrecht, H. Lütcke, T. Auer, W. I. Dewiputri, R. Schweizer, G. Moll, H. Heinrich, and A. Rothenberger, “Neurofeedback of slow cortical potentials: neural mechanisms and feasibility of a placebo-controlled design in healthy adults,” *Front. Hum. Neurosci.*, vol. 8, p. 990, Dec. 2014.
- [117] D. Regan, “Steady-state evoked potentials,” *J. Opt. Soc. Am.*, vol. 67, pp. 1475–1489, Nov. 1977.
- [118] S. T. Morgan, J. C. Hansen, and S. A. Hillyard, “Selective attention to stimulus location modulates the steady-state visual evoked potential,” *Proc. Natl. Acad. Sci. U. S. A.*, vol. 93, pp. 4770–4774, May 1996.
- [119] M. Middendorf, G. McMillan, G. Calhoun, and K. S. Jones, “Brain-computer interfaces based on the steady-state visual-evoked response,” *IEEE Transactions on Rehabilitation Engineering*, vol. 8, no. 2, pp. 211–214, 2000.
- [120] G. R. Müller-Putz, R. Scherer, C. Brauneis, and G. Pfurtscheller, “Steady-state visual evoked potential (SSVEP)-based communication: impact of harmonic frequency components,” *J. Neural Eng.*, vol. 2, pp. 123–130, Dec. 2005.
- [121] N. J. Hill and B. Schölkopf, “An online brain–computer interface based on shifting attention to concurrent streams of auditory stimuli,” *J. Neural Eng.*, vol. 9, p. 026011, Feb. 2012.
- [122] M.-A. Lopez, H. Pomares, F. Pelayo, J. Urquiza, and J. Perez, “Evidences of cognitive effects over auditory steady-state responses by means of artificial neural networks and its use in brain–computer interfaces,” *Neurocomputing*, vol. 72, pp. 3617–3623, Oct. 2009.
- [123] M. Schreuder, B. Blankertz, and M. Tangermann, “A new auditory multi-class brain-computer interface paradigm: Spatial hearing as an informative cue,” *PLOS ONE*, vol. 5, pp. 1–14, 04 2010.
- [124] C. Breitwieser, C. Pokorny, and G. R. Müller-Putz, “A hybrid three-class brain–computer interface system utilizing SSSEPs and transient ERPs,” *J. Neural Eng.*, vol. 13, p. 066015, Oct. 2016.
- [125] G. Müller-Putz, *New Concepts in Brain-Computer Communication: Use of Steady-State Somatosensory Evoked Potentials, User Training by Telesupport and Control of Functional Electrical Stimulation*. PhD thesis, Graz, University of Technology, 2004.

- [126] G. Müller-Putz, R. Scherer, C. Neuper, and G. Pfurtscheller, “Steady-state somatosensory evoked potentials: Suitable brain signals for brain–computer interfaces?,” *IEEE transactions on neural systems and rehabilitation engineering : a publication of the IEEE Engineering in Medicine and Biology Society*, vol. 14, pp. 30–7, 04 2006.
- [127] W. R. Howard, “Pattern recognition and machine Learning20072Christopher m. bishop. pattern recognition and machine learning. heidelberg, germany: Springer 2006. i-xx, 740 pp., ISBN: 0-387-31073-8 \$74.95 hardcover,” *Kybernetes*, vol. 36, no. 2, pp. 275–275, 2007.
- [128] O. Ledoit and M. Wolf, “A well-conditioned estimator for large-dimensional covariance matrices,” *Journal of Multivariate Analysis*, vol. 88, no. 2, pp. 365–411, 2004.
- [129] B. Blankertz, S. Lemm, M. Treder, S. Haufe, and K.-R. Müller, “Single-trial analysis and classification of ERP components—a tutorial,” *Neuroimage*, vol. 56, no. 2, pp. 814–825, 2011.
- [130] T. Hastie, R. Tibshirani, and J. Friedman, *The Elements of Statistical Learning: Data Mining, Inference, and Prediction*. Springer Science & Business Media, Nov. 2013.
- [131] D. Steyrl, R. Scherer, O. Förstner, and G. R. Müller-Putz, “Motor imagery brain-computer interfaces: random forests vs regularized LDA-non-linear beats linear,” in *Proceedings of the 6th International Brain-Computer Interface Conference*, pp. 241–244, 2014.
- [132] D. Steyrl, R. Scherer, and G. R. Müller-Putz, “Random forests for feature selection in non-invasive Brain-Computer interfacing,” in *Human-Computer Interaction and Knowledge Discovery in Complex, Unstructured, Big Data*, pp. 207–216, Springer Berlin Heidelberg, 2013.
- [133] D. Steyrl, R. Scherer, J. Faller, and G. R. Müller-Putz, “Random forests in non-invasive sensorimotor rhythm brain-computer interfaces: a practical and convenient non-linear classifier,” *Biomed. Tech.*, vol. 61, pp. 77–86, Feb. 2016.
- [134] G. Pfurtscheller, G. R. Müller, J. Pfurtscheller, H. J. Gerner, and R. Rupp, “‘Thought’ – control of functional electrical stimulation to restore hand grasp in a patient with tetraplegia,” *Neuroscience Letters*, vol. 351, no. 1, pp. 33–36, 2003.
- [135] G. Pfurtscheller and T. Solis-Escalante, “Could the beta rebound in the eeg be suitable to realize a “brain switch”?,” *Clinical Neurophysiology*, vol. 120, no. 1, pp. 24 – 29, 2009.

- [136] G. Pfurtscheller, T. Solis-Escalante, R. Ortner, P. Linortner, and G. Müller-Putz, “Self-paced operation of an ssvep-based orthosis with and without an imagery-based “brain switch:” a feasibility study towards a hybrid bci,” *IEEE transactions on neural systems and rehabilitation engineering*, vol. 18, pp. 409–14, 02 2010.
- [137] T. Solis-Escalante, G. Müller-Putz, C. Brunner, V. Kaiser, and G. Pfurtscheller, “Analysis of sensorimotor rhythms for the implementation of a brain switch for healthy subjects,” *Biomedical Signal Processing and Control*, vol. 5, no. 1, pp. 15 – 20, 2010.
- [138] R. Scherer, G. R. Müller, C. Neuper, B. Graimann, and G. Pfurtscheller, “An asynchronously controlled EEG-based virtual keyboard: improvement of the spelling rate,” *IEEE Trans. Biomed. Eng.*, vol. 51, pp. 979–984, June 2004.
- [139] B. Blankertz, G. Dornhege, M. Krauledat, M. Schröder, J. Williamson, R. Murray-Smith, and K.-R. Müller, “The berlin Brain-Computer interface presents the novel mental typewriter Hex-o-Spell,” in *Proceedings of the 3rd International Brain-Computer Interface Workshop and Training Course 2006*, pp. 108–109, 2006.
- [140] R. Scherer, M. Billinger, J. Wagner, A. Schwarz, D. T. Hettich, E. Bolinger, M. Lloria Garcia, J. Navarro, and G. Müller-Putz, “Thought-based row-column scanning communication board for individuals with cerebral palsy,” *Ann. Phys. Rehabil. Med.*, vol. 58, pp. 14–22, Feb. 2015.
- [141] R. Scherer, A. Schwarz, G. R. Müller-Putz, V. Pammer-Schindler, and M. L. Garcia, “Game-Based BCI training: Interactive design for individuals with cerebral palsy,” in *2015 IEEE International Conference on Systems, Man, and Cybernetics*, pp. 3175–3180, Oct. 2015.
- [142] R. Scherer, A. Schwarz, G. R. Müller-Putz, V. Pammer-Schindler, and M. L. Garcia, “Lets play Tic-Tac-Toe: A Brain-Computer interface case study in cerebral palsy,” in *2016 IEEE International Conference on Systems, Man, and Cybernetics (SMC)*, pp. 003736–003741, Oct. 2016.
- [143] G. Townsend, B. Graimann, and G. Pfurtscheller, “Continuous EEG classification during motor imagery–simulation of an asynchronous BCI,” *IEEE Trans. Neural Syst. Rehabil. Eng.*, vol. 12, pp. 258–265, June 2004.
- [144] B. Blankertz, G. Dornhege, M. Krauledat, K.-R. Müller, and G. Curio, “The non-invasive berlin Brain–Computer interface: Fast acquisition of effective performance in untrained subjects,” *Neuroimage*, vol. 37, pp. 539–550, Aug. 2007.
- [145] G. Krausz, R. Scherer, G. Korisek, and G. Pfurtscheller, “Critical decision-speed and information transfer in the Graz brain–computer interface,” *Applied psychophysiology and biofeedback*, vol. 28, pp. 233–40, 10 2003.

- [146] F. Nijboer, A. Furdea, I. Gunst, J. Mellinger, D. J. McFarland, N. Birbaumer, and A. Kübler, “An auditory brain–computer interface (BCI),” *J. Neurosci. Methods*, vol. 167, pp. 43–50, Jan. 2008.
- [147] A. Herweg, J. Gutzeit, S. Kleih, and A. Kübler, “Wheelchair control by elderly participants in a virtual environment with a brain-computer interface (BCI) and tactile stimulation,” *Biol. Psychol.*, vol. 121, pp. 117–124, Dec. 2016.
- [148] P. E. Patterson and J. A. Katz, “Design and evaluation of a sensory feedback system that provides grasping pressure in a myoelectric hand,” *J. Rehabil. Res. Dev.*, vol. 29, no. 1, pp. 1–8, 1992.
- [149] P. Bach-y Rita and S. W Kercel, “Sensory substitution and the human-machine interface,” *Trends Cogn. Sci.*, vol. 7, pp. 541–546, Dec. 2003.
- [150] F. Cincotti, L. Kauhanen, F. Aloise, T. Palomäki, N. Caporusso, P. Jylänki, D. Mattia, F. Babiloni, G. Vanacker, M. Nuttin, M. G. Marciani, and J. del R. Millán, “Vibrotactile feedback for Brain-Computer interface operation,” *Computational Intelligence and Neuroscience*, vol. 2007, pp. 1–12, 2007.
- [151] F. Cincotti, L. Kauhanen, F. Aloise, T. Palomaki, N. Caporusso, P. Jylanki, F. Babiloni, G. Vanacker, M. Nuttin, M. G. Marciani, J. del R. Millan, and D. Mattia, “Preliminary experimentation on vibrotactile feedback in the context of mu-rhythm based BCI,” *2007 29th Annual International Conference of the IEEE Engineering in Medicine and Biology Society*, 2007.
- [152] G. R. Müller-Putz, P. Ofner, J. Pereira, A. Pinegger, A. Schwarz, M. Zube, U. Eck, B. Hessing, M. Schneiders, and R. Rupp, “Applying intuitive EEG-controlled grasp neuroprostheses in individuals with spinal cord injury: Preliminary results from the MoreGrasp clinical feasibility study,” in *2019 41st Annual International Conference of the IEEE Engineering in Medicine and Biology Society (EMBC)*, pp. 5949–5955, July 2019.
- [153] P. H. Peckham, J. T. Mortimer, and E. B. Marsolais, “Controlled prehension and release in the C5 quadriplegic elicited by functional electrical stimulation of the paralyzed forearm musculature,” *Ann. Biomed. Eng.*, vol. 8, no. 4-6, pp. 369–388, 1980.
- [154] T. R. Scott, P. H. Peckham, and M. W. Keith, “Upper extremity neuroprostheses using functional electrical stimulation,” *Baillieres. Clin. Neurol.*, vol. 4, pp. 57–75, Apr. 1995.
- [155] G. Müller-Putz, R. Scherer, G. Pfurtscheller, and R. Rupp, “Eeg-based neuroprosthesis control: A step towards clinical practice,” *Neuroscience letters*, vol. 382, pp. 169–74, 07 2005.

- [156] R. Rupp and H. J. Gerner, “Neuroprosthetics of the upper extremity - clinical application in spinal cord injury and challenges for the future,” *Acta neurochirurgica. Supplement*, vol. 97, pp. 419–26, 02 2007.
- [157] B. Fromm, R. Rupp, and H. J. Gerner, “[the freehand system: an implantable neuroprosthesis for functional electrostimulation of the upper extremity],” *Handchirurgie, Mikrochirurgie, plastische Chirurgie : Organ der Deutschsprachigen Arbeitsgemeinschaft für Handchirurgie*, vol. 33, pp. 149–52, 06 2001.
- [158] J. M. Heasman, T. R. D. Scott, L. Kirkup, R. Y. Flynn, V. A. Vare, and C. R. Gschwind, “Control of a hand grasp neuroprosthesis using an electroencephalogram-triggered switch: demonstration of improvements in performance using wavepacket analysis,” *Med. Biol. Eng. Comput.*, vol. 40, pp. 588–593, Sept. 2002.
- [159] P. H. Peckham, K. L. Kilgore, M. W. Keith, A. M. Bryden, N. Bhadra, and F. W. Montague, “An advanced neuroprosthesis for restoration of hand and upper arm control using an implantable controller,” *J. Hand Surg. Am.*, vol. 27, pp. 265–276, Mar. 2002.
- [160] G. R. Müller-Putz and G. Pfurtscheller, “Control of an electrical prosthesis with an SSVEP-Based BCI,” *IEEE Transactions on Biomedical Engineering*, vol. 55, pp. 361–364, Jan. 2008.
- [161] R. Ortner, B. Z. Allison, G. Korisek, H. Gaggl, and G. Pfurtscheller, “An SSVEP BCI to control a hand orthosis for persons with tetraplegia,” *IEEE Trans. Neural Syst. Rehabil. Eng.*, vol. 19, pp. 1–5, Feb. 2011.
- [162] G. Müller-Putz, R. Scherer, G. Pfurtscheller, and C. Neuper, “Temporal coding of brain patterns for direct limb control in humans,” *Front. Neurosci.*, vol. 4, June 2010.
- [163] M. Tavella, R. Leeb, R. Rupp, and J. D. R. Millan, “Towards natural non-invasive hand neuroprostheses for daily living,” *Conf. Proc. IEEE Eng. Med. Biol. Soc.*, vol. 2010, pp. 126–129, 2010.
- [164] G. R. Müller-Putz, C. Breitwieser, F. Cincotti, M. Leeb, R. amd Schreuder, F. Leotta, M. Tavella, L. Bianchi, A. Kreilinger, A. Ramsay, M. Rohm, M. Sagebaum, L. Tonin, C. Neuper, and J. Millan, “Tools for brain-computer interaction: a general concept for a hybrid BCI,” *Frontiers in Neuroinformatics*, vol. 5, 2011.
- [165] G. Pfurtscheller, B. Z. Allison, C. Brunner, G. Bauernfeind, T. Solis-Escalante, R. Scherer, T. O. Zander, G. Mueller-Putz, C. Neuper, and N. Birbaumer, “The hybrid BCI,” *Front. Neurosci.*, vol. 4, p. 30, Apr. 2010.
- [166] M. Rohm, M. Schneiders, C. Müller, A. Kreilinger, V. Kaiser, G. R. Müller-Putz, and R. Rupp, “Hybrid brain–computer interfaces and hybrid neuroprostheses for

- restoration of upper limb functions in individuals with high-level spinal cord injury,” *Artif. Intell. Med.*, vol. 59, pp. 133–142, Oct. 2013.
- [167] A. Kreiling, M. Rohm, V. Kaiser, R. Leeb, R. Rupp, and G. Müller-Putz, “Neuroprosthesis control via a noninvasive hybrid brain-computer interface,” *Intelligent Systems, IEEE*, vol. 28, 09 2013.
- [168] D. B. Popović and T. Sinkjær, “Central nervous system lesions leading to disability,” *Automatica*, vol. 18, no. 2, pp. 11–23, 2008.
- [169] B. O. Bergum, J. Long, and A. Baddeley, “Attention and performance IX,” *The American Journal of Psychology*, vol. 95, no. 4, p. 706, 1982.
- [170] M. Jeannerod, “The timing of natural prehension,” *J. Mot. Behav.*, vol. 16, pp. 201–211, 1994.
- [171] L. S. Jakobson and M. A. Goodale, “Factors affecting higher-order movement planning: a kinematic analysis of human prehension,” *Exp. Brain Res.*, vol. 86, no. 1, pp. 199–208, 1991.
- [172] U. Castiello, “The neuroscience of grasping,” *Nat. Rev. Neurosci.*, vol. 6, pp. 726–736, Sept. 2005.
- [173] T. Pistohl, A. Schulze-Bonhage, A. Aertsen, C. Mehring, and T. Ball, “Decoding natural grasp types from human ECoG,” *Neuroimage*, vol. 59, pp. 248–260, Jan. 2012.
- [174] T. Pistohl, T. S. B. Schmidt, T. Ball, A. Schulze-Bonhage, A. Aertsen, and C. Mehring, “Grasp detection from human ECoG during natural reach-to-grasp movements,” *PLoS One*, vol. 8, p. e54658, Jan. 2013.
- [175] T. Milekovic, J. Fischer, T. Pistohl, J. Ruescher, A. Schulze-Bonhage, A. Aertsen, J. Rickert, T. Ball, and C. Mehring, “An online brain-machine interface using decoding of movement direction from the human electrocorticogram,” *J. Neural Eng.*, vol. 9, p. 046003, June 2012.
- [176] P. Ofner and G. Müller-Putz, “Decoding of velocities and positions of 3d arm movement from eeg,” in *Proceedings of the IEEE Engineering in Medicine and Biology Society. IEEE Engineering in Medicine and Biology Society. Conference*, vol. 2012, pp. 6406–9, 08 2012.
- [177] T. J. Bradberry, R. J. Gentili, and J. L. Contreras-Vidal, “Reconstructing three-dimensional hand movements from noninvasive electroencephalographic signals,” *J. Neurosci.*, vol. 30, pp. 3432–3437, Mar. 2010.
- [178] S. Waldert, T. Pistohl, C. Braun, T. Ball, A. Aertsen, and C. Mehring, “A review on directional information in neural signals for brain-machine interfaces,” *J. Physiol. Paris*, vol. 103, pp. 244–254, Sept. 2009.

- [179] A. Schwarz, P. Ofner, J. Pereira, A. I. Sburlea, and G. R. Müller-Putz, “Decoding natural reach-and-grasp actions from human EEG,” *J. Neural Eng.*, vol. 15, p. 016005, Feb. 2018.
- [180] A. Schwarz, M. K. Höller, J. Pereira, P. Ofner, and G. R. Müller-Putz, “Decoding hand movements from human EEG to control a robotic arm in a simulation environment,” *J. Neural Eng.*, vol. 17, p. 036010, may 2020.
- [181] M. Billinger, I. Daly, V. Kaiser, J. Jin, B. Z. Allison, G. R. Müller-Putz, and C. Brunner, “Is it significant? guidelines for reporting BCI performance,” *Towards Practical Brain-Computer Interfaces*, pp. 333–354, 2012.
- [182] G. Müller-Putz, R. Scherer, C. Brunner, R. Leeb, and G. Pfurtscheller, “Better than random: a closer look on BCI results,” *Int. J. Bioelectromagn.*, vol. 10, no. ARTICLE, pp. 52–55, 2008.
- [183] A. Schwarz, J. Pereira, R. Kobler, and G. R. Müller-Putz, “Unimanual and bimanual Reach-and-Grasp actions can be decoded from human EEG,” *IEEE Trans. Biomed. Eng.*, vol. 67, pp. 1684–1695, Sept. 2019.
- [184] P. Ofner, A. Schwarz, J. Pereira, D. Wyss, R. Wildburger, and G. R. Müller-Putz, “Attempted arm and hand movements can be decoded from Low-Frequency EEG from persons with spinal cord injury,” *Sci. Rep.*, vol. 9, p. 7134, May 2019.
- [185] Y. Blokland, R. Vlek, B. Karaman, F. Özin, D. Thijssen, T. Eijsvogels, W. Colier, M. Floor-Westerdijk, J. Bruhn, and J. Farquhar, “Detection of event-related desynchronization during attempted and imagined movements in tetraplegics for brain switch control,” *Conf. Proc. IEEE Eng. Med. Biol. Soc.*, vol. 2012, pp. 3967–3969, 2012.
- [186] R. Betz, F. Biering-Sørensen, S. Burns, W. Donovan, D. Graves, J. Guest, L. Jones, S. Kirshblum, A. Krassioukov, M. Mulcahey, M. Schmidt Read, G. Rodriguez, R. Rupp, C. Schuld, K. Tansey, and K. Walden, “The 2019 revision of the international standards for neurological classification of spinal cord injury (isnc-sci)—what’s new?,” *Spinal Cord*, vol. 57, 09 2019.
- [187] C. Breitwieser, A. Kreiling, C. Neuper, and G. R. Müller-Putz, “The TOBI hybrid BCI—the data acquisition module,” in *Proceedings of the First TOBI Workshop*, vol. 58, 2010.
- [188] C. Breitwieser, I. Daly, C. Neuper, and G. R. Müller-Putz, “Proposing a standardized protocol for raw biosignal transmission,” *IEEE Transactions on Biomedical Engineering*, vol. 59, no. 3, pp. 852–859, 2012.
- [189] L. C. Parra, C. D. Spence, A. D. Gerson, and P. Sajda, “Recipes for the linear analysis of EEG,” *Neuroimage*, vol. 28, pp. 326–341, Nov. 2005.



- [190] R. J. Kobler, A. I. Sburlea, and G. R. Müller-Putz, “Tuning characteristics of low-frequency EEG to positions and velocities in visuomotor and oculomotor tracking tasks,” *Sci. Rep.*, vol. 8, p. 17713, Dec. 2018.
- [191] R. J. Kobler, A. I. Sburlea, and G. R. Müller-Putz, “A comparison of ocular artifact removal methods for block design based electroencephalography experiments,” in *Proceedings of the 7th Graz Brain-Computer Interface Conference*, pp. 236–241, 2017.
- [192] W. Skrandies, “Global field power and topographic similarity,” *Brain Topogr.*, vol. 3, no. 1, pp. 137–141, 1990.
- [193] J. Schmitz, J. Packheiser, T. Birnkraut, N.-A. Hinz, P. Friedrich, O. Güntürkün, and S. Ocklenburg, “The neurophysiological correlates of handedness: Insights from the lateralized readiness potential,” *Behav. Brain Res.*, vol. 364, pp. 114–122, May 2019.
- [194] M. G. H. Coles, “The lateralized readiness potential: Past, present, and future,” in *Psychophysiology*, vol. 33, pp. S3–S3, 1996.
- [195] A. Vuckovic, S. Pangaro, and P. Finda, “Unimanual versus bimanual motor imagery classifiers for assistive and rehabilitative brain computer interfaces,” *IEEE Trans. Neural Syst. Rehabil. Eng.*, vol. 26, pp. 2407–2415, Dec. 2018.
- [196] I. Daly, R. Scherer, M. Billinger, and G. Müller-Putz, “FORCe: Fully online and automated artifact removal for Brain-Computer interfacing,” *IEEE Trans. Neural Syst. Rehabil. Eng.*, vol. 23, pp. 725–736, Sept. 2015.
- [197] A. Schwarz, J. Pereira, L. Lindner, and G. Müller-Putz, “Combining frequency and time-domain EEG features for classification of self-paced reach-and-grasp actions,” in *Proceedings of the 41st International Engineering in Medicine and Biology Conference*, 2019.
- [198] Peh, R. Duda, P. Hart, and D. Stork, *Pattern Classification*. New York: John Wiley & Sons, 2001.
- [199] M. Jochumsen, I. K. Niazi, K. Dremstrup, and E. N. Kamavuako, “Detecting and classifying three different hand movement types through electroencephalography recordings for neurorehabilitation,” *Med. Biol. Eng. Comput.*, vol. 54, pp. 1491–1501, Oct. 2016.
- [200] S. Oda and T. Moritani, “Movement-related cortical potentials during handgrip contractions with special reference to force and electromyogram bilateral deficit,” *Eur. J. Appl. Physiol. Occup. Physiol.*, vol. 72, no. 1-2, pp. 1–5, 1995.
- [201] P. Ofner, A. Schwarz, J. Pereira, and G. R. Müller-Putz, “Upper limb movements can be decoded from the time-domain of low-frequency EEG,” *PLoS One*, vol. 12, p. e0182578, Aug. 2017.

- [202] M. Jeannerod, J. Long, and A. Baddeley, *Attention and performance XIII*. Psychology Press, 1981.
- [203] M. Jeannerod, “The timing of natural prehension movements,” *J. Mot. Behav.*, vol. 16, pp. 235–254, Sept. 1984.
- [204] L. Randazzo, I. Iturrate, R. Chavarriaga, R. Leeb, and J. R. Del Millan, “Detecting intention to grasp during reaching movements from EEG,” *Conf. Proc. IEEE Eng. Med. Biol. Soc.*, vol. 2015, pp. 1115–1118, Aug. 2015.
- [205] I. Iturrate, R. Chavarriaga, M. Pereira, H. Zhang, T. Corbet, R. Leeb, and J. D. R. Millán, “Human EEG reveals distinct neural correlates of power and precision grasping types,” *Neuroimage*, vol. 181, pp. 635–644, Nov. 2018.
- [206] B. Blankertz, F. Losch, M. Krauledat, G. Dornhege, G. Curio, and K. Müller, “The berlin Brain-Computer interface: Accurate performance from first-session in BCI-naive subjects,” *IEEE Transactions on Biomedical Engineering*, vol. 55, pp. 2452–2462, Oct. 2008.
- [207] A. Schwarz, D. Steyrl, and G. R. Müller-Putz, “Brain-computer interface adaptation for an end user to compete in the cybathlon,” in *2016 IEEE International Conference on Systems, Man, and Cybernetics (SMC)*, pp. 001803–001808, Oct. 2016.
- [208] K. LaFleur, K. Cassady, A. Doud, K. Shades, E. Rogin, and B. He, “Quadcopter control in three-dimensional space using a noninvasive motor imagery-based brain-computer interface,” *J. Neural Eng.*, vol. 10, p. 046003, June 2013.
- [209] J. Meng, S. Zhang, A. Bekyo, J. Olsoe, B. Baxter, and B. He, “Noninvasive electroencephalogram based control of a robotic arm for reach and grasp tasks,” *Sci. Rep.*, vol. 6, p. 38565, Dec. 2016.
- [210] H. Ramoser, J. Müller-gerking, and G. Pfurtscheller, “Designing optimal spatial filters for single-trial EEG classification in a movement task,” *IEEE Trans. Rehabil. Eng.*, vol. 8, pp. 441–446, 1999.
- [211] Y. Blokland, L. Spyrou, J. Lerou, J. Mourisse, G. Jan Scheffer, G.-J. van Geffen, J. Farquhar, and J. Bruhn, “Detection of attempted movement from the EEG during neuromuscular block: proof of principle study in awake volunteers,” *Sci. Rep.*, vol. 5, p. 12815, Aug. 2015.
- [212] A. Rastogi, C. E. Vargas-Irwin, F. R. Willett, J. Abreu, D. C. Crowder, B. A. Murphy, W. D. Memberg, J. P. Miller, J. A. Sweet, B. L. Walter, S. S. Cash, P. G. Rezaii, B. Franco, J. Saab, S. D. Stavisky, K. V. Shenoy, J. M. Henderson, L. R. Hochberg, R. F. Kirsch, and A. B. Ajiboye, “Neural representation of observed, imagined, and attempted grasping force in motor cortex of individuals with chronic tetraplegia,” *Sci. Rep.*, vol. 10, p. 1429, Jan. 2020.

- [213] K. K. Ang, Z. Y. Chin, C. Wang, C. Guan, and H. Zhang, “Filter bank common spatial pattern algorithm on BCI competition IV datasets 2a and 2b,” *Front. Neurosci.*, vol. 6, p. 39, Mar. 2012.
- [214] D. Coyle, G. Prasad, and T. M. McGinnity, “A time-series prediction approach for feature extraction in a brain-computer interface,” *IEEE Transactions on Neural Systems and Rehabilitation Engineering*, vol. 13, no. 4, pp. 461–467, 2005.
- [215] A. Korik, R. Sosnik, N. Siddique, and D. Coyle, “Decoding imagined 3d hand movement trajectories from eeg: Evidence to support the use of mu, beta, and low gamma oscillations,” *Frontiers in Neuroscience*, vol. 12, p. 130, 2018.
- [216] C. Vidaurre, C. Sannelli, K.-R. Müller, and B. Blankertz, “Co-adaptive calibration to improve BCI efficiency,” *J. Neural Eng.*, vol. 8, p. 025009, Apr. 2011.
- [217] C. Vidaurre, M. Kawanabe, P. von Büna, B. Blankertz, and K. R. Müller, “Toward unsupervised adaptation of LDA for Brain-Computer interfaces,” *IEEE Transactions on Biomedical Engineering*, vol. 58, pp. 587–597, Mar. 2011.
- [218] P. Shenoy, M. Krauledat, B. Blankertz, R. P. N. Rao, and K.-R. Müller, “Towards adaptive classification for BCI,” *J. Neural Eng.*, vol. 3, pp. R13–23, Mar. 2006.
- [219] J. Faller, C. Vidaurre, T. Solis-Escalante, C. Neuper, and R. Scherer, “Autocalibration and recurrent adaptation: towards a plug and play online ERD-BCI,” *IEEE Trans. Neural Syst. Rehabil. Eng.*, vol. 20, pp. 313–319, May 2012.
- [220] J. Faller, R. Scherer, U. Costa, E. Opisso, J. Medina, and G. R. Müller-Putz, “A co-adaptive brain-computer interface for end users with severe motor impairment,” *PLoS One*, vol. 9, p. e101168, July 2014.
- [221] A. Schwarz, J. Brandstetter, J. Pereira, and G. R. Müller-Putz, “Direct comparison of supervised and semi-supervised retraining approaches for co-adaptive BCIs,” *Med. Biol. Eng. Comput.*, vol. 57, pp. 2347–2357, Sept. 2019.
- [222] K. Statthaler, A. Schwarz, D. Steyrl, R. Kobler, M. K. Höller, J. Brandstetter, L. Hehenberger, M. Bigga, and G. Müller-Putz, “Cybathlon experiences of the graz BCI racing team mirage91 in the brain-computer interface discipline,” *J. Neuroeng. Rehabil.*, vol. 14, p. 129, Dec. 2017.
- [223] S. Slobounov, M. Hallett, and K. M. Newell, “Perceived effort in force production as reflected in motor-related cortical potentials,” *Clin. Neurophysiol.*, vol. 115, pp. 2391–2402, Oct. 2004.
- [224] G. R. Müller-Putz, P. Ofner, A. Schwarz, J. Pereira, G. Luzhnica, C. di Sciascio, E. Veas, S. Stein, J. Williamson, R. Murray-Smith, C. Escolano, L. Montesano, B. Hessing, M. Schneiders, and R. Rupp, “MoreGrasp: Restoration of upper limb function in individuals with high spinal cord injury by multimodal neuroprostheses

- for interaction in daily activities,” in *Proceedings of the 7th Graz Brain-Computer Interface Conference 2017* (G. R. Müller-Putz, D. Steyrl, S. C. Wriessnegger, and R. Scherer, eds.), pp. 338–343, Sept. 2017.
- [225] S. Blum, S. Debener, R. Emkes, N. Volkening, S. Fudickar, and M. G. Bleichner, “EEG recording and online signal processing on android: A multiapp framework for Brain-Computer interfaces on smartphone,” *Biomed Res. Int.*, vol. 2017, p. 3072870, Nov. 2017.

## 4 Appendix

### 4.1 Appendix A: Author Contributions

Schwarz Andreas, Ofner Patrick, Pereira Joana, Sburlea Andreea and Gernot Müller-Putz, “Decoding natural reach-and-grasp actions from human EEG.”, *Journal of Neural Engineering*, Feb 2018; 15(1):016005, url<https://doi.org/10.1088/1741-2552/aa8911>  
Distribution of work: AS (75%), OP(10%), JP(5%), SbA(5%), GMP (5%)

---

Schwarz Andreas, Maria Katharina Höller, Joana Pereira and Gernot Müller-Putz, “Decoding hand movements from human EEG to control a robotic arm in a simulation environment.”, *Journal of Neural Engineering*, 17(3):030610,2020 <https://doi.org/10.1088/1741-2552/ab882e>.  
Distribution of work: AS (70%), MKH(15%), JP(5%), PO(5%), GMP (5%)

---

Schwarz Andreas, Pereira Joana, Kobler Reinmar, Gernot Müller-Putz, “Unimanual and Bimanual Reach-and-Grasp Actions Can Be Decoded From Human EEG.”, *IEEE Transactions on Biomedical Engineering (TBME)*, 09/2019, epub ahead of print, <https://dx.doi.org/10.1109/TBME.2019.2942974>  
Distribution of work: AS (80%), JP(10%), RK (5%), GMP (5%)

---

Schwarz Andreas, Pereira Joana, Lindner Lydia, Gernot Müller-Putz, “Combining frequency and time-domain EEG features for classification of self-paced reach-and-grasp actions.”, *Proc. of the 41st Annual International Conference of the IEEE Engineering in Medicine and Biology Society (EMBC)*, Berlin, Germany. <https://doi.org/10.1109/EMBC.2019.8857138>  
Distribution of work: AS (70%), JP(10%), LL (15%), GMP (5%)

## 4.2 Appendix B: Core Publications

# Decoding natural reach-and-grasp actions from human EEG

Andreas Schwarz<sup>1</sup>, Patrick Ofner<sup>1</sup>, Joana Pereira<sup>1</sup>,  
Andreea Ioana Sburlea<sup>1</sup> and Gernot R Müller-Putz<sup>1</sup>

Institute of Neural Engineering, Graz University of Technology, Stremayrgasse 16/IV, 8010 Graz, Austria

E-mail: [gernot.mueller@tugraz.at](mailto:gernot.mueller@tugraz.at)

Received 15 May 2017, revised 25 July 2017

Accepted for publication 30 August 2017

Published 6 December 2017




CrossMark

## Abstract

**Objective.** Despite the high number of degrees of freedom of the human hand, most actions of daily life can be executed incorporating only palmar, pincer and lateral grasp. In this study we attempt to discriminate these three different executed reach-and-grasp actions utilizing their EEG neural correlates. **Approach.** In a cue-guided experiment, 15 healthy individuals were asked to perform these actions using daily life objects. We recorded 72 trials for each reach-and-grasp condition and from a no-movement condition. **Main results.** Using low-frequency time domain features from 0.3 to 3 Hz, we achieved binary classification accuracies of 72.4%, STD  $\pm$  5.8% between grasp types, for grasps versus no-movement condition peak performances of 93.5%, STD  $\pm$  4.6% could be reached. In an offline multiclass classification scenario which incorporated not only all reach-and-grasp actions but also the no-movement condition, the highest performance could be reached using a window of 1000 ms for feature extraction. Classification performance peaked at 65.9%, STD  $\pm$  8.1%. Underlying neural correlates of the reach-and-grasp actions, investigated over the primary motor cortex, showed significant differences starting from approximately 800 ms to 1200 ms after the movement onset which is also the same time frame where classification performance reached its maximum. **Significance.** We could show that it is possible to discriminate three executed reach-and-grasp actions prominent in people's everyday use from non-invasive EEG. Underlying neural correlates showed significant differences between all tested conditions. These findings will eventually contribute to our attempt of controlling a neuroprosthesis in a natural and intuitive way, which could ultimately benefit motor impaired end users in their daily life actions.


Keywords: reach-and-grasp decoding, EEG, grasp neural correlates, grasp motor decoding, motor-related cortical potential, movement-related cortical potential

 Supplementary material for this article is available [online](#)

(Some figures may appear in colour only in the online journal)

## Introduction

When asking a tetraplegic spinal cord injured (SCI) person, from which lost function they would benefit most, three quarters make regaining arm/hand function their priority choice [1, 2] (2nd elimination of Dysreflexia, 3rd sexual function).

 Original content from this work may be used under the terms of the [Creative Commons Attribution 3.0 licence](#). Any further distribution of this work must maintain attribution to the author(s) and the title of the work, journal citation and DOI.

Yet up to this point this population is waiting for an intervention that will improve their functional ability [3].

Neuroprosthesis based on functional electrical stimulation (FES) may present a technical solution. Small electric pulses stimulate still innervated paralysed arm muscles. In this way, the neuroprosthesis is able to restore hand functions, especially different grasps [4, 5] on demand. Studies from the early 2000s show that neuroprosthetic control can be achieved with non-invasive brain-computer interfaces (BCI) [6, 7].

These non-invasive BCIs enable its users to interact with their environment by means of changes in brain activity captured by the electroencephalographic signals (EEG). BCI control strategies usually rely on focused attention to an external stimuli [8–11] or on specific mental strategies [12–14].

Pfurtscheller *et al* [15] applied combined BCI-FES technology to restore left hand functions of a tetraplegic end user (complete SCI, lesion height C5, neither hand nor finger function, residual elbow function). After ten months of FES muscle training (five times a week, 45 min each session) and a period of four months of BCI training, the end user was able to perform a palmar grasp and use a glass using motor imagination (MI) of repeated foot movement as a control signal. In later studies [16, 17], Rohm *et al* refined the approach by also including functional control of the elbow. They extended BCI control by introducing new mental tasks and temporal coded [18] BCI commands.

So far, BCI-based neuroprosthesis control has strongly relied on the (repeated) imagination of basic motor tasks e.g. repeated planar extension/flexion of both feet [15], or repeated MI of opening/closing left or right hand [16, 17]. From a user's perspective it seems rather unnatural to perform specific foot MI for controlling one's hand functions. Even contralateral hand MI [6, 16, 17, 19] feels unnatural and does not support a natural feeling of control.

We believe that for a more natural and intuitive control of an upper limb neuroprosthesis it is essential to focus on the successful decoding of more complex and natural hand/arm movements, such as different grasp actions. In most daily life scenarios, a grasp is combined with a reaching movement towards an object. Studies investigating grasp kinematics imply that the hand preshapes already during the reaching phase, whereas maximum grip aperture occurs within 70% of movement completion [20, 21]. Although the human hand incorporates a large amount of degrees of freedom, yet only three main grasps—palmar, pincer and lateral grasp—are necessary to perform most daily life actions [22].

Previously, it has been shown that it is possible to detect and discriminate different reach-and-grasp actions from human electrocorticogram (ECoG) [23, 24]. Results indicated that discriminative information for movement detection and classification can be found in the amplitude modulations of frequencies below 6 Hz.

In the time domain, cortical activations in this frequency range are known as movement-related cortical potentials (MRCP). They are described by a negative shift in amplitude during movement preparation, reaching its maximum negativity imminently to the actual movement onset (Bereitschaftspotential). Thereafter a positive rebound occurs which ultimately returns to a baseline level [25]. The shape of these potentials may vary depending on various factors, such as the movement task [26–28], force [29, 30] or movement speed [31].

EEG based studies investigating MRCPs [25] indicate that this information can also be exploited non-invasively, not only for directional information [26], but also for the analysis of hand shape during a grasping movement [32], to study the effects of grasp force [33] and ultimately to discriminate

different grasps [31, 34–36]. The intention of movement has been investigated in palmar, pincer and lateral grasps [31].

Of particular interest are two studies from Agashe *et al* [32, 37] who attempted low-frequency reach-to-grasp decoding and classification incorporating palmar and lateral-precision grasp on various objects. In a follow-up multi-session study incorporating two amputee end users controlling a robotic hand, they show the feasibility and success of their efforts.

In our current study we want to add up to their prior work and further investigate the whole reach-and-grasp process in a daily life setting using common objects of daily life.

In our experimental setup we chose three different reach-and-grasp actions most commonly used in daily life: (i) palmar grasp, (ii) pincer grasp and (iii) lateral (key) grasp. We hypothesize that these executed reach-and-grasp actions can be discriminated significantly better than chance (I) against each other and (II) against the no-movement condition, based on low frequency EEG activity. We test our hypothesis in 15 healthy volunteers using binary and multiclass classification approaches and also show the difference between the low frequency neural correlates of the movements. Finally we discuss the potential of our results for online application to facilitate artificial control.

## Methods

### Subjects

The study was approved by the ethics committee of the Medical University of Graz (ek28-108 15/16). Fifteen right-handed subjects, seven male, eight female, aged between 23 and 37 years, participated in the experiment. Subjects were without any known medical conditions and had normal or corrected-to-normal vision. Each subject was explained the aim of the study, signed an informed consent and was paid for participating in the study.

### Experimental task

Recordings took place in an electromagnetic and noise shielded room to facilitate consistent measurement conditions over all subjects. Subjects were seated in a comfortable chair. Right in front of them we placed a table with a built-in 22 inch screen. Subjects were asked to place their right hand on a pressure button located on the desk between them and the screen. We positioned four objects on pre-defined positions in a semi-circle on the screen so that the distance to the right hand of the user was equidistant for all four objects (figure 1). The objects were (i) a glass (for palmar grasp), (ii) a needle (for pincer grasp), (iii) a key (for lateral grasp) and (iv) an empty plexiglass tile (for no-movement condition). Both the needle and the key were placed in plexiglass retainers not only to facilitate comfortable grasping conditions but to incorporate them in positions of everyday use: the key was placed in a keyhole ready to be turned, the needle was stuck at a 45 degree angle in the plexiglass retainer, ready to be picked up (figure 1).

In this setup we used a cue-based paradigm as shown in figure 2. At second 0, the subjects were presented with a



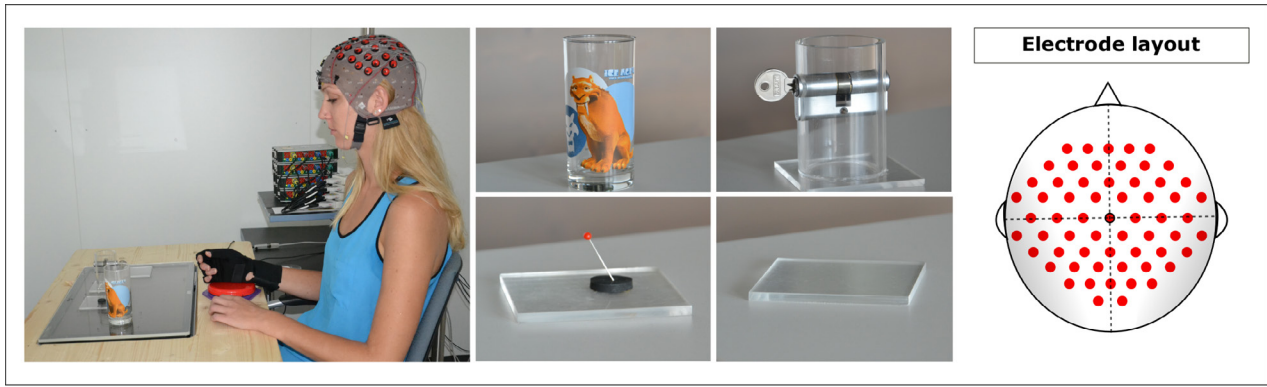


**Figure 1.** Experimental setup. Left: the subject is seated at the prepared table. Center: objects of the reach-and-grasp tasks: glass (palmar grasp), key including lock in a plexiglass retainer (lateral grasp), needle (pincer grasp) and a plexiglass tile for the no-movement condition. Right: electrode layout of the experiment. The center electrode (black ringed) is located at position Cz.

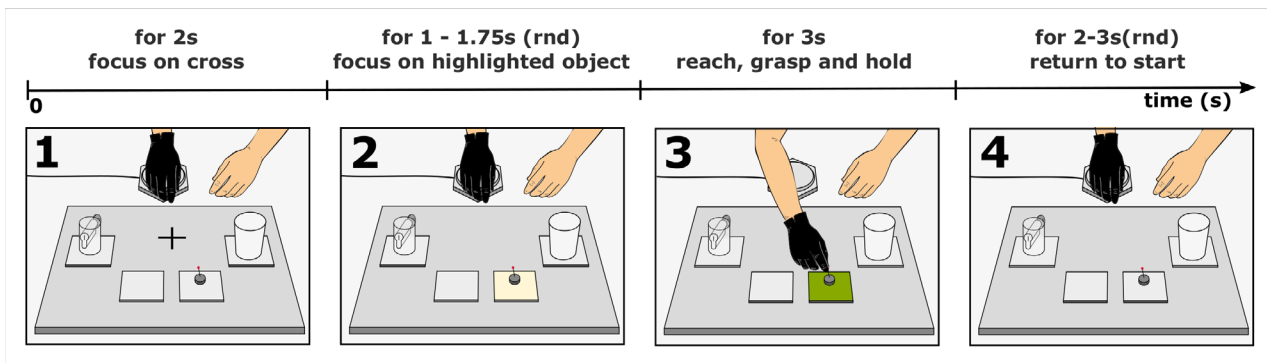


**Figure 2.** Experimental paradigm, sequential view. At trial start subjects focused on the cross shown on the screen (1), thereafter, the tile underneath one of the objects was highlighted in white and subjects switched their focus to the highlighted object (2). Once the highlighting turned green (3) subjects grasped the designated object and held it until the highlighting vanished. Thereafter they moved the hand back to the starting position (4). This figure was created and designed with friendly assistance of nu-art [38].

fixation cross located in the center of the screen, together with an auditory beep. Subjects were instructed to look at the cross. After 2 s, one of the objects was randomly highlighted by illuminating the underneath tile in white. Subjects were instructed to focus their gaze on the highlighted object. After a varying time period of 1–1.75 s, the white illumination turned green for 3 s. Subjects were instructed to reach, grasp and hold the object for as long as the underneath tile was illuminated in green. Thereafter, subjects released the object and returned the hand to the starting position on the pressure button. In case the empty tile was illuminated, subjects were asked to focus on the tile and avoid any eye or body movement. After each trial we introduced a break for 2–3 s.

We recorded 72 trials for each condition over eight consecutive runs. After each run, objects were repositioned clockwise, so that every object was located on each position equally often. Furthermore we recorded a three times 1 min of rest as well as 1 min of eye-movements at the beginning, half-time and end of the session.

**Data recording**

For EEG recording we used four biosignal amplifiers with 61 active electrodes (g.tec medical engineering, Austria). Electrodes were positioned over frontal, parietal and temporal

lobes (see figure 1, right). For reference we used the right earlobe and for ground the AFz channel. EEG was sampled with 512 Hz and pre-filtered between 0.01 and 200 Hz using an 8th order Chebyshev filter. To remove power line noise, we applied a notch filter at 50 Hz. Electrode positions were captured using a ELPOS system by Zebris (Zebris Medical GmbH, Germany).

In addition we used three active electrodes for recording electrooculographic signals (EOG). We positioned them above the nasion and below the outer canthi of the eyes to form a rectangular triangle [39], and used the same recording settings as for the EEG data. To record hand and finger movements during the experiments, we used a 5DT data glove (5DT, USA). For movement onset detection we used a pressure button. Data recording and synchronization was performed using MATLAB R2012b (Mathworks, Massachusetts, USA) and TOBI SignalServer [40].

**Movement detection**

For detecting the movement onset of each reach-and-grasp condition we used the rising flank (button release) of the pressure button. Time-locking the no-movement condition to the onset of the green cue would make the comparison with the reach-and-grasp conditions unfair. A cue-related visually

evoked potential could increase classification accuracies above chance-level not because of any motor potential involved, but because of the presence of the cue-related event.

Therefore, we calculated mean and standard deviation of the reaction time of each subject based on the period between the onset of the green cue and the movement onset indicated by the pressure button. Thereafter we added the mean plus a random percentage of the standard deviation to the onset of the green cue. In this way we allow fair comparison between movement and no-movement conditions.

In addition to the movement onset we were interested in the timing when subjects finished their grasps. For this matter, we investigated the data collected using the data glove. In this experiment we used 15 sensors of the data glove which were located at the joints of the finger phalanges. To reduce the dimensionality of the movement data collected with the glove, we performed principle component analysis (PCA) for each reach-and-grasp condition. We used only the first PCA component for further analysis. We epoched the component according to movement onsets and calculated a subject-specific mean for each reach-and-grasp condition. We determined the timepoint of the peak in the variance as the point where subjects finished their grasp. In a similar way, we determined the timepoint when subjects released their grasp, after holding the object.

#### *Artefact avoidance and rejection strategies*

EEG analysis, especially in the low frequency range is highly vulnerable to ocular based artefacts [41]. Our strategy in dealing with artefacts, especially eye movements, was based on artefact avoidance and trial rejection based on statistical parameters. To avoid unnecessary eye-movement during trial execution, we aligned the cue presentation and the target into the same field of view. In this matter we introduced the ‘white phase’ into our paradigm (see figure 2, step 2). Subjects were specifically asked to focus on the object above the tile highlighted in white. This procedure allowed the participants to maintain their focus on the designated object and to execute the designated task once the highlighting turned green (figure 2, step 3). We also repositioned each object clockwise after each run to minimize the impact of the position itself.

Preceding further analysis, we discarded all trials in which subjects did not lift their hand within 2s after start of the green highlighting. We filtered EEG between 0.3 and 35 Hz using a zerophase 4th order Butterworth filter. Thereafter, we rejected artefact contaminated trials using statistical parameters: (1) amplitude threshold (amplitude exceeds  $\pm 125 \mu\text{V}$ ), (2) abnormal joint probability (3) and abnormal kurtosis. As threshold for the last two we used four times the standard deviation (STD). Using similar statistics, we also performed channel based rejection. On average we rejected 12% of the recorded trials and kept 59 EEG channels. Rejected channels were mainly located on the edges of the electrode grid on the right side. Our approach has no need for additional measurement channels and has already been used successfully in both offline [35] and online BCI scenarios [42–44].

#### *Binary single trial classification*

The aims of performing binary single trial classification were twofold. First, we were interested in the discriminability between reach-and-grasp actions. Second, we wanted to discriminate individual reach-and-grasp actions from the no-movement condition.

We common average referenced (CAR) the EEG to increase the signal to noise ratio and resampled the signal to 16 Hz to facilitate computational performance. Thereafter the signal was bandpass filtered from 0.3 to 3 Hz using a 4th order zero-phase Butterworth filter. We epoched our trials based on the movement onset captured by the pressure button to define our time region of interest (tROI). The tROI started 2s before and ended 3s after movement onset. Using 10 times 5 fold cross-validation, we divided the recorded trials into test and training data. For further classification we used all available channels. For training the shrinkage based linear discriminant analysis classifier (sLDA) [45], we used a time window of 1s taking amplitude values in 125ms steps as features. In steps of 1/16 of a second we moved this window over the defined tROI of training and test trials. This means, that we trained and tested a classification model every 1/16 of a second in the tROI (in total 80 models over the whole tROI). In each cross-validation fold, the classifier was trained based on training data and evaluated on the test data. We repeated the 5 fold cross validation 10 times and report the mean of the accuracies. Based on these accuracies, we also calculated the information transfer rate (ITR) according to Wolpaw’s bit rate [46, 47]. On average 6.7 trials were shown to each participant per minute.

For the binary classification strategy we performed this procedure for each possible class combination (6 in total).

#### *Multiclass single trial classification*

Our approach for multiclass classification was similar to the binary classification methodology, but we used a multiclass sLDA model instead [48]. Furthermore we investigated how the window size for feature extraction impacts on the overall performance. Here we analyzed four time-window sizes: one sample, 500ms, 1000ms and 1500ms. Table 1 describes the windows and their features in detail.

Since our classification approach resulted in its own classification model every 1/16 of a second, we were also able to investigate time point specific confusion matrices. Therefore we calculated them for each subject for each time point and in grand average within the tROI. We also performed row-wise normalization so that for each row the sum of all predicted class rates adds up to 100%.

Additionally to the implications of the window size, we were interested in the classification performance when reducing electrodes. Therefore we performed multiclass classification not only with our full setup of 61 electrodes but also with three reduced setups (see also figure 9):

- 5 channel layout: (Fz, C1, Cz, C2, CPz)
- 15 channel layout: (FC3, FC1, FCz, FC2, FC4, C3, C1, Cz, C2, C4, CP3, CP1, CPz, CP2, CP4)

**Table 1.** Window sizes investigated for the multiclass classification approach. Features were extracted in steps of 125 ms starting from the actual sample to the designated window size.

Window size	Number of features per channel (taken in 125 ms steps from the window)	Average number of features extracted per trial	Trial-to-feature ratio
1 sample	1	59	4.88
500 ms	5	295	0.97
1000 ms	9	531	0.54
1500 ms	13	767	0.37

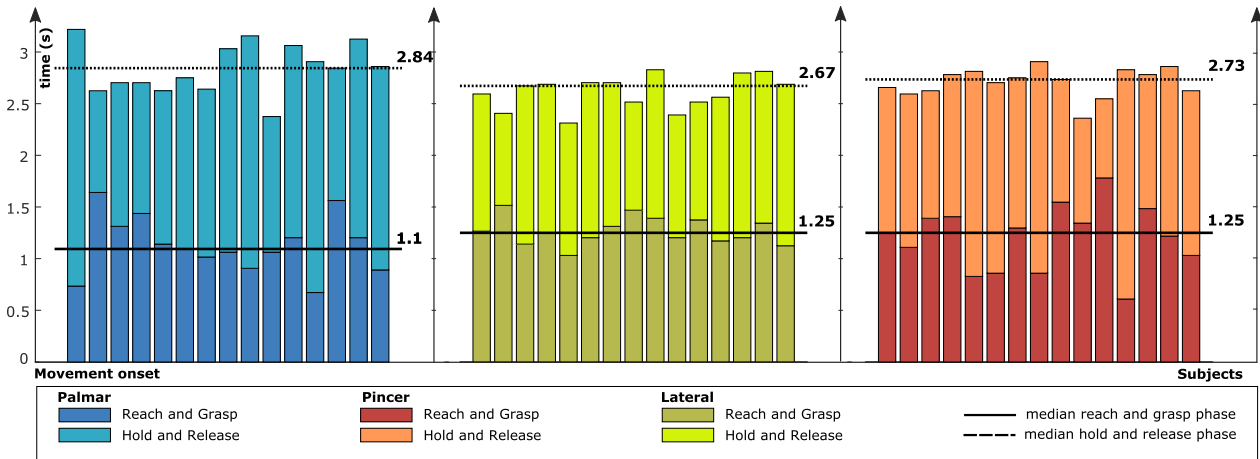


**Figure 3.** Behavioural analysis. Subject-specific behavioural analysis with respect to the movement onset. Darker colors represent the time taken from movement onset to the final grasp position. Lighter colors indicate the phase from hold to release. Horizontal lines indicate the median over all subjects for the reach-and-grasp (bold) and the hold and release (dashed).

- 25 channel layout: F3, F1, Fz, F2, F4, FC3, FC1, FCz, FC2, FC4, C3, C1, Cz, C2, C4, CP3, CP1, CPz, CP2, CP4, P3, P1, Pz, P2, P4).

For each setup we calculated the multiclass performance as already described using the 1000ms feature window. Additionally, we statistically compared the layouts with respect to subjects peak performance using a one-way repeated measure ANOVA.

*Movement-related cortical potentials (MRCPs)*

Apart from classification we were also interested to analyze the underlying differences in the MRCP neural correlates of grasps.

To analyse MRCPs we used the CAR-filtered EEG data and resampled it to 16 Hz to ease computational effort. Thereafter we bandpassed the signal using a 4th order zero-phase Butterworth filter between 0.3 to 3 Hz and epoched data from -2s to 3s with respect to the movement onset. For each condition we calculated the confidence interval (alpha = 0.05) across all trials of all subjects using nonparametric t-percentile bootstrap statistics. MRCP calculations were done for each channel separately, however we only show a selection of channels located primarily over the motor cortex.

In addition, we performed sample-wise statistical testing using the nonparametric Wilcoxon Rank Sum Test. We applied the false discovery rate (FDR) procedure to correct for multiple comparisons.

**Results**

*Behavioural analysis*

In figure 3 we show a summary of the behavioural analysis of all subjects for each reach-and-grasp condition. All scaling is done relative to the movement onset of each subject, whereas the reach-and-grasp phase as well as the hold and release phase were calculated using data from the 5DT data glove. We observed similar timings for the reach-and-grasp-phases, as well as for the hold and release phases. We calculated a repeated-measures one-way ANOVA with the reach-and-grasp time as factor (three levels) for palmar, pincer and lateral grasp onset. Mauchly’s test indicated that the assumption of sphericity was not violated. There was no significant effect for the grasp onsets  $F(2.28 = 1.473, p > 0.24)$ .

*Movement-related cortical potentials (MRCPs)*

Figure 4 shows the confidence interval (alpha = 0.05) of the MRCPs for each condition for channels FCz, C1, Cz and C2 with respect to the movement onset (second 0). A broader selection of channels can be viewed in the supplementary material ([stacks.iop.org/JNE/15/016005/mmedia](https://stacks.iop.org/JNE/15/016005/mmedia)).

In the top left quadrant, all conditions are plotted together. For all grasping conditions a strong negative shift can be observed starting around 250 to 350ms before the movement onset. Imminent to the movement onset the negative shift

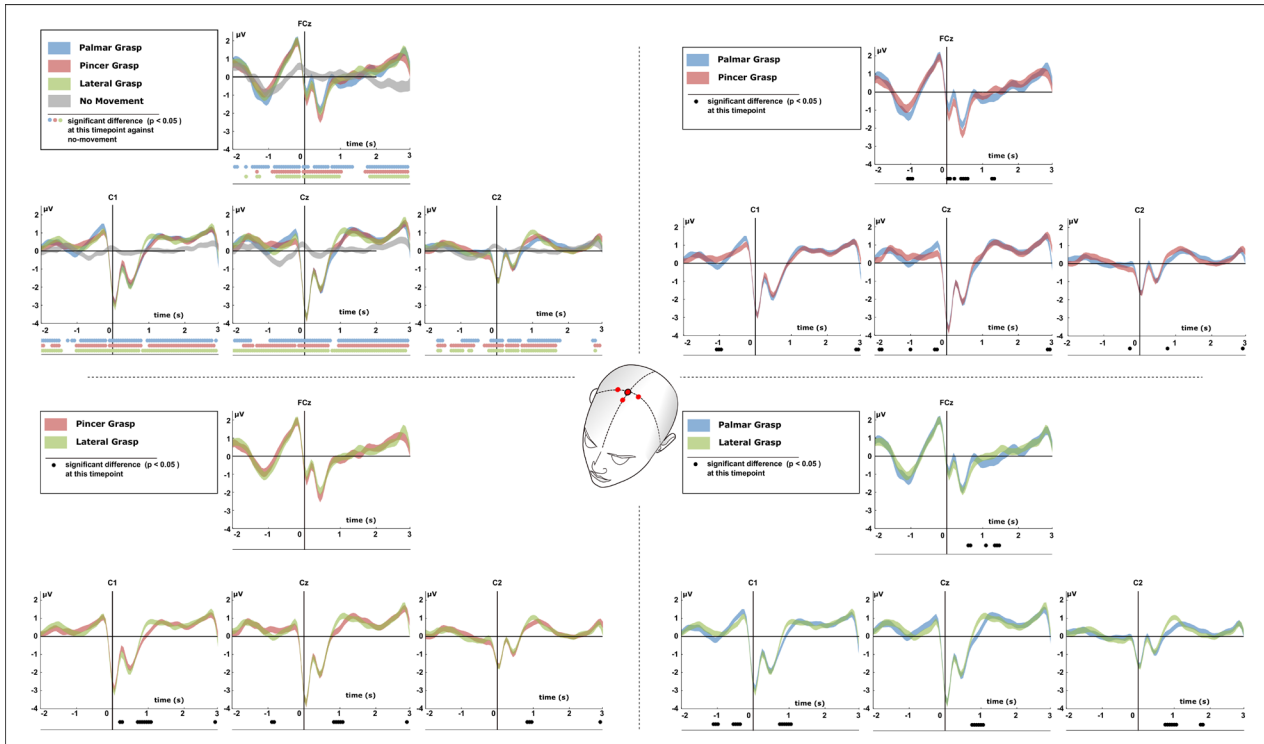


**Figure 4.** Grand average of all trials of the movement-related cortical potentials (MRCPs) with respect to the movement onset for all the conditions. Colored shaded areas show the mean confidence interval of the designated grasp ( $\alpha = .05$ ). In the top left panel MRCPs of all grasp conditions and the no-movement condition are plotted together. The other panels show the MRCPs for every pair of grasps. Below each channel we marked significantly different ( $p < 0.05$ ) timepoints resulting from the Wilcoxon Rank Sum Test. In the top left panel, this is shown for every reach-and-grasp condition (in their designated colors) against the no-movement class. In the other three panels, we show the significant differences for the grasp versus grasp conditions each.

reaches its maximum at around  $-4 \mu V$ . After 200 ms, all grasp conditions show an intermediate strong positive rebound followed by a second positive rebound which is different for each grasp condition. For all grasp conditions, significant differences can be observed against the no-movement condition starting from 2 s before the cue.

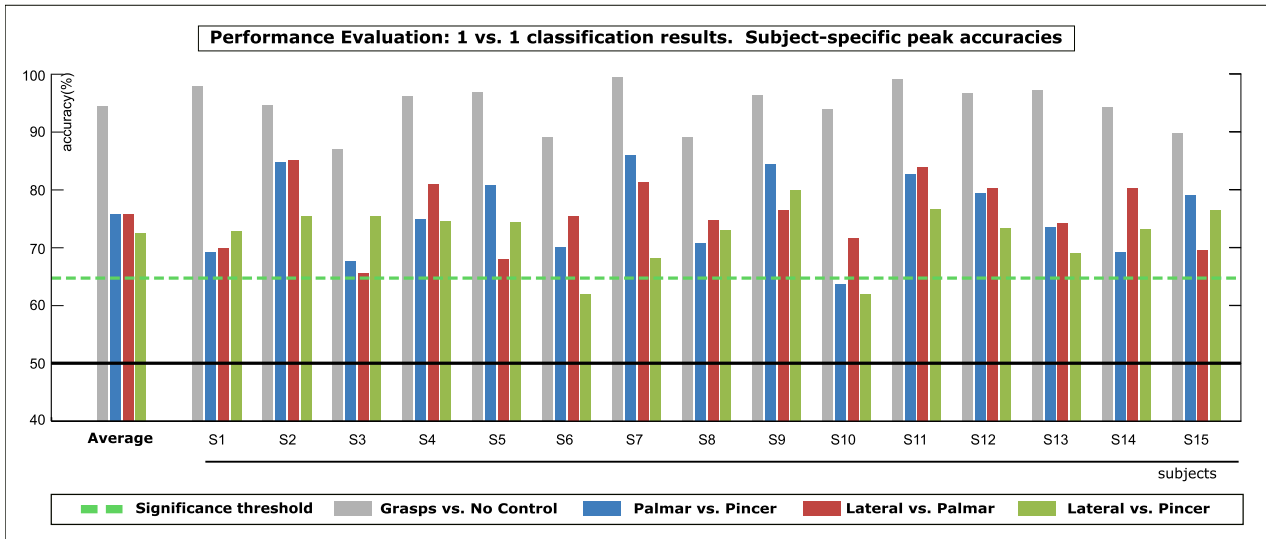
Significant differences can be observed up to 3 s after the cue for all electrodes over the central motor cortex. Most pronounced differences can be observed at Cz and C1. The remaining three quadrants show all possible pairings of grasps. In all comparisons between reach-and-grasp conditions, significant differences can be observed from  $-1$  s seconds before until 1.5 s after the movement onset. Moreover, at the occurrence of the second positive rebound at around second 1, differences are most pronounced. These differences are the smallest in the palmar versus pincer comparison and only significant ipsilaterally at C2 (see top right quadrant). For the comparison of pincer and palmar grasp conditions versus the lateral grasp condition significant differences over C1, Cz and C2 can be observed. Moreover, a time difference between the positive peak of the second positive rebound can be observed among conditions, especially at central electrode Cz. The lateral grasp condition reaches peak rebound almost  $\sim 250$  ms earlier than the pincer and the palmar grasp condition. In both cases this difference is significant in all central electrodes.

#### Binary classification approach

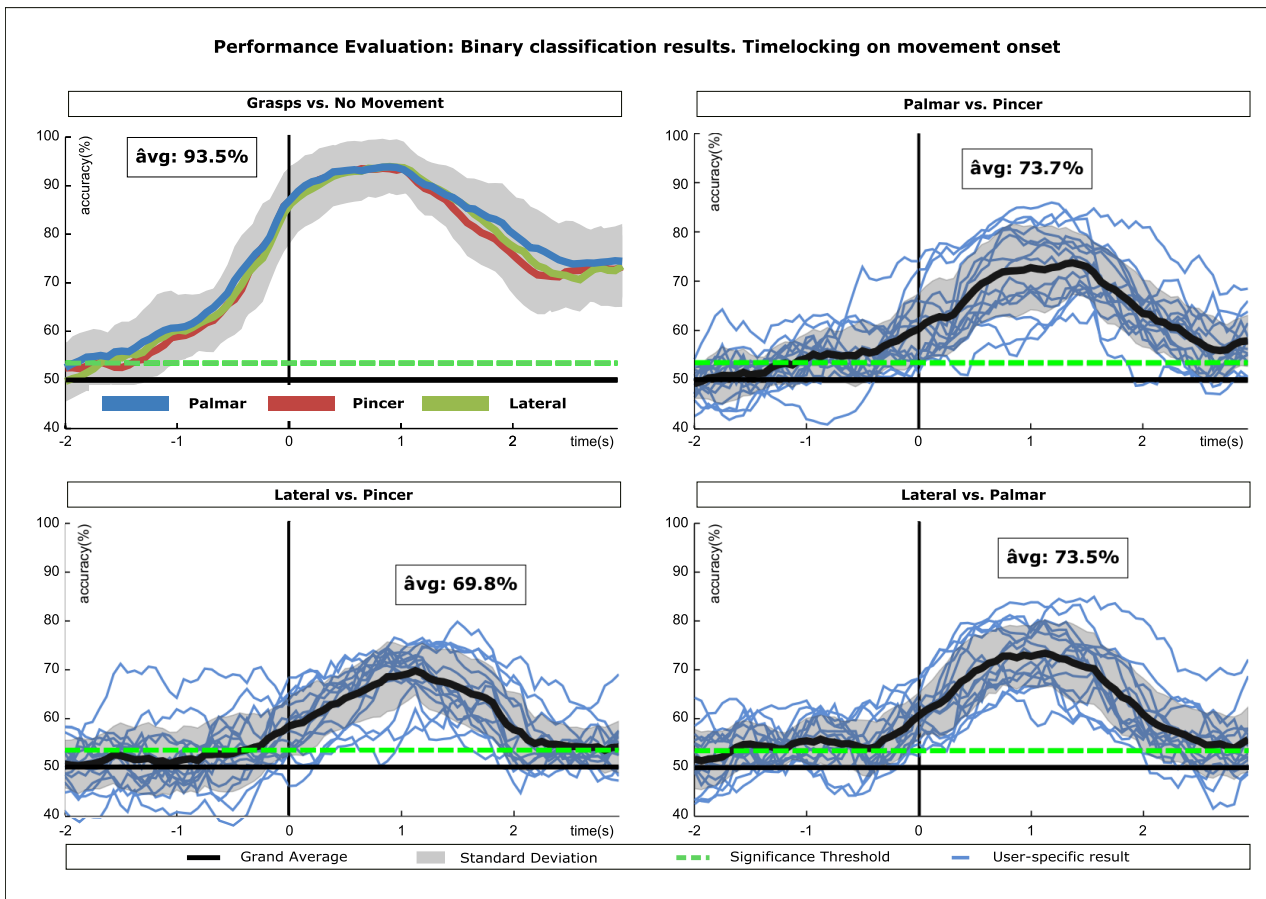
As a first step we performed one versus one classification of all task pairs. Figures 5 and 6 display classification results for all subjects and their grand average over all tasks pairs. We defined the time region of interest (tROI) from 2 s before to 3 s after the movement onset. The subject-specific chance level for binary classification is 63.3% ( $\alpha = 0.05$ , adjusted Wald-interval) and is Bonferroni corrected for multiple comparisons of the sample-wise classification approach (see [49, 50]). For the grand average over all subjects chance level is 53.5%. For this classification approach we used features from a time window of one second.

In figure 5 we show the subject-specific peak accuracies of the tROI. Grasps versus no-movement achieve average peak accuracies of 94.5%, while grasps versus grasp peak performance average at 75.8% (palmar versus pincer, blue), 75.9% (lateral versus palmar, red) and 72.3% (lateral versus pincer, green). Only the classification results of two subjects (S6: Lateral versus Palmar; S10: Palmar versus Pincer, Lateral versus Pincer) were below the subject-specific chance level in a grasp versus grasp condition.

In table 2 we show the peak performance of the grand average of each class combination percent and bits per minute as well as its time of occurrence relative to the movement onset.



**Figure 5.** Binary classification results—peak accuracies over all trials. The first bar group displays the average peak accuracies of all subjects (grand average). Bar group S1 to S15 display subject-specific peak accuracies. Notice that only the accuracy of S6 and S10 are below the single subject significance threshold (dashed green line) of 63.2%.



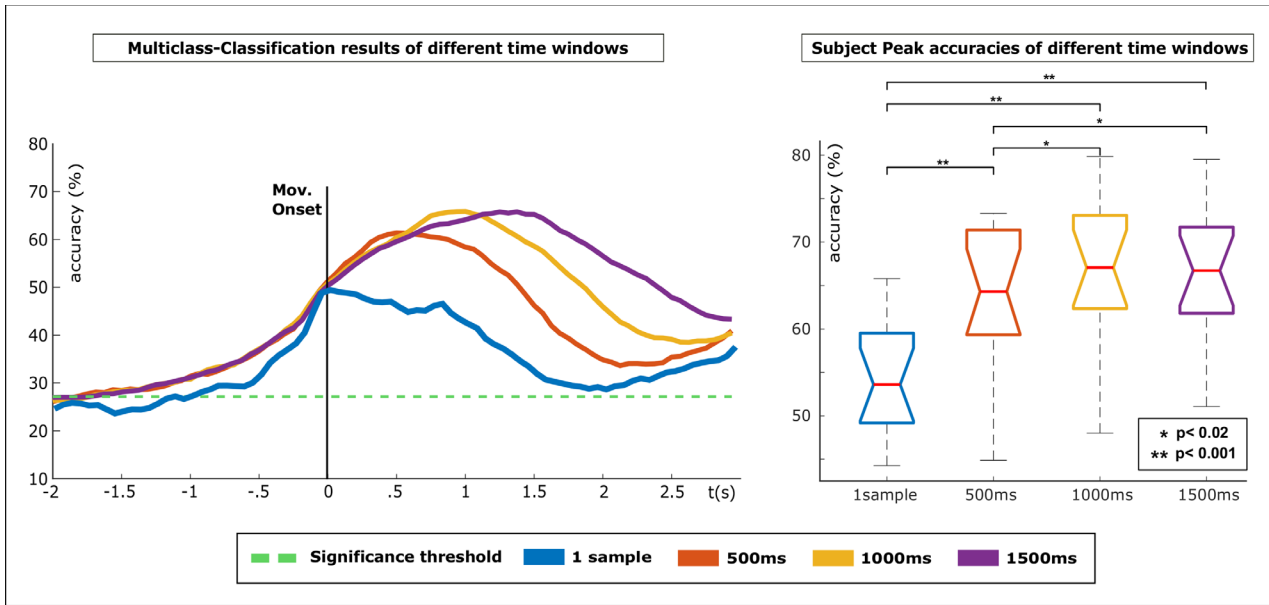
**Figure 6.** Binary classification results. Subject-specific and grand average classification accuracies with respect to the movement onset. The black perpendicular line at second 0 marks the movement onset. Textboxes indicate the grand average peak accuracy. Top left plot shows the grand average for all investigated grasps versus the no-movement condition including its standard deviation. Plots on top right corner and on the bottom indicate the performance of grasp versus grasp evaluations.

Figure 6 shows the subject-specific classification performance and the grand average performance over the tROI. All grasps show similar classification behaviour against the no-movement condition (as shown in the top left plot). Better-than-chance

classification performance could already be reached 1.4s before the actual movement onset. Performance of at least 90% remained stable over the first second after the movement onset. Grand average peak performance was 93.5%. For grasp

**Table 2.** Grand average peak performance in percentage and bits per minute for all class combinations and their corresponding time point.

Task combination	Peak accuracy (%)	Peak performance (bits min <sup>-1</sup> )	Time point relative to movement onset (s)
Grasps versus no-movement	93.5 STD ± 4.2	4.37	+0.875
Palmar versus pincer	73.7 STD ± 6.1	1.13	+1.125
Palmar versus lateral	73.5 STD ± 6.6	1.12	+1.375
Lateral versus pincer	69.8 STD ± 4.8	0.78	+1.125



**Figure 7.** Multiclass classification results based on different time windows. The figure on the left side displays the grand average of the multiclass performance for each investigated time window (colored bold lines). The green dashed line shows the significance threshold at 27.4%. With increasing size of the time window, peak accuracy for the classification delays in time. The boxplots on the right show the range of peak accuracies for all subjects in each time window evaluation.

**Table 3.** Grand average peak performance in percentage and bits per minute for different window sizes and their corresponding time point.

Window size	Peak accuracy (%)	Peak performance (bits min <sup>-1</sup> )	Time point (s, relative to movement onset)
1 sample	50.3, STD ± 6.6	1.42	+0.06
500 ms	61.8, STD ± 8.7	2.92	+0.62
1000 ms	65.9, STD ± 8.1	3.57	+1.0
1500 ms	65.8, STD ± 7.5	3.56	+1.43

versus grasp conditions better-than-chance performance could be achieved on grand average up to 1 s before movement onset for palmar versus pincer, respective 400ms and 300ms for palmar versus lateral and lateral versus pincer. Grand average peak accuracies occurred after movement onset between 1.125 s and 1.375 s. Grand-average peak accuracy culminates at 73.7% (palmar versus pincer), 69.8% (lateral versus pincer) and 73.5% (lateral versus palmar).

*Multiclass classification approach*

Similar to the binary classification approach, we defined the time region of interest from 2 s before to 3 s after the movement onset. The subject-specific chance level for the multiclass approach lies at 33.5% (alpha = 0.05, adjusted Wald-interval, Bonferroni corrected for multiple comparisons). For the grand average, chance level lies at 27.1%. Figure 7 shows the grand

average performance of the multiclass classification for the four different time windows tested. We were interested to evaluate the impact of window size on the overall performance. For all approaches better-than-chance classification was already possible in a time range between -0.5 s to 1 s relative to the movement onset (see figure 7, left plot). There is also almost no difference between the 1000 ms and the 1500 ms window in terms of performance. However, peak accuracy and its timing shifted with increasing window size as shown in table 3. We also investigated the subject-specific peak accuracies for each time window as shown in figure 7 (right plot). We conducted a one way repeated-measures ANOVA over the peak accuracies of all subjects per window size (4 levels). Mauchly’s test for sphericity indicated correction of the p-values. Correction was done using the Greenhouse–Geisser criterion. Their differences between peak accuracies for each time window were significant ( $F(3, 42) = 84.6, p < 0.001$ ).

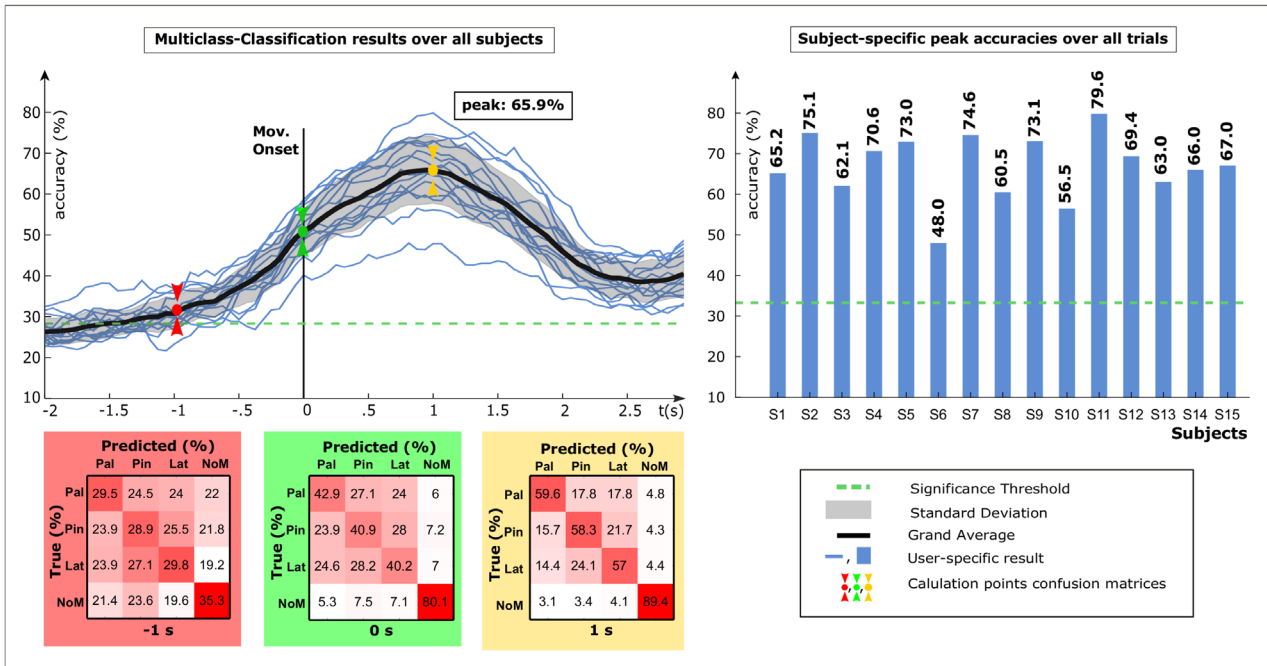


**Figure 8.** Multiclass classification results for a 1000 ms time-window. Top left plot displays the grand average classification performance including its standard deviation and subject-specific results. Colored marker represents calculation time points for the subjacent confusion matrices. Confusion matrices are normalized by row and display rates in percentage. The right plot shows subject-specific peak accuracies over all trials. Notice that the green dashed line represents the significant threshold in both plots (left plot for grand average over all subjects, right subject-specific level).

Post-hoc test for multiple comparison using the Tukey–Kramer criterion revealed that window-based performance is significantly better than the one sample approach. We also found that the 1000 ms and the 1500 ms perform significantly better ( $p = 0.02$ ) than the 500 ms window.

For the rest of the analysis we chose the classification approach using the time window of 1000 ms. Figure 8 displays multiclass-classification results for all subjects using the 1000 ms time window. We attained the grand average peak accuracy of 65.9%. As shown in figure 7 better-than-chance classification was already possible more than 1 s before movement onset.

Apart from the classification results for participants S6 and S10, all peak accuracies exceeded 60%. In figure 8 top right, we show the subject-specific peak accuracies which result on average in 66.9%. This value differs from the grand average due to the variance in peak time per subject.

Since our method incorporates its own classification model every 1/16 of a second, we were able to show condition specific confusion matrices at several timepoints of interest (figure 8, bottom). In this case we chose 1 s before movement onset (i, red), movement onset (ii, green) and 1 s after the cue (iii, yellow). While the true positive rate is similar for all contributing classes in (i), the true positive rate of the no-movement condition is almost twice as high in (ii) and almost a third higher in (iii). This resembles the results we presented previously in the binary classification approach (grasp versus no movement) and the underlying MRCPs, in which distinct differences between grasping movements and no movement could be seen on a broad time interval (–1 to 1 relative to the movement onset). However, in (iii) true positive rates for the grasp classes also reached values of almost 60%.

Incorporating the 1000 ms window for feature extraction, we also investigated three additional electrode setups with reduced number of electrodes, as can be seen in figure 9. For all tested layouts better than chance accuracies could be achieved. With increasing number of electrodes, performance increased for all subjects. We conducted a one-way repeated-measures ANOVA over the peak accuracies of all subjects per channel layout (four levels). Mauchly’s test for sphericity indicated no need for correction. The differences between peak accuracies for each channel layout were significant ( $F(3, 42) = 78.505$ ,  $p < 0.001$ ). Post-hoc test for multiple comparison using the Tukey–Kramer criterion revealed that all channel-layouts are significantly different from each other.

## Discussion

In this paper we show that it is possible to discriminate three executed reach-and-grasp actions prominent in everyday life using their EEG neural correlates. Furthermore, we show that these actions can be discriminated against no-movement with high accuracy. In the binary classification scenario, performance for grasp versus grasp conditions peaked on average at 72.4% (STD  $\pm$  5.8%), for grasps versus the no-movement peak performances of 93.5% (STD  $\pm$  4.6%) could be reached. For the multiclass classification scenario which incorporated all reach-and-grasp conditions and the no-movement condition, maximum performance (65.9%, STD  $\pm$  8.1%) could be reached using a feature window of 1000 ms. Underlying MRCPs of the reach-and-grasp actions investigated over the primary motor cortex showed significant differences starting from approximately 800 ms to 1200 ms after the movement

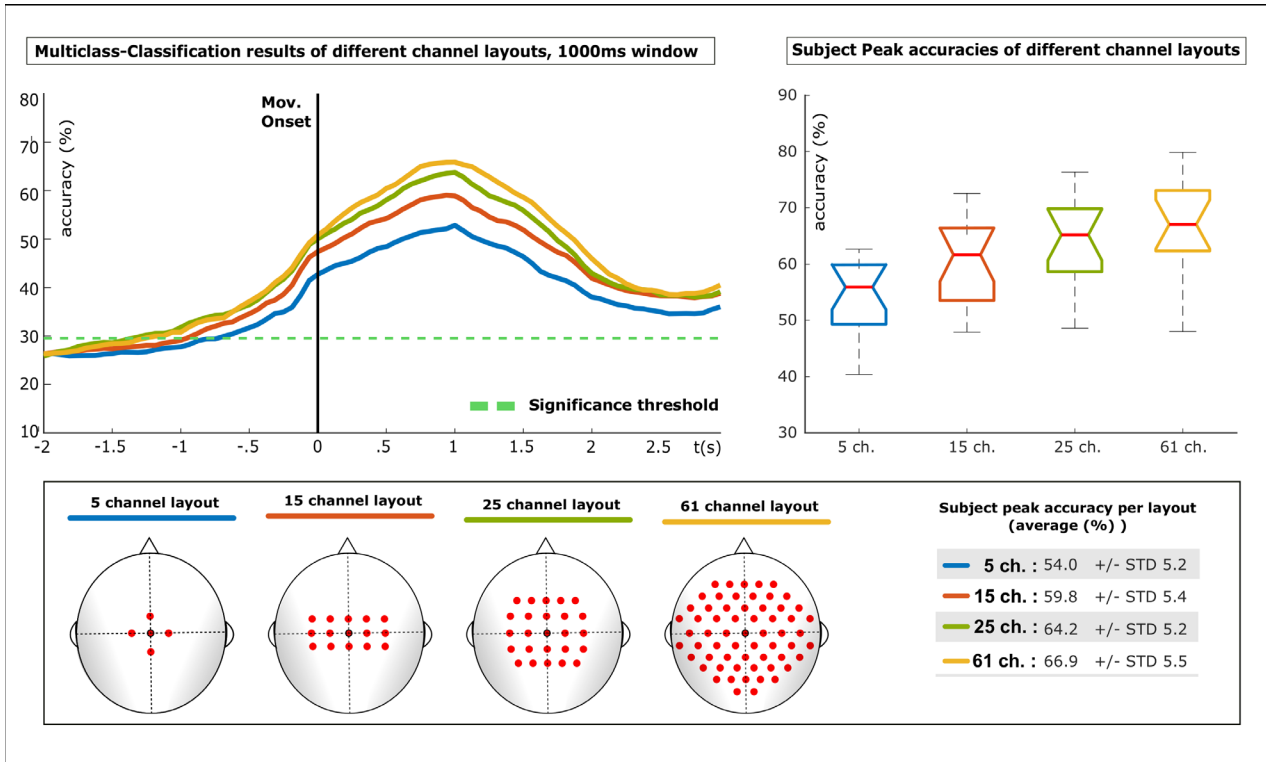


**Figure 9.** Multiclass evaluation of different electrode layouts using the 1000 ms time-window. Top left plot displays the multiclass classification accuracy for all four layouts (color-coded). The boxplots on the right show the range of peak accuracies for all subjects for each electrode layout. In the bottom part of the figure we visualize the four different electrode layouts.

onset which is the same time frame where classification performance reached its maximum.

*Movement-related cortical potentials*

Analysis of the MRCPs for each reach-and-grasp condition showed the maximum negative shift imminent to the movement onset, as previously described by Shibasaki et al in [25] and presented also in other studies that investigate the neural correlates of upper limb movements such as Gu et al [51, 52], Jochumsen et al [30, 53] or Oda et al [54]. Our analysis shows that the maximum negative shift occurs over the central motor cortex (Cz) imminent to the movement onset and is more pronounced on the contralateral side (C1) than on the ipsilateral side (C2). This effect can be seen further in the extended MRCPs analysis provided as supplementary material.

Comparisons between all conditions reveal that all reach-and-grasp conditions show significant differences to the no-movement condition over the whole tROI.

In all grasp-versus-grasp conditions we found significant differences ( $p < 0.05$ ) emerging around one second before the movement onset, however most pronounced differences are found around 0.8 s ms to 1.2 s after the movement onset.

Interestingly we found a time shift in the peaks of this positive rebound potential for the reach-and-grasp conditions. This time shift is pronounced strongest in condition combinations involving the lateral grasp. This potential produced by the lateral grasp appears the earliest of all reach-and-grasp conditions. It can be seen not only at contralateral, but also at central and ipsilateral sides.

The behavioural analysis indicate that subjects finished grasping objects on average between 1.1 s and 1.25 s after the movement onset. This falls in the same time frame where the significant differences between the MRCPs can be found.

*Single trial classification*

Binary single trial classifications show high classification results for movement versus no-movement conditions with subject-specific accuracies over 90%. Even for subjects (S6, S10) with unfavourable grasp versus grasp classification performance detection rates reach performances of 85% and more. Peak accuracies were reached within the first second after the movement onset. The movement intention could be detected before the actual movement with performance rates exceeding 80% in grand average over all subjects. These performance results are similar to the findings reported by other studies regarding the detection of upper limb movement intention [31, 34, 55] and [56] (online).

Binary grasp versus grasp classification performance ranged from ~70% to 73% on grand average. Subject-specific accuracies were usually higher (~+3%) due to variances in peak timing. Only for two subjects (S6, S10) any grasp versus grasp combination scored lower than chance (S6: Lateral versus Palmar; S10: Palmar versus Pincer, Lateral versus Pincer). We could also observe significant classification performance imminently before the movement onset ranging from 57%–59%. These results are in line with the findings of Jochumsen et al [31] who investigated strategies for discriminating grasp intentions. Using



temporal features in the range of 0.01–5 Hz, they obtained similar performance results. However, the focus of their study was only on the movement intention and it does not reflect the whole movement process including reaching. We obtained grand average peak accuracies around 1–1.5 s after movement onset.

Peak accuracies correspond to changes in amplitude in the neural correlates in which we observed significant differences regarding the emerging of a positive rebound potential of the reach-and-grasp conditions as well as in their time shift.

Regarding the multi-class classification approach significant classification results could also be reached up to 1 s before the movement onset. In the multi-class classification approach confusion matrices reveal a disproportionate contribution to the true positive rate by the movements versus no-movement condition. Despite true-positive rates being significantly higher than chance level for all movement versus movement conditions, the movement versus no-movement condition contribute almost twice as high to the overall performance at movement onset. In the multiclass scenario, peak accuracy of 65.9% was reached one second after the movement onset. Again, confusion matrices show high contribution of movement versus no-movement conditions, however also grasp versus grasp conditions contributed equally to the overall performance (~ two third ratio).

With respect to the previously mentioned findings of Agashe *et al* [32], a direct comparison of performance results is difficult due to differences in the methodological approach and in the experimental setup. We also investigated the no-movement condition in the multiclass scenario, which was not incorporated in their study. However, in their study, participants reached peak accuracy for classification already 250 ms after the movement onset which is approximately 750 ms earlier than we report in our findings (1 s after movement onset). This suggests that they find their most discriminant information already within the early reaching phase to the object, while our results indicate peak accuracy during the grasping itself.

#### *Implications of the window size and electrode setup*

Regarding our investigations on different window sizes in the multiclass approach we show that all window-based approaches could outperform single sample based classification significantly ( $p < 0.001$ ).

Interestingly, we also found a significant difference in performance ( $p = 0.02$ ) between 500 ms and the 1000 ms window, which suggests that discriminative information for different reach-and-grasp actions is spread over a longer period of time than 500 ms. Our behavioural analysis also shows that all reach-and-grasp actions are on average slightly longer than 1000 ms (1100 ms to 1250 ms) which also implies that the 1000 ms window allows better coverage of the whole reach-and-grasp action than a shorter one. We also tested a 1500 ms window, though performance compared to the 1000 ms window was almost identical and no significant differences could be found ( $p > 0.86$ ). However, we observed a delay in peak performance of around 400 ms.

Our investigation towards different electrode setups clearly showed that with increasing number of electrodes also peak performance increases. This effect is present for each subject and lead to the significant ( $p < 0.05$ ) differences between all evaluated electrode setups. However, by reducing the number of electrodes (and therefore the feature space for the classifier) by almost two thirds to 25 electrodes, peak performance decreases by less than 3%, which suggests a possible trade-off between performance and usability in e.g. an out-of-the-lab scenario incorporating potential end users.

#### *Limitations*

In this study we used a cue-based protocol and conducted an offline analysis. In this regard we used zero-phase bandpass filtering EEG to compensate for the group delay. In an online scenario, non-causal filtering is not possible.

To allow a fair comparison between movement and no-movement conditions we time-locked the no-movement condition according to a virtual onset calculated from the subject's reaction time. In our opinion, these no-movement epochs are not comparable to real resting periods since these epochs are interspersed in a cue guided experiment setting which demands the subjects attention and action. In an online scenario, a real resting period would persist over a longer period or during a phase in which subjects intentionally do not attempt any form of control (e.g. while watching a movie).

With increasing window size the increasing number of features becomes an issue. The larger the number of features included the more unfavourable the trial to feature ratio, which ultimately results in an increased validation error. Empirical evaluation of this issue was already performed by Blankertz *et al* [45]. With a linear increase of features used, the dimensionality of the feature space grows exponentially. This results in a poor estimation of the covariance matrix for the classification model and has a high negative impact on classification performance ('curse of dimensionality').

One possibility to overcome this issue would be to use a feature reduction technique to keep only features containing high discriminative information, such as sequential forward selection (SFS, already applied in [31]) or the smooth and decimation approach used in [57]. In our experimental setup we used a causal sliding window for extracting features for classification. In an online scenario, any window based approach will introduce a delay with regard to the reach-and-grasp action of the subject. Although this is a static delay, increasing window size will also increase the delay and introduce an offset time in any BCI control scenario. However, this applies to any causal online scenario and is not solely a limitation of this specific experiment.

#### *Transfer to online control and future work*

So far we showed in offline analysis that three reach-and-grasp movements towards different objects can be discriminated from low-frequency EEG time domain features.

Our offline analysis showed better-than-chance performance in single trial classification, however the generation

of robust motor commands needs to be investigated further in online setups. Our results show peak accuracies around 75% on grand average, which suggest that at best three out of four reach-and-grasp commands could be decoded correctly. In previous sensori-motor rhythm (SMR) based BCI studies [58–60] incorporating cerebral palsy end users, we investigated possibilities to accumulate multiple control commands for one single decision. This evidence accumulation strategy demanded three ‘correct’ commands out of e.g. five to finally trigger the correct action. Though the whole process of decision making is prolonged, erroneous commands are less probable.

Another idea for boosting BCI performance would be to incorporate error-related potentials (ErrP) into the decision process, as already briefly introduced by Kreilinger *et al* [61] using motor imagery tasks (MI). The idea here would be to use a hybrid combination of EEG based detectors for grasps and ErrP. Whenever a misclassification of the designated grasp happens, the triggered ErrP could be used for undo. We hypothesize that this combination could lead to increased overall performance, however data collection for calibration will require a more complex paradigm since not only grasps, but also ErrP data has to be collected.

In this study we rejected on average around 12% of trials due to artefact contamination which would affect at least every tenth grasp attempt in an online scenario. Though artefacts may not be avoided completely, we believe that with proper end user training this percentage can be decreased. Still, for robust grasp control these contaminated attempts need to be handled accordingly e.g. by signaling the end user to repeat the current action.

For this experiment we used a high density electrode grid of 61 electrodes placed on frontal, central and parietal areas over the scalp. Our investigations show that this grid can be reduced by almost two thirds to 25 electrodes, while still maintaining similar performance. This factor might become critical when attempting to leave a controlled laboratory environment and, for instance, when working together with end users in their own homes.

Successful online control requires reliable movement intention detection since the exploited MRCPs are time-locked to the movement onset. In this study, we showed high detection accuracies for movements versus no-movement conditions. In an online scenario, a hierarchical classification model could be used to detect the movement intention of the user and rely on this detection point as a timelock for grasp versus grasp discrimination. This approach has already been used offline in several studies incorporating complex hand movements [31, 33, 62].

Further studies incorporating high spinal cord injured end users will finally assess whether our current results can be translated to the targeted end user group. The command strategy in our study relied on executed movements and it is still unknown whether similar classification results could be achieved in end users. Studies from Blokland *et al* [63, 64] and Verbaarschot *et al* [65] indicate that attempted movements may present a better command strategy than imagined

movements. Also Lacourse *et al* [66] indicated higher correlations between attempted and imagined movements of tetraplegic end users than between executed and imagined movements of a healthy control group. Our first experiments incorporating high SCI end users performing attempted complex hand movements confirm [67] that attempted grasps of end users can be discriminated better than chance.

## Conclusion

In this study we showed that it is possible to discriminate three executed reach-and-grasp actions prominent in people’s everyday use from non-invasive EEG. Based on their neural correlates, we could show differentiation against each other and also against a no-movement condition. Furthermore we could identify significant differences in the underlying movement-related cortical potentials.

This findings will eventually contribute to our attempt of controlling a neuroprosthesis in a natural and intuitive way and a step closer to a successful and reliable intervention for end users with high spinal cord injury.



## Acknowledgments

This work was funded by the Horizon 2020 programme project ‘MoreGrasp’ (643955) and the ERC Consolidator Grant ‘FeelYourReach’ (681231). Special thanks to Dietmar Josef Schäffauer who helped manufacturing the plexiglass objects and the monitor table. We also thank Michael Burtscher for design support in creating figure 2.

## Author contributions

AS, GRMP and PO designed the study; AS performed the experiment; AS performed the analysis; AS, PO, GRMP, JP and AIS wrote the paper.

## ORCID iDs

Andreas Schwarz  <https://orcid.org/0000-0002-3883-4989>  
 Patrick Ofner  <https://orcid.org/0000-0001-7169-4300>  
 Joana Pereira  <https://orcid.org/0000-0002-2032-8981>  
 Andreea Ioana Sburlea  <https://orcid.org/0000-0001-6766-3464>  
 Gernot R. Müller-Putz  <https://orcid.org/0000-0002-0087-3720>

## References

- [1] Snoek G J, IJzerman M J, Hermens H J, Maxwell D and Biering-Sorensen F 2004 Survey of the needs of patients with spinal cord injury: impact and priority for improvement in hand function in tetraplegics *Spinal Cord* **42** 526–32
- [2] Anderson K D 2004 Targeting recovery: priorities of the spinal cord-injured population *J. Neurotrauma* **21** 1371–83

- [3] Anderson K D 2009 Consideration of user priorities when developing neural prosthetics *J. Neural Eng.* **6** 055003
- [4] Peckham P H *et al* 2002 An advanced neuroprosthesis for restoration of hand and upper arm control using an implantable controller *J. Hand Surg. Am.* **27** 265–76
- [5] Rupp R and Gerner H J 2007 Neuroprosthetics of the upper extremity—clinical application in spinal cord injury and challenges for the future *Acta Neurochir. Suppl.* **97** 419–26
- [6] Müller-Putz G R, Scherer R, Pfurtscheller G and Rupp R 2005 EEG-based neuroprosthesis control: a step towards clinical practice *Neurosci. Lett.* **382** 169–74
- [7] Müller-Putz G R, Scherer R, Pfurtscheller G and Rupp R 2006 Brain–computer interfaces for control of neuroprostheses: from synchronous to asynchronous mode of operation *Biomed. Tech.* **51** 57–63
- [8] Halder S *et al* 2015 Brain-controlled applications using dynamic P300 speller matrices *Artif. Intell. Med.* **63** 7–17
- [9] Farwell L A and Donchin E 1988 Talking off the top of your head: toward a mental prosthesis utilizing event-related brain potentials *Electroencephalogr. Clin. Neurophysiol.* **70** 510–23
- [10] Kaufmann T, Schulz S M, Grünzinger C and Kübler A 2011 Flashing characters with famous faces improves ERP-based brain–computer interface performance *J. Neural Eng.* **8** 056016
- [11] Müller-Putz G R, Scherer R, Neuper C and Pfurtscheller G 2006 Steady-state somatosensory evoked potentials: suitable brain signals for brain–computer interfaces? *IEEE Trans. Neural. Syst. Rehabil. Eng.* **14** 30–7
- [12] Pfurtscheller G and Lopes da Silva F H 1999 Event-related EEG/MEG synchronization and desynchronization: basic principles *Clin. Neurophysiol.* **110** 1842–57
- [13] Friedrich E V C, Neuper C and Scherer R 2013 Whatever works: a systematic user-centered training protocol to optimize brain–computer interfacing individually *PLoS One* **8** e76214
- [14] Pfurtscheller G and Neuper C 2001 Motor imagery and direct brain–computer communication *Proc. IEEE* **89** 1123–34
- [15] Pfurtscheller G, Gert P, Müller G R, Jörg P, Gerner H J and Rüdiger R 2003 ‘Thought’—control of functional electrical stimulation to restore hand grasp in a patient with tetraplegia *Neurosci. Lett.* **351** 33–6
- [16] Rohm M *et al* 2013 Hybrid brain–computer interfaces and hybrid neuroprostheses for restoration of upper limb functions in individuals with high-level spinal cord injury *Artif. Intell. Med.* **59** 133–42
- [17] Kreiling A, Rohm R, Kaiser V, Leeb R, Rupp R and Müller-Putz G R 2013 Neuroprosthesis control via a noninvasive hybrid brain–computer interface *IEEE Intell. Syst.* **28** 40–3
- [18] Müller-Putz G R, Scherer R, Pfurtscheller G and Neuper C 2010 Temporal coding of brain patterns for direct limb control in humans *Front. Neurosci.* **4** 34
- [19] Rupp R, Rüdiger R, Martin R, Matthias S, Alex K and Müller-Putz G R 2015 Functional rehabilitation of the paralyzed upper extremity after spinal cord injury by noninvasive hybrid neuroprostheses *Proc. IEEE* **103** 954–68
- [20] Jakobson L S and Goodale M A 1991 Factors affecting higher-order movement planning: a kinematic analysis of human prehension *Exp. Brain Res.* **86** 199–208
- [21] Castiello U 2005 The neuroscience of grasping *Nat. Rev. Neurosci.* **6** 726–36
- [22] Popovic D, Dejan P and Thomas S 2008 Central nervous system lesions leading to disability *Automatica* **18** 11–23
- [23] Pistohl T, Schulze-Bonhage A, Aertsen A, Mehring C and Ball T 2012 Decoding natural grasp types from human ECoG *Neuroimage* **59** 248–60
- [24] Pistohl T, Schmidt T S B, Ball T, Schulze-Bonhage A, Aertsen A and Mehring C 2013 Grasp detection from human ECoG during natural reach-to-grasp movements *PLoS One* **8** e54658
- [25] Shibasaki H, Hiroshi S and Mark H 2006 What is the Bereitschaftspotential? *Clin. Neurophysiol.* **117** 2341–56
- [26] Waldert S, Pistohl T, Braun C, Ball T, Aertsen A and Mehring C 2009 A review on directional information in neural signals for brain–machine interfaces *J. Physiol. Paris* **103** 244–54
- [27] Vuckovic A and Sepulveda F 2008 Delta band contribution in cue based single trial classification of real and imaginary wrist movements *Med. Biol. Eng. Comput.* **46** 529–39
- [28] Ofner P, Schwarz A, Pereira J and Müller-Putz G R 2016 Movements of the same upper limb can be classified from low-frequency time-domain EEG signals *Proc. of the Sixth International Brain–Computer Interface Meeting: BCI Past, Present, and Future (June 2016)* (Verlag der technischen Universität Graz)
- [29] Slobounov S, Hallett M and Newell K M 2004 Perceived effort in force production as reflected in motor-related cortical potentials *Clin. Neurophysiol.* **115** 2391–402
- [30] Jochumsen M, Niazi I K, Mrachacz-Kersting N, Farina D and Dremstrup K 2013 Detection and classification of movement-related cortical potentials associated with task force and speed *J. Neural Eng.* **10** 056015
- [31] Jochumsen M, Niazi I K, Dremstrup K and Kamavuako E N 2016 Detecting and classifying three different hand movement types through electroencephalography recordings for neurorehabilitation *Med. Biol. Eng. Comput.* **54** 1491–501
- [32] Agashe H A, Paek A Y, Zhang Y and Contreras-Vidal J L 2015 Global cortical activity predicts shape of hand during grasping *Front. Neurosci.* **9** 121
- [33] Jochumsen M, Niazi I K, Taylor D, Farina D and Dremstrup K 2015 Detecting and classifying movement-related cortical potentials associated with hand movements in healthy subjects and stroke patients from single-electrode, single-trial EEG *J. Neural Eng.* **12** 056013
- [34] Randazzo L, Luca R, Inaki I, Ricardo C, Robert L and Del Millan J R 2015 Detecting intention to grasp during reaching movements from EEG *2015 37th Annual Int. Conf. of the IEEE Engineering in Medicine and Biology Society (EMBC)* (<https://doi.org/10.1109/EMBC.2015.7318561>)
- [35] Schwarz A, Ofner P, Pereira J and Müller-Putz G R 2016 Time domain classification of grasp and hold tasks *Proc. of the Sixth International Brain–Computer Interface Meeting: BCI Past, Present, and Future (June 2016)* ed G R Müller-Putz *et al* (Verlag der Technischen Universität Graz) p 76
- [36] Itturate I, Leeb R, Chavarriaga R and Millan J 2016 Decoding of two hand grasping types from EEG *Proc. of the 6th Int. Brain–Computer Interface Meeting: BCI Past, Present, and Future (June 2016)* (Verlag der Technischen Universität Graz) p 66
- [37] Agashe H A, Paek A Y and Contreras-Vidal J L 2016 Multisession, noninvasive closed-loop neuroprosthetic control of grasping by upper limb amputees *Prog. Brain Res.* **228** 107–28
- [38] Burtscher M Nu-art, michael burtscher, grafk, design, illustrationen *Nu-Art* (cited 27 Mar 2017) (Available at: <http://nu-art.at/>)
- [39] Schlögl A, Keinrath C, Zimmermann D, Scherer R, Leeb R and Pfurtscheller G 2007 A fully automated correction method of EOG artifacts in EEG recordings *Clin. Neurophysiol.* **118** 98–104
- [40] Breitwieser C, Daly I, Neuper C and Müller-Putz G R 2012 Proposing a standardized protocol for raw biosignal transmission *IEEE Trans. Biomed. Eng.* **59** 852–9
- [41] Fatourechi M, Bashashati A, Ward R K and Birch G E 2007 EMG and EOG artifacts in brain computer interface systems: a survey *Clin. Neurophysiol.* **118** 480–94
- [42] Faller J, Vidaurre C, Solis-Escalante T, Neuper C and Scherer R 2012 Autocalibration and recurrent adaptation:

- towards a plug and play online ERD-BCI *IEEE Trans. Neural. Syst. Rehabil. Eng.* **20** 313–9
- [43] Schwarz A, Andreas S, Reinhold S, David S, Josef F and Müller-Putz G R 2015 A co-adaptive sensory motor rhythms brain–computer interface based on common spatial patterns and Random Forest *2015 37th Annual Int. Conf. of the IEEE Engineering in Medicine and Biology Society (EMBC)* (<https://doi.org/10.1109/EMBC.2015.7318545>)
- [44] Schwarz A, Steyrl D and Müller-Putz G R 2016 Brain–computer interface adaptation for an end user to compete in the Cybathlon 2016 *IEEE Int. Conf. on Systems, Man, and Cybernetics (SMC)* (<https://doi.org/10.1109/SMC.2016.7844499>)
- [45] Blankertz B, Lemm S, Treder M, Haufe S and Müller K-R 2011 Single-trial analysis and classification of ERP components—a tutorial *Neuroimage* **56** 814–25
- [46] Thomas E, Dyson M and Clerc M 2013 An analysis of performance evaluation for motor-imagery based BCI *J. Neural Eng.* **10** 031001
- [47] Wolpaw J R, Ramoser H, McFarland D J and Pfurtscheller G 1998 EEG-based communication: improved accuracy by response verification *IEEE Trans. Rehabil. Eng.* **6** 326–33
- [48] Duda R O, Hart P E and Stork D G 2012 *Pattern Classification* (New York: Wiley)
- [49] Billinger M et al 2012 Is it significant? guidelines for reporting BCI performance *Biological and Medical Physics, Biomedical Engineering* (Berlin: Springer) pp 333–54
- [50] Müller-Putz G R, Scherer R, Brunner C, Leeb R and Pfurtscheller G 2008 Better than Random? A closer look on BCI results *Int. J. Bioelectromagn.* **10** 52–5
- [51] Gu Y, Dremstrup K and Farina D 2009 Single-trial discrimination of type and speed of wrist movements from EEG recordings *Clin. Neurophysiol.* **120** 1596–600
- [52] Gu Y, do Nascimento O F, Lucas M-F and Farina D 2009 Identification of task parameters from movement-related cortical potentials *Med. Biol. Eng. Comput.* **47** 1257–64
- [53] Jochumsen M, Niazi I K, Mrachacz-Kersting N, Jiang N, Farina D and Dremstrup K 2015 Comparison of spatial filters and features for the detection and classification of movement-related cortical potentials in healthy individuals and stroke patients *J. Neural Eng.* **12** 056003
- [54] Oda S and Moritani T 1995 Movement-related cortical potentials during handgrip contractions with special reference to force and electromyogram bilateral deficit *Eur. J. Appl. Physiol. Occup. Physiol.* **72** 1–5
- [55] Niazi I K, Jiang N, Tiberghien O, Nielsen J F, Dremstrup K and Farina D 2011 Detection of movement intention from single-trial movement-related cortical potentials *J. Neural Eng.* **8** 066009
- [56] Xu R, Jiang N, Lin C, Mrachacz-Kersting N, Dremstrup K and Farina D 2014 Enhanced low-latency detection of motor intention from EEG for closed-loop brain–computer interface applications *IEEE Trans. Biomed. Eng.* **61** 288–96
- [57] Pinegger A, Faller J, Halder S, Wriessnegger S C and Müller-Putz G R 2015 Control or non-control state: that is the question! An asynchronous visual P300-based BCI approach *J. Neural Eng.* **12** 014001
- [58] Scherer R, Schwarz A, Müller-Putz G R, Pammer-Schindler V and Garcia M L 2016 Lets play Tic-Tac-Toe: a brain–computer interface case study in cerebral palsy *2016 IEEE Int. Conf. on Systems, Man, and Cybernetics (SMC)* (<https://doi.org/10.1109/SMC.2016.7844815>)
- [59] Scherer R et al 2015 Thought-based row-column scanning communication board for individuals with cerebral palsy *Ann. Phys. Rehabil. Med.* **58** 14–22
- [60] Scherer R, Schwarz A, Müller-Putz G R, Pammer-Schindler V and Garcia M L 2015 Game-based bci training: interactive design for individuals with cerebral palsy *2015 IEEE Int. Conf. on Systems, Man, and Cybernetics* (<https://doi.org/10.1109/SMC.2015.551>)
- [61] Kreilinger A, Hiebel H and Müller-Putz G R 2016 Single versus multiple events error potential detection in a bci-controlled car game with continuous and discrete feedback *IEEE Trans. Biomed. Eng.* **63** 519–29
- [62] Omedes J, Schwarz A, Monsanto L and Müller-Putz G R 2017 Hierarchical decoding of grasping commands from EEG *Proc. of the 39th Annual Int. Conf. of the IEEE Engineering in Medicine and Biology Society (EMBC'17)*
- [63] Blokland Y et al 2012 Detection of event-related desynchronization during attempted and imagined movements in tetraplegics for brain switch control *Conf. Proc. IEEE Eng. Med. Biol. Soc.* **2012** 3967–9
- [64] Blokland Y et al 2015 Detection of attempted movement from the EEG during neuromuscular block: proof of principle study in awake volunteers *Sci Rep.* **5** 12815
- [65] Verbaarschot C, Farquhar J and Haselager P 2015 Lost in time *Conscious Cogn.* **33** 300–15
- [66] Lacourse M G, Cohen M J, Lawrence K E and Romero D H 1999 Cortical potentials during imagined movements in individuals with chronic spinal cord injuries *Behav. Brain Res.* **104** 73–88
- [67] Müller-Putz G R, Ofner P, Schwarz A and Pereira J 2017 MoreGrasp: restoration of upper limb function in individuals with high spinal cord injury by multimodal neuroprostheses for interaction in daily activities *Proc. of the 7th Graz Brain–Computer Interface Conf.* (<https://doi.org/10.3217/978-3-85125-533-1-62>)



## PAPER

## OPEN ACCESS

RECEIVED  
6 December 2019REVISED  
27 March 2020ACCEPTED FOR PUBLICATION  
9 April 2020PUBLISHED  
28 May 2020

Original content from  
this work may be used  
under the terms of the  
[Creative Commons  
Attribution 4.0 licence](#).

Any further distribution  
of this work must  
maintain attribution to  
the author(s) and the title  
of the work, journal  
citation and DOI.



# Decoding hand movements from human EEG to control a robotic arm in a simulation environment

Andreas Schwarz<sup>1</sup> , Maria Katharina Höller<sup>1</sup>, Joana Pereira<sup>1</sup> , Patrick Ofner<sup>1,2</sup>   
and Gernot R Müller-Putz<sup>1,3</sup>

<sup>1</sup> Institute of Neural Engineering, Graz University of Technology, Stremayrgasse 16/IV, Graz 8010, Austria

<sup>2</sup> Know-Center GmbH, Graz 8010, Austria

<sup>3</sup> Author to whom any correspondence should be addressed.

E-mail: [gernot.mueller@tugraz.at](mailto:gernot.mueller@tugraz.at)

**Keywords:** movement-related cortical potential, MRCP, grasping, brain-computer interface, BCI, simulation environment, movement decoding

Supplementary material for this article is available [online](#)

## Abstract

**Objective.** Daily life tasks can become a significant challenge for motor impaired persons. Depending on the severity of their impairment, they require more complex solutions to retain an independent life. Brain-computer interfaces (BCIs) are targeted to provide an intuitive form of control for advanced assistive devices such as robotic arms or neuroprostheses. In our current study we aim to decode three different executed hand movements in an online BCI scenario from electroencephalographic (EEG) data. **Approach.** Immersed in a desktop-based simulation environment, 15 non-disabled participants interacted with virtual objects from daily life by an avatar's robotic arm. In a short calibration phase, participants performed executed palmar and lateral grasps and wrist supinations. Using this data, we trained a classification model on features extracted from the low frequency time domain. In the subsequent evaluation phase, participants controlled the avatar's robotic arm and interacted with the virtual objects in case of a correct classification. **Main results.** On average, participants scored online 48% of all movement trials correctly (3-condition scenario, adjusted chance level 40%,  $\alpha = 0.05$ ). The underlying movement-related cortical potentials (MRCPs) of the acquired calibration data show significant differences between conditions over contralateral central sensorimotor areas, which are retained in the data acquired from the online BCI use. **Significance.** We could show the successful online decoding of two grasps and one wrist supination movement using low frequency time domain features of the human EEG. These findings can potentially contribute to the development of a more natural and intuitive BCI-based control modality for upper limb motor neuroprostheses or robotic arms for people with motor impairments.

## 1. Introduction

Motor impairment has a significant effect on a person's daily life. Depending on the severity of their impairment, persons may not be able to walk, eat, drink or even brush their teeth without the help of a caregiver anymore. Motor impairment can have a broad variety of causes ranging from severe trauma to the spinal cord (SCI) and neuropathological conditions to stroke. Naturally, affected persons seek intervention to cushion the resulting effects such as muscle and tendon transfers for tetraplegic SCI persons [1–4], extensive stroke rehabilitation [5] or in the case

of motor neuron diseases, delay and reduce its symptoms [6, 7]. When surgical or physiotherapeutic interventions reach their limits, assistive devices attempt to bridge the gap towards a comparatively independent life. The more severe the grade of impairment, the higher the need for more customized assistive devices become.

Non-invasive brain-computer interfaces (BCIs), though still in a prototype stage, can potentially provide a customized control modality for even the most severe cases of motor impairment. They attempt to decode brain signals acquired in real time ('online') by using the electroencephalogram (EEG). Using state

of the art machine learning methods [8, 9], a control signal can be generated for controlling assistive devices [10], e.g. a robotic arm [11] or an upper limb motor neuroprosthesis [12–15].

So far, BCIs intended for control of assistive devices often relied on repetitive mental imagery (MI) and oscillation based features for generating control signals [12–15].

Recent studies however have shown that movement-related cortical potentials (MRCPs) [16–18], extracted from the low frequency time domain (LFTD), hold sufficient information for decoding singular, non-repetitive movements: They have been shown to encode information about both singular lower limb [19–22] as well as upper limb movements [23–28] including grasp force and speed [26, 29] and even directional information from reaching movements [30].

In the field of stroke rehabilitation, Mrachacz-Kersting *et al* already successfully integrated an MRCP-based BCI in lower limb rehabilitation for stroke survivors: the BCI decodes in real-time EEG correlates of stroke patients performing lower limb movements, which in turn activates non-invasive transcranial magnetic stimulation (TMS). Their results show in both chronic and subacute patients neuroplastic changes and further significant improvements in regaining movement functionality (clinical scales) [31–34]. In the same field of research, this approach is already investigated for upper limb movements [35].

MRCPs are also investigated for the purpose of control. Especially in the case of persons with high spinal cord injury, BCIs are primarily intended to control artificial limbs, such as robotic arms [11] or upper limb motor neuroprosthesis [36]. Studies conducted in non-disabled populations have shown offline that MRCPs hold sufficient information to decode upper limb movements [25] including complex reach and grasp movements [23, 24, 37]. However, to our knowledge only one proof-of concept study with one participant has applied this online in a BCI [38]. Recently, Ofner *et al* showed offline that MRCPs of tetraplegic end users ( $n = 10$ ) still retain sufficient information for decoding upper limb movements [38]. Additionally, they showed in a proof-of-concept study asynchronous online decoding of hand open vs. palmar grasp attempts in one participant with tetraplegia.

Their offline analysis further revealed that the EEG potentials associated with the motor task in a cue-locked paradigm are contaminated by potentials which are related with the processing of the cue itself. This effect can be problematic: if one wants to develop an online classifier for asynchronous use, the EEG potentials around the movement onset in a cue-free scenario consist solely of the MRCPs itself, without time-locked influences of visual cues (see also [25, 39]). It is therefore imperative to study new

possibilities to gather calibration data that is equally properly labelled, but in which movement-related features are not masked by the presentation of cues.

Hence, the aims of our current study were two-fold: First, while most studies have investigated MRCPs for upper limb decoding rely on offline analysis, we wanted to assess the feasibility of MRCPs in an online system, i.e. allowing for BCI control. Our second goal was to minimize the influence of discrete visual cues in the EEG signals, since such cues could mask discriminable information in the low-frequency time-domain.

Therefore, we measured 15 healthy participants that performed three different hand movements of daily life: (i) palmar grasp, (ii) lateral grasp and (iii) wrist supination. We presented the instructions in a realistic simulation environment, engaging study participants in daily life actions (e.g. grasping a glass with a palmar grasp). After recording data for a calibration (calibration phase), we used features extracted from the LFTD to train a classification model. In a subsequent evaluation phase, we gave discrete feedback based on the participants' hand movements and evaluated the performance of the three-class online classifier.

## 2. Methods

### 2.1. Participants

Fifteen healthy participants aged between 21 and 35 years (median 26, eight male, seven female) took part in the experiment. The study was approved by the local ethics committee of the Medical University of Graz. Participants were briefed about the aims of the study and gave written informed consent to participate. They also received monetary compensation for their efforts. To evaluate their handedness, we performed the three stage hand dominance test developed by Steingrübler [40]. The test assesses the individual hand dominance quantifying the results of three exercises: (i) draw a line within a prescribed path, (ii), dot unaligned circles and (iii) dot horizontally aligned squares. Results show that 13 participants were right-handed and two left handed (see [stacks.iop.org/JNE/17/036010/mmedia](https://stacks.iop.org/JNE/17/036010/mmedia) supplementary table 1 for detailed results).

### 2.2. Experimental setup and paradigm—simulation of daily activities

We conducted all recordings at the BCI-Lab of the Institute of Neural Engineering at Graz University of Technology. Participants were seated in a noise and electromagnetically shielded room to facilitate a stable measurement environment. A monitor was placed in front of them which showed the paradigm. Participants positioned their right hand in an upright position comfortably on the armrest of the chair.

We designed a simulation environment for presenting instructions in a daily life setting: A motor

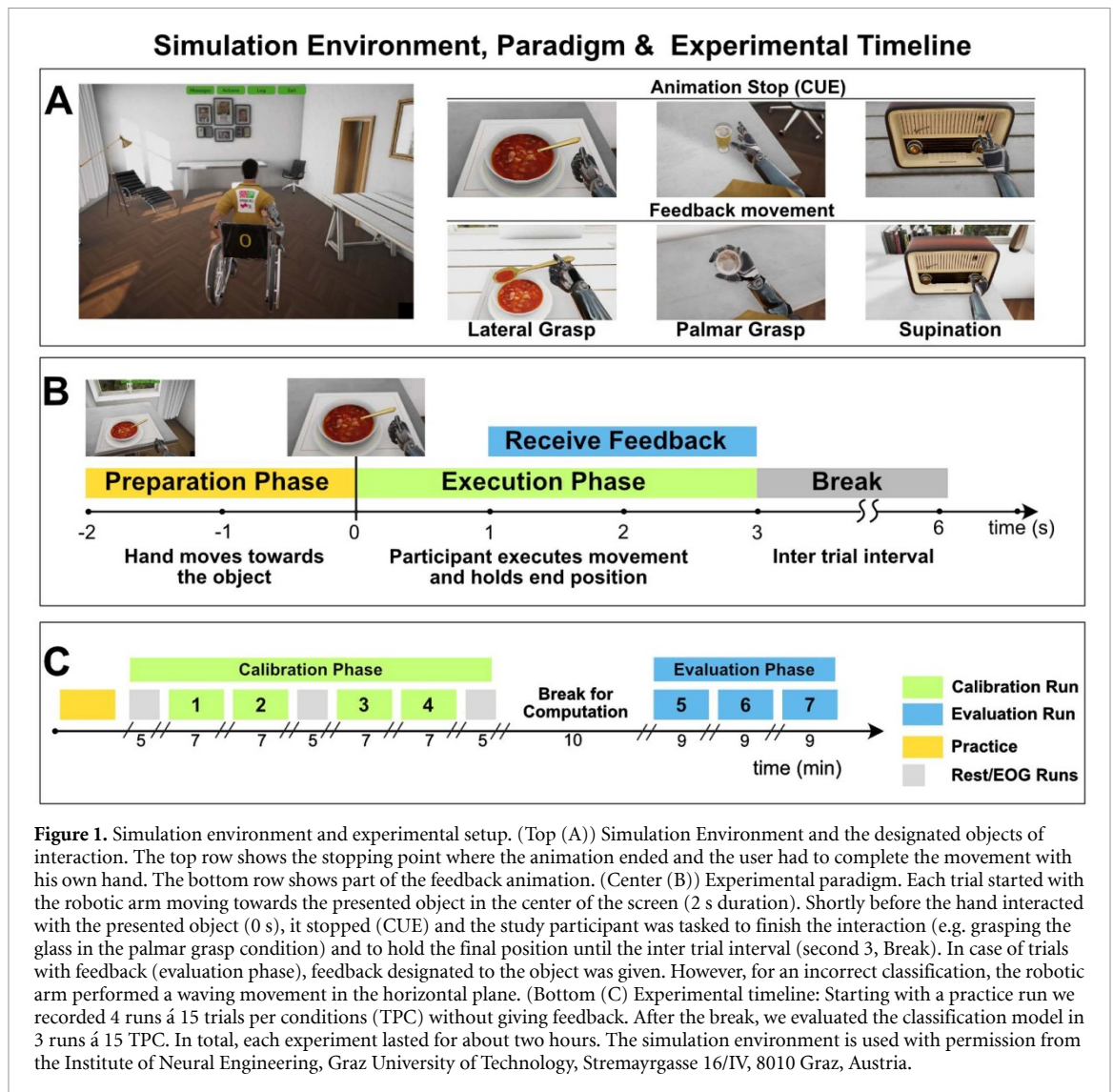


**Figure 1.** Simulation environment and experimental setup. (Top (A)) Simulation Environment and the designated objects of interaction. The top row shows the stopping point where the animation ended and the user had to complete the movement with his own hand. The bottom row shows part of the feedback animation. (Center (B)) Experimental paradigm. Each trial started with the robotic arm moving towards the presented object in the center of the screen (2 s duration). Shortly before the hand interacted with the presented object (0 s), it stopped (CUE) and the study participant was tasked to finish the interaction (e.g. grasping the glass in the palmar grasp condition) and to hold the final position until the inter trial interval (second 3, Break). In case of trials with feedback (evaluation phase), feedback designated to the object was given. However, for an incorrect classification, the robotic arm performed a waving movement in the horizontal plane. (Bottom (C)) Experimental timeline: Starting with a practice run we recorded 4 runs á 15 trials per conditions (TPC) without giving feedback. After the break, we evaluated the classification model in 3 runs á 15 TPC. In total, each experiment lasted for about two hours. The simulation environment is used with permission from the Institute of Neural Engineering, Graz University of Technology, Stremayrgasse 16/IV, 8010 Graz, Austria.

impaired avatar with a robotic right arm reaches for objects of daily life presented on a table. In front of the avatar we showed one of three objects in random order, (i) a glass, (ii) a bowl of soup with a spoon and (iii) a radio with knobs (figure 1(A)). At the beginning of each trial the robotic right arm of the avatar started moving towards the designated objects, but stopped shortly before interaction (CUE). We instructed the participants to finish the designated movements with their own right hand (see figure 1(B)). For the (i) glass, a palmar grasp, for the (ii) bowl of soup, a lateral grasp and for the (iii) radio, a wrist supination. Participants held the movement until the end of the trial time = 3 s and went back to the starting position (start of inter trial interval). The object on the desk vanished (time = 3 s) and an inter-trial-interval of random length between 2 and 3 s followed. Before the start of the actual recording, each participant performed a practice run for performing the movements correctly and to avoid artifacts in subsequent runs. This training run was not part of any subsequent analysis.

We organized the experiment in two consecutive phases: calibration and evaluation (see figure 1(C)). For the calibration phase no feedback was given to the participants and the trial ended 3 s after the robotic arm of the avatar stopped before the object. However, in the evaluation phase participants received feedback based on their actions online. Whenever a participant's movement was recognized correctly, the avatar's robotic arm completed the designated movement. In case of the (i) glass, and (ii) spoon the hand grasped them and brought them towards the avatars mouth, in case of the (iii) radio, the robotic arm turned the knob on the radio. In the case of an incorrect recognition, the avatar's arm performed a repetitive shaking movement in the horizontal plane.

In this manner we recorded 4 runs with 15 trials per condition (TPC) for the calibration phase (in total 60 TPC). At the beginning, half time and end of calibration phase we recorded 3 min of rest as well as 2 min of eye movements or blinks using a cue-guided paradigm presented in [41, 42].

Using the data acquired in the calibration phase, we trained a classification model. In the subsequent evaluation phase, we recorded 3 runs á 15 TPC, where we gave feedback to the participants.

### 2.3. Data recording

We recorded EEG with 57 active electrodes covering frontal, central, parietal and temporal areas according to the 5% layout described by Oostenfeld and Praamstra [43]. Additionally, 6 electrodes positioned at the outer canthi, infra and superior orbital to left and right eye were used for recording ocular activity (EOG). However, EOG recordings were not part of the analysis described in this work. EEG and EOG were recorded using four biosignal amplifiers (g.USBamp) and a g.GAMMASys/g.LADYbird active electrode system (g.tec medical engineering GmbH, Austria). Signals were recorded with a sampling rate of 512 Hz and prefiltered using an 8th order Chebyshev filter in the range of 0.01 to 200 Hz. A photodiode was positioned on the screen to measure the exact cue onset (the stopping of the hand). In addition, we recorded hand movements during the experiment using a data glove (5DT Technologies, Orlando, CA, USA). Data recording and synchronization was achieved via TOBI Signal Server [44] and MATLAB 2015b (Mathworks, Natick, MA, USA). The online evaluation was implemented in Simulink (Mathworks, Natick, MA, USA). For sending commands and receiving timed triggers between the online evaluation and the paradigm, we used a customized protocol based on TCP/IP.

### 2.4. Movement detection and artefact avoidance and rejection strategies

For determining a reliable single trial movement onset, we used the participant-specific movement data recorded by the data glove. We evaluated 15 sensors positioned at the joints of the finger phalanxes. We epoched all movement trials of the calibration dataset from  $-3$  to  $3$  s with respect to the movement onset. To reduce the dimensionality of the data, we performed principal component analysis (PCA) on the movement data for each condition and used the first component to extract the movement onset.

To avoid movement-related artifact contamination of the calibration data, our strategy in this experiment was twofold: First, we carefully instructed participants to fixate their gaze on the object presented on the table and to avoid any unnecessary body and eye movements during the trial phase. As a second step we performed steps to exclude potential artifact contaminated trials from the calibration set [45–47]. We rejected contaminated trials using statistical methods. Concretely, we filtered all available EEG data between 0.3–35 Hz and epoched each trial from  $[-1\ 2]$  s with respect to the movement onset. Thereafter we rejected trials based on amplitude threshold (exceeding limits

of  $\pm 125\ \mu\text{V}$ ), channel variance, abnormal joint probability and abnormal kurtosis. For the latter three, we used four times the standard deviation as a threshold for trial rejection. On average we retained 52 trials per condition of the calibration data.

### 2.5. Offline single-trial multiclass classification and calibration

We used the data of the calibration phase to train a classification model for the subsequent online evaluation. After excluding any potential artifact contaminated trials, we causally filtered the raw EEG using a 4th order Butterworth filter in the range between 0.3 and 3 Hz. Additionally we applied common average reference (CAR) filtering and resampled the signal to 16 Hz to ease computational load. Previous studies [24, 25, 46, 48] have shown that the most discriminant features for decoding upper limb movements in the low frequency time domain can be found within the first second after the movement onset. Therefore, we defined for each trial a window of interest (WOI) from  $[0\ 2]$  s with respect to the movement onset calculated from the data of the data glove (For offline analysis, we extended the WOI to  $[-1\ 2]$  s). For each participant we epoched trials according to the WOI and divided them in a training and evaluation set using a  $5 \times 5$  cross validation procedure. For each timepoint within the WOI we calculated a shrinkage linear discriminant analysis classification model (sLDA) [49] using the training set and evaluated its performance on the evaluation set. As features, we used the amplitude values from each channel extracted in steps of 0.125 s of the preceding second with respect to the actual investigated time point  $[-0.975: 0.125:0]$  s. In this way, we extracted 8 features per channel resulting in a total of  $8 \times 57 = 456$  features per trial (observation). As a measure of performance, we used the average accuracy on the evaluation folds of the cross validation. The classification model of the time point yielding the highest classification accuracy was then further used in the online BCI evaluation.

### 2.6. Online evaluation

The online BCI model was implemented in Simulink (Mathworks, Natick, MA, USA). Communication between BCI and the Unity based paradigm was done via a customized protocol based on TCP/IP. The incoming EEG was causally filtered using a 4th order Butterworth bandpass filter in the range of 0.3–3 Hz and resampled to 16 Hz. Thereafter, we applied CAR filtering on the signal. Features were again extracted in 0.125 s steps from the preceding one second  $[-0.975: 0.125:0]$  s (whereas 0 s is the actual sample).

The previously calculated sLDA classification model was used to continuously discriminate the input between conditions. Shrinkage based LDA is widely used in the field of BCI research [9, 49]. However, so far it has not been applied in combination



with MRCPs as features to decode singular arm movements online on a large population.

Final discrimination between conditions was achieved by averaging the linear distances of the last three classified samples and selecting the condition with the maximum distance. Eventually, we determined the condition by using a discrete time point in the trial. To determine this time point we deliberately did not use any movement data potentially provided by the data glove to detect the movement onset. Instead we used the time point where the robotic arm of the avatar stopped its movement (CUE) as a reference. Additionally, we appended a participant specific delay which was calculated from the calibration data: With respect to the CUE we added (i) the mean difference between the movement onset and the CUE onset, (ii) network delay and (iii) the time of maximum performance of the classification model.

We gave immediate feedback based on the output of the classifier of this time point. In correct classified trials the avatar completed the movement, otherwise the avatars hand performed a shaking movement in the horizontal plane.

Additionally, we implemented this BCI also as an offline simulation. Using the Evaluation Data set we replaced the estimated onset point with the actual movement onset extracted from the data glove data and compared the achieved performances between real and estimated movement onset.

## 2.7. Analysis of the movement-related cortical potentials (MRCPs)

We analyzed the low-frequency EEG correlates of both calibration and evaluation datasets. We filtered the EEG using a causal 4th order Butterworth band-pass filter in the range between 0.3–3 Hz and resampled it to 16 Hz to reduce computational load. Thereafter we applied CAR filtering and epoched the EEG into trials starting from  $[-2\ 2]$  s with respect to the movement onset acquired by data from the data glove. We were interested in the differences between conditions as well as the differences between the data acquired from calibration and the evaluation phase (non-feedback vs. feedback). For each participant, we calculated the participant specific averages for each condition and its 95% confidence interval using t-percentile bootstrap statistics ( $\alpha = 0.05$ ). We then calculated the group average over all participants.

Additionally, we calculated topographical maps of the grand averages for each condition and their differences. This approach closely follows the analysis described in [46]: differences were calculated by subtraction (e.g.  $\text{cond}(A) - \text{cond}(B)$ ) and visualized using the EEGLAB toolbox [50]. To assess significant differences between conditions we used non-parametric paired sample two-tailed permutation tests based on t-statistics ( $\alpha = 0.05$ ) [51]: in steps of 0.125 s we performed individual tests per time point and channel. In 5000 permutations, we applied t-statistics,

extracted the maximum t-statistic (t-max) for each permutation and generated a t-max reference distribution which is already adjusted for false discoveries [52, 53]. We eventually visualized significant different channels in the topographical difference plots between conditions.

## 3. Results

### 3.1. Single trial classification

The analysis of the single trial classification results followed two consecutive steps: First, we evaluated for each participant the results of the  $5 \times 5$  cross validation on the calibration set. Second, we evaluated the online results (evaluation set). Figure 2 (left) shows the grand average of the best performing classification mode) and its time point of maximum accuracy, which was 56.5% at around 1 s after the movement onset. The confusion matrix in figure 2 (middle) depicts the grand average of the participant-specific peak accuracy (row-wise normalized). On average, true positive rates (normalized true positives in percent, TPR) are between 54% and 64% (supination highest with 63.8%). False positive and false negative rates (normalized false positives/negatives in percent, FPR/FNR) between grasps (finger joints versus finger joints) yield around 25% whereas they are lower for grasp versus wrist supination comparisons (finger joints versus wrist joints), with around 19%. On the right side of figure 2 we show the confusion matrix for the performance of the BCI. In comparison to the calibration phase the TPRs decreased leading to a decreased classification performance for all conditions—most notably for the lateral grasp condition which decreased by more than 20% in TPR.

Table 1 illustrates all classification results of both calibration and evaluation phase on the participant level. As for the calibration phase, all participants scored better than chance level which was at 44.4% (adjusted Wald interval,  $\alpha = 0.05$  [54, 55], corrected for multiple comparisons,  $n = 48$ ). Peak accuracy was in the range from 47% (e.g. participant S13) to up to 76.5% (participant S05) and were achieved in the first second after the movement onset ( $\text{STD} \pm 0.35$  s, table 1, 2nd column). For the online classification of the evaluation phase we did not rely on the movement onset anymore, rather than a combination of visual stopping cue of the paradigm, the participants individual reaction time and a technical network delay. The overall delay (participants' reaction time to the CUE plus the technical delay) and final classification time point for the online evaluation can be found in columns 4 and 5 of table 1. While the technical delay was  $0.11 \text{ s} \pm 0.01 \text{ s}$ , the reaction time to the cue was participant dependent for each participant. The last two columns of table 1 show the results of the online evaluation. With the exception of S13, all participants scored significantly better than chance (chance level 40.4% adjusted Wald interval,

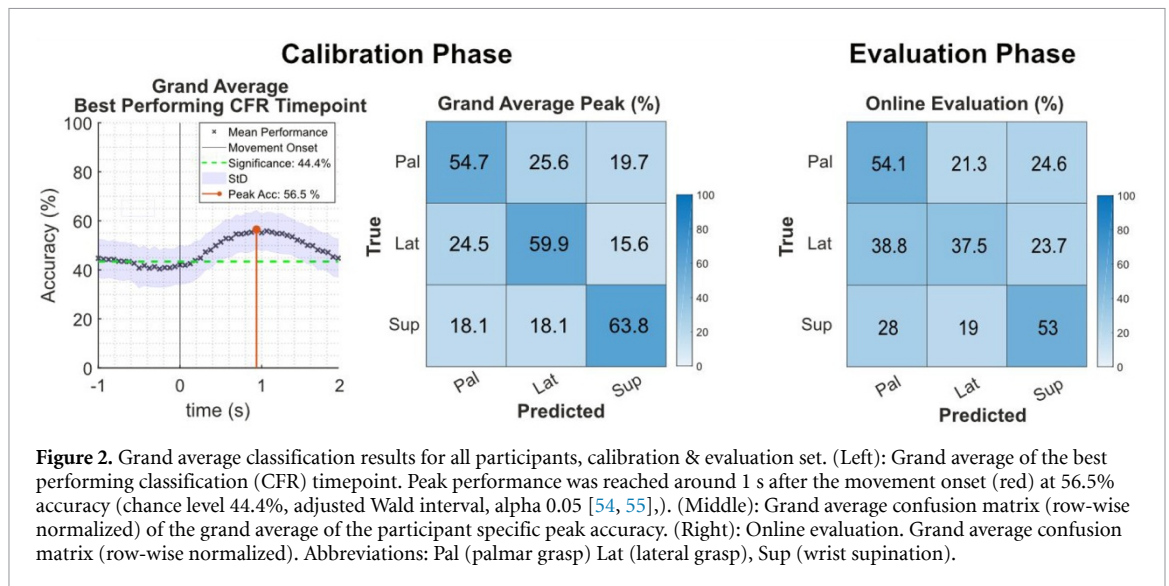


**Figure 2.** Grand average classification results for all participants, calibration & evaluation set. (Left): Grand average of the best performing classification (CFR) timepoint. Peak performance was reached around 1 s after the movement onset (red) at 56.5% accuracy (chance level 44.4%, adjusted Wald interval, alpha 0.05 [54, 55]). (Middle): Grand average confusion matrix (row-wise normalized) of the grand average of the participant specific peak accuracy. (Right): Online evaluation. Grand average confusion matrix (row-wise normalized). Abbreviations: Pal (palmar grasp) Lat (lateral grasp), Sup (wrist supination).

**Table 1.** Participant specific classification results for the calibration phase and the corresponding evaluation phase. Offline calibration (Columns 2–5): Participant specific peak accuracy (accuracy including standard deviation, Acc  $\pm$  STD) of the  $5 \times 5$  cross validated (CV) results. The fifth column shows the best time point for online classification (CFR TP) in seconds. Columns 6 to 7 show the correct classified trials in the evaluation phase as well as their designated overall accuracy (Acc) in percent. The last line displays the grand average over all subjects (AVG).

	Calibration phase Cross validated ( $5 \times 5$ )				Evaluation phase	
	Offline Acc $\pm$ STD (%) Chance: 44%	Offline Acc Time (s)	Overall delay std (%)	Online CFR TP (s)	Correct trials (max. 135) Chance: 54	Online Acc (%) Chance: 40.4%
S01	63.6 $\pm$ 8.4	1.19	0.35	1.54	63	46.7
S02	59.5 $\pm$ 10.4	0.75	0.42	1.17	71	52.6
S03	70.9 $\pm$ 5.9	0.56	0.34	0.90	78	57.8
S04	55.7 $\pm$ 7.7	1.31	0.52	1.83	66	48.9
S05	76.5 $\pm$ 5.5	0.94	0.46	1.40	65	48.1
S06	57.5 $\pm$ 6.9	1.13	0.45	1.57	74	54.8
S07	64.5 $\pm$ 7.4	1.06	0.17	1.23	63	46.7
S08	49.1 $\pm$ 8.9	1.06	0.28	1.35	64	47.4
S09	53.5 $\pm$ 6.8	0.69	0.87	1.56	63	46.7
S10	61.6 $\pm$ 8.1	0.5	0.49	1.00	63	46.7
S11	56.9 $\pm$ 1.9	1.69	0.19	1.88	67	49.6
S12	56.5 $\pm$ 7.7	1.5	0.49	1.99	67	49.6
S13	47.6 $\pm$ 6.5	0.81	0.53	1.34	47	34.8
S14	51.8 $\pm$ 8.1	1.63	0.63	2.26	62	45.9
S15	67.8 $\pm$ 7.8	0.69	0.35	1.04	63	46.7
AVG	59.55 $\pm$ 7.2	1.0 $\pm$ 0.35	0.43	1.4	65.01	48.2

alpha = 0.05). On average participants scored 65 (correct trials) out of 135 trials (min. 47 (S13), max. 78 (S03)).

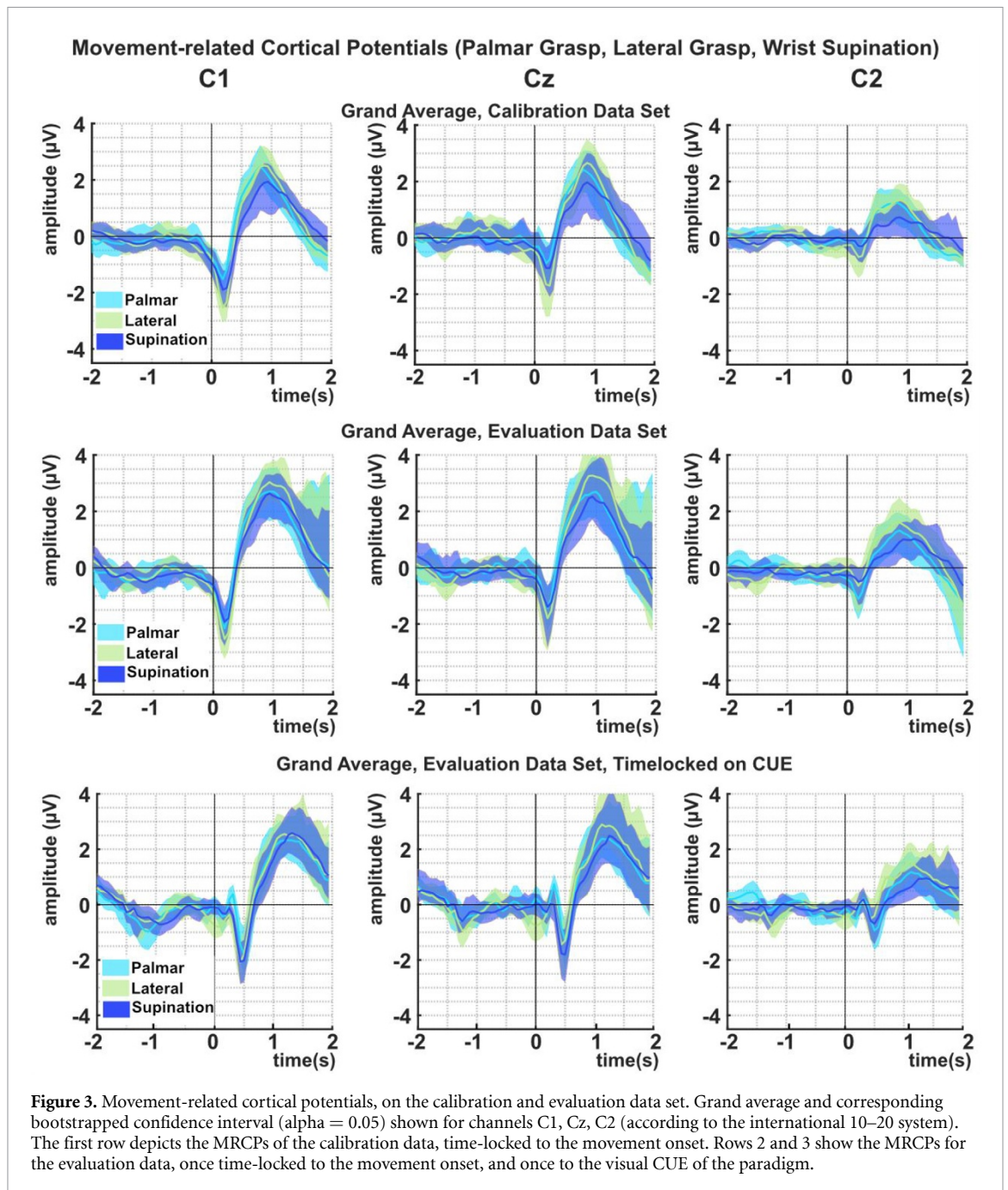
In an additional analysis we created an offline BCI simulation and used as time-locking point not the estimated movement onset as in the online BCI rather than the real movement onset calculated from the data glove data. Results indicate that when time-locking on the real movement onset a significant (Wilcoxon rank sum test,  $p < 0.05$ ) performance increase of about 4.5% could be reached. Detailed results can be found in the supplementary section 3.

### 3.2. Movement-related cortical potentials (MRCPs)

Figure 3 depicts the MRCPs in the low frequency range from 0.3 to 3 Hz. We show the grand average

MRCPs for each condition over all participants as well as the 95% confidence interval of the mean calculated using non-parametric t-percentile bootstrap tests. We show the MRCPs on the channels over the central motor cortex (C1, Cz, C2). We defined the time window of interest as  $[-2 \ 2]$  s with respect to the movement onset for both calibration and evaluation data sets. Furthermore, we investigated the evaluation data set further when time-locking to the visual CUE, with a time-window of interest  $[-2 \ 2]$  s.

For both data sets and time-locking points, a negative deflection (Bereitschaftspotential) [17], can be observed starting before the movement onset (strongest for lateral grasp condition) followed by a positive rebound around 1 to 1.5 s after the movement onset. This rebound is pronounced stronger

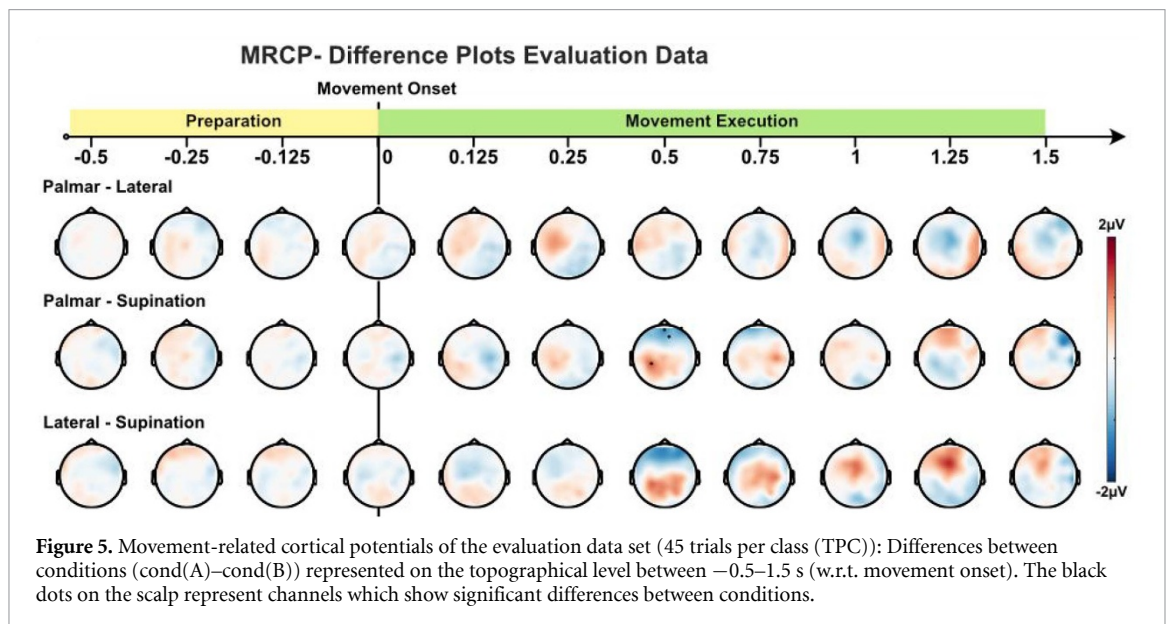
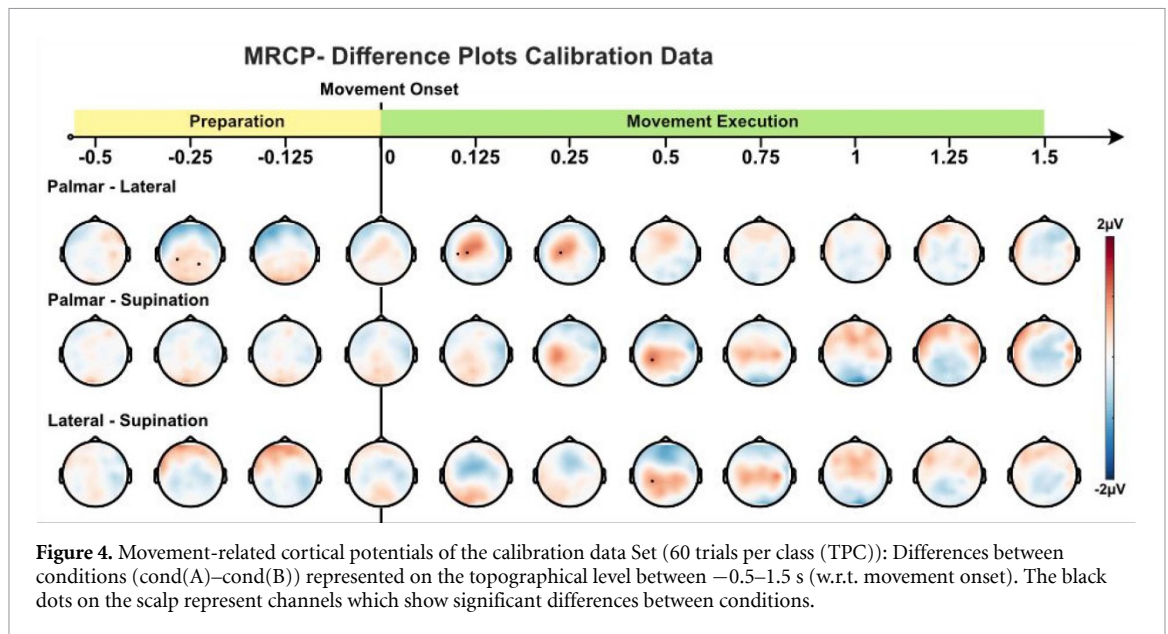


on the evaluation set. On a grand average basis, no significant differences between conditions can be observed. Apart from that, we found a strong lateralization effect towards the contralateral side (left) to the executing hand (right).

Especially for the evaluation data set (figure 3, rows 2 & 3), the confidence intervals for all conditions are broader, especially around 0.8 s after the movement onset which falls in line with the time period where feedback was presented to the participants. When time locking on the visual CUE rather than the real movement onset, the negative deflection of the Bereitschaftspotential shifts by 0.3–0.4 s, which is explained by the reaction time of the participants, but also its intensity is diminished by around  $1 \mu\text{V}$ . The positive rebound effect remains the same.

Figure S1 (see supplementary material) shows the grand average for each condition on the topographical level for the Calibration and Evaluation data set. Time = 0 s represents the movement onset acquired using data of the data glove.

Additionally, we investigated both calibration and evaluation data sets for differences between conditions on a topographical level. We calculated this difference by subtraction of two conditions (e.g.  $\text{cond}(A) - \text{cond}(B)$ ). Figures 4 and 5 show these condition based differences for the calibration and evaluation data sets in the range from  $[-0.5 \text{ } 1.5] \text{ s}$  with respect to the movement onset. Black dots on the topographical plots notate channels which show significant differences between conditions



(assessed using permutation tests based on t-statistics,  $p < 0.05$  [51]). We also analysed each condition on a topographical level separately (see supplementary figure S1).

For the calibration data set, significant differences can be found in all condition combinations, especially between the palmar and lateral grasp conditions (row 1): Before the movement onset ( $-0.25$  s) significant differences emerge on central-parietal areas (channels CCp3 h, CP2). After the movement onset (0.125 to 1 s), a lateralized pattern emerges at the primary motor cortex at channel locations C1 and C3. For combinations between both grasps and wrist supination, we found a pattern around 0.5 s after the movement onset over central/central parietal areas. These differences become significant for both grasping conditions versus wrist supination on the contralateral side at location CP3 h.

When looking at the topographical difference plots of the evaluation data set, in general, the difference patterns are similar to the calibration data set, but less pronounced. Hence, for palmar versus lateral grasp differences, the differences in the contralateral areas of the motor cortex turn out not to be significant anymore. Contrary, for grasp conditions versus wrist supination, the differences found in the evaluation set are similar to the findings in the calibration set in both distinction and timing. For palmar grasp versus wrist supination additional significant differences in central frontal channels (Fz, FFC2 h) can be found.

#### 4. Discussion

In this study we could show the successful online decoding of three upper-limb movements (palmar

grasp, lateral grasp and wrist supination), using low frequency time domain features of the human EEG. For all 15 study participants we gathered a set of calibration data to determine the best performing time point and classification model. Offline analysis of this data yielded a peak accuracy of about 60% ( $\pm 7.2\%$ ) (three condition problem, adjusted significance threshold 44%) about 1 s after the detected movement onset. When using the obtained classification model in the subsequent online BCI scenario, 14 out of 15 participants could retain better than chance performance with an average of 65 correctly classified trials out of 135 trials (48% correct trials, adjusted chance level 40%,  $\alpha = 0.05$ ). Underlying movement-related cortical potentials show no indications of being masked by VEPs at the movement onset. Moreover, significant differences in the calibration data between conditions in the first 0.5 s after the movement onset are mainly located over contralateral sensorimotor areas. These differences are retained to a large extent when looking at the data gathered from the evaluation phase. In either case, these differences lie within the same time period which was used to train the participant specific classification models.

#### 4.1. Movement-related cortical potentials

Contrary to our initial approaches [24, 25, 46, 48], we refrained in this study from using non-causal (zero-phase) filtering approaches to be homogenous in preprocessing for both offline and online application. However, when plotting the EEG potentials, one needs to be aware that this processing does not account for additional filter effects such as e.g. phase shifts, which have a potential influence on the signal.

Analysis of the grand average of the MRCPs shows similar morphology for all three investigated conditions: Shortly before the movement onset a negative deflection from the baseline starts, culminating in a negative peak which is characteristic for the Bereitschaftspotential [16, 17]. In this case, the negative peak happens after the movement onset rather than before, which we attribute to a delayed onset detection of the data-glove.

The peak negative deflection is lateralized (lateralized readiness potential (LRP)) [46, 56], meaning that the negative deflection is stronger on the contralateral side of the executing (right) hand. Following the negative deflection, a strong positive swing can be observed, which peaks around 1 s after the movement onset and is more pronounced on both grasp conditions (see supplementary figure 1) than the wrist supination condition. Furthermore, this positive swing is stronger pronounced in the evaluation data set than in the calibration data set.

Though we did not encounter this positive swing in previous works [24, 25, 46], we attribute this as an

effect of the visual paradigm and feedback presentation as well as the causal filtering approach. When looking at figure 3, 2nd row, the confidence interval becomes considerably broader around 1 s after the movement onset, especially for channels Cz and C1 which we also attribute to feedback presentation.

We were also interested in changes in the MRCP morphology when time locking on the CUE (the robotic arm stops before the interaction with the objects) rather than the calculated movement onset from the data glove (see figure 3 rows 2 and 3 for comparison): our analysis shows, apart from a delayed negative peak of the Bereitschaftspotential (due to reaction time to the CUE), that the morphology of the MRCPs is still preserved, with only a minimal decrease in grand average amplitude.

Naturally, we were also interested in the differences between conditions. Our analysis of the calibration data in channel space shows that the main differences can be found within the first 0.5 s after the movement onset, mainly over the contralateral primary motor cortex (locations C3, C1). Only for the grasp versus grasp comparison, significant differences can already be found 0.25 s before the movement onset. These findings go in line with the results shown in Ofner *et al* [25] and Itturate *et al* [23] who both report similar findings regarding effect timing and location. Moreover, we could show that these differences are also still present in the online experiment, though the patterns are diminished. Especially for the grasp versus grasp comparison, no significant differences can be found. On the other hand, we see additional differences over the frontal area (Fz), for grasp conditions versus supination around 0.5 s after the movement onset. Though they only become significant for palmar grasp versus supination, these differences can also be observed in the lateral versus supination comparison.

Summarizing, we found significant differences between different grasp conditions within the first 0.5 s after the movement onset, mainly over the contralateral sensorimotor areas. This finding goes in line with the findings of Agashe *et al* [28] in grasps (five grasping tasks, information content peaks around 250 ms), as well Ofner *et al* [25] who investigated a set of upper limb movements (six movements).

#### 4.2. Single trial classification

Our offline results for the calibration data show that the movement decoding performance was about 60% over all participants (chance level  $\sim 44\%$ , adjusted Wald interval,  $\alpha = 0.05$ ). These findings are within the same range as the performances achieved in [23–25, 46, 57, 58]. However a direct comparison is difficult since the number of conditions, trials per condition and especially the paradigm greatly differ.

Peak accuracies were found on average one second after the movement onset. Our classification model was trained using features of the preceding 1 s time

window, which includes the time frame where we found significant differences over the contralateral sensorimotor areas between conditions. Analysis of the offline grand average confusion matrix of the participants peak accuracy showed that false positive and false negative rates between grasps (finger joints versus finger joints) were higher than for grasps versus wrist supination (finger joints versus wrist joints). This confirms the findings made by Ofner *et al* [25] who also found these error rates highest for conditions involving the same joint (e.g. hand open vs hand close; wrist pronation vs. wrist supination).

In the online evaluation, participants scored on average 65 out of 135 trials correctly (~48%, adjusted chance level 40%,  $\alpha = 0.05$ ). Fourteen out of fifteen participants scored higher than chance, however compared to the offline results, performance decreased by about 11%. When looking at the TPR of the confusion matrix, we see that the TPRs for the lateral grasp and supination conditions have dropped by 10% to 20%. Furthermore, true positive and false negative rates for all conditions are now in the same range. When transferring an offline calibrated classification model to online use, a certain drop in performance is to be expected [59]. However, in this cue-based online scenario, several additional factors have to be taken into account:

(i) MRCPs are a time and phase-locked phenomenon [16, 17]. For the online BCI scenario, we *estimated* this time point using participant specific behavioural data (timing between the stopping point of the robotic arm and the participants actual movement onset on the calibration data), which is afflicted with a certain variance. Although we attempted to compensate by smoothing the classification output, the classification output is still prone to deviations in the exact timing of the task execution.

To fully understand the impact of using this estimated onset, we performed an offline BCI simulation using the evaluation data set (see supplementary chapter 3 and table S2): We replaced the estimated onset with the real movement onset extracted from the data glove and recalculated the classification accuracy using the same classification model: Results indicate that the overall classification improved significantly (Wilcoxon rank sum test,  $p < 0.05$ ) from previously 65 to 71 out of 135 (45 TPC) correctly classified trials, which represents a performance increase on average of about 4.5%. We realize that this offline simulation cannot account for feedback-dependent effects such as e.g. showing more positive feedback due to improved classification or improved motivation, however, it underlines the importance of an adequate time-locking point for BCI classification.

(ii) With the presentation of feedback to the participants, we introduced an additional variable potentially influencing the performance of the participant specific classification model. The analysis of the MRCP for the evaluation data set shows that

the positive deflection starting around 0.5 s after the movement onset is more pronounced than in the calibration phase. Additionally, channels in central frontal areas (Fz, FFC2 h) show increased activity which are both factors potentially influencing the classification performance. Further studies need to investigate whether this effect can be attributed to e.g. a change in state of mind (excitement, pressure to perform) or feedback presentation.

In either case, the BCI implemented in this study relies on a fixed classification model based on the calibration set data. Studies have shown that there is evidence that co-adaptive training approaches can potentially remedy the performance loss from offline to online BCI models [45, 47, 60–62]. In a co-adaptive BCI concept not only the machine learning algorithm is acknowledged as a ‘learner’ but the users operating the BCI too: both parties are engaged in a closed loop mutual learning environment: A co-adaptive BCI collects data online and adapts its classification models in operative use, while users adapt to the feedback received by the BCI. In this way, performance loss due to changes in brain patterns (e.g. by feedback presentation or EEG nonstationarities) could be attenuated due to the co-adaptive training [63, 64]. However, to our knowledge, the co-adaptive training approach has only been applied on BCIs using non-phase locked, oscillation based features and it remains to be seen if this concept can be translated using MRCPs seamlessly.

So far, only few non-invasive EEG studies have successfully shown online decoding attempts of upper limb movements/grasps using MRCPs as features for discrimination.

Ofner *et al* [38] could show in a self-paced proof-of-concept online approach in one SCI end user to successfully discriminate between opening and closing the hand. Unfortunately a direct comparison is not possible due to substantial differences in the approach and paradigm (e.g. self-paced vs. cue paced). When comparing in general with the online performances of BCIs, e.g. oscillation based approaches based on repetitive mental tasks presented in [63, 65–67], the results of this study are below the average of 75% peak for two conditions (see [59]).

### 4.3. Study limitations

In our current study, we show in a cue-based scenario that online decoding of grasp and hand movements is possible. However, the approach still contains considerable constraints and challenges before a stable BCI control for robotic arms or upper limb motor neuroprostheses conceivable.

For training the classification model, we still relied on the real movement onset, a parameter which is not necessarily available for the targeted end user population. While we compensated for this in the

evaluation phase by using the CUE as time-locking point, this contributed to a decreased performance.

The main challenge still remains in improving the decoding performance of the BCI, especially when exploiting the low frequency time domain for discriminable features. Though the results in this study confirm that discriminable information can be found in MRCPs and transferred to an online BCI, its performance is rather low. Various studies by Itturate *et al* [23], Vuckovic *et al* [68] and Jochumsen *et al* [26, 37] have already shown by offline analysis that additional discriminable information between grasp and hand movements can also be found in alpha and beta range [69]. We have investigated the combination of time domain features extracted from MRCPs with frequency domain features from alpha and beta range [48]. Though it did not have a substantial effect on grasp versus grasp classification, it led to an increased decoder performance in movement detection against the rest condition. In the current study, we used a cue-guided protocol which allowed us to have a fixed time-locking point rather than detecting the occurrence of the grasp in an asynchronous way. In a scenario of daily life, these reference points would be absent, and any classification model applied would continuously process the data for detecting any upper limb movement intention (e.g. a continuous classification of movement versus rest). However this was not subject to the actual study since our goal was to show the feasibility of grasp discrimination using EEG signals.

#### 4.4. Transfer to end users

We conducted this study as a precursor for investigating MRCP-based BCIs for control for severely motor impaired end users (e.g. users with high spinal cord injury). Therefore one of our main interests in this study was to determine whether the discrimination of hand/arm movements can be done on an online BCI control scenario in healthy participants. Now that we showed the feasibility of the approach in healthy participants, we want to discuss its transfer to the final target population.

Firstly, it is imperative to assess the movement capabilities of the potential neuroprosthesis users, since their residual upper limb functions vary [36]. In case of no residual grasp function, we believe that using low-frequency time-domain EEG as a control signal could offer a possibility for an intuitive robotic arm or neuroprostheses control.

Secondly, while in our study we instructed the participants to execute the movements, this is not possible for the targeted end user group. Recent findings suggest that executed movements provide a similar neural representation to that of attempted movements and can as well be decoded from EEG [38, 70, 71]. So, it is necessary to evaluate the performance of the online decoder while end-users attempt to perform the upper-limb movements.

Additionally, combinations of movement execution and movement attempts, depending on the residual functions of the user, could be explored. For instance, combining non-functional hand/grasp movements with a movement the end user is still capable of, e.g. a reaching movement. A number of studies in healthy participants have already shown offline that different reach-and-grasp actions can be discriminated using EEG [23, 24, 26, 46, 58]. In this way, end users would execute the reach and could attempt to perform the designated grasp/supination.

Thirdly, the simulation environment presented in this study can be useful for the end-users since it allows a smoother transition between the virtual and the daily-life scenarios, when compared to the presentation of abstract cues. In the simulation environment, participants interact with virtual objects to perform daily life actions, which we consider to be more immersive. While we did not investigate the effect of training over several sessions, it would be interesting to use this simulation environment for training over multiple sessions with end-users and test whether such training has an impact in the overall performance on a free-control of, e.g. a neuroprostheses. It is also relevant to mention that the simulation is not exclusive to the 3 movements investigated in this study, and it encompasses more objects for a larger set of upper-limb movements (including additional grasps and elbow movements), which allows adaptation according to the users' own needs and final application.

Despite these challenges and limitations, we have already started to assess the feasibility of our findings in a group of tetraplegic participants: Within the MoreGrasp ([www.moregrasp.eu](http://www.moregrasp.eu)) feasibility study, we assess their capabilities of using a BCI to control an upper limb motor neuroprosthesis in several stages [36, 40, 72]. Analogue to the current study, they perform singular, attempted hand movements to generate control signals for the BCI. In the last stage, study participants are going to train with their mobile, customized BCIs *at their homes* using a tablet version of the simulation environment evaluated in the current study. Our initial findings so far confirmed that also attempted movement can be used for decoding ([36, 72], analogue to Ofner *et al* [38]).

## 5. Conclusion

In this study we have successfully shown the online decoding of two grasps and one wrist supination movement using low frequency time domain features of the human EEG. In the BCI scenario, 14 out of 15 healthy participants achieved decoding accuracy higher than chance level (three conditions, 40%, adjusted Wald interval,  $\alpha = 0.05$  [54, 55]), with an average accuracy of 48%. Underlying EEG correlates of the acquired calibration data show significant

differences over the contralateral central sensorimotor areas, which are retained to a large extent for the data acquired from online BCI use. These findings can potentially contribute to the development of a more natural and intuitive BCI-based control modality for assistive devices such as upper limb motor neuroprostheses for people with motor impairments.

## Acknowledgments

The authors thank Harald Czar for his (tireless) effort in implementing and adjusting the paradigm to our quite specific needs, as well as Andreas Pinegger for the support in the paradigm interface. We also want to acknowledge David Steyrl and Rüdiger Rupp for fruitful discussions during the initial phase of the experiment. This work was partly supported by EU Horizon 2020 Project MoreGrasp ('643955') and ERC-Cog2015 681231 'Feel Your Reach'. Supported by TU Graz Open Access Publishing Fund.

## ORCID iDs

Andreas Schwarz  <https://orcid.org/0000-0002-3883-4989>

Joana Pereira  <https://orcid.org/0000-0002-2032-8981>

Patrick Ofner  <https://orcid.org/0000-0001-7169-4300>

Gernot R Müller-Putz  <https://orcid.org/0000-0002-0087-3720>

## References

- [1] House J H 2003 Surgical rehabilitation of the upper limb in tetraplegia *J. Hand Surg. Am.* **28** 356
- [2] Keith M W and Lacey S H 1991 Surgical rehabilitation of the tetraplegic upper extremity *Neurorehabil. Neural Repair* **8** 75–87
- [3] Gohritz A, Turcsányi I and Fridén J 2017 Surgical rehabilitation of the tetraplegic upper extremity *Rehabil. Surg.* pp 233–47
- [4] Hentz V R and Leclercq C 2002 *Surgical Rehabilitation of the Upper Limb in Tetraplegia* (University of Michigan: W.B Saunders)
- [5] Coleman E R, Moudgal R, Lang K, Hyacinth H I, Awosika O O, Kissela B M et al 2017 Early rehabilitation after stroke: a narrative review *Curr. Atherosclerosis Rep.* **19** 59
- [6] Feinstein A, Freeman J and Lo A C 2015 Treatment of progressive multiple sclerosis: what works, what does not, and what is needed *Lancet Neurol.* **14** 194–207
- [7] Petrov D, Mansfield C, Moussy A and Hermine O 2017 ALS clinical trials review: 20 years of failure are we any closer to registering a new treatment? *Front Aging Neurosci.* **9** 68
- [8] Steyrl D, Scherer R, Faller J and Müller-Putz G R 2016 Random forests in non-invasive sensorimotor rhythm brain-computer interfaces: a practical and convenient non-linear classifier *Biomed. Tech.* **61** 77–86
- [9] Lotte F, Bougrain L, Cichocki A, Clerc M, Congedo M, Rakotomamonjy A et al 2018 A review of classification algorithms for EEG-based brain-computer interfaces: a 10 year update *J. Neural Eng.* **15** 031005
- [10] Wolpaw J R, Birbaumer N, McFarland D J, Pfurtscheller G and Vaughan T M 2002 Brain-computer interfaces for communication and control *Clin. Neurophysiol.* **113** 767–91
- [11] Meng J, Zhang S, Bekyo A, Olsoe J, Baxter B and He B 2016 Noninvasive electroencephalogram based control of a robotic arm for reach and grasp tasks *Sci. Rep.* **6** 38565
- [12] Müller-Putz G R, Ofner P, Pereira J, Pinegger A, Schwarz A, Zube M et al Applying intuitive EEG-controlled grasp neuroprostheses in individuals with spinal cord injury: The MoreGrasp clinical feasibility study submitted *Ann. Int. Conf. IEEE Eng. Med. Biol. Soc.* pp 5949–55
- [13] Müller-Putz G R, Scherer R, Pfurtscheller G and Rupp R 2006 Brain-computer interfaces for control of neuroprostheses: from synchronous to asynchronous mode of operation *Biomed. Tech.* **51** 57–63
- [14] Pfurtscheller G, Müller G R, Pfurtscheller J, Gerner H J and Rupp R 2003 "Thought"-control of functional electrical stimulation to restore hand grasp in a patient with tetraplegia *Neurosci. Lett.* **351** 33–36
- [15] Müller-Putz G R, Scherer R, Pfurtscheller G and Rupp R 2005 EEG-based neuroprosthesis control: a step towards clinical practice *Neurosci. Lett.* **382** 169–74
- [16] Kornhuber H H and Deecke L 1965 Hirnpotentialänderungen bei willkürbewegungen und passiven Bewegungen des menschen: bereitschaftspotential und reafferente potentiale *Pflügers Archiv für die gesamte Physiologie des Menschen und der Tiere* **284** 1–17
- [17] Shibasaki H and Hallett M 2006 What is the Bereitschaftspotential? *Clin. Neurophysiol.* **117** 2341–56
- [18] Jahanshahi M and Hallett M 2003 The Bereitschaftspotential: what does it measure and where does it come from? *The Bereitschaftspotential* (Boston, MA: Springer) pp 1–17
- [19] Jiang N, Gizzi L, Mrachacz-Kersting N, Dremstrup K and Farina D 2015 A brain-computer interface for single-trial detection of gait initiation from movement related cortical potentials *Clin. Neurophysiol.* **126** 154–9
- [20] Niazi I K, Jiang N, Jochumsen M, Nielsen J E, Dremstrup K and Farina D 2013 Detection of movement-related cortical potentials based on subject-independent training *Med. Biol. Eng. Comput.* **51** 507–12
- [21] Liu D, Chen W, Chavarriaga R, Pei Z and Millán J D R 2017 Decoding of self-paced lower-limb movement intention: a case study on the influence factors *Front Hum. Neurosci.* **11** 560
- [22] Sburlea A I, Montesano L and Minguez J 2017 Advantages of EEG phase patterns for the detection of gait intention in healthy and stroke subjects *J. Neural Eng.* **14** 036004
- [23] Iturrate I, Chavarriaga R, Pereira M, Zhang H, Corbet T, Leeb R et al 2018 Human EEG reveals distinct neural correlates of power and precision grasping types *Neuroimage* **181** 635–44
- [24] Schwarz A, Ofner P, Pereira J, Sburlea A I and Müller-Putz G R 2018 Decoding natural reach-and-grasp actions from human EEG *J. Neural Eng.* **15** 016005
- [25] Ofner P, Schwarz A, Pereira J and Müller-Putz G R 2017 Upper limb movements can be decoded from the time-domain of low-frequency EEG *PLoS One* **12** e0182578
- [26] Jochumsen M, Rovsing C, Rovsing H, Niazi I K, Dremstrup K and Kamavuako E N 2017 Classification of hand grasp kinetics and types using movement-related cortical potentials and EEG rhythms *Comput. Intell. Neurosci.* **2017** 7470864
- [27] Agashe H A, Paek A Y and Contreras-Vidal J L 2016 Multisession, noninvasive closed-loop neuroprosthetic control of grasping by upper limb amputees *Prog. Brain Res.* **228** 107–28
- [28] Agashe H A, Paek A Y, Zhang Y and Contreras-Vidal J L 2015 Global cortical activity predicts shape of hand during grasping *Front Neurosci.* **9** 121
- [29] Jochumsen M, Niazi I K, Mrachacz-Kersting N, Farina D and Dremstrup K 2013 Detection and classification of



- movement-related cortical potentials associated with task force and speed *J. Neural Eng.* **10** 056015
- [30] Kim J-H, Bießmann F and Lee S-W 2015 Decoding three-dimensional trajectory of executed and imagined arm movements from electroencephalogram signals *IEEE Trans. Neural Syst. Rehabil. Eng.* **23** 867–76
- [31] Mrachacz-Kersting N, Kristensen S R, Niazi I K and Farina D 2012 Precise temporal association between cortical potentials evoked by motor imagination and afference induces cortical plasticity *J. Physiol. (Lond.)* **590** 1669–82
- [32] Xu R, Jiang N, Mrachacz-Kersting N, Lin C, Prieto G A, Moreno J C et al 2014 A closed-loop brain–computer interface triggering an active ankle–foot orthosis for inducing cortical neural plasticity *IEEE Trans. Biomedical Eng.* **61** 2092–101
- [33] Mrachacz-Kersting N, Jiang N, Stevenson A J T, Niazi I K, Kostic V, Pavlovic A et al 2016 Efficient neuroplasticity induction in chronic stroke patients by an associative brain–computer interface *J. Neurophysiol.* **115** 1410–21
- [34] Mrachacz-Kersting N, Jiang N, Dremstrup K and Farina D 2014 A novel brain–computer interface for chronic stroke patients *Brain-Comp. Interface Res.* (Berlin: Springer) pp 51–61
- [35] Mrachacz-Kersting N, Dosen S, Aliakbarhosseinabadi S, Pereira E M, Stevenson A J T, Jiang N et al 2019 Brain-state dependent peripheral nerve stimulation for plasticity induction targeting upper-limb *Converging Clin. Eng. Res. Neurorehabil. III* 1061–5
- [36] Müller-Putz G R, Ofner P, Pereira J, Pinegger A, Schwarz A, Zube M et al 2019 Applying intuitive EEG-controlled grasp neuroprostheses in individuals with spinal cord injury: preliminary results from the MoreGrasp clinical feasibility study 2019 41st Annual Int. Conf. of the IEEE Eng. Med. Biol. Proc. (EMBC) pp 5949–55
- [37] Jochumsen M, Niazi I K, Taylor D, Farina D and Dremstrup K 2015 Detecting and classifying movement-related cortical potentials associated with hand movements in healthy subjects and stroke patients from single-electrode, single-trial EEG *J. Neural Eng.* **12** 056013
- [38] Ofner P, Schwarz A, Pereira J, Wyss D, Wildburger R and Müller-Putz G R 2019 Attempted arm and hand movements can be decoded from low-frequency EEG from persons with spinal cord injury *Sci. Rep.* **9** 7134
- [39] Ofner P, Kersch P and Müller-Putz G 2017 Visual input affects the decoding of imagined movements of the same limb *Proc. of the 7th Graz Brain-Computer Interface Conf. 2017—From Vision to Reality* ed G R Müller-Putz, D Steyrl, S C Wriessnegger and R Scherer pp 367–71
- [40] Steingrüber H-J 1976 *Hand-Dominanz-Test: H-D-T* (Göttingen: Hogrefe Verlag GmbH & Vo.KG)
- [41] Kobler R J, Sburlea A I and Müller-Putz G R 2018 Tuning characteristics of low-frequency EEG to positions and velocities in visuomotor and oculomotor tracking tasks *Sci. Rep.* **8** 17713
- [42] Kobler R J, Sburlea A I and Müller-Putz G R A comparison of ocular artifact removal methods for block design based electroencephalography experiments *Proc. of the 7th Graz Brain-Computer Interface Conf.* pp 236–41
- [43] Oostenveld R and Praamstra P 2001 The five percent electrode system for high-resolution EEG and ERP measurements *Clin. Neurophysiol.* **112** 713–19
- [44] Breitwieser C, Daly I, Neuper C and Müller-Putz G R 2012 Proposing a standardized protocol for raw biosignal transmission *IEEE Trans. Biomed. Eng.* **59** 852–9
- [45] Faller J, Vidaurre C, Solis-Escalante T, Neuper C and Scherer R 2012 Autocalibration and recurrent adaptation: towards a plug and play online ERD-BCI *IEEE Trans. Neural Syst. Rehabil. Eng.* **20** 313–19
- [46] Schwarz A, Pereira J, Kobler R and Müller-Putz G R 2019 Unimanual and bimanual reach-and-grasp actions can be decoded from human EEG *IEEE Trans. Biomed. Eng.* pp 1–12
- [47] Schwarz A, Scherer R, Steyrl D, Faller J and Müller-Putz G R 2015 A co-adaptive sensory motor rhythms brain–computer interface based on common spatial patterns and random forest *Conf. Proc. IEEE Eng. Med. Biol. Soc.* **2015** 1049–52
- [48] Schwarz A, Pereira J, Lindner L and Müller-Putz G R 2019 Combining frequency and time-domain EEG features for classification of self-paced reach-and-grasp actions 2019 41st Annual Int. Conf. of the IEEE Engineering in Medicine and Biology Society Eng. Med. Biol. Soc. (EMBC) pp 3036–41
- [49] Blankertz B, Lemm S, Treder M, Haufe S and Müller K-R 2011 Single-trial analysis and classification of ERP components—a tutorial *NeuroImage* **56** 814–25
- [50] Brunner C, Delorme A and Makeig S 2013 Eeglab—an open source matlab toolbox for electrophysiological research Biomedical Engineering/Biomedizinische Technik (<https://www.degruyter.com/downloadpdf/j/bmte.2013.58.issue-s1-G/bmt-2013-4182/bmt-2013-4182.pdf>)
- [51] Westfall P H and Stanley Young S 1993 *Resampling-Based Multiple Testing: Examples and Methods for p-Value Adjustment* (New York: Wiley)
- [52] Blair R C and Karniski W 1993 An alternative method for significance testing of waveform difference potentials *Psychophysiology* **30** 518–24
- [53] Holmes A P, Blair R C, Watson J D and Ford I 1996 Nonparametric analysis of statistic images from functional mapping experiments *J. Cereb. Blood Flow Metab.* **16** 7–22
- [54] Billinger M, Daly I, Kaiser V, Jin J, Allison B Z, Müller-Putz G R et al 2012 Is it significant? guidelines for reporting BCI performance *Towards Pract. Brain-Comp. Interfaces* **333–54**
- [55] Müller-Putz G R, Scherer R, Brunner C, Leeb R and Pfurtscheller G 2008 Better than Random? A closer look on BCI results *Int. J. Biomagnetism* **10** 5
- [56] Schmitz J, Packheiser J, Birnkraut T, Hinz N-A, Friedrich P, Güntürkün O et al 2019 The neurophysiological correlates of handedness: insights from the lateralized readiness potential *Behav. Brain Res.* **364** 114–22
- [57] Ofner P, Schwarz A, Pereira J, Wyss D, Wildburger R and Müller-Putz G R Attempted arm and hand movements can be decoded from low-frequency EEG from persons with spinal cord injury submitted *Sci. Rep.* **9** 7134
- [58] Randazzo L, Iturrate I, Chavarriaga R, Leeb R and Del Millan J R 2015 Detecting intention to grasp during reaching movements from EEG *Conf. Proc. IEEE Eng. Med. Biol. Soc.* **2015** 1115–18
- [59] Acqualagna L, Botrel L, Vidaurre C, Kübler A and Blankertz B 2016 Large-scale assessment of a fully automatic co-adaptive motor imagery-based brain computer interface *PLoS One* **11** e0148886
- [60] Vidaurre C, Sannelli C, K-r M and Blankertz B 2011 Co-adaptive calibration to improve BCI efficiency *J. Neural Eng.* **8** 025009
- [61] Vidaurre C, Kawanabe M, von Bünau P, Blankertz B and Müller K R 2011 Toward unsupervised adaptation of LDA for brain–computer interfaces *IEEE Trans. Biomedical Eng.* **58** 587–97
- [62] Shenoy P, Krauledat M, Blankertz B, Rao R P N and Müller K-R 2006 Towards adaptive classification for BCI *J. Neural Eng.* **3** R13–23
- [63] Schwarz A, Brandstetter J, Pereira J and Müller-Putz G R 2019 Direct comparison of supervised and semi-supervised retraining approaches for co-adaptive BCIs *Med. Biol. Eng. Comput.* **57** 2347–57
- [64] Vidaurre C, Sannelli C, K-r M and Blankertz B 2010 Machine-learning based co-adaptive calibration: a perspective to fight BCI illiteracy *Lecture Notes Comp. Sci.* pp 413–20
- [65] Faller J, Scherer R, Costa U, Opiso E, Medina J and Müller-Putz G R 2014 A co-adaptive brain–computer interface for end users with severe motor impairment *PLoS One* **9** e101168

- [66] Yao L, Mrachacz-Kersting N, Sheng X, Zhu X, Farina D and Jiang N 2018 A multi-class BCI based on somatosensory imagery *IEEE Trans. Neural Syst. Rehabil. Eng.* **26** 1508–15
- [67] Statthaler K, Schwarz A, Steyrl D, Kobler R, Höller M K, Brandstetter J *et al* 2017 Cybathlon experiences of the Graz BCI racing team Mirage91 in the brain-computer interface discipline *J. Neuroeng. Rehabil.* **14** 129
- [68] Vuckovic A, Pangaro S and Finda P 2018 Unimanual versus bimanual motor imagery classifiers for assistive and rehabilitative brain computer interfaces *IEEE Trans. Neural Syst. Rehabil. Eng.* **26** 2407–15
- [69] Edelman B J, Baxter B and He B 2016 EEG source imaging enhances the decoding of complex right-hand motor imagery tasks *IEEE Trans. Biomed. Eng.* **63** 4–14
- [70] Blokland Y, Spyrou L, Lerou J, Mourisse J, Jan Scheffer G, G-j V G *et al* 2015 Detection of attempted movement from the EEG during neuromuscular block: proof of principle study in awake volunteers *Sci. Rep.* **5** 12815
- [71] Blokland Y, Vlek R, Karaman B, Özin F, Thijssen D, Eijssvogels T *et al* 2012 Detection of event-related desynchronization during attempted and imagined movements in tetraplegics for brain switch control *Conf. Proc. IEEE Eng. Med. Biol. Soc.* **2012** 3967–9
- [72] Müller-Putz G R, Ofner P, Schwarz A, Pereira J, Pinegger A, Dias C L *et al* 2017 Towards non-invasive EEG-based arm/hand-control in users with spinal cord injury 2017 5th *Int. Winter Conf. on Brain-Computer Interface (BCI)* pp 63–5

# Unimanual and Bimanual Reach-and-Grasp Actions Can Be Decoded From Human EEG

Andreas Schwarz , Joana Pereira , Reinmar Kobler, and Gernot R. Müller-Putz 

**Abstract**—While most tasks of daily life can be handled through a small number of different grasps, many tasks require the action of both hands. In these bimanual tasks, the second hand has either a supporting role (e.g. for fixating a jar) or a more active role (e.g. grasping a pot on both handles). In this study we attempt to discriminate the neural correlates of unimanual (performed with left and right hand) from bimanual reach-and-grasp actions using the low-frequency time-domain electroencephalogram (EEG). In a self-initiated movement task, 15 healthy participants were asked to perform unimanual (palmar and lateral grasps with left and right hand) and bimanual (double lateral, mixed palmar/lateral) reach-and-grasps on objects of daily life. Using EEG time-domain features in the frequency range of 0.3–3 Hz, we achieved multiclass-classification accuracies of  $38.6 \pm 6.6\%$  (7 classes, 17.1% chance level) for a combination of 6 movements and 1 rest condition. The grand average confusion matrix shows highest true positive rates (TPR) for the rest (63%) condition while TPR for the movement classes varied between 33 to 41%. The underlying movement-related cortical potentials (MRCPs) show significant differences between unimanual (e.g. left hand vs. right hand grasps) as well unimanual vs. bimanual conditions which both can be attributed to lateralization effects. We believe that these findings can be exploited and further used for attempts in providing persons with spinal cord injury a form of natural control for bimanual neuroprostheses.

**Index Terms**—Unimanual reach-and-grasp action, bimanual reach-and-grasp action, movement-related cortical potential, grasp decoding, brain-computer interface, electroencephalogram (EEG).

## I. INTRODUCTION

PERSONS with high spinal cord injury (SCI) have lost a substantial part of their motor functions. In contrary to a paraplegic person, also upper limb function is critically affected, making fundamental actions of daily life like personal hygiene, eating and drinking not accomplishable without help. Unsurprisingly, surveys with tetraplegic persons show that improving hand function is their top priority [1], [2]. If surgical

rehabilitation, such as tendon and muscle transfers are not possible or feasible [3], [4], there are still possibilities to restore or replace lost hand and arm functions. This includes the use of exoskeletons [5]–[7], or even to utilize muscles of the paralysed arm itself. The latter can be accomplished by an upper limb motor neuroprosthesis based on functional electrical stimulation (FES), in which the innervated muscles are stimulated by periodic small electrical impulses to form basic grasps [8].

It has been shown that FES-based grasp neuroprostheses can be controlled via brain-computer interfaces (BCI), in which brain activity is recorded using EEG [9]–[11]. While these first attempts relied on an abstract form of control, e.g. users would repeatedly imagine a plantar flexion/dorsiflexion of both feet to open/close the hand, we have recently proposed [12]–[14] to use more natural control strategies: Our future goal is to use the actual movement attempted by the user e.g. a palmar grasp or a hand rotation, for control of a upper limb motor neuroprosthesis. Initial studies in healthy participants have shown that several non-repetitive upper limb movements, as well as combined reach and grasp actions of palmar, lateral and pincer grasps can be decoded from the low frequency domain of the EEG and potentially used for control of a neuroprosthesis [15], [16]. In these studies, movement-related cortical potentials (MRCP) [17], [18] in the low frequency band from 0.3 to 3 Hz were extracted as features to classify several executed upper-limb movements. These findings go along with Pistohl *et al.*, who achieved similar results using ECoG [19], [20], Agashe *et al.* who analyzed grasp kinematics [21] or Jochumsen *et al.*, who discriminated different levels of grasp force, speed and eventually different grasps in the low frequency band [22], [23]. Itturate *et al.* confirmed recently, in a self-initiated task (the movement initiation was not cued by means of visual or auditory stimulus), that the most discriminable features for decoding can be found in the frequency range from 0.3 to 6 Hz [24].

While the previous studies were conducted on a population of participants without motor disabilities, MRCPs can also be detected and classified offline in SCI participants: In [25], [26], participants were not able to execute the screened movements anymore, and therefore they were instructed to attempt performing the cued movements. Very recently, in a proof-of-concept study in one person with SCI, Ofner *et al.* showed for the first time that it is possible to discriminate movement attempts of hand open vs. palmar grasp online using low-frequency time-domain features. [25].

While our research focuses on enabling people with motor impairments to control assistive devices using a BCI, MRCPs

Manuscript received August 23, 2019; accepted September 14, 2019. Date of publication September 23, 2019; date of current version May 20, 2020. This work was supported in part by EU Horizon 2020 Project MoreGrasp ('643955') and ERC-Cog-2015 681231 'Feel Your Reach'. (Corresponding author: Gernot R. Müller-Putz.)

A. Schwarz, J. Pereira, and R. Kobler are with the Institute of Neural Engineering, Graz University of Technology.

G. R. Müller-Putz is with the Institute of Neural Engineering, Graz University of Technology, 8010 Graz, Austria (e-mail: gernot.mueller@tugraz.at).

This article has supplementary downloadable material available at <http://ieeexplore.ieee.org>, provided by the authors.

Digital Object Identifier 10.1109/TBME.2019.2942974

also have an impact in a multitude of applications in rehabilitation engineering [27]: Most prominently, Mrachacz-Kersting *et al.*, showed that their EEG (MRCP) assisted stroke rehabilitation induces neural plasticity and thus has measurable positive impact in regaining functionality of lower limbs [28], [29].

During our work with end users we came to understand that unimanual upper-limb neuroprostheses control is necessary but not sufficient: Self-care tasks (such as eating, drinking, personal hygiene) often demand bimanual hand control. In some cases, the second hand plays a supporting role, e.g. when getting jam out of a glass with a spoon, a palmar grasp is executed with one hand to stabilize the glass while the other hand performs a lateral grasp to operate the spoon. In other situations, it has a more active role, e.g. when lifting up a cooking pot by its handles (in which a double lateral grasp is necessary).

In this work, we present the first steps to overcome this obstacle and investigate the possibility of bimanual natural control. For that, we conducted an experiment in which healthy participants ( $n = 15$ ) performed self-initiated reach-and-grasp actions on objects of daily life suitable for unimanual and bimanual grasps.

Our hypothesis is that MRCPs hold enough discriminable information not only for decoding unimanual reach-and-grasp actions (executed with left or right hand), but also for discriminating unimanual from bimanual conditions.

We then discuss the contribution of our findings for a possible application in bimanual grasp neuroprostheses.

## II. METHODS

### A. Participants

This study was approved by the local ethics committee of the Medical University of Graz (EK: 30-439 ex 17/18). Fifteen healthy participants aged between 21 and 30 years (median 26) participated in the study. They reported to be right handed and without any known medical condition. To confirm the handedness, each participant performed a three stage Hand-Dominance-Test first described by H.J. Steingrüber [30]. This gender specific, pen and paper test assesses the hand dominance in three exercises performed by each hand individually: (i) draw a line within a prescribed path, (ii) puncture unaligned circles and (iii) puncture horizontally aligned squares. Each participant was informed about the procedure and scientific aims of the study. All gave written informed consent and received monetary compensation for their participation.

### B. Experiment Setup and Paradigm

All recordings were conducted at the BCI-Lab of the Institute of Neural Engineering of the Graz University of Technology. Participants were seated on a chair in an electromagnetic and noise shielded room. In front of them there was a table with a built-in monitor. On the monitor we placed real objects of everyday use for reach-and-grasping. Table I lists the objects, the associated grasps and the experimental conditions. For the unimanual conditions, we placed an empty jar (for the palmar grasp) and a spoon (for the lateral grasp). For the bimanual conditions, we placed a pot (double lateral grasp on the handles) and

TABLE I  
EXPERIMENTAL CONDITIONS

TYPE	OBJECT	GRASP TYPE
<b>Unimanual</b> (performed w. left or right hand separately)	Jar	Palmar
	Spoon	Lateral
<b>Bimanual</b>	Pot with Handles	Double Lateral
	Jar with Spoon	Palmar (left Hand) Lateral (right Hand)
<b>Rest</b>	Cross on Screen	No movement performed
<b>Eye Movement</b>	Moving dot on screen	Dot moving horizontally and vertically on the screen; Text insert <i>Blink</i> for performing eye blinks.

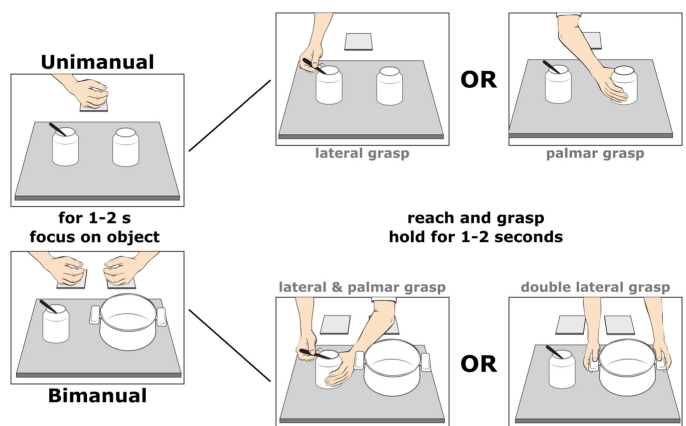


Fig. 1. Paradigm for unimanual and bimanual tasks. For all tasks, participants were asked to focus their gaze on the object they wanted to grasp for 1 to 2 s before performing the movement. Thereafter, participants performed the suitable reach-and-grasp and held the object for 1 to 2 s before moving back to the starting position. This grasp could be an unimanual lateral grasp or palmar grasp, or a bimanual task combination of palmar grasp (executed with the left hand, holding the jar) with a lateral grasp (right hand) or double lateral grasp (holding the handles of the pot).

the jar with the spoon (mixed grasping of palmar (left hand) and lateral (right hand)). The objects and associated reach-and-grasp actions are shown in Fig. 1. Depending on the run type (i.e. unimanual or bimanual), we positioned the two designated objects on the table on predefined positions. In unimanual runs the participants' hand (either left or right) was positioned centered on a pressure plate to detect the movement onset in a comfortable reaching distance in front of the objects. For bimanual runs, both hands were located on two pressure plates equally distant to the center to capture the movement onsets of both hands. After each run we switched the positions of the objects so that each object was on each location equally often.

The participants were asked to perform the reach-and-grasp actions in a self-initiated manner (i.e. decide freely when to start the movement and also which object to grasp), however in a preceding instruction run we introduced them to some task requirements: We instructed them to first fixate their gaze on the object for 1-2 s before they started the movement (Fig. 1). Each object had its own fixation point, e.g. the pot had a small black dot inside and for the spoon, participants focused on its

tip. Thereafter, participants performed the reach-and-grasp and held the object for 1 to 2 s before moving back to the starting position. Once they returned to the starting position, a small insert on the bottom of the screen informed them about the number of times they grasped the object in the current run (e.g. Spoon 5/20). Before the next trial, participants were asked to perform a break of at least 4 s.

One run consisted of 20 trials per condition. After each run we introduced a short break. In total we recorded 80 trials for each condition, which results in  $80 * 2$  (grasps)  $* 3$  (movement types, unimanual left, unimanual right, bimanual) = 480 reach-and-grasp actions per participant. Data recorded in the instruction run was not part of the analysis. At the beginning, half time and the end of experiment we recorded 3 min of rest as well as 2 min of eye movements or blinks for potential removal of artefacts based on blinks or eye movements. We recorded this data according to a visually guided paradigm also shown in [31], [32]: In 6 trials á 10 s, participants had to follow a white dot moving horizontally or vertically across the built-in screen (deprived of any real objects). In 3 additional trials á 10 s participants performed eyeblinks.

### C. Data Recording

We measured EEG with 58 active electrodes covering frontal, central, parietal and temporal areas. In addition, we measured the electrooculogram (EOG) using 6 active electrodes positioned at the outer canthi, infra and superior orbital to the left and right eye. The reference electrode was placed on the right earlobe, ground on position AFF2h. The EEG layout corresponds to the 5% layout described by Oostenveld *et al.* [33]. We recorded the EEG and EOG using four biosignal amplifiers (g.USBamp) and a g.GAMMAsys/g.LADYbird active electrode system (g.tec medical engineering GmbH, Austria). Signals were sampled at 256 Hz and band-pass filtered from 0.01 Hz to 100 Hz (8th order Chebyshev filter). Power line interference was suppressed with a notch filter at 50 Hz.

We used isolated force-sensing resistor (FSR) sensors to record the movement onset from the starting position and also the grasping time point (with FSR sensors attached to the objects). Sensor output was digitized using a battery operated Arduino microcontroller. Time synchronization with the EEG and EOG was made via the galvanic decoupled TTL input of the master g.USBamp amplifier.

### D. Behavioural Analysis

We analyzed the behaviour of the participants during the executed reach-and-grasp actions. Concretely, we analyzed the duration of the reach-and-grasp action for each grasp type. The time information provided by the force sensitive resistors was extracted from all trials. Then, for each participant and each condition the average duration was calculated. To check for significant differences in duration among conditions, a repeated measures ANOVA with 6 levels (conditions) was performed. We also tested the repeated measures model for sphericity using Mauchly's test.

### E. Artefact Avoidance, Correction, and Rejection Strategies

Our procedure to deal (i.e. avoid, correct, and reject) with artefacts [34] consisted of three parts:

1) *Avoidance*: We carefully instructed the participants and created gaze fixation points, so that during the movement task itself, no eye movements would occur: The participants were instructed to focus their gaze on the object 1-2 s before the movement. Moreover, we explained the general importance of reducing blinks and eye movements to a minimum, and avoiding any other movement not associated with the task. Lastly, inter-trial as well as inter-run breaks were introduced, in which participants could have a break.

2) *Correction*: EEG in the low frequency range can easily get contaminated with ocular artefacts. Therefore, after the recordings, we applied a subspace subtraction algorithm [35] to attenuate ocular artefacts related to eye movements and eye blinks. The algorithm corrects ocular artefacts in a three step procedure. First, it finds the subspaces that maximally explain the variance during horizontal and vertical eye movements and blinks. The subspaces are estimated by computing an unmixing matrix that linearly combines all channels. Second, a mixing matrix that defines the contribution of each artefact subspace to the EEG channels is estimated. Third, the subspace that contains the ocular artefacts is subtracted from the raw signals [31], [32].

3) *Rejection*: Subsequent to EOG correction we rejected potential artefact contaminated trials using statistical parameters. We therefore filtered the EEG between .3 and 35 Hz and rejected trials by (1) amplitude threshold (amplitude exceeds  $\pm 125 \mu\text{V}$ ), (2) abnormal joint probability and (3) abnormal kurtosis by threshold of 4 times the standard deviation. This approach had already been used in several studies ([36]–[38]). On average, 11% of the trials were rejected due to artefact contamination.

### F. Data Preprocessing

EEG, EOG, and sensor data were processed using MATLAB R2017b. EEG and EOG data were high pass filtered using a zero-phase 4th order high pass Butterworth filter with the cut-off frequency set at 0.3 Hz. Incorporating the recorded rest and eye movement runs, we calculated and applied the artefact subspace filter for removing ocular based artefacts. Preceding any further step we analysed the synchronized sensor data of the force-sensing resistors and excluded any trials in which participants did not meet the instructions given with respect to timing. Exclusion parameters were set to: (i) more than 3s from movement onset to finalizing the grasp at the object, (ii) less than one second holding the object, (iii) more than 3s from the holding position back to the starting position. Thereafter we defined a window of interest (WOI) for each trial with 2s before and 3s after the movement onset  $[-2\ 3]$ s, with 0 referring to the movement onset. In the case of bimanual trials, in which we recorded movement onsets from both hands, we defined the movement onset for analysis as the first onset detected, regardless the hand. Additionally, we extracted 81 rest trials from the rest runs. The rest trials had a duration of 5s (i.e., similar to the WOI duration)

with a 1s gap between consecutive rest trials. Thereafter we applied the statistical outlier rejection mentioned above [36], [38] on the trials. Trials marked for rejection were excluded from subsequent analysis.

### G. Low Frequency Correlates: Movement-Related Cortical Potentials (MRCPs)

For obtaining the low frequency EEG correlates of the movement conditions, we applied common average reference (CAR) filtering and resampled the preprocessed EEG to 16 Hz to ease computational effort. Thereafter, we applied a 4th order zero-phase lowpass Butterworth filter at the cut-off frequency of 3 Hz. We calculated the global field power (GFP) as the standard-deviation across channels [39]. The participant-specific scalp potentials were then normalized by the average GFP during the rest condition. Thereafter, we epoched the data for each condition from  $-2$  s to 3 s with respect to the movement onset and calculated the average over epochs for each condition, for each participant individually. To obtain the grand-average MRCP, we calculated the mean over the participant-specific average and its respective confidence interval using non-parametric t-percentile bootstrap statistics ( $\alpha = 0.05$ ).

Naturally we were interested in the differences among conditions. For the sake of clarity we decided in a first step to group conditions of the same hand as well as both bimanual conditions. The new resulting conditions were: ‘Left Hand,’ ‘Right Hand’ and ‘Bimanual’. For each condition, we calculated the grand-average MRCPs as well as their differences in channel space, by simply subtracting the grand-averages (condition(A)-condition(B)). Concretely, the following differences between conditions were calculated: i.) left minus right, ii.) left minus bimanual, iii.) right minus bimanual, iv.) all movement trials minus rest.

In a second step we calculated the differences of the grand-averages of the same hand conditions (e.g. left hand palmar minus left hand lateral) and of the bimanual conditions (bimanual double lateral (pot) minus bimanual mixed palmar/lateral (jar)). These differences were then observed on topographical plots in which the channel locations were extracted from a template (obtained from [33]) using the EEGlab toolbox [40].

Differences between the MRCPs for each condition were assessed using nonparametric paired-sample two-tailed permutation tests based on t-statistics ( $\alpha = 0.05$ ) on the  $[-1 \ 1.5]$  s window with respect to the movement onset [41]. Concretely, individual tests at each time point and channel were performed (steps of 125 ms). For each permutation, t-statistics were obtained and the maximal t-statistic ( $t$ -max) was extracted. After all 1000 permutations, a  $t$ -max reference distribution was obtained, and the  $p$ -values of each comparisons were derived from this reference distribution, which is adjusted to reflect the chance of false discoveries [42], [43]. For visualization, we marked the significantly different channels over the topographical plots representing the difference between conditions.

### H. Single Trial Classification

We performed both binary (1 versus 1 condition) as well as multiclass classification on the recorded data (7 conditions).

Both approaches were conducted in the same manner but with a different number of conditions. For the multiclass single trial classification approach we used all available conditions, including 81 rest trials extracted from the recorded rest runs (7 conditions in total), for the binary version we compared all possible 2 condition combinations (yielding in 21 binary combinations). Our approach consisted of two main steps: First, find the time-point of the best performing classification model in terms of accuracy within the designated window of interest (WOI) from  $-2$  s to 3 s through cross-validation. Second, use this classification model associated to that time-point, and test its performance on a previously unseen set of test data. For that we split the data in two independent data sets. The first 66% of all trials (Calibration set, on average 52 TPC) were used for finding and calibrating the best performing classifier while the remaining 34% (Evaluation set, on average 23 TPC) were used to evaluate this classification model.

Initially, we resampled all preprocessed EEG signal to 16 Hz and applied CAR filtering. We used a zero-phase, 4th order low-pass Butterworth filter with a cut-off frequency of 3 Hz to filter the EEG signal. For finding the best classification model we epoched all trials of the calibration set according to the WOI. For each time point within the WOI, an individual classification model was calculated as follows: Using a 10 times 5-fold cross-validation evaluation procedure, we divided the trials into training and validation sets. We trained a shrinkage based linear discriminant analysis (sLDA) classifier [44] with features extracted from the training set. The features corresponded to the amplitudes of all 58 EEG channels extracted in 125 ms steps of a causal 1 s window (e.g. for the classification model trained on the time point  $t = 1$  s, 9 amplitude values at  $[0: 0.125:1]$  s (w.r.t. movement onset) were used). For each trial on the training set, we extracted 9 features per channel, yielding in total 522 features. We tested the resulting classification model on the validation trials selected by the cross-validation. We repeated this procedure for each point within the WOI, thus obtaining 80 different classification models for the whole WOI. As a measure of performance we analysed the mean of the accuracies resulting from the validation sets of each fold and its corresponding confusion matrices.

Thereafter we selected the best performing classification model and applied it on the previously unseen trials of the Evaluation set (using the same preprocessing as before). We report the mean of the accuracies of all trials within the Evaluation set within the WOI. We additionally calculated the information transfer rate (ITR) according to Wolpaw’s Bit rate [45], [46]. We estimated that each participant performed on average 6 reach-and-grasp actions per minute.

## III. RESULTS

### A. Movement-Related Cortical Potentials (MRCPs)

**1) Unimanual vs. Bimanual:** We analysed the MRCPs as the low-frequency EEG correlates of unimanual and bimanual reach-and-grasp conditions. Fig. 2, shows the grand-average MRCPs and respective bootstrapped confidence interval ( $\alpha = 0.05$ ) for conditions ‘Left Hand,’ ‘Right Hand’ and ‘Bimanual’ over channels C1, Cz and C2, located over the central

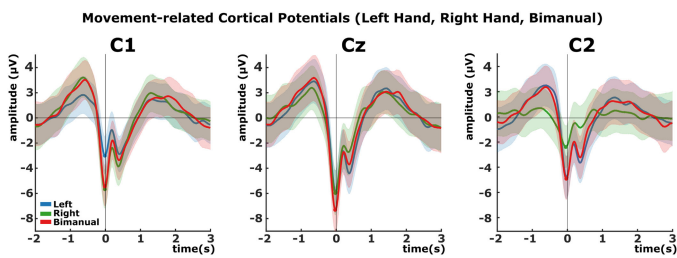


Fig. 2. Movement-related cortical potentials of unimanual and bimanual reach-and-grasp actions. Grand-average and respective bootstrapped confidence interval ( $\alpha = 0.05$ ) for conditions 'Left Hand,' 'Right Hand' and 'Bimanual' for channels C1, Cz and C2. Time = 0 s represents the movement onset.

motor cortex. Time = 0 s represents the movement onset within the window of interest  $[-2\ 3]$  s. For these three conditions, a positive peak is observed around 0.5 s before the actual movement onset. Thereafter a strong negative shift (Bereitschaftspotential, [17], [18]) imminent to the movement onset can be observed. For both positive and negative peaks the absolute amplitude is significantly stronger (Wilcoxon rank sum test (WRS),  $p < 0.05$ ) on electrodes contralateral to the executing hand for unimanual conditions. For the bimanual condition, the positive peak in the preparation phase is not lateralized and occurs on both hemispheres with almost equal amplitude. The negative peak (Cz,  $-7.3\ \mu\text{V}$ ) in the bimanual condition is more pronounced than in both unimanual conditions (Cz,  $-6\ \mu\text{V}$ ), however, not significant throughout the population of participants (WRS,  $p = 0.104$ ). In both unimanual and bimanual conditions, the strong negative peak is followed by a second intermediate negative peak of smaller amplitude around 250 ms after the movement onset, before returning to a positive level.

Fig. 3 shows the differences between conditions plotted as topographical maps in a time window from  $[-1\ 1.5]$  s with respect to the movement onset. Differences between conditions were calculated by subtraction ( $\text{cond}(A) - \text{cond}(B)$ ). Black dots on the topographical maps represent the significantly different channels (permutation tests based on  $t$ -statistics,  $p < 0.05$ , [41]) between conditions. Most prominent between movement conditions are the differences between 'Left Hand' and 'Right Hand' grasp conditions (Fig. 3, first row). Starting around 1 s before the movement till around movement onset, significant differences emerge at central/central-parietal channels (at  $-1$  s: CCP4h; at  $-0.5$  s: FCC3h, C3, C1, C2, C4, CCP4h) on the left and the right hemispheres. At  $-0.5$  s two significant areas over the motor cortex on both hemispheres can be identified (FCC3h, C3, C1 and C2, C4, CCP4h). Polarities of both regions are opposite to each other, which is in consistency to the MRCPs depicted in Fig. 2. Most pronounced differences between conditions can be observed imminently to the movement onset (0 s). Significant differences occur again in two separate areas over the central/central parietal motor cortex (FCC3h, CCP3h, C1, CP2, CP4, CCP4h, CCP6h).

We also investigated the differences between both unimanual (left or right) and the bimanual conditions (Fig. 3, rows 2

and 3 respectively). Significant differences emerge already in the preparation phase and are most prominent around movement onset and thereafter (till 0.5 s after movement), however, there are fewer significant electrodes. For both comparisons (i.e. left vs. bimanual and right vs. bimanual) these differences emerge only on one hemisphere mainly over central/parietal regions: For left hand vs. bimanual, significant differences can be seen on the channels located over the left motor cortex (at 0 s: C1; at 0.125 s FCC3h FCC1h C1), whereas for right hand vs. bimanual significant differences are found mainly over the right motor cortex (at  $-0.5$  s: C2, CCP4h; at 0 s: C2, CCP2h CCP4h, CP2). For the last row of Fig. 3 we averaged all movement conditions and calculated the differences to the rest condition. Again significant differences emerged in the preparation phase mainly over the central electrodes over the motor cortex (especially C1, Cz and C2 and adjacent channels). Imminently to movement onset and thereafter, significant differences were localized mainly over central/central parietal areas.

**2) Inner Conditions:** Naturally we were also interested in the differences between grasp types (i.e. lateral vs. palmar with right or left hands, and lateral vs. mixed bimanual conditions). Hence we calculated the grand-average over participants and the confidence interval ( $\alpha = 0.05$ ) of each condition (see Fig. 4). Fig. 4 shows the grand-average MRCPs for each of the reach and grasp conditions. For better understanding we grouped them per performing hand, and both bimanual conditions. As with Fig. 4, we show channels C1, Cz and C2. Similar to Fig. 2, we observe a lateralization and higher negative peak around movement onset in the bimanual conditions. However, differences between grasp conditions are found scarcely: While pre-movement and reaching phases seem almost identical within all pairs (left palmar vs. left lateral; right palmar vs. right lateral; palmar bimanual vs. mixed bimanual), the positive rebound  $[1.25\ 1.5]$  s for the lateral conditions is stronger over the central position (Cz). A similar effect can be observed for bimanual conditions: Here the positive double lateral rebound around 1.5 s after movement onset exceeds the mixed palmar/lateral grasp combination. A similar effect can be observed for bimanual conditions: Here the positive double lateral rebound around 1.5 s after movement onset exceeds the mixed palmar/lateral grasp combination in amplitude by approximately  $1\ \mu\text{V}$ . In both cases the stronger rebound for the lateral conditions turned out to be not significant ( $\alpha = 0.05$ , see Fig. 4).

Fig. 5 shows the differences between conditions represented as topographical maps in the time-window  $[-1\ 1.5]$  s with respect to the movement onset. Again, differences between conditions were calculated by subtraction ( $\text{cond}(A) - \text{cond}(B)$ ). Black dots on the topographical maps represent channels considered significantly different (assessed using permutation tests based on  $t$ -statistics,  $p < 0.05$ , [41]) between conditions. For the same hand unimanual conditions, no clear topographical difference is observed. Between the bimanual conditions, few sparsely distributed channels are significantly different (e.g. at  $-0.125$  s: Fz), however, as expected from Fig. 4 no striking pattern can be identified in the channel space.

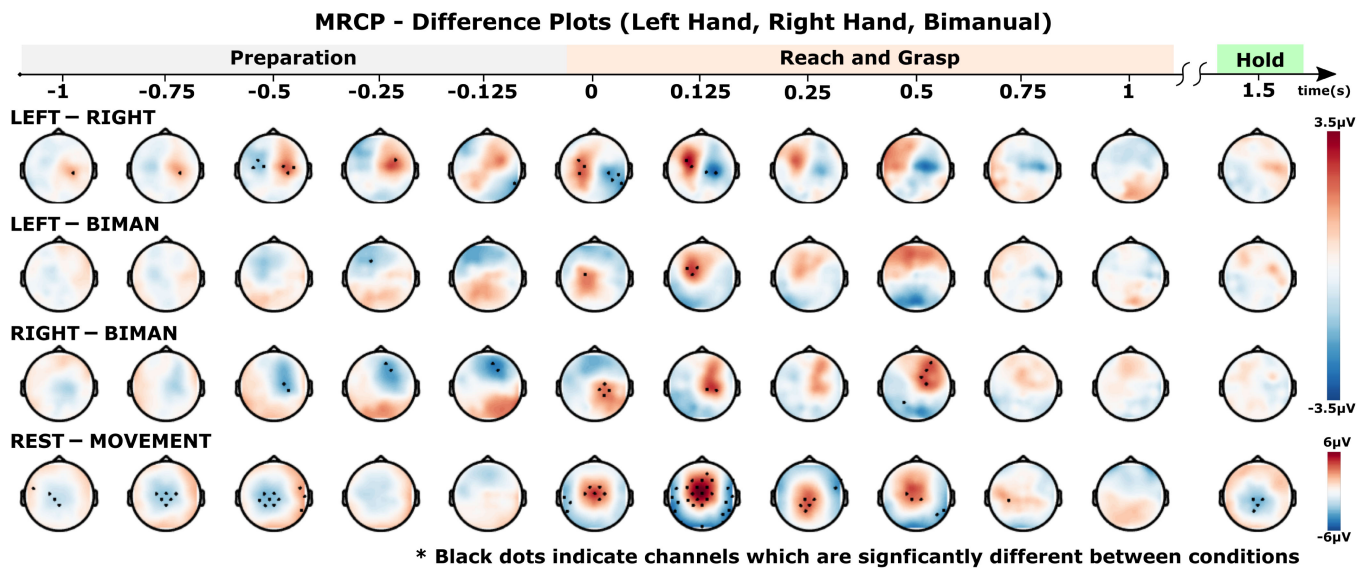


**Fig. 3.** Topographical plots representing the difference between conditions (cond(A)-cond(B)) for time-points between  $[-1, 1.5]$  s with respect to the movement onset. Black dots over the maps represent the significantly different channels between conditions (assessed used permutation tests based on  $t$ -statistics,  $p < 0.05$  [41]).

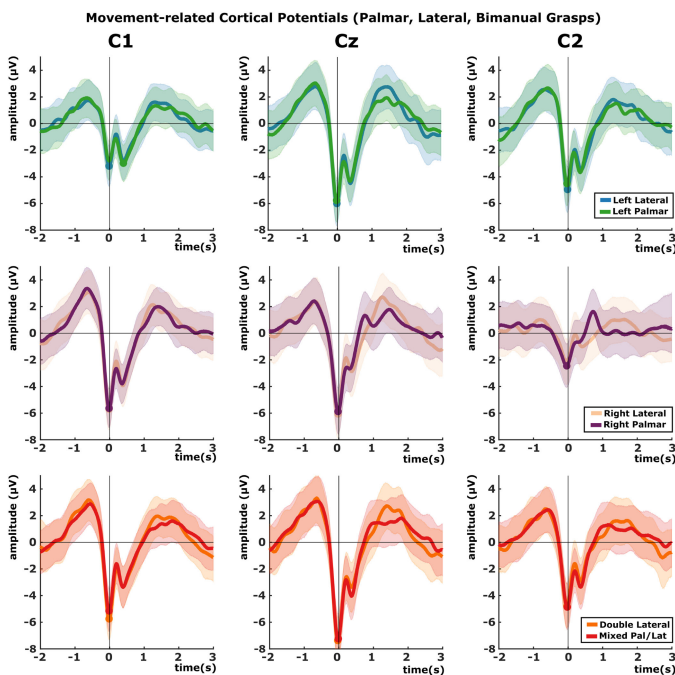


**Fig. 4.** Movement-related cortical potentials of same hand and bimanual reach-and-grasp actions. grand-average and respective bootstrapped confidence interval ( $\alpha = 0.05$ ) for conditions palmar and lateral graspings and bimanual conditions for channels C1, Cz and C2. Time = 0 s represents the movement onset.

## B. Single-Trial Classification

Single trial classification followed two approaches, a binary (1 vs. 1 condition, in total 21) and multiclass approach. We show the results of the grand average of the participant-specific peak accuracies of the Calibration and Evaluation set (see Table II). All binary results were better than chance level (61.4%, adjusted

Wald interval,  $\alpha = 0.05$ ) for all participants. Highest performances could be reached between unimanual and bimanual movement conditions (70-80%) or movement versus rest conditions (80-90%). Also unimanual left versus right combinations scored in the range between 70 and 80%. Condition combinations of the same hand (e.g. l-lat vs. l-pal) or bimanual versus bimanual conditions reached performances in the range of 66-70%. More detailed results regarding binary classification can be found in the supplementary Figure S3.

For the multiclass classification we discriminated all 6 movement classes as well as rest trials extracted from the rest runs. Figure 6 illustrates the determination of the best classification model (Calibration set). We show the grand-average over all participants of the classification accuracy when evaluating each time-point within the window of interest with a different classification model. The best performing classification time-point was (on average) at 1 s after the movement onset with peak accuracy of 42.7%. The chance level lies at 20.7% ( $\alpha = 0.05$ , adjusted Wald-interval [47]) and is Bonferroni corrected for multiple comparisons (80 calculated classification models). Additionally we calculated the grand average of the individual confusion matrices for each subject at the point of peak accuracy and at the point of the movement onset (Fig. 6, bottom). For both shown confusion matrices, unsurprisingly, the true positive rate (TPR) of the rest condition exceeds TPRs of any movement classes by 20 to 25%. TPRs of movement conditions at the point of peak accuracy are higher by 10-15% compared to TPRs at movement onset. In general, false positive rates (FPR) of same hand conditions (e.g. Left Palmar, Left Lateral) as well as for both bimanual conditions are considerably higher than when compared to opposite hand or unimanual versus bimanual conditions.

Fig. 7 (left) shows the results of the best performing classification model applied on the unseen data of the Evaluation set.



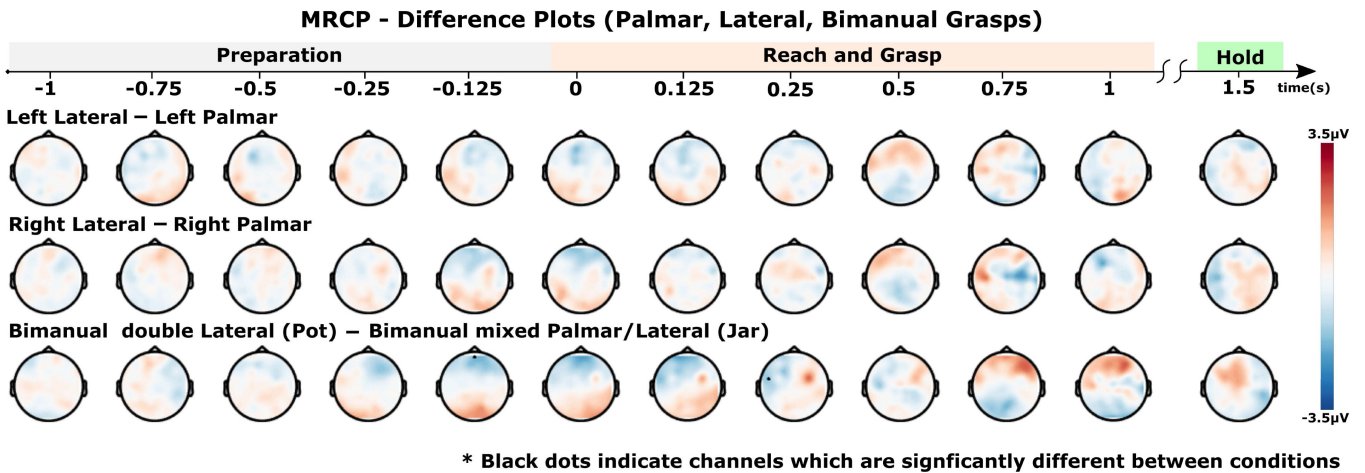


Fig. 5. Topographical plots representing the difference between grasp conditions (cond(A)-cond(B)) for time-points between [-1 1.5]s with respect to the movement onset. Black dots represent channels with significant differences (assessed using permutation tests,  $p < 0.05$ ).

TABLE II

BINARY CLASSIFICATION RESULTS, PARTICIPANT-SPECIFIC PEAK ACCURACIES IN PERCENT FOR CALIBRATION AND EVALUATION SET. THE UPPER TRIANGLE MATRIX SHOWS THE RESULTS FOR THE EVALUATION SET (HIGHLIGHTED GREEN), THE LOWER TRIANGLE MATRIX SHOWS THE RESULTS FOR THE CALIBRATION SET (HIGHLIGHTED RED). CONDITION ABBREVIATIONS: rest (REST); l-pal (LEFT PALMAR); l-lat (LEFT LATERAL); r-pal (RIGHT PALMAR); r-lat (RIGHT LATERAL); bi-dlat (BIMANUAL DOUBLE LATERAL); bi-mix (BIMANUAL MIXED PALMAR/LATERAL)

	l-lat	l-pal	r-lat	r-pal	bi-dlat	bi-Mix	rest
l-lat		68	77.2	79.3	73.7	74.5	84.1
l-pal	66.2		75.8	74.1	70.8	70.4	82.9
r-lat	74.4	78.4		66.3	74.3	70.8	83.6
r-pal	79.2	78.7	69.4		73.9	75.8	83.6
bi-dlat	74.9	76.3	74.8	76.6		65.5	87.1
bi-mix	76.3	74.6	76.4	76.9	69.2		87.1
rest	83.1	83.7	83.9	83.6	89.1	87.9	

We show the grand average over all participants (black bold line) as well as participant specific performances (thin gray lines). Again all participants scored significantly higher than chance level (24.2%, adjusted Wald-interval [47], Bonferroni corrected for 80 comparisons). Both peak accuracy (38.6%) and timing (1.1 s) are within the same range when compared to the results of the Calibration set (see Table III for detailed comparison). Due to the participants' variation in time-course of accuracy, the peak of the grand-average accuracy is understandably lower (38.6%) than when performing the average of the individual peak accuracies (31.3%). Fig. 7 (right) shows the associated confusion matrix of the grand average of the participant specific peak accuracies. Again the TPR for the rest condition is higher than for all movement conditions. TPRs for the movement conditions range between 30 and 41%. As could already be seen in for the results of the Calibration set, the false positive rates (FPR) of same hand conditions (e.g. Left Palmar, Left Lateral) as well as for both bimanual conditions are higher than when compared to opposite hand or unimanual versus bimanual

Calibration - Best Performing Classification Timepoint (66% of available data used)

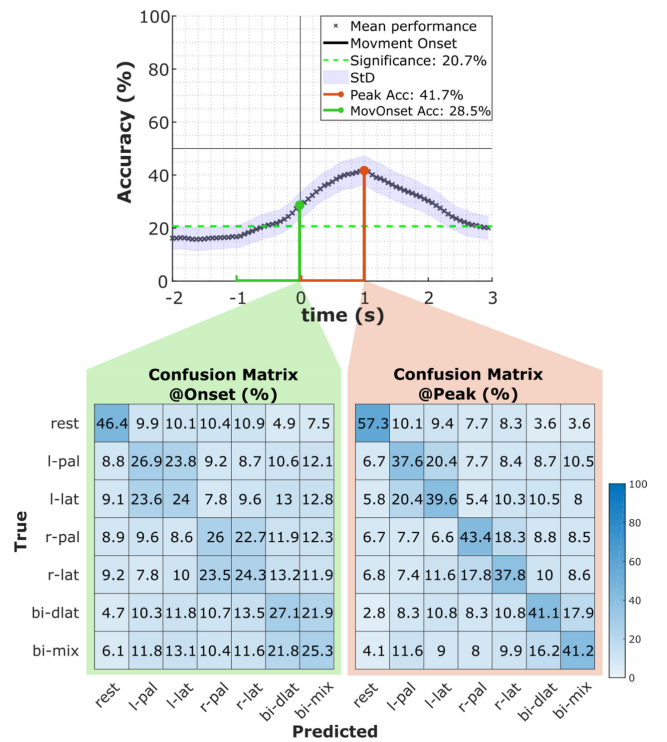


Fig. 6. Calibration set, offline classification results for all participants ( $n = 15$ ). Top: Grand Average of the best performing classification time point. Peak performance is reached at 1 s after the movement onset (red dot), which incorporates time domain features from [0 1]. Bottom: C: Row-wise normalized confusion matrices of the grand-average calculated over the timepoints of movement onset (time = 0 s) and participant-specific peak performance. Condition abbreviations: rest (Rest); l-pal (Left Palmar); l-lat (Left Lateral); r-pal (Right Palmar); r-lat (Right Lateral); bi-dlat (Bimanual double Lateral); bi-mix (Bimanual mixed Palmar/Lateral).

conditions. For the Evaluation set results we also calculated the information transfer rate (ITR) using Wolpaw's Bit rate (see Table III). On average participants scored 1.6 +/- 0.8 bits/min.

TABLE III

PARTICIPANT-SPECIFIC PEAK ACCURACIES FOR CALIBRATION AND EVALUATION SET. THE LAST COLUMN SHOWS THE INFORMATION TRANSFER RATE (ITR) ACCORDING TO WOLPAW'S BIT RATE CALCULATION (EVALUATION SET ONLY)

#	Calibration set			Evaluation set		
	Peak %	Std %	Time s	Peak %	Time s	ITR bit/min
S1	46.1	5.22	0.69	37	0.81	1.4
S2	37.6	4.62	1.00	31.5	1.13	0.8
S3	38.1	4.62	1.00	33.1	1.19	1.0
S4	47.2	4.35	0.81	36.9	0.94	1.4
S5	42.1	5.47	1.13	42.3	1.31	2.0
S6	41.7	4.96	1.06	37.3	1.19	1.4
S7	34.3	4.96	1.06	36	1.19	1.3
S8	49.8	3.62	0.88	43.6	1.00	2.2
S9	40.7	5.47	1.13	32.9	1.25	1.0
S10	49.2	5.35	0.75	49.1	0.88	3.0
S11	41.5	4.62	1.00	37	1.13	1.4
S12	44.8	4.62	1.00	49.1	1.06	3.0
S13	32.1	6.09	1.56	25.3	1.63	0.4
S14	49.8	3.62	0.88	47.9	0.94	2.8
S15	45.1	4.62	1.00	40.4	1.06	1.8
grand average	42.7	4.81	1.00	38.6	1.11	1.6

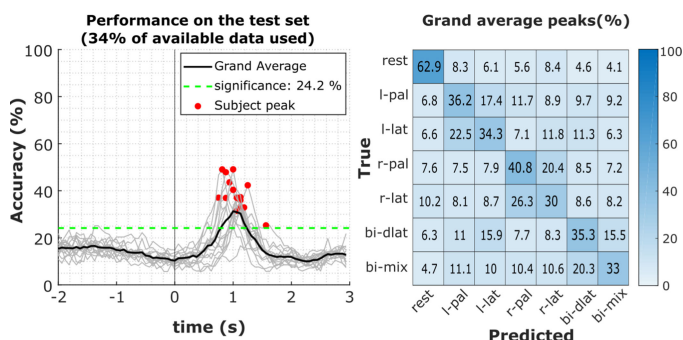


Fig. 7. Evaluation set, offline classification results for all participants ( $n = 15$ ). Left: Grand average over all participants of the best performing classification model applied on the unseen data of the Evaluation set (black line). Red dots indicate the participant-specific peak accuracies. The green dotted line marks the task-related chance level. Right: Row-wise normalized confusion matrix of the grand average of the participant-specific peak accuracies.

### C. Behavioural Analysis

Results from the Hand-Dominance-Test confirmed that all participants were right handed (see Supplementary Figure S1). The reach-and-grasp durations of all participants are shown in Figure 8 as boxplots, separated by condition. We performed a repeated measures one-way ANOVA to test for significant differences in the reach-and-grasp time among the conditions (6 levels). Mauchly's test indicated that the assumption of sphericity was not violated. There was a significant effect for the reach-and-grasp duration  $F(5,70) = 9.16$ ,  $p < 0.01$ . Post hoc pairwise multiple comparison tests using the Tukey-Kramer

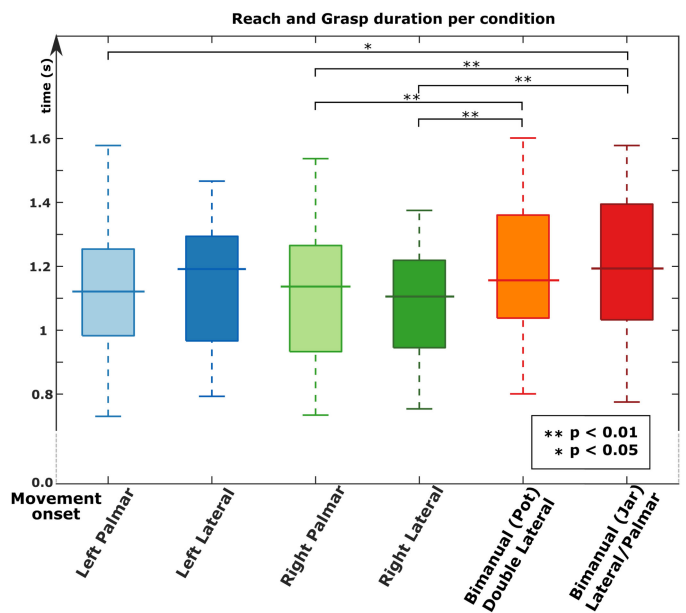


Fig. 8. Behavioural analysis. Box-plots of the reach-and-grasp durations of all participants. The reach-and-grasp duration is calculated from lifting the hand off the pressure sensor until triggering the pressure sensor on the object.

criterion showed that bimanual conditions were performed significantly slower than unimanual conditions with the exception of lateral grasping with the left hand. For all the significant differences the effect size was between 110 and 140 ms. For the bimanual trials we also calculated the median difference between the movement onset between the left and right hand. The time difference between these movement onsets resulted at  $32 \text{ ms} \pm 10 \text{ ms}$ . Detailed results can be found in the supplementary material (Figure S2, right).

## IV. DISCUSSION

In this study, we could show that unimanual and bimanual reach-and-grasp actions can be successfully decoded against each other using the low-frequency time-domain features of the EEG. Our multiclass classification approach, which incorporated all six reach-and-grasp movements and a rest condition resulted in a peak performance on average of  $38.6 \pm 6.6\%$  (achieved on the unseen data of the Evaluation set, chance level at 24.2%). Peak accuracy was reached on average within the first second after the movement onset. Low frequency EEG correlates which were exploited by the classifier show significant differences between unimanual and bimanual conditions already preceding the movement onset.

### A. Movement-Related Cortical Potentials

In general, MRCPs of all the reach-and-grasp conditions investigated in this work are similar in morphology to our previous study described in [16], [48]: Imminently to the movement onset, a strong negative deflection occurs, which we associate to the Bereitschaftspotential described in [17], [18] and in other EEG based studies on MRCPs such as [15], [22], [49]–[51].

Around 250 ms after the movement onset a reafferent potential emerges, which was already identified in previous experiments [16], [48], [52] and seems to be characteristic of reach and grasp movement tasks. When comparing combined conditions of 'Left Hand,' 'Right Hand' and 'Bimanual,' significant lateralization effects can be observed not only in direct MRCP comparison but also in the difference topoplots for 'left-right,' as well as 'left-bimanual' and 'right-bimanual'. In all difference plot combinations lateralized effects already occur from 1 s before the actual movement over the motor cortex and culminate prominently at or shortly after the movement is initiated (movement onset). No distinct lateralization effect can be observed in the bimanual conditions. Here both hands are actively engaged in the task and show similar MRCP morphology. However when looking at the difference topoplots between unimanual and bimanual conditions, significant differences emerge ipsilateral to the involved unimanual condition (e.g. for 'right-bimanual' significant differences can be found on the right side since the left hand is only engaged in the bimanual task, while the right hand is active in both unimanual and bimanual tasks). While lateralization effects are known since the first experiments of Kornhuber and Deecke in 1965, [18] and have been subsequently investigated in some movement tasks [53]–[54], we show that this effect is also observable in the context of reach-and-grasp movements. As for comparison between same-hand conditions, we did not find significant differences in any combinations. However, when comparing unimanual to the bimanual conditions, a stronger negativity of the Bereitschaftspotential at second 0 can be observed (about  $-1.3 \mu\text{V}$ ) for bimanual conditions. Similar to our previous study [16], we observed a stronger rebound effect for the lateral grasp conditions, when compared to palmar grasp, regardless of the hand. This is visible between 1 to 2 s after the movement onset, over central position Cz (this occurs when the grasping is already finished and the hand is in the holding phase). This effect is also visible in the bimanual conditions whereas the condition pot (double lateral grasp) is more pronounced than the condition jar (mixed, palmar/lateral grasp).

The analysis of the reach-and-grasp durations show that in general, bimanual tasks were performed significantly slower (110–140 ms.) than unimanual grasps, with the exception of the left-hand lateral grasp condition. We surmise that this increased duration reflects the additional effort for a coordinated bimanual movement and in the case of the left lateral grasp, the unfamiliar activity. Interestingly, the timing from our previous experiment [16] and its cue guided paradigm yielded similar reach and grasp timings (1.1–1.125 s). Nevertheless no apparent differences regarding the timing with respect to the morphology of the EEG correlates of the unimanual conditions can be observed.

### B. Single-Trial Classification

Our classification approach targeted to simulate a BCI online scenario, therefore we initially split our data in a Calibration set for calculating a classification model and an Evaluation set of unseen data.

Results from the binary approach achieved on the Evaluation set show that same hand condition combinations as well as the bimanual versus bimanual combination resulted on average in accuracies between 66 and 70%. Condition combinations involving a mixture of unimanual and bimanual conditions and especially involving the rest condition yield highest performance results, on average between 74% to 90%. For most condition combinations, subject specific peak accuracies were achieved around 1 s after the movement onset. However for same hand, respective bimanual versus bimanual condition combinations, timings are more diverse which is reflected in grand average (see supplementary Figure S3).

Calibration set results generally yielded about 3–4% higher peak performances, but are still in the same range as for the Evaluation set. Notable, these results are comparable to binary results achieved [15], [16], since analysis and number of trials are similar.

For the multiclass approach, our participants achieved on average  $38.6 \pm 6.6\%$  accuracy on the unseen data of the Evaluation set exceeding chance level by more than 18% (7 conditions). Participant specific peak accuracies were achieved around 1 s  $\pm 200$  ms after the movement onset.

Our classification approach used the preceding window of 1 s to extract the features, e.g. the classification model obtained at 1 s used features from the movement onset [0:0.125:1] s. This goes in line with the significant differences found between the low frequency EEG correlates of all conditions. With regards to the length of our feature extraction window of 1 s, this means that these classification models were trained exclusively on the reach-and-grasp movement towards the object.

Analysis of the multiclass based confusion matrices of indicate that the true positive rates (TPRs) for the rest condition exceeds any other movement related TPRs by more than 20–25%. This effect was expected and has also been observed by our previous experiment series [16], [48] and can be attributed to the significant differences of the low frequency EEG correlates observed between rest and movement conditions. We also see that discrimination between conditions of the same hand as well as discrimination between bimanual conditions yield highest false positive and false negative rates within the confusion matrix (17–25%). However, condition combinations involving different types of movement, e.g. unimanual versus bimanual or unimanual left versus unimanual right, false positive and false negative rates are lower (4–12%). This was also expected since their low frequency EEG correlates showed an increased number of significantly different channels due to lateralization effects.

Our analysis on the data of the Calibration set indicated in general higher peak performances per participant, however the timing was in the same range. Better than chance classification could already be reached 1 s before the actual movement onset which is also in line with previous studies [15], [16], [22]. Unfortunately, direct performance comparison to other grasp decoding studies in the field such as Itturate *et al.* [24], Randazzo *et al.* [55] or Jochumsen *et al.* [22] and Agashe *et al.* [21] are difficult due to varying numbers of conditions or fundamental differences in experimental setup and paradigm design.

Our findings in this study show that unimanual and bimanual reach-and-grasp actions can be successfully decoded from low-frequency EEG and hence implementation in assistive devices for tetraplegic end users seems imminent. Nevertheless, there are still issues to be solved which could potentially put this idea in the dim future.

MRCPs used in this work for decoding are a time and phase-locked phenomenon. They are time-locked to an event, e.g. the finishing of a grasp [24], [55] or, as in the present study and [15], [48] to the movement onset [56]–[58]. While time-locking to executed movements is a feasible approach for people without motor disabilities, an accurate time-locking event can become difficult to obtain in tetraplegic persons who often do not have a measurable movement onset, not to mention an actual grasping trigger. Brisk visual or auditory cues could also be applied, however they usually elicit potentials which might mask the MRCP (see [14]). Recently, new paradigm approaches were proposed in [25], [59] in which continuous visual input is presented to the participants, in an attempt to avoid such potentials.

As we have seen in the classification results of the current study, applying the classification model over a larger window of interest leads to a good discrimination limited to a 1 s window on which the model was trained on. Outside this 1 s window, mean classification results are at chance level. This also applies for the rest condition which is trained on the same 1 s window. This suggests that if the timing of the reach and grasp action differs (e.g. slower movement or different distance for reaching the object), discrimination performance would be greatly reduced.

It is important to point out that our classification approach relied solely on low-frequency time-domain features. However, state-of-the-art BCIs based on mental imagery strategies rely on event-related desynchronization (ERD) phenomena to create a signal for control. In these studies, the participants imagine inter alia repetitive hand or feet movements, to generate a control signal [60]–[64]. Aside from unimanual movements, also bimanual tasks have been investigated, leading to a notable control [65]–[67]. While those BCIs usually provide a satisfying degree of control, they depend on strategies which feel unnatural to the users, since there is often a mismatch between the intended movement (e.g. repetitive feet MI) and the actual movement executed by the control device (e.g. hand open command for a neuroprosthesis). While we could already show, for a set of unimanual reach-and-grasp movements, that the performance associated with the rest condition could be boosted and stabilized by incorporating features from alpha and beta band EEG, this did not significantly improve the discrimination between different grasp types [48]. Additionally, Iturrate *et al.* have shown, for precision and power grasps, that discriminable information for reach-and-grasp decoding can be found in higher bands, despite the highest decoding performances being achieved using features from 1-6 Hz [24], [48], [68]. Future work should therefore consider the possibility of using a combination of time-domain and frequency features and, eventually, a participant-specific tuning of the relevant frequency bands. Since the classification of movement vs. rest is boosted by frequency-domain features, it might be beneficial to implement other classification approaches, like the hierarchical approach described in [69].

Furthermore, we still face the challenge of transferring these results to actual end users: It is still unclear whether combined reach-and-grasp actions can be decoded from a person without voluntary hand/finger control: While the reaching towards an object can still be executed the grasp itself is only attempted (due to lack of voluntary finger control). Future investigations - in close cooperation with tetraplegic end users - will show whether this combination of executed and attempted movement can be detected.

Naturally, the task becomes even more complex when targeting a population without any voluntary upper limb control left. So far, it has already been shown that unimanual attempted hand movements can be decoded [25], [26], [70] in principal, as well as MRCPs from imagined movements [59]. However, further studies on a larger population are necessary to evaluate the decoding performance and thus control possibilities.

## V. CONCLUSION

We show that unimanual and bimanual reach-and-grasp actions can be decoded from the low frequency EEG. Significant lateralization effects were identified in the EEG neural correlates for left versus right unimanual hand conditions, whereas bimanual conditions elicited bilaterally with no perceivable lateralization. We believe, that despite issues such as asynchronous classification performance and transfer to end users, which still need addressing, our findings can potentially lead to an EEG-driven bimanual control of neuroprostheses.

## ACKNOWLEDGMENT

The authors thank R. Rupp for fruitful discussions that inspired this work, S. Wriessnegger for the discussions on the experimental paradigm, M. K. Höller for the development of the sensor system and assisting in the measurements, M. Burtscher (www.nu-art.at) for the creation of Figure 1. The authors also thank P. Ofner, A. Pinegger, and all members of the EU Horizon 2020 Project ‘MoreGrasp’ (‘643955’) for building the solid foundation for this research.

## REFERENCES

- [1] G. J. Snoek *et al.*, “Survey of the needs of patients with spinal cord injury: Impact and priority for improvement in hand function in tetraplegics,” *Spinal Cord*, vol. 42, no. 9, pp. 526–532, Sep. 2004.
- [2] K. D. Anderson, “Targeting recovery: Priorities of the spinal cord-injured population,” *J. Neurotrauma*, vol. 21, no. 10, pp. 1371–1383, Oct. 2004.
- [3] V. R. Hentz and C. Leclercq, *Surgical Rehabilitation of the Upper Limb in Tetraplegia*. Philadelphia, PA, USA: Saunders Limited, 2002.
- [4] C. Leclercq, M.-A. Lemouel, and T. Albert, “[Surgical rehabilitation procedures of the upper limbs in tetraplegic patients],” *Handchir. Mikrochir. Plast. Chir.*, vol. 37, no. 4, pp. 230–237, Aug. 2005.
- [5] S. Crea *et al.*, “Feasibility and safety of shared EEG/EOG and vision-guided autonomous whole-arm exoskeleton control to perform activities of daily living,” *Sci. Rep.*, vol. 8, no. 1, Jul. 2018, Art. no. 108238.
- [6] N. A. Bhagat *et al.*, “Design and optimization of an EEG-based brain machine interface (BMI) to an upper-limb exoskeleton for stroke survivors,” *Frontiers Neurosci.*, vol. 10, 2016, doi: 10.3389/fnins.2016.00122.
- [7] J. Cantillo-Negrete *et al.*, “Motor imagery-based brain-computer interface coupled to a robotic hand orthosis aimed for neurorehabilitation of stroke patients,” *J. Healthc. Eng.*, vol. 2018, Apr. 2018, Art. no. 1624637.
- [8] R. Rupp and H. J. Gerner, “Neuroprosthetics of the upper extremity—Clinical application in spinal cord injury and challenges for the future,” *Acta Neurochir. Suppl.*, vol. 97, no. Pt 1, pp. 419–426, 2007.

- [9] G. R. Müller-Putz *et al.*, "EEG-based neuroprosthesis control: A step towards clinical practice," *Neurosci. Lett.*, vol. 382, no. 1-2, pp. 169–174, Apr. 2005.
- [10] G. Müller-Putz *et al.*, "Brain-computer interfaces for control of neuroprostheses: From synchronous to asynchronous mode of operation," *Biomed. Tech.*, vol. 51, no. 2, pp. 57–63, Jul. 2006.
- [11] G. Pfurtscheller *et al.*, "'Thought'- control of functional electrical stimulation to restore hand grasp in a patient with tetraplegia," *Neurosci. Lett.*, vol. 351, no. 1, pp. 33–36, 2003. [Online]. Available: <http://www.sciencedirect.com/science/article/pii/S0304394003009479>
- [12] G. R. Müller-Putz *et al.*, "From classic motor imagery to complex movement intention decoding: The noninvasive Graz-BCI approach," *Prog. Brain Res.*, vol. 228, pp. 39–70, May 2016.
- [13] G. Müller-Putz *et al.*, "Steuerung von Neuroprothesen bei Querschnittlähmung: Der nichtinvasive Graz-BCI-Ansatz," *NeuroRehabilitation*, vol. 8, no. 3, pp. 126–133, 2016.
- [14] G. R. Müller-Putz *et al.*, "MoreGrasp: Restoration of upper limb function in individuals with spinal cord injury by multimodal neuroprostheses for interaction in daily life activities," in *Proc. 7th Graz Brain-Comput. Interface Conf.*, 2017, pp. 338–343.
- [15] P. Ofner *et al.*, "Upper limb movements can be decoded from the time-domain of low-frequency EEG," *PLoS One*, vol. 12, no. 8, Aug. 2017, Art. no. e0182578.
- [16] A. Schwarz *et al.*, "Decoding natural reach-and-grasp actions from human EEG," *J. Neural Eng.*, vol. 15, no. 1, Feb. 2018, Art. no. 016005.
- [17] H. Shibasaki and M. Hallett, "What is the Bereitschaftspotential?" *Clin. Neurophysiol.*, vol. 117, no. 11, pp. 2341–2356, 2006.
- [18] H. H. Kornhuber and L. Deecke, "Hirnpotentialänderungen bei willkürbewegungen und passiven bewegungen des menschen: Bereitschaftspotential und reafferente potentiale," *Pflugers Arch. Gesamte Physiol. Menschen Tiere*, vol. 284, no. 1, pp. 1–17, 1965.
- [19] T. Pistohl *et al.*, "Decoding natural grasp types from human ECoG," *NeuroImage*, vol. 59, no. 1, pp. 248–260, Jan. 2012.
- [20] T. Pistohl *et al.*, "Grasp detection from human ECoG during natural reach-to-grasp movements," *PLoS One*, vol. 8, no. 1, Jan. 2013, Art. no. e54658.
- [21] H. A. Agashe *et al.*, "Global cortical activity predicts shape of hand during grasping," *Frontiers Neurosci.*, vol. 9, Apr. 2015, Art. no. 121.
- [22] M. Jochumsen *et al.*, "Detecting and classifying three different hand movement types through electroencephalography recordings for neurorehabilitation," *Med. Biol. Eng. Comput.*, vol. 54, no. 10, pp. 1491–1501, Oct. 2016.
- [23] M. Jochumsen *et al.*, "Detection and classification of movement-related cortical potentials associated with task force and speed," *J. Neural Eng.*, vol. 10, no. 5, Oct. 2013, Art. no. 056015.
- [24] I. Iturrate *et al.*, "Human EEG reveals distinct neural correlates of power and precision grasping types," *NeuroImage*, vol. 181, pp. 635–644, 2018.
- [25] P. Ofner *et al.*, "Attempted arm and hand movements can be decoded from low-frequency EEG from persons with spinal cord injury," *Sci. Reports*, vol. 9, 2019, Art. no. 7134.
- [26] G. R. Müller-Putz *et al.*, "Applying intuitive EEG-controlled grasp neuroprostheses in individuals with spinal cord injury: The MoreGrasp clinical feasibility study," in *Proc. 41st Conf. Eng. Med. Biol.*, 2019, p. 7.
- [27] K. Dremstrup *et al.*, "Rehabilitation using a brain computer interface based on movement related cortical potentials—A review," in *Proc. 13th Mediterranean Conf. Med. Biol. Eng. Comput.*, 2014, pp. 1659–1662.
- [28] N. Mrachacz-Kersting *et al.*, "Precise temporal association between cortical potentials evoked by motor imagination and afference induces cortical plasticity," *J. Physiol.*, vol. 590, no. 7, pp. 1669–1682, Apr. 2012.
- [29] N. Mrachacz-Kersting *et al.*, "Brain-state dependent peripheral nerve stimulation for plasticity induction targeting upper-limb," in *Proc. Int. Conf. NeuroRehabil.*, 2019, pp. 1061–1065.
- [30] H.-J. Steingruber, *Hand-Dominanz-Test: H-D-T; Manual*. Göttingen, Germany: Hogrefe, 2011.
- [31] R. J. Kobler, A. I. Sburlea, and G. R. Müller-Putz, "Tuning characteristics of low-frequency EEG to positions and velocities in visuomotor and oculomotor tracking tasks," *Sci. Rep.*, vol. 8, no. 1, Dec. 2018, Art. no. 17713.
- [32] R. Kobler, A. Sburlea, and G. R. Müller-Putz, "A comparison of ocular artifact removal methods for block design based electroencephalography experiments," in *Proc. 7th Graz Brain-Comput. Interface Conf.*, 2017, pp. 236–241.
- [33] R. Oostenveld and P. Praamstra, "The five percent electrode system for high-resolution EEG and ERP measurements," *Clin. Neurophysiol.*, vol. 112, no. 4, pp. 713–719, Apr. 2001.
- [34] M. Fatourechchi *et al.*, "EMG and EOG artifacts in brain computer interface systems: A survey," *Clin. Neurophysiol.*, vol. 118, no. 3, pp. 480–494, Mar. 2007.
- [35] L. C. Parra *et al.*, "Recipes for the linear analysis of EEG," *NeuroImage*, vol. 28, no. 2, pp. 326–341, 2005.
- [36] J. Faller *et al.*, "Autocalibration and recurrent adaptation: Towards a plug and play online ERD-BCI," *IEEE Trans. Neural Syst. Rehabil. Eng.*, vol. 20, no. 3, pp. 313–319, May 2012.
- [37] K. Statthaler *et al.*, "Cybathlon experiences of the Graz BCI racing team Mirage 91 in the brain-computer interface discipline," *J. Neuroeng. Rehabil.*, vol. 14, no. 1, Dec. 2017, Art. no. 129.
- [38] A. Schwarz *et al.*, "A co-adaptive sensory motor rhythms brain-computer interface based on common spatial patterns and random forest," *Conf. Proc. IEEE Eng. Med. Biol. Soc.*, vol. 2015, pp. 1049–1052, Aug. 2015.
- [39] W. Skrandies, "Global field power and topographic similarity," *Brain Topogr.*, vol. 3, no. 1, pp. 137–141, 1990.
- [40] C. Brunner, A. Delorme, and S. Makeig, "Eeglab—An open source Matlab toolbox for electrophysiological research," *Biomed. Tech.*, vol. 58, Suppl. 1, pp. 1–2, Aug. 2013, doi: [10.1515/bmt-2013-4182](https://doi.org/10.1515/bmt-2013-4182).
- [41] P. H. Westfall, S. Stanley Young, and Young, *Resampling-Based Multiple Testing: Examples and Methods for P-Value Adjustment*. Hoboken, NJ, USA: Wiley, Jan. 1993.
- [42] R. C. Blair, R. Clifford Blair, and W. Karniski, "An alternative method for significance testing of waveform difference potentials," *Psychophysiology*, vol. 30, no. 5, pp. 518–524, 1993.
- [43] A. P. Holmes *et al.*, "Nonparametric analysis of statistic images from functional mapping experiments," *J. Cereb. Blood Flow Metab.*, vol. 16, no. 1, pp. 7–22, Jan. 1996.
- [44] B. Blankertz *et al.*, "Single-trial analysis and classification of ERP components—A tutorial," *NeuroImage*, vol. 56, no. 2, pp. 814–825, 2011.
- [45] E. Thomas, M. Dyson, and M. Clerc, "An analysis of performance evaluation for motor-imagery based BCI," *J. Neural Eng.*, vol. 10, no. 3, Jun. 2013, Art. no. 031001.
- [46] J. R. Wolpaw *et al.*, "EEG-based communication: Improved accuracy by response verification," *IEEE Trans. Rehabil. Eng.*, vol. 6, no. 3, pp. 326–333, Sep. 1998.
- [47] M. Billinger *et al.*, "Is it significant? guidelines for reporting BCI performance," in *Proc. Biol. Med. Phys., Biomed. Eng.*, 2012, pp. 333–354.
- [48] A. Schwarz *et al.*, "Combining frequency and time-domain EEG features for classification of self-paced reach-and-grasp actions," in *Proc. 41st Conf. Eng. Med. Biol.*, Jul. 23–27, 2019, doi: [10.1109/EMBC.2019.8857138](https://doi.org/10.1109/EMBC.2019.8857138).
- [49] M. Jochumsen *et al.*, "Comparison of spatial filters and features for the detection and classification of movement-related cortical potentials in healthy individuals and stroke patients," *J. Neural Eng.*, vol. 12, no. 5, Oct. 2015, Art. no. 056003.
- [50] J. Pereira *et al.*, "EEG neural correlates of goal-directed movement intention," *NeuroImage*, vol. 149, pp. 129–140, Apr. 2017.
- [51] S. Oda and T. Moritani, "Movement-related cortical potentials during handgrip contractions with special reference to force and electromyogram bilateral deficit," *Eur. J. Appl. Physiol. Occup. Physiol.*, vol. 72, no. 1/2, pp. 1–5, 1995.
- [52] C. Bozzacchi, R. L. Cimmino, and F. Di Russo, "The temporal coupling effect: Preparation and execution of bimanual reaching movements," *Biol. Psychol.*, vol. 123, pp. 302–309, Feb. 2017.
- [53] F. T. Y. Smulders and J. O. Miller, "The lateralized readiness potential," in *The Oxford Handbook of Event-Related Potential Components*. Oxford, U.K.: Oxford Univ. Press, 2011.
- [54] J. Schmitz *et al.*, "The neurophysiological correlates of handedness: Insights from the lateralized readiness potential," *Behav. Brain Res.*, vol. 364, pp. 114–122, May 2019.
- [55] L. Randazzo *et al.*, "Detecting intention to grasp during reaching movements from EEG," *Conf. Proc. IEEE Eng. Med. Biol. Soc.*, vol. 2015, pp. 1115–1118, Aug. 2015.
- [56] I. K. Niazi *et al.*, "Detection of movement intention from single-trial movement-related cortical potentials," *J. Neural Eng.*, vol. 8, no. 6, Dec. 2011, Art. no. 066009.
- [57] E. López-Larraz *et al.*, "Continuous decoding of movement intention of upper limb self-initiated analytic movements from pre-movement EEG correlates," *J. Neuroeng. Rehabil.*, vol. 11, Nov. 2014, Art. no. 153.
- [58] I. K. Niazi *et al.*, "Detection of movement-related cortical potentials based on subject-independent training," *Med. Biol. Eng. Comput.*, vol. 51, no. 5, pp. 507–512, May 2013.
- [59] J. Pereira, A. I. Sburlea, and G. R. Müller-Putz, "EEG patterns of self-paced movement imaginations towards externally-cued and internally-selected targets," *Sci. Rep.*, vol. 8, no. 1, Sep. 2018, Art. no. 13394.

- [60] G. Pfurtscheller and C. Neuper, "Motor imagery and direct brain-computer communication," *Proc. IEEE*, vol. 89, no. 7, pp. 1123–1134, Jul. 2001.
- [61] B. Blankertz *et al.*, "The Berlin brain-computer interface: Accurate performance from first-session in BCI-naive subjects," *IEEE Trans. Biomed. Eng.*, vol. 55, no. 10, pp. 2452–2462, Oct. 2008.
- [62] A. Schwarz, D. Steyrl, and G. R. Müller-Putz, "Brain-computer interface adaptation for an end user to compete in the Cybathlon," in *Proc. IEEE Int. Conf. Syst., Man, Cybern.*, 2016, pp. 001803–001808.
- [63] J. R. Millan *et al.*, "Noninvasive brain-actuated control of a mobile robot by human EEG," *IEEE Trans. Biomed. Eng.*, vol. 51, no. 6, pp. 1026–1033, Jun. 2004.
- [64] R. Scherer *et al.*, "Toward self-paced brain-computer communication: Navigation through virtual worlds," *IEEE Trans. Biomed. Eng.*, vol. 55, no. 2, pp. 675–682, Feb. 2008.
- [65] K. LaFleur *et al.*, "Quadcopter control in three-dimensional space using a noninvasive motor imagery-based brain-computer interface," *J. Neural Eng.*, vol. 10, no. 4, Aug. 2013, Art. no. 046003.
- [66] J. Meng *et al.*, "Noninvasive electroencephalogram based control of a robotic arm for reach and grasp tasks," *Sci. Rep.*, vol. 6, Dec. 2016, Art. no. 38565.
- [67] A. Vuckovic, S. Pangaro, and P. Finda, "Unimanual versus bimanual motor imagery classifiers for assistive and rehabilitative brain computer interfaces," *IEEE Trans. Neural Syst. Rehabil. Eng.*, vol. 26, no. 12, pp. 2407–2415, Dec. 2018.
- [68] A. Korik *et al.*, "Decoding imagined 3D hand movement trajectories from EEG: Evidence to support the use of mu, beta, and low gamma oscillations," *Frontiers Neurosci.*, vol. 12, Mar. 2018, Art. no. 130.
- [69] J. Omedes *et al.*, "Hierarchical decoding of grasping commands from EEG," *Conf. Proc. IEEE Eng. Med. Biol. Soc.*, vol. 2017, pp. 2085–2088, Jul. 2017.
- [70] Y. Blokland *et al.*, "Detection of attempted movement from the EEG during neuromuscular block: Proof of principle study in awake volunteers," *Sci. Rep.*, vol. 5, Aug. 2015, Art. no. 12815.

# Combining frequency and time-domain EEG features for classification of self-paced reach-and-grasp actions

Andreas Schwarz<sup>1</sup>, Joana Pereira<sup>1</sup>, Lydia Lindner<sup>1</sup> and Gernot R. Müller-Putz<sup>1</sup>, *Member IEEE*

**Abstract**—Brain-computer interfaces (BCIs) might provide an intuitive way for severely motor impaired persons to operate assistive devices to perform daily life activities. Recent studies have shown that complex hand movements, such as reach-and-grasp tasks, can be decoded from the low frequency of the electroencephalogram (EEG). In this work we investigated whether additional features extracted from the frequency-domain of alpha and beta bands could improve classification performance of rest vs. palmar vs. lateral grasp. We analysed two multi-class classification approaches, the first using features from the low frequency time-domain, and the second in which we combined the time-domain with frequency-domain features from alpha and beta bands. We measured EEG of ten participants without motor disability which performed self-paced reach-and-grasp actions on objects of daily life. For the time-domain classification approach, participants reached an average peak accuracy of 65%. For the combined approach, an average peak accuracy of 75% was reached. In both approaches and for all subjects, performance was significantly higher than chance level (38.1%, 3-class scenario). By computing the confusion matrices as well as feature rankings through the Fisher score, we show that movement vs. rest classification performance increased considerably in the combined approach and was the main responsible for the multi-class higher performance. These findings could help the development of BCIs in real-life scenarios, where decreasing false movement detections could drastically increase the end-user acceptance and usability of BCIs.

## I. INTRODUCTION

Brain-computer interfaces (BCIs) enable its users to interact with their environment by deliberate or evoked changes in brain activity. One possible target group would be persons with high spinal cord injury (SCI): while their upper limb function is critically impaired, a BCI might enable them to control an robotic arm [1] or a upper limb motor neuroprosthesis [2] just by thought. BCI control strategies for such applications typically rely on repetitive imagination of mental tasks, e.g. motor imagination of repeated hand or foot movements [3], [4] [5]. In recent years, we have focused our research [6]–[10] in finding new control strategies [10]: We investigated the possibility of using the actual (single) movement intended by the user, e.g. reaching for a glass or grasping a spoon. Our studies have shown that the electroencephalographic (EEG) correlates of movement in the low frequency range hold sufficient information to discriminate up to three different grasps. The EEG neural correlate which amplitude is modulated by the different types of grasps is

a slow cortical potential measured around the movement onset and known as movement related cortical potential (MRCP) [11]. MRCPs manifest as a negative deflection of the amplitude before an actual movement onset, reaching its maximum peak negativity imminently to the movement onset, then followed by a positive rebound. They have been found to provide information regarding force and speed [12] as well as different reach and grasp actions in non-motor impaired participants [6], [13], [14]. In our recent project, (Horizon 2020, “MoreGrasp”) we are transferring these findings to actual end users with SCI, who perform single movement attempts like a palmar or lateral grasp to control an upper limb neuroprosthesis by means of a BCI [15]. Our findings indicate that these potentials are also present in individuals with SCI, however the initial decoding performances are rather low. Hence we keep investigating means for increasing BCI performance.

So far, we have restricted our feature space to the low frequency time-domain signals for discriminating between different executed or attempted reach and grasp actions. Investigations by Jochumsen et al. on grasp intention decoding [12] have shown that an inclusion of spectral feature components could lead to increased classification performance. Hence in the current study, we investigate the effects of combining time-domain features with additional frequency features from alpha and beta ranges. We hypothesize that combining frequency and time-domain features significantly improves the classification performance of rest vs. palmar vs. lateral grasps. We measured the EEG of ten right handed participants without motor disability during a self-paced reach-and-grasp experiment which included inter alia palmar (grasping a glass) and lateral (grasping a spoon) grasps. Finally, we discuss the contribution of both types of features using a topographical ranked metric for feature quality through the Fisher score [16].

## II. METHODS

### A. Participants, Experimental setup and Paradigm

This study was approved by the local ethics committee of the Medical University of Graz (EK: 30-439 ex 17/18). Ten right handed participants took part in this study. Each participant was informed about the study goals and gave written informed consent. At the beginning of each session, we tested their handedness using the Hand-Dominance-Test described in [17]. Participants were seated in an electromagnetically shielded room and we placed a table with an in-built monitor in front of them. On the horizontally positioned screen we placed two objects, an empty jar and a jar with

\*This work was supported by EU Horizon 2020 Project ‘MOREGRASP’ (643955) and partly by ERC consolidator Grant No ‘681231’

<sup>1</sup>Institute of Neural Engineering, Stremayrgasse 16/ IV, Graz, University of Technology, Austria andreas.schwarz@tugraz.at, gernot.mueller@tugraz.at

a spoon (fixed within the jar). During rest and breaks, the participants' right hand laid on a pressure sensor centrally positioned between the objects, in comfortable reaching and grasping range, as illustrated in Figure 1.

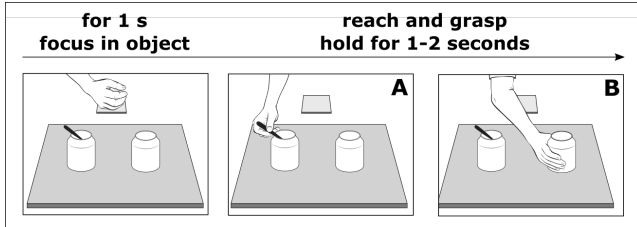


Fig. 1. **Paradigm for self-paced reach-and-grasp actions.** Participants were asked to focus on the object for at least one second before initiating the reach-and-grasp action. They grasped and held the object eventually for 1-2 seconds.

Our participants were instructed to reach and grasp the objects in a self-paced manner, however we instructed them to first focus their gaze on the object they wanted to grasp for at least 1 second. Thereafter, they performed a steady reach and grasp towards either a spoon (with a lateral grasp, see Figure 1 A), or the glass (with a palmar grasp, see Figure 1, B), followed by an holding period of at least 1 second. Aside from these two movement conditions, additional conditions were recorded in which participants were asked to perform grasps with both hands. These results are not the target of this paper, and will be published elsewhere. Participants were then asked to move their hand back on the pressure plate. On completion, a small insert showed them the amount of grasps they performed on the object. Between these reach-and-grasp actions we asked them to perform a break for at least 4 seconds. We recorded 80 trials per class (TPC) distributed over 4 runs á 20 TPC. After each run, we switched the positions of the objects so that each object was positioned left or right equally often. Additionally, we recorded at the beginning, halftime and end of the experiment 3 minutes of rest where participants were asked to focus their gaze on a dot shown on the center of the screen. Other than that, we also recorded eye movements and blinks by moving this dot horizontally and vertically on the screen, on a paradigm described in [18]. We measured EEG and EOG with 58 and 6 active electrodes (g.tec medical engineering GmbH, Austria), respectively. For recording the movement onset we used a pressure plate, localized centrally between both objects and synchronized its data to the EEG. EEG was recorded with a sampling frequency of 256 Hz and prefiltered using an 8th order Chebyshev filter between 0.01 and 100Hz. Power line interferences were dampened using a notch filter at 50Hz.

### B. Single Trial Multiclass Classification

We performed single trial multiclass classification incorporating two different approaches: The first approach (time-domain-only) relied solely on using features from the low frequency time-domain, while the second (combined model) relied on features extracted from the time-domain as well as from the frequency-domain. For both classification

approaches we preprocessed the data using a 4th order zero-phase high pass filter at 0.3 Hz. To counter any influence of eye-movements we used the eye movement and blink runs and applied the EOG-subspace method described in [18]. Thereafter, we excluded remaining artefact contaminated trials based on statistical parameters (amplitude threshold, kurtosis, probability density function) as described in [6], [19]. For both grasp conditions we defined a window of interest (WOI) of [-2 3]s with respect to the movement onset. For the rest condition we epoched the recorded rest runs in trials of 5 second length (1 second interval) and hence extracted 81 rest condition trials.

1) *Time Domain Feature Classification:* The time-domain-only classification follows closely our initial approach described in [6]: For each participant, we resampled the preprocessed EEG signal to 16 Hz and applied common average reference filter (CAR). Thereafter we low-pass filtered the signal with a cut-off frequency of 3 Hz to retain only its desired low frequency components and epoched it into trials according to the previously defined WOI. Using a 10 times 5 fold cross validation technique we divided each participants' trials into training and testing sets. We trained a shrinkage based linear discriminant analysis (sLDA) classifier [20] on features extracted from a 1 second window. Concretely, on this 1 second window, we took 9 amplitude values as features in 125ms steps per channel, i.e. we took 522 features in total per observation. For every sample, we moved this 1-second window over the WOI. This means that for every point within the WOI, we trained and tested an individual classification model. In this way, we were able to determine the best performing classification model within the WOI. For each fold, we evaluated the accuracy of the best performing classification model on the testing set throughout the WOI and averaged over all testing folds. We report the grand-average over all participants.

2) *Combined model: Time Domain / Frequency Domain Feature Classification:* For each participant we resampled the EEG to 128 Hz and applied CAR filtering. The WOI as well as the 10 times 5 fold cross validation procedure were the same as described above. Additionally to the 522 time-domain features extracted from the 1 second window, we calculated its power spectral density estimate (PSD), yielding for every frequency from 1 to 64 Hz a power value. We took the mean of 7 overlapping power bins covering alpha [8:12 Hz; 10:14 Hz;] and beta frequency ranges [14:19 Hz; 17:22Hz; 20:25 Hz; 23:28Hz; 26:31 Hz] and therefore extracted 7 new features per EEG channel (406). After normalization and calculation of the base 10 logarithm, these features were concatenated with the time-domain features from the same extraction window. In total we extracted 928 features (522 time-domain + 406 frequency domain) per observation. Again these features were classified using an sLDA classifier.

### C. Power Spectral Density Estimate and EEG correlates

We also performed analysis of the frequency-domain using the power spectral density estimate (PSD) as well as the



low frequency EEG correlates of all available conditions. Following the same artefact correction steps, we resampled the signal to 128 Hz and applied CAR filtering. For each participant, we epoched trials from  $[-1 \ 0]$ s with respect to the time point of peak performance in the combined classification model and calculated their PSD. Thereafter, we calculated the PSD mean of each condition. Additionally, we report the grand average PSD of all subjects per condition. As for the time-domain based low-frequency correlates, we resampled the EEG to 128 Hz, applied CAR filtering and bandpass filtered the signal between .3 and 3 Hz (4th order, zero-phase Butterworth). We calculated the global field potential using the rest data [21] to normalize the signal. For each subject we calculated the average for each condition over the WOI  $[-2 \ 3]$  and calculated the 95% confidence interval ( $\alpha = 0.05$ ) using non-parametric t-percentile bootstrap statistics. We report the grand averages over all subjects per condition.

#### D. Feature rating

We were also interested in a global rating of the features extracted from the time-domain as well as the frequency-domain, especially for the newly applied combined model. We used all available trials and conditions for this analysis. For each participant, we epoched trials from  $[-1 \ 0]$ s with respect to the time point of peak accuracy and calculated both time domain and frequency-domain features (see combined model). The subsequent feature rating was performed using the basic Fisher score approach described in [16]. For the time-domain features we summed up all scores per channel and calculated the grand average over all participants; for the frequency-domain features we calculated the grand average over all participants per frequency band.

### III. RESULTS

Figure 2 shows the single trial classification performance achieved solely with features extracted from the time-domain (top) as well as from the combined classification approach (bottom). The left column shows the grand average classification performance of all subjects for each classification model calculated within the WOI. The red vertical line shows the grand average point of peak performance. The green dashed line depicts the chance level with 38.9% ( $\alpha = 0.05$ , adjusted Wald interval, corrected for multiple comparisons [22]). The center column displays performance when the best performing classifier is applied over the whole WOI. Grey traces show the individual subject performances, and peak accuracies are marked with red dots. The matrices in the right column show the grand average of the individual subject confusion matrices, calculated at the point of peak accuracy for both classification approaches. We applied row-wise normalization. It can clearly be seen that the true positive rate of the rest conditions is higher than for movement classes while the error rate for false positives and false negatives is considerably lower. Table I depicts the subject specific peak accuracies for both classification approaches.

On average, the combined approach shows an increase in performance by 10%. Statistical comparison between both peak accuracies and standard deviation revealed this difference to be significant (Wilcoxon rank sum test  $p < 0.05$ ). Figure 3 shows the low frequency correlates of all conditions with respect to the movement onset (second 0). We observe an overlap between the confidence intervals (CI) of the movement classes. Significant differences ( $p < 0.05$ ) between grand averages of movements versus the rest condition emerge on the electrodes covering contralateral areas before and after the movement onset (see non overlapping areas). Regarding the PSD analysis (Figure 4) distinct differences between movement and rest conditions can be observed, especially in the alpha and beta frequency ranges.

Finally, we evaluated the results from the feature ranking provided by the Fisher Score (see Figure 5). Here we show the grand average over all participants. The first column shows scoring results of the time-domain features for all possible binary combinations. Distinct higher scores can be observed between movement classes over the whole motor cortex, especially around C3, Cz and C2. However, for movement vs. rest the highest scores are obtained on more central and contralateral areas within the motor cortex (Cz, C1, C3). As for the frequency-domain based ratings (column 2 to 7), no distinct scores can be observed between movement vs. movement comparisons. For movement conditions vs. rest, distinct scores can be seen on the channels over contralateral motor areas, most distinctively in alpha band (e.g. 9-13 Hz) but also in the beta band (21-26Hz, 24-29Hz). The rating for the frequency range additionally shows scoring on some peripheral electrodes when comparing movement conditions vs. rest. Concretely, these corresponded to increased scores on occipital areas for the alpha range, and increased scores for the frontal ipsilateral areas for the beta range.

We also investigated the reach-and-grasp duration for both conditions. On average, it took participants  $1.1 \pm 0.2$  s from the movement onset to grasp any object.

### IV. DISCUSSION

In this paper we could confirm that different reach and grasp actions can be decoded from the low frequency-domain incorporating MRCPs as a primary neural correlate for discrimination. Our results go in line with previous findings [6] [14], [23] and notably [24]. For both approaches, all participants could score peak accuracies significantly higher than chance level (38.09%) at  $65.03 \%$   $\pm$  STD 6.51 for the time-domain-only approach and  $75.09 \%$   $\pm$  STD 5.76 for the combined approach. Participant specific peak accuracies occur on average 1 to 1.3 seconds after the movement onset for both investigated approaches which corresponds to the reach-and-grasp duration for both conditions. This means that peak accuracy is reached within the final stages of grasping the designated object, which is in accordance with previous findings [6]. Such timings would allow in an online scenario for a sufficient close to real time control. Regarding the combined approach, we could show that overall classification performance significantly improves

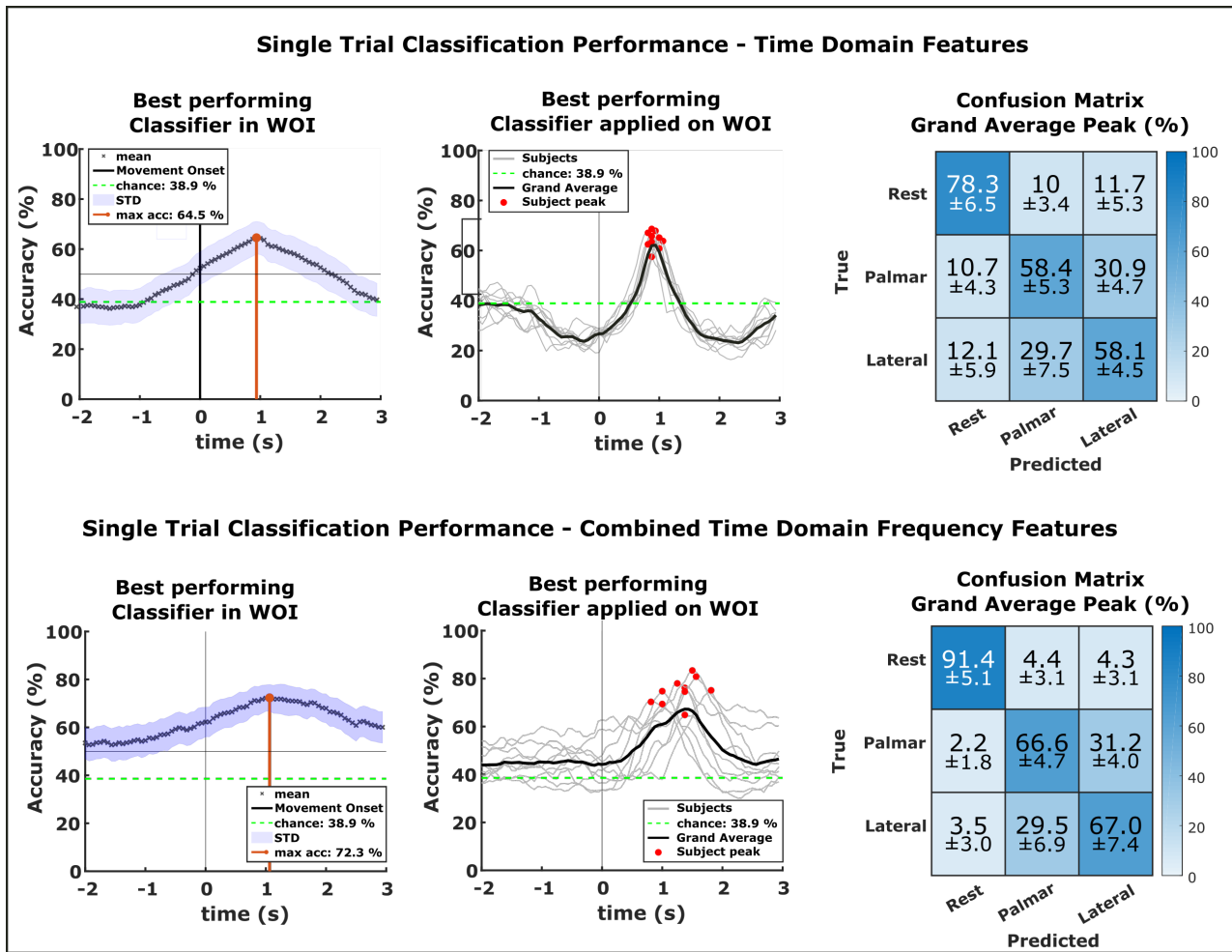


Fig. 2. Single trial classification performance based on time domain features (Top Row) and combined time domain and frequency domain features (Bottom Row). (Left Column): Grand average classification performance within the WOI. (Center Column): Grand average of the best performing classifier applied over the WOI. Grey lines represent individual subject performance, red dots their peak performances (Right Column): Row-wise normalized confusion matrix of the grand average calculated over the individual peak performance per subject.

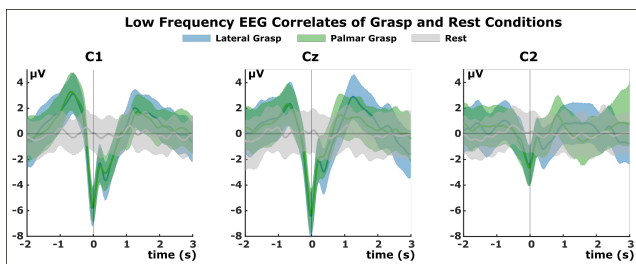


Fig. 3. Low frequency EEG correlates of grasp and rest conditions of channels C1, Cz and C2. Colored shaded areas show the confidence interval, bold lines the grand average of the designated reach-and-grasp-ation. The thin perpendicular line at second zero represents the movement onset.

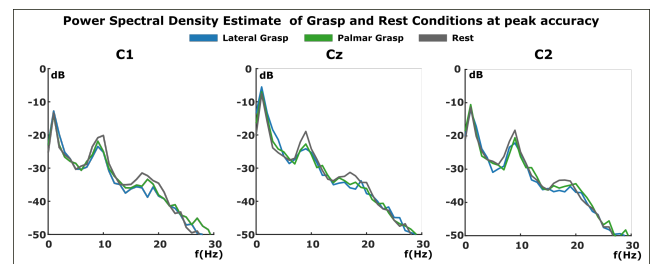


Fig. 4. Grand average PSD of the peak accuracy feature window for channels C1, Cz and C2. Bold lines show the condition specific PSDs.

when extending the feature space to the frequency-domain incorporating alpha and beta band from the same WOI. Our results show that a significant average peak performance increase of 10% could be reached. The confusion matrices

calculated at the point of peak accuracy reveal that this performance boost is due to a considerable improvement in classifying movements vs. rest condition. In comparison to the time-domain-only classification model, the true positive rate of the rest condition increases by more than 20% while the rates for false positives and false negatives with regards

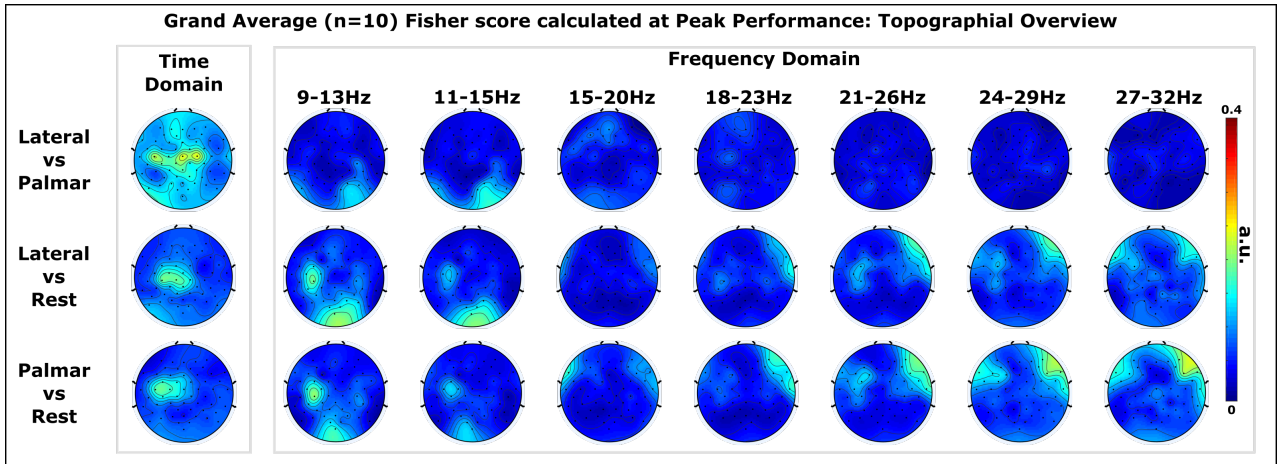


Fig. 5. Topographical overview of the feature ranking provided by the fisher score. The first column summarizes the time domain features, columns 2 to 7 show scoring for the different frequency bands.

TABLE I

SUBJECT SPECIFIC PEAK ACCURACIES (ACC) INCLUDING STANDARD DEVIATION (STD) AND TIME OF OCCURRENCE (WITH RESPECT TO THE MOVEMENT ONSET) FOR BOTH TIME-DOMAIN AND COMBINED CLASSIFICATION APPROACHES.

#	time-domain-only		combined	
	ACC±STD (%)	(s)	ACC±STD (%)	(s)
S1	69.34 ± 5.9	0.94	76.14 ± 5.9	1.4
S2	63.63 ± 6.2	0.88	77.02 ± 5.3	1.3
S3	69.27 ± 6.4	0.88	83.10 ± 4.9	1.5
S4	68.09 ± 6.3	0.81	75.57 ± 5.2	1
S5	63.95 ± 6.6	1.1	74.28 ± 5.4	1.82
S6	61.26 ± 7.6	1	65.81 ± 7.1	1.4
S7	68.72 ± 6.0	0.88	81.26 ± 5.0	1.6
S8	57.78 ± 7.2	0.88	72.27 ± 5.4	0.81
S9	62.75 ± 6.8	0.81	7.23 ± 6.5	1
S10	65.50 ± 6.1	1	74.23 ± 6.9	1.4
AVG	<b>65.0 ± 6.5</b>	<b>0.92 ± 0.1</b>	<b>75.1 ± 5.8</b>	<b>1.2 ± 0.3</b>

to the movement conditions decrease from 10-12% to 2-4%. Furthermore, the combined model results for movement vs. movement conditions increased true positive rates of about 9%, however their false positive and false negative rates are almost identical to the time-domain-only classification model. This indicates that the actual performance gain was achieved mainly by the increased classification performance of movement conditions vs. rest rather than between movement conditions. We also see that for the combined model, accuracies are already elevated above chance level two seconds before the movement onset, contrary to results for the time-domain-only model. The classification accuracy 2 s before the movement onset indicates that the true positive rates for the rest condition are responsible for this effect. This goes in line with findings of Pfurtscheller [25] [26] and their

research on event-related desynchronization who showed that already 2 seconds preceding the movement power changes happen in alpha and beta ranges.

The results of the Fisher score ranking show that for movement vs. movement and the time-domain, high score features are mainly located at the motor cortex, whereas for the frequency-domain, no distinct high scores are obtained. As for movement vs. rest discrimination, in both time-domain and frequency-domain, the highest scores are obtained for central and contralateral channels over the motor cortex. For the frequency-domain the largest contribution is on the alpha frequency range, but high scores are also observed on the lower beta frequencies. High scores were additionally found on other channels in the alpha and high-beta ranges: For the alpha range, also occipital channels seem to be relevant, which can be explained by increased alpha activity typically associated with resting conditions. However, for the high-beta range, higher scores on the frontal lateral channels are most likely associated with the presence of muscular artifacts, especially since the associated channels are located ipsilaterally with respect to the movement. While we applied a trial-based artefact rejection, this result indicates that not all artefact contaminated trials could be successfully removed with our procedure. One must therefore take this point into consideration when interpreting the results, since this effect could have partially contributed to an increase in classification performance of movement vs. rest.

The PSD analysis performed on the time window of peak performance shows higher power values for the rest condition than for both movements, especially in alpha and beta range which adds further strength to our hypothesis. Ultimately, we investigated the low-frequency correlates of all conditions. The movement vs. movement conditions show distinct MRCPs, which were characterized by a negative deflection around the movement onset followed by a reafferent potential which occurred about 300 ms after the peak negativity.

Thereafter a second positive rebound occurs before the EEG returns back to baseline. This second positive rebound is on average stronger for the condition involving the lateral grasp when comparing to the palmar grasp condition, which is in consistency with our previous findings [6]. When comparing the confidence intervals of both movement classes to the rest condition, significant differences around the movement onset on central and contralateral electrodes can be found.

We are aware that the target population is not able to execute grasping movements, however they are able to execute the reach (which allows us to detect the movement onset) and attempt grasping. Preliminary results have already shown that movement attempts lead to similar neural correlates in SCI [15]. Therefore, we expect that our methods can be successfully validated in end users eligible for an upper limb grasp neuroprosthesis.

## V. CONCLUSION

In this work, we could show that a combined classification model of time-domain and frequency-domain features leads to significantly higher classification performances for multiclass classification of reach-and-grasp and rest conditions. While the contribution of the frequency-domain features for the classification of movement vs. movement classification is minimal, these additional features considerably boost movement vs. rest classification. This could be used to decrease false positive rates and therefore the system reliability. We believe that these findings will effectively contribute to our research on BCI-controlled neuroprosthesis for persons with high spinal cord injury.

## ACKNOWLEDGEMENTS

The Authors would like to thank Maria Katharina Höller, MSc. for her tireless effort in supporting measurements and development of the synchronized pressure sensor system. Furthermore, the authors deeply thank Patrick Ofner, MSc. and all members of the EU Horizon 2020 Project MOREGRASP (643955), who build undoubtedly the solid foundation of this research.

## REFERENCES

- [1] J. Meng, S. Zhang, A. Bekyo, J. Olsoe, B. Baxter, and B. He, "Noninvasive electroencephalogram based control of a robotic arm for reach and grasp tasks," *Sci. Rep.*, vol. 6, no. 1, 2016.
- [2] R. Rupp, M. Rohm, M. Schneiders, A. Kreiling, and G. R. Müller-Putz, "Functional rehabilitation of the paralyzed upper extremity after spinal cord injury by noninvasive hybrid neuroprostheses," *Proc. IEEE*, vol. 103, no. 6, pp. 954–968, 2015.
- [3] E. V. C. Friedrich, C. Neuper, and R. Scherer, "Whatever works: a systematic user-centered training protocol to optimize brain-computer interfacing individually," *PLoS One*, vol. 8, no. 9, p. e76214, Sept. 2013.
- [4] M. Rohm, M. Schneiders, C. Müller, A. Kreiling, V. Kaiser, G. R. Müller-Putz, and R. Rupp, "Hybrid brain-computer interfaces and hybrid neuroprostheses for restoration of upper limb functions in individuals with high-level spinal cord injury," *Artif. Intell. Med.*, vol. 59, no. 2, pp. 133–142, 2013.
- [5] G. Pfurtscheller, G. R. Müller, J. Pfurtscheller, H. J. Gerner, and R. Rupp, "'thought' – control of functional electrical stimulation to restore hand grasp in a patient with tetraplegia," *Neurosci. Lett.*, vol. 351, no. 1, pp. 33–36, 2003.
- [6] A. Schwarz, P. Ofner, J. Pereira, A. I. Sburlea, and G. R. Müller-Putz, "Decoding natural reach-and-grasp actions from human EEG," *J. Neural Eng.*, vol. 15, no. 1, p. 016005, Feb. 2018.
- [7] P. Ofner, A. Schwarz, J. Pereira, and G. R. Müller-Putz, "Upper limb movements can be decoded from the time-domain of low-frequency EEG," *PLoS One*, vol. 12, no. 8, p. e0182578, Aug. 2017.
- [8] J. Omedes, A. Schwarz, G. R. Müller-Putz, and L. Montesano, "Factors that affect error potentials during a grasping task: toward a hybrid natural movement decoding BCI," *J. Neural Eng.*, vol. 15, no. 4, p. 046023, Aug. 2018.
- [9] J. Pereira, A. I. Sburlea, and G. R. Müller-Putz, "EEG patterns of self-paced movement imaginations towards externally-cued and internally-selected targets," *Sci. Rep.*, vol. 8, no. 1, p. 13394, Sept. 2018.
- [10] G. R. Müller-Putz, A. Schwarz, J. Pereira, and P. Ofner, "From classic motor imagery to complex movement intention decoding: The noninvasive Graz-BCI approach," *Prog. Brain Res.*, vol. 228, pp. 39–70, May 2016.
- [11] H. Shibusaki and M. Hallett, "What is the Bereitschaftspotential?" *Clin. Neurophysiol.*, vol. 117, no. 11, pp. 2341–2356, Nov. 2006.
- [12] M. Jochumsen, I. K. Niazi, N. Mrachacz-Kersting, D. Farina, and K. Dremstrup, "Detection and classification of movement-related cortical potentials associated with task force and speed," *J. Neural Eng.*, vol. 10, no. 5, p. 056015, Oct. 2013.
- [13] H. A. Agashe, A. Y. Paek, Y. Zhang, and J. L. Contreras-Vidal, "Global cortical activity predicts shape of hand during grasping," *Frontiers in Neuroscience*, vol. 9, p. 121, 2015. [Online]. Available: <https://www.frontiersin.org/article/10.3389/fnins.2015.00121>
- [14] I. Iturrate, R. Chavarriaga, M. Pereira, H. Zhang, T. Corbet, R. Leeb, and J. D. R. Millán, "Human EEG reveals distinct neural correlates of power and precision grasping types," *Neuroimage*, vol. 181, pp. 635–644, Nov. 2018.
- [15] G. R. Müller-Putz, P. Ofner, A. Schwarz, J. Pereira, G. Luzhnic, and R. Rupp, "MoreGrasp: Restoration of upper limb function in individuals with high spinal cord injury by multimodal neuroprostheses for interaction in daily life activities," in *Proceedings of the 7th Graz Brain-Computer Interface Conference 2017*, Müller-Putz, Steyrl, Wriessnegger, and Scherer, Eds. Verlag der TU Graz, Graz University of Technology, pp. 338–343.
- [16] "R.O. Duda, P.E. Hart, and D.G. Stork, pattern classification, New York: John Wiley & Sons, 2001, pp. xx 654, ISBN: 0-471-05669-3," *J. Classification*, vol. 24, no. 2, pp. 305–307, 2007.
- [17] H.-J. Steingrüber, *Hand-Dominanz-Test: H-D-T ; Manual*. HOGREFE, 2011.
- [18] R. J. Kobler, A. I. Sburlea, and G. R. Müller-Putz, "Tuning characteristics of low-frequency EEG to positions and velocities in visuomotor and oculomotor tracking tasks," *Sci. Rep.*, vol. 8, no. 1, p. 17713, Dec. 2018.
- [19] J. Fallor, C. Vidaurre, T. Solis-Escalante, C. Neuper, and R. Scherer, "Autocalibration and recurrent adaptation: towards a plug and play online ERD-BCI," *IEEE Trans. Neural Syst. Rehabil. Eng.*, vol. 20, no. 3, pp. 313–319, May 2012.
- [20] B. Blankertz, S. Lemm, M. Treder, S. Haufe, and K.-R. Müller, "Single-trial analysis and classification of ERP components—a tutorial," *Neuroimage*, vol. 56, no. 2, pp. 814–825, May 2011.
- [21] W. Skrandies, "Global field power and topographic similarity," *Brain Topogr.*, vol. 3, no. 1, pp. 137–141, 1990.
- [22] M. Billinger, I. Daly, V. Kaiser, J. Jin, B. Z. Allison, G. R. Müller-Putz, and C. Brunner, "Is it significant? guidelines for reporting BCI performance," in *Biological and Medical Physics, Biomedical Engineering*, 2012, pp. 333–354.
- [23] L. Randazzo, I. Iturrate, R. Chavarriaga, R. Leeb, and J. R. Del Millán, "Detecting intention to grasp during reaching movements from EEG," *Conf. Proc. IEEE Eng. Med. Biol. Soc.*, vol. 2015, pp. 1115–1118, Aug. 2015.
- [24] M. Jochumsen, I. K. Niazi, K. Dremstrup, and E. N. Kamavuako, "Detecting and classifying three different hand movement types through electroencephalography recordings for neurorehabilitation," *Med. Biol. Eng. Comput.*, vol. 54, no. 10, pp. 1491–1501, Oct. 2016.
- [25] G. Pfurtscheller and A. Aranibar, "Evaluation of event-related desynchronization (ERD) preceding and following voluntary self-paced movement," *Electroencephalogr. Clin. Neurophysiol.*, vol. 46, no. 2, pp. 138–146, Feb. 1979.
- [26] G. Pfurtscheller and C. Neuper, "Motor imagery and direct brain-computer communication," *Proc. IEEE*, vol. 89, no. 7, pp. 1123–1134, 2001.

## 4.3 Appendix C: Publication List (peer reviewed)

### 4.3.0.1 2020

1. Kobler R, Sburlea A.I., Lopes-Dias C., **Schwarz A.**, Hirata M., Müller-Putz G.R., Corneo-retinal-dipole and blink related eye artifacts can be corrected of-line and online in electroencephalographic and magnetoencephalographic signals, Neuroimage, 2020, accepted
2. **Schwarz A.**, Höller, M.K., Pereira J., Müller-Putz G.R., Decoding hand movements from human EEG to control a robotic arm in a simulation environment, Journal of Neural Engineering, <https://doi.org/10.1088/1741-2552/ab882e>
3. Ditz J., **Schwarz A.**, Müller-Putz G.R., Perturbation-Evoked Potential can be classified from single-trial EEG, Journal of Neural Engineering <https://doi.org/10.1088/1741-2552/ab89fb>

### 4.3.0.2 2019

4. **Schwarz A.**, Pereira J., Kobler R., Müller-Putz G.R., Unimanual and Bimanual Reach-and-Grasp Actions Can Be Decoded From Human EEG, IEEE Transactions on Biomedical Engineering, 67(6) p.1684-1695, 09/2019, <https://dx.doi.org/10.1109/TBME.2019.2942974>
5. **Schwarz A.**, Lindner L., Pereira J., Müller-Putz G.R., Combining frequency and time-domain EEG features for classification of self-paced reach-and-grasp actions, 41st Annual International Conference of the IEEE Engineering in Medicine and Biology Society (EMBC), Berlin, Germany, 2019, 3036-3041, <https://doi.org/10.1109/EMBC.2019.8857138>
6. **Schwarz A.**, Brandstetter J., Pereira J., Müller-Putz G.R., Direct comparison of supervised and semi-supervised retraining approaches for co-adaptive BCIs, Medical & Biological Engineering and Computing, 57(11), 2347-2357, 2019, <https://dx.doi.org/10.1007/s11517-019-02047-1>
7. Ofner P., **Schwarz A.**, Pereira J., Wyss D., Wildburger R., Müller-Putz G.R., Attempted Arm and Hand Movements can be Decoded from Low-Frequency EEG from Persons with Spinal Cord Injury. Scientific Reports, 9(1), 7134, 2019, <https://doi.org/10.1038/s41598-019-43594-9>
8. Ofner P., Pereira, J., **Schwarz A.**, Müller-Putz G.R., Online detection of hand open vs palmar grasp attempts in a person with spinal cord injury, 8th Graz Brain-Computer Interface Conference 2019, Graz, Austria ,188.193, 2019, [doi.org/10.3217/978-3-85125-682-6-35](https://doi.org/10.3217/978-3-85125-682-6-35)

9. Müller-Putz G.R., Ofner P., Pereira J., Pinegger A., **Schwarz A.** et al. , Applying intuitive EEG-controlled grasp neuroprostheses in individuals with spinal cord injury: Preliminary results from the MoreGrasp clinical feasibility study, 41st Annual International Conference of the IEEE Engineering in Medicine and Biology Society (EMBC), Berlin, Germany, 5949-5955, <https://doi.org/10.1109/EMBC.2019.8856491>

#### 4.3.0.3 2018

10. **Schwarz A.**, Ofner P., Pereira J., Sburlea I.A., Müller-Putz G.R. ,Decoding natural reach-and-grasp actions from human EEG, Journal of Neural Engineering, 15(1), 2018, <https://doi.org/10.1088/1741-2552/aa8911>
11. Omedes J., **Schwarz A.**, Müller-Putz G.R., Monsanto L., Factors that affect error potentials during a grasping task: towards a hybrid natural movement decoding BCI, Journal of Neural Engineering 15(4), 2018, <https://doi.org/10.1088/1741-2552/aac1a1>
12. Müller-Putz G.R., Pereira J., Ofner P., **Schwarz A.**, et al., Towards non-invasive Brain-Computer Interfaces for hand/arm control in users with spinal cord injury. 6th International Winter Conference on Brain-Computer Interface (pp. 65-68), Korea, <https://doi.org/10.1109/IWW-BCI.2018.8311498>

#### 4.3.0.4 2017

13. Ofner P., **Schwarz A.**, Pereira J., Müller-Putz G.R., Upper limb movements can be decoded from the time-domain of low-frequency EEG, PloS one 12 (8), e0182578, 2017, <https://doi.org/10.1371/journal.pone.0182578>
14. Statthaler K., **Schwarz A.**, Steyrl D., Kobler R, et al., Cybathlon experiences of the Graz BCI racing team Mirage91 in the brain-computer interface discipline, Journal of neuroengineering and rehabilitation, 14(1), 129ff., 2017, <http://doi.org/10.1186/s12984-017-0344-9>
15. Omedes J., **Schwarz A.**, Montesano L., Müller-Putz G.R., Hierarchical decoding of grasping commands from EEG, Engineering in Medicine and Biology Society (EMBC), 2017 39th Annual International Conference of the IEEE, p.2085-2088, <https://doi.org/10.1109/EMBC.2017.8037264>
16. Pereira J., Ofner J., **Schwarz A.**, Sburlea A.I., Müller-Putz G.R., EEG neural correlates of goal-directed movement intention, Neuroimage 149, 129-140, 2017, <https://doi.org/10.1016/j.neuroimage.2017.01.030>
17. Müller-Putz G.R., Ofner P., **Schwarz A.**, Pereira J., Pinegger A., Lopes Dias C. et al. Towards non-invasive EEG-based arm/hand-control in users with spinal cord

injury, 2017 5th International Winter Conference on Brain-Computer Interface (BCI), p. 63-65, <http://doi.org/10.1109/IWW-BCI.2017.7858160>

18. Müller-Putz G.R., Ofner P., **Schwarz A.**, Pereira J. et al., MoreGrasp: Restoration of upper limb function in individuals with high spinal cord injury by multimodal neuroprostheses for interaction in daily activities, 7th Graz Brain-Computer Interface Conference 2017 (pp.338-343), <http://doi.org/10.3217/978-3-85125-533-1-62>

#### 4.3.0.5 2016

19. Müller-Putz G.R., **Schwarz A.**, Pereira J., Ofner P., From classic motor imagery to complex movement intention decoding: The noninvasive Graz-BCI approach, 228, p. 39-70, Elsevier, 2017, <https://doi.org/10.1016/bs.pbr.2016.04.017>
20. Müller-Putz G.R., **Schwarz A.**, Pereira J., Ofner P., Steuerung von Neuroprothesen bei Querschnittlähmung: der nichtinvasive Graz-BCI-Ansatz, *neuroreha*, 8(3), 126-133, Georg Thieme Verlag, <https://doi.org/10.1055/s-0042-111672>
21. **Schwarz A.**, Steyrl D., Müller-Putz G.R., Brain-computer interface adaptation for an end user to compete in the Cybathlon, 2016 IEEE International Conference on Cybathlon, Systems, Man, and Cybernetics (SMC), 1803-1808 <https://doi.org/10.1109/SMC.2016.7844499>
22. **Schwarz A.**, Ofner P., Pereira J., Müller-Putz G.R., Time domain classification of grasp and hold tasks, Sixth International Brain-Computer Interface Meeting: BCI Past, Present, and Future, Asilomar, CA, USA, 2016 6, p.76, <https://doi.org/DOI:10.3217/978-3-85125-467-9-76>
23. Ofner, P., **Schwarz, A.**, Pereira, J., Müller-Putz, G.R., Movements of the same upper limb can be classified from low-frequency time-domain EEG signals, Proceedings of the Sixth International Brain-Computer Interface Meeting: BCI Past, Present, and Future, pp. 69, [urlhttps://doi.org/10.3217/978-3-85125-467-9-69](https://doi.org/10.3217/978-3-85125-467-9-69)
24. Pereira J., Ofner P., **Schwarz A.**, Müller-Putz, G.R., Discriminating goal-directed from non-goal-directed movements for BCI control, Proceedings of the 6th International Brain-Computer Interface Meeting , pp.67, <https://doi.org/10.3217/978-3-85125-467-9-67>
25. Scherer, R., **Schwarz, A.**, Müller-Putz, G. et al., Lets play Tic-Tac-Toe: A Brain-Computer Interface case study in cerebral palsy. In Systems, Man, and Cybernetics (SMC), 2016 IEEE International Conference on (pp. 003736 - 003741), [urlhttps://doi.org/10.1109/SMC.2016.7844815](https://doi.org/10.1109/SMC.2016.7844815)

#### 4.3.0.6 2015

26. **Schwarz A.**, Scherer R., Steyrl D., Faller J., Müller-Putz G.R., A co-adaptive sensory motor rhythms brain-computer interface based on common spatial patterns and random forest, Engineering in Medicine and Biology Society (EMBC15), 2015 37th Annual International Conference of the IEEE, p.1049-1052, Milan, 2015, url<https://doi.org/10.1109/embc.2015.7318545>
27. Scherer R., Billinger M., Wagner J., **Schwarz A.**, Hettich DT., Bolinger E., Garcia ML. and Gernot R. Müller-Putz, Thought-based row-column scanning communication board for individuals with cerebral palsy, *Annals of Physical Medicine and Rehabilitation*, 58(1), p.14-22, <https://doi.org/10.1016/j.rehab.2014.11.005>
28. Scherer R., **Schwarz A.**, Müller-Putz G.R. et al., Game-based BCI training: Interactive design for individuals with cerebral palsy. In IEEE International Conference on Systems, Man, and Cybernetics (pp. 3175-3180), <https://doi.org/10.1109/SMC.2015.551>